Stochastic Dynamics of Hysteretic Structures

J.E. Hurtado

Monograph CIMNE IS-25 1998

Monograph Series in Earthquake Engineering

Edited by A.H. Barbat

Stochastic Dynamics of Hysteretic Structures

J.E. Hurtado
Universidad Nacional de Colombia

Monograph CIMNE IS-25 1998

INTERNATIONAL CENTER FOR NUMERICAL METHODS IN ENGINEERING
Edificio C1, Campus Norte UPC
C/ Gran Capitán, s/n
08034 Barcelona, Spain

Monograph Series in Earthquake Engineering
Edited by A.H. Barbat

ISSN: 1134-3249

STOCHASTIC DYNAMICS OF HYSTERETIC STRUCTURES
Monograph CIMNE IS-25

ISBN: 84-89925-09-7
Depósito Legal: B-9265-98

IMPRESO EN ESPAÑA - PRINTED IN SPAIN

Acknowledgements

Finantial supports for performing this research at the Technical University of Catalonia have been given to the author by the Colombian Science Institute, *Colciencias* and the National University of Colombia. The supports of are gratefully acknowledged.

Contents

Introduction

1. Motivation

Many structural and mechanical systems are subject to external actions that are random in time and nature, i.e. not only the moment of their ocurrence in a macro-scale is uncertain but also their time variation in the micro-scale. Earthquakes, wind loads, ocean waves etc., can be classified into this cathegory. Since their time variation is usually fast they produce vibration in the structure and, therefore, one has to deal with random dynamic responses produced by random time-variant actions. Furthermore, the uncertainty of the structural performance increases if account is taken of the randomness associated to structural parameters such as mass, stiffness, strength, etc. It is clear that the problem must be examined from a probabilistic point of view by means of the theories of stochastic processes and random vibration.

A general method that can be applied to any type of linear or nonlinear structure for obtaining statistical measures of its response is the *Monte Carlo simulation*, which consists in the synthetic generation of a large number of realizations of the random process under study and the calculation of a set of structural response histories with a deterministic algorithm. The large computational effort required by this technique, which makes it well neigh an unadmissible task in case of large nonlinear structures, explains why random vibration theory is mainly concerned with analytical methods for assessing such measures at a lower cost. Monte Carlo simulation is commonly employed only for judging the accuracy of analytical methods on small structural systems.

The analysis of the structural random vibration caused by earthquakes using analytical techniques is more involved than for other random loads, due to the fact that they usually entail nonlinear structural response - let alone the difficulties for a correct stochastic description of earthquake acceleration processes. While methods for characterizing the vibration of linear structures in probabilistic terms are well established, for nonlinear systems the available methods are limited in their application. In fact, either they can be applied only to structures having weak nonlinear behaviour and otherwise they become inaccurate, or they give good estimations only for certain cases of severe nonlinear response. Moreover, the structural size that can be managed when using some of them is

usually very limited for mathematical or computational reasons. Finally, some of the above limitations are more serious for a class of nonlinear systems, namely those exhibiting hysteretic behaviour, whose mathematical description makes difficult or impossible the application of some established techniques.

2. Outline

This monograph deals with methods for analysing the random vibration of deterministic or uncertain hysteretic structures under any type of external random dynamic load. However, more attention is given to the modelling of seismic random vibration of structures.

Chapter 1 is devoted to a cursory account of background concepts on random processes and stochastic calculus. It is intended to be helpful to the general reader for a better understanding of the subsequent developments. The topics examined are the stationary and nonstationary processes, Markov processes, basic and advanced stochastic calculus and stochastic differential equations. In chapter 2 the stochastic modelling of earthquake actions is dealt with. Both stationary and nonstationary models are examined, with a special emphasis placed on the instantaneous spectrum, which is used in later applications of random vibration methods to the analysis of base isolated buildings. The next chapter summarizes the basic concepts of the method of stochastic equivalent linearization as well as methods for assessing the distribution of response maxima and the influence of model uncertainties.

Chapter 4 discusses the application of the method of stochastic linearization to hysteretic structures using the hypothesis of joint Gaussian behaviour of the response variables which is frequently resorted to in random vibration analyses. It is shown that the method is subject to errors that can be enormous in some cases. In chapter 5 a non Gaussian method aimed at obtaining better estimations is introduced. It is based on combinations of Dirac and Gauss densities poised in accordance to the departure from the linear state of the system. Its superiority over the conventional Gaussian approach is demonstrated through a series of examples. The chapter ends with the derivation of the equations necessary to compute the influence of model uncertainty according to the general second-order method described in chapter 3.

In chapter 6 a method intended to extend the applicability of stochastic linearization to large nonlinear structures using eigendecomposition that has been proposed by several authors is discussed. It is shown that when used for nonstationary analyses, the response estimations it gives are tightly dependent on the time step used for the calculation, which is tantamount to saying that the method is not suitable for practical application. An algorithm that overcomes this drawback is introduced. It is shown that it is mathematically equivalent

in the eigenspace to the direct method used in chapters 3 to 5 in the physical space.

Chapter 7 begins with a discussion on methods for estimating the higher order stochastic response of hysteretic structures. It follows with an analysis of the numerical weaknesses of the method of maximum entropy, which emerges as the best to that purpose from the previous examination. However, the method is fraught with numerical pitfalls, the most important of which lies in the ill-conditioning of a core matrix, whose entries are multidimensional integrals that must be calculated at each time step. A procedure for calculating the integrals, based on Fourier transforms, is then introduced. It is demonstrated that it leads to a solution for the joint probability density while normal integration techniques carry the solution to numerical collapse. In the last chapter the method of stochastic equivalent linearization is applied to the study of the seismic random vibration of two types of base isolation systems. Both are found to be highly sensitive to some nonstationary details of the seismic action. Other aspects, such as the influence of the structural nonlinear behaviour and the uncertainty of device strength are examined.

Chapter 1

Random processes and stochastic calculus

1.1 Introduction

By the expression *random* or *stochastic process* it is meant a scalar or vector random variable which evolves in time. This means that the value of the function $x(t)$ at any time is unpredictable and so it is a random variable $X(t)$ which can only be described in a probabilistic sense*. According to this definition, the relationship existing between the theory of random processes to that of random variables is similar to that linking dynamics with statics in structural theory. Figure 1.1 shows a realization of a random process (an earthquake accelerogram in this case). Unlike the common deterministic view of structural dynamics problems, which would take such accelerogram as the "true" excitation, from an stochastic viewpoint it is only a matter of chance that just this recorded acceleration history has ocurred and any other with the same probabilistic structure could be claimed to be considered with equal rigth. The structural responses to several random excitations, of course, would differ, especially if the system is nonlinear. Thus, both the input and output time histories could be regarded as random processes.

The mentioned probabilistic structure of the random process is the subject under study. That is, if the discrete states of the (in general, vector) random variable $\boldsymbol{X}(t)$ are $\boldsymbol{X}_1, \boldsymbol{X}_2, \boldsymbol{X}_3, \ldots$ at times $t_1 \leq t_2 \leq t_3, \ldots$ the interest lies on the determination of probabilistic measures common for all posible realizations of that sequence. According to the information conveyed by the measures one can order them into a hierachy. The most complete description of a stochastic

* Throughout this work a distinction is made between deterministic and stochastic time functions, which are denoted with lower- and upper-case letters, respectively. The realizations of a stochastic process are also denoted with lower-case symbols.

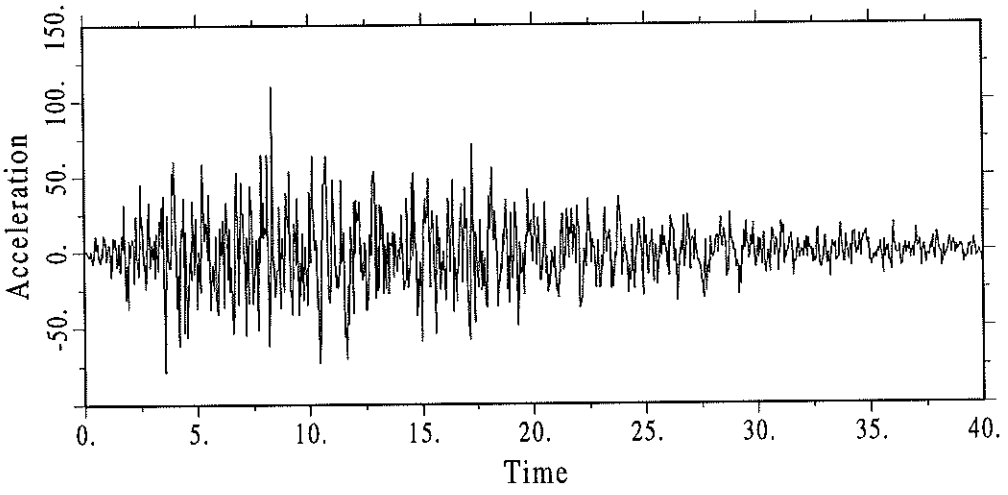

Figure 1.1 An earthquake motion record (units: s, cm/s^2)

process would be the set of joint probability distribution functions of the type

$$F(\boldsymbol{x}_1, t_1) = P[\boldsymbol{X}_1(t_1) \leq \boldsymbol{x}_1]$$

$$F(\boldsymbol{x}_1, t_1; \boldsymbol{x}_2, t_2) = P[\boldsymbol{X}_1(t_1) \leq \boldsymbol{x}_1 \cap \boldsymbol{X}_2(t_2) \leq \boldsymbol{x}_2]$$

$$F(\boldsymbol{x}_1, t_1; \boldsymbol{x}_2, t_2 \ldots \boldsymbol{x}_m, t_m) = P[\boldsymbol{X}_1(t_1) \leq \boldsymbol{x}_1 \cap \ldots \boldsymbol{X}_m(t_m) \leq \boldsymbol{x}_m] \tag{1.1}$$

if they can be found. The corresponding probability density functions are defined as their partial derivatives with respect to all their arguments. For a scalar process we have

$$f(x_1, t_1; x_2, t_2 \ldots x_m, t_m) = \frac{\partial^m F(x_1, t_1; x_2, t_2 \ldots x_m, t_m)}{\partial x_1 \partial x_2 \ldots \partial x_m} \tag{1.2}$$

An important class of processes for which the overall probabilistic description (1.1) can be greatly simplified is constituted by the *Markov diffusion processes.* As will be shown later in this chapter, these processes can be completely specified in terms of second order, conditional probability densities of the type

$$f(\boldsymbol{x}_2, t_2 | \boldsymbol{x}_1, t_1) \tag{1.3}$$

which expresses the probability of finding the process in state $\boldsymbol{x}_2$ at time t_2 given that it was in state $\boldsymbol{x}_1$ at time t_1. This notion has opened the way to the development of the theory of stochastic differential equations.

In many cases, however, even the determination of such elementary conditional probabilities is difficult, in which case the analysis of a vector process can only achieve the estimation of some moments of the components of the vector, i.e.

$$\mu_{|\boldsymbol{k}|}(\boldsymbol{X};t) = \int x_1^{k_1} x_2^{k_2} \dots x_n^{k_n} f(\boldsymbol{x},t)\mathrm{d}\boldsymbol{x} \tag{1.4}$$

where $\boldsymbol{k}$ is the multi-index of powers of the associated random variables

$$\boldsymbol{k} = [k_1, k_2, \dots] \tag{1.5}$$

and $|\boldsymbol{k}|$ is the sum of its elements:

$$|\boldsymbol{k}| = k_1 + k_2 + \dots \tag{1.6}$$

These moments represent, of course, a poorer probabilistic information about the process than the density functions. The lowest position in this hierarchy correspond to the case where only the moments of the first two orders ($|\boldsymbol{k}| = 1, 2$) can be obtained. However, if the process is Gaussian (that is, the marginal and joint probabilistic densities obey a normal law) such second order description determines completely the whole probabilistic evolution of the Markov diffusion process. If not, it can nevertheless be useful for the assessment of other important measures of the process, such as first passage times, expected maximum values, etc., as detailed in chapter 3.

The present work is concerned with methods for estimating second as well as higher order stochastic response of hysteretic structures under different types of Gaussian excitation. To facilitate the understanding of the implied methods, concepts and results it is necessary to provide the reader with an exposition on the theory of random processes and stochastic differential equations. Since a detailed and rigorous treatment of such a wide subject will occupy several volumes, this chapter is only purported to give a brief account of it. The exposition is restricted to the concepts that will be needed in the subsequent chapters. Moreover they will be treated in a somewhat cursory manner, i.e. only few derivations will be perfomed and for most of them the reader is referred to basic treatises, such as those by Gardiner (1985), Kloeden and Platen (1995), Nigam (1983), Priestley (1981), Soong (1973), Soong and Grigoriu (1993), and Tikhonov (1982) which have been used in the composition of this summary.

1.2 Elements of stochastic calculus

The very fact that the realizations of a stochastic process are uncertain implies that conventional notions of Riemann calculus, such as continuity, differentiability and integrability need to be reformulated. That is, the uncertainty about the path of all the realizations requires those concepts to be defined in a probabilistic rather than in the usual deterministic sense. The following is a brief summary of some milestones of stochastic calculus.

1. *Norm of a random variable.*
   A random variable X is said to be of *second order* when its variance $\mathrm{E}[X^2]$ is finite. For such a variable the *norm* is defined as

$$||X|| = (\mathrm{E}[X^2])^{\frac{1}{2}} \tag{1.7}$$

It can be shown that the above expectation satisfies inner product properties.

2. *Distance between random variables.*
   The distance between variables X_1 and X_2 is defined as

$$d(X_1, X_2) = ||X_1 - X_2|| \tag{1.8}$$

A space of random variables provided with the above inner product, norm and distance is called a $L_2-space$, which can be demonstrated to be complete a Banach and Hilbert space. In particular, the important property that there exists a unique limit for a sequence X_n in a L_2-space must be stressed, since it is the basis for the following notions.

3. *Convergence in mean square.*
   A sequence of random variables X_n is said to *converge in mean square* to a random variable X if

$$\lim_{n\to\infty} ||X_n - X|| = \text{m.s.} \lim_{n\to\infty} X_n = 0 \tag{1.9}$$

4. *Continuity in mean square.*
   A second order stochastic process is *continuous in mean square* if the function

$$R_X(t, s) = \mathrm{E}[X(t)X(s)] \tag{1.10}$$

is continuous at $s = t$. This function is called *auto-correlation function* and plays an important role in the theory of stochastic processes.

5. *Differentiation in mean square.*

The *mean square derivative* $\dot{X}(t)$ of a process $X(t)$ is defined as the mean square limit

$$\text{m.s.} \lim_{\tau \to 0} \frac{X(t+\tau) - X(t)}{\tau} \tag{1.11}$$

if it exists. The condition for the existence of the limit is that the second generalized derivative of the auto-correlation function, namely,

$$\lim_{\tau,\sigma \to 0} \frac{1}{\tau\sigma}[R_X(t+\tau, s+\sigma) - R_X(t+\tau, s) - R_X(t, s+\sigma) + R_X(t, s)] \tag{1.12}$$

exists at (t, t) and is finite. An important result that will often be used in this work is that if a stochastic process is N times m.s. differentiable then

$$\mathrm{E}\Big[\frac{\mathrm{d}^n X(t)}{\mathrm{d}t^n}\Big] = \frac{\mathrm{d}^n}{\mathrm{d}t^n}\mathrm{E}[X(t)] \tag{1.13}$$

Also, if $X^{(n)}(t)$ denotes the derivative $\frac{\mathrm{d}^n X(t)}{\mathrm{d}t^n}$, then

$$R_X^{(n,m)}(t, s) = \mathrm{E}[X^{(n)}(t)X^{(m)}(s)] = \frac{\partial^{n+m} R_X(t, s)}{\partial t^n \partial s^m} \tag{1.14}$$

if the implied derivatives exist.

6. *Integration in mean square*

The concept of mean square Riemann or Riemann-Stieltjes integrals requires some previous definitions. Consider a $N-$partition of the interval $[t_0, t_N] \subset T$, i.e. the points $t_k, k = 0, 1, 2, \ldots, N$ such that $t_0 < t_1 < t_2 < \ldots t_N$ and define

$$\Delta_N = \max(t_k - t_{k-1}) \tag{1.15}$$

Let $X(t)$ be a stochastic process with finite second order moments defined on $[t_0, t_N]$, and $f(t, u)$ a deterministic function defined in the same interval and integrable in the ordinary Riemann sense for every $u \in U$. The variable

$$Y_N(u) = \sum_{k=1}^{N} f(\tau_k, u)X(\tau_k)(t_k - t_{k-1}) \tag{1.16}$$

in which τ_k is an arbitrary point in the interval $[t_{k-1}, t_k)$, will then be a random variable of u defined for each of such partitions. If, for every $u \in U$ the limit

$$\text{m.s.} \lim_{\substack{N\to\infty \\ \Delta_N \to 0}} Y_N = Y(u) \tag{1.17}$$

exists for some sequence of subdivisons of $[t_0, t_N]$, it is called the *mean square Riemann integral* of $f(t,u)$ over the interval $[t_0, t_N]$ and it is denoted by

$$Y(u) = \int_{t_0}^{t_N} f(t,u)X(t)\mathrm{d}t \tag{1.18}$$

The necessary and suficient condition for the existence of the m.s. Riemann integral is that the ordinary double Riemann integral

$$\int_{t_0}^{t_N}\int_{t_0}^{t_N} f(t,u)f(s,u)R_X(t,s)\mathrm{d}t\,\mathrm{d}s \tag{1.19}$$

exists and is finite.

Mean square Riemann-Stieltjes integrals can be developed similarly. For example, the integral

$$I = \int_{t_0}^{t_N} X(t)\mathrm{d}F(t) \tag{1.20}$$

in which $X(t)$ is a stochastic process and $F(t)$ is a (deterministic or stochastic) function not necessarily continuous, can be expressed as the mean square limit

$$I = \text{m.s.} \lim_{\substack{N\to\infty \\ \Delta_N \to 0}} I_N \tag{1.21}$$

where

$$I_N(u) = \sum_{k=1}^{N} X(\tau_k)[F(t_k) - F(t_{k-1})] \tag{1.22}$$

A sufficient condition for the existence of the above limit is that $F(t)$ has a bounded variation, i. e.

$$\sum_{k=1}^{N} |F(t_k) - F(t_{k-1})| < M \tag{1.23}$$

where M is a finite number. This condition is violated by stochastic functions such as a the Wiener process. Since it is quite useful in the development of stochastic differential equations, special mathematical tools are required for the evaluation of stochastic integrals involving it. These are the Ito and Stratonovich integrals which are defined later.

1.3 Stationary processes

1.3.1 Definition

An important class of processes is constituted by those whose probabilistic structure do not vary with time. More rigorously, a *stationary process in strict sense* is such that its distributions do not change under an arbitrary translation of the time axis, τ, i.e.,

$$F(x_1, x_2, \ldots x_m; t_1, t_2, \ldots t_m) = F(x_1, x_2, \ldots x_m; t_1 + \tau, t_2 + \tau, \ldots t_m + \tau) \quad (1.24)$$

By setting $\tau = -t_1$ it can be seen that the probability distributions will not depend on the absolute position of the origin but only on the time lag.

For the specific case of the first order distribution ($m = 1$) there will be no dependence on any time measure at all and hence the moments of the process will be constant, i.e.

$$\mathrm{E}[X^i(t)] = \text{const}, \quad i = 1, 2, \ldots \quad (1.25)$$

Moreover, second order moments will depend only on the difference $\tau = t_2 - t_1$ and then

$$\mathrm{E}[X(t_1)X(t_2)] = \mathrm{E}[X(t)X(t+\tau)] = R_X(\tau) \quad (1.26)$$

An important measure of stochastic process is the *auto-covariance function*, defined as

$$\Sigma_X(t_1, t_2) = \mathrm{E}[\{X(t_1) - \mu(t_1)\}\{X(t_2) - \mu(t_2)\}] \quad (1.27)$$

where $\mu(t_i)$ is the *mean* of the process at time t_i,

$$\mu(t_i) = \mathrm{E}[X(t_i)], \qquad i = 1, 2 \quad (1.28)$$

In the special case of a stationary process the auto-covariance function simplifies to

$$\Sigma_X(t_1, t_2) = R_X(\tau) - \mu^2 \tag{1.29}$$

for $\tau = t_2 - t_1$.

The condition for having a strict-sense stationary process can be relaxed to introduce a more practical class of processes called *weakly stationary*. They are defined by the following conditions: (a) the moments of first and second orders are constant and (b) the auto-correlation function only depends on the time lag as in equation (1.26). No condition is imposed on third and higher orders of expectations. Since these conditions are also satisfied by strictly stationary processes it can be said that weak stationarity does not imply strict stationarity. The only exemption is the Gaussian process, which is completely determined by expectations of the first two orders.

1.3.2 Auto-Correlation and spectral density functions

An important weakly stationary process is that having *independent* or *orthogonal increments*. It can be defined on the basis of the analysis of the following process:

$$X(t) = Z_1 \mathrm{e}^{\mathrm{i}\omega_1 t} + Z_2 \mathrm{e}^{\mathrm{i}\omega_2 t} \tag{1.30}$$

where Z_1 and Z_2 are zero-mean complex-valued random variables, $\mathrm{i}^2 = -1$ and ω_1, ω_2 are constants. The mean of the process is, clearly,

$$\mathrm{E}[X(t)] = 0 \tag{1.31}$$

due to the harmonic nature of the complex-exponential. The auto-correlation function is

$$\mathrm{E}[X(t)X^{\mathrm{C}}(t+\tau)] = \mathrm{E}[Z_1 Z_1^{\mathrm{C}}]\mathrm{e}^{-\mathrm{i}\omega_1\tau} + \mathrm{E}[Z_1 Z_2^{\mathrm{C}}]\mathrm{e}^{\mathrm{i}[\omega_1 t - \omega_2(t+\tau)]} +$$

$$\mathrm{E}[Z_2 Z_1^{\mathrm{C}}]\mathrm{e}^{\mathrm{i}[\omega_2 t - \omega_1(t+\tau)]} + \mathrm{E}[Z_2 Z_2^{\mathrm{C}}]\mathrm{e}^{-\mathrm{i}\omega_2\tau} \tag{1.32}$$

For the process to be weakly stationary it is necessary that $\mathrm{E}[Z_1 Z_2^{\mathrm{C}}] = \mathrm{E}[Z_2 Z_1^{\mathrm{C}}] = 0$ so that the auto-correlation function does not depend on t (whence the orthogonalaty labeling). Under such a restriction the auto-correlation becomes

$$\mathrm{E}[X(t)X^{\mathrm{C}}(t+\tau)] = \mathrm{E}[|Z_1|^2]\mathrm{e}^{-\mathrm{i}\omega_1\tau} + \mathrm{E}[|Z_2|^2]\mathrm{e}^{-\mathrm{i}\omega_2\tau} \tag{1.33}$$

Generalizing, a stationary process with auto-correlation

$$R_X(\tau) = \mathrm{E}[X(t)X^{\mathrm{C}}(t+\tau)] = \sum_{k=1}^{n} \mathrm{E}[\,|Z_k|^2\,]\mathrm{e}^{-\mathrm{i}\omega_k\tau} \tag{1.34}$$

can be built by the sum of harmonics

$$X(t) = \sum_{k=1}^{n} Z_k \mathrm{e}^{\mathrm{i}\omega_k t} \tag{1.35}$$

under the condition $\mathrm{E}[Z_j Z_k^{\mathrm{C}}] = 0, j \neq k$. The continous version of this process gives origin to the so-called *spectral representation* of stationary process. It is given by the Fourier-Stieltjes stochastic integral

$$X(t) = \int_{-\infty}^{\infty} \mathrm{e}^{\mathrm{i}\omega t}\mathrm{d}Z(\omega) \tag{1.36}$$

in which $Z(\omega)$ is a complex-valued stochastic process with independent increments, i.e.,

$$\mathrm{E}[\mathrm{d}Z(\omega_1)\mathrm{d}Z(\omega_2)^{\mathrm{C}}] = 0, \omega_1 \neq \omega_2 \tag{1.37}$$

and

$$\mathrm{E}[|\mathrm{d}Z(\omega)|^2] = \mathrm{d}\Phi(\omega) \tag{1.38}$$

where $\Phi(\omega)$ is some random function that needs not to be continuous. The difference between this representation and that of a conventional Fourier-Stieltjes integral of ordinary calculus lies in the fact that function $Z(\omega)$ is itself a random process, which implies that it will be diferent for all the realizations of the process $X(t)$. Therefore, the differentials and integrals involved in these equations are to be understood in stochastic (mean square) sense as was explained in the preceding paragraph.

According to the above derivations, the auto-correlation function of this process is given by

$$R_X(\tau) = \int_{-\infty}^{\infty} \mathrm{E}[|\mathrm{d}Z(\omega)|^2]\mathrm{e}^{-\mathrm{i}\omega t} = \int_{-\infty}^{\infty} \mathrm{e}^{-\mathrm{i}\omega t}\mathrm{d}\Phi(\omega) \tag{1.39}$$

If function $\Phi(\omega)$ is absolutely continuous its differential can be represented as

$$d\Phi(\omega) = S_X(\omega)d\omega \tag{1.40}$$

and then the auto-correlation function is given by the following Fourier transform:

$$R_X(\tau) = \int_{-\infty}^{\infty} e^{-i\omega t} S_X(\omega)d\omega \tag{1.41}$$

Function $S_X(\omega)$, which can be obtained by inverting the above expression

$$S_X(\omega) = \frac{1}{2\pi}\int_{-\infty}^{\infty} e^{i\omega t} R_X(\tau)d\tau \tag{1.42}$$

is called the *power spectral density function* of the process. These Fourier-type relationships are called the *Wiener-Khintchine formulas.*

The spectral density is a real and nonnegative function that plays a similar role as the Fourier transform does in the analysis of deterministic signals. In fact, it provides a description of the distribution of the (expected) energy associated to the several frequencies which are present in the realizations of the process. The link between both frequency functions is given by the definition of the spectral density used in signal processing

$$S_X(\omega) = \lim_{s\to\infty} \frac{E[|\tilde{X}(\omega)|^2]}{2\pi s} \tag{1.43}$$

Here $\tilde{X}(\omega)$ stands for the Fourier transform of realizations of a stationary process $X(t)$ of duration s. Through a somewhat tedious derivation it can be shown that this equation reduces to the above definition of the spectral density (1.42). In signal processing practice, the density is estimated by the aproximation

$$\hat{S}_X(\omega) \approx \frac{|\tilde{X}(\omega)|^2}{2\pi s} \tag{1.44}$$

which is called *periodogram.* The high variance inherent to this estimation is reduced by means of the so-called *spectral windows* (Priestley 1981). Alternatively, the power spectrum can be estimated by the spectral method based on the principle of maximum entropy, which coincides with that resulting from auto-regressive (AR) modelling (Kapur 1989; Papoulis 1991).

Finally, it must be noted that the use of the *one-sided power spectral density*

$$G_X(\omega) = 2S_X(\omega), \quad \omega > 0 \tag{1.45}$$

is conventional in engineering applications due to the non-negativity of physical frequencies.

1.3.3 White noise

An important stationary stochastic process is *white noise*, $W(t)$, which can be defined as a process having a constant spectral density function over the whole frequency axis, i.e.,

$$S_W(\omega) = \text{const} \tag{1.46}$$

meaning that an equal amount of energy is associated to each frequency (whence the term "white"). The autocorrelation function is obtained by Fourier-transforming the above density,

$$R_W(\tau) = 2\pi S_W \delta(\tau) \tag{1.47}$$

where $\delta(\cdot)$ is the Dirac delta function. The meaning of this equation is that any value of the process is correlated only with itself. If, in addition, the noise is Gaussian, it is completely independent of the next or previous ones. This is, of course, a highly idealized situation which is impossible to find in the physical world. Albeit a purely mathematical idealization, however, the white noise process is very useful in theoretical derivations and practical analysis in the field of random vibration. It can be simulated by means of the following algorithm (Clough and Penzien 1993; Nigam and Narayanan 1994):

1. Generate a set of uniformly distributed random numbers $\{x_1, x_2, \ldots x_n\}$ in the range $[0, 1]$.

2. Make the transformation

$$y_i = \sqrt{-2\ln x_i}\cos 2\pi x_{i+1}$$

$$y_{i+1} = \sqrt{-2\ln x_i}\sin 2\pi x_{i+1} \tag{1.48}$$

3. Multiply all the numbers y_i by the intensity of the process $2\pi S_W$ and assign them to time values equally spaced at intervals h.

It can be shown that the resulting process tends to a a white noise as $h \to 0$. Figure 1.2 shows an approximation to a realization of a white noise process of $S_W = 1$ obtained in this way. The importance of white noise in mechanics lies

in the fact that many random loads (and, in general, natural phenomena) can be modelled either as white noise or as the response of certain filters to white excitation. This issue will be dealt with in the following chapter in the specific case of earthquake excitation.

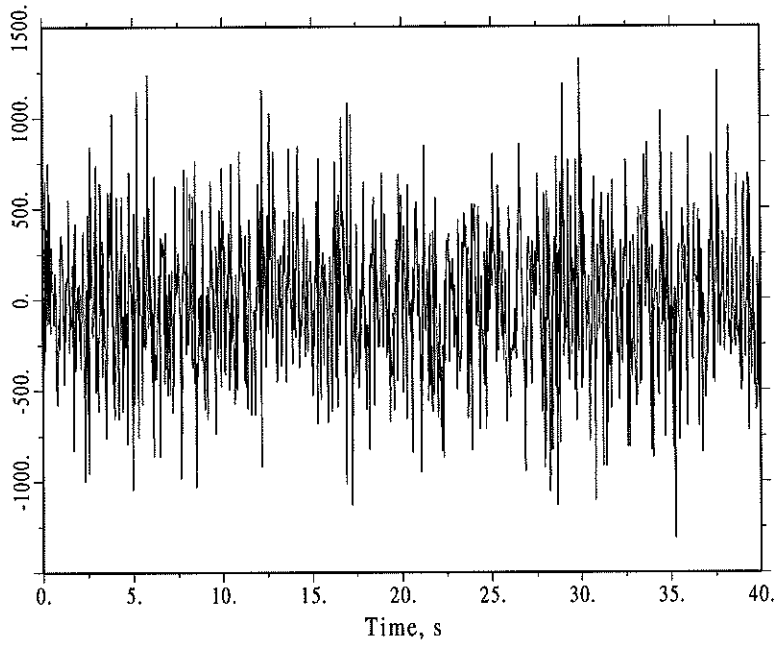

Figure 1.2 A white noise realization

1.3.4 Ergodicity

An important subject for the derivation of statistical parameters of a stationary stochastic process from its physical realizations is that of *ergodicity*, by which it is meant the kind of relationship existing between averages obtained in the sample space and those calculated from a single realization on the time axis. Specifically, if $x(t)$ is a certain realization of the stochastic process $X(t)$, the time average of a deterministic function of this realization, $g[x(t)]$ is given by

$$< g[x(t)] >= \lim_{T\to\infty} \frac{1}{2T} \int_{-T}^{T} g[x(t)]\,\mathrm{d}t \tag{1.49}$$

Accordingly, a stochastic process is said to be *ergodic* with respect to the space of functions $\mathcal{G}$ if, for every $g[x(t)] \in \mathcal{G}$ the time average obtained on $g[\cdot]$ equals the ensemble average with probability one. That is,

$$< g[X(t)] >= \mathrm{E}[g[X(t)]] \tag{1.50}$$

In practice, the interest lies mainly on ergodicity with respect to common averages such as mean, mean square and auto-correlation. The conditions for existence of such types of ergodicity can be read in basic texts on random processes.

1.4 Nonstationary processes

It was said before that a stationary random process admits a spectral representation of the type

$$X(t) = \int_{-\infty}^{\infty} \mathrm{e}^{\mathrm{i}\omega t} \mathrm{d}Z(\omega) \tag{1.51}$$

where $Z(\omega)$ is a complex-valued random process with independent increments. This equation means that any stationary process can be decomposed into a infinite sum of harmonics of random amplitudes, which can be statistically related to their respective frequency through a random function having a spectral nature. This decomposition constitutes, in fact, the essentials of the simulation of random processes, as it will be shown in chapter 2. When dealing with nonstationary processes, however, it is no longer possible to represent them as a sum of sine and cosine functions because these are stationary. Since the spectral representation has both a theoretical and practical appealing in that the spectrum of the process is involved in its definition, some authors have proposed nonstationary models of similar kind. The most spread is the theoretically sound proposal due to Priestley (1981). Given that the Fourier transform of a sine or cosine function is a Dirac pulse located at the respective frequency, while that of a exponentially damped harmonic is a Gaussian function centered around it, Priestley proposed to interpret the later as the Fourier transform of a wave with evolutionary amplitude and, consequently, developped the theory of *oscillatory functions* and *evolutionary spectrum*. The theory generalizes the concept of frequency and allows the preservation of the meaning of spectral density in the case of nonstationary processes. In the present work, however, it is only possible to summarize briefly the notion of evolutionary spectrum. This is given by

$$S_X(\omega, t) = |\xi(\omega, t)|^2 S_Y(\omega) \tag{1.52}$$

where $S_Y(\omega)$ is the power spectral density of an associated process $Y(t)$ and $\xi(\omega, t)$ is a (in general, complex) smooth oscillatory function which controls the evolution of the process in both amplitude and frequency with time. This equation is based on the spectral representation of nonstationary processes proposed by Priestley

$$X(t) = \int_{-\infty}^{\infty} \xi(\omega, t) \mathrm{e}^{\mathrm{i}\omega t} \mathrm{d}Z(\omega) \tag{1.53}$$

which is possible if some conditions imposed on $\xi(\omega, t)$ are satisfied. A widely used simplification of this model is the *uniformly modulated process*, in which the modulating function is real and not dependent on frequency, i.e.,

$$\xi(\omega, t) \equiv \xi(t) \tag{1.54}$$

so that it only controls the amplitude of the process. The evolutionary spectral density simplifies to

$$S_X(\omega, t) = \xi(t)^2 S_Y(\omega) \tag{1.55}$$

Another approach to the spectral description of nonstationary porcesses is due to Bendat and Piersol (1971) who propose to describe the nonstationary process by means of the local auto-correlation function

$$R_X(t, \tau) = \mathrm{E}\Big[X\Big(t - \frac{\tau}{2}\Big) X\Big(t + \frac{\tau}{2}\Big)\Big] \tag{1.56}$$

A time-dependent power spectral density can be derived as the Fourier transform

$$S_X(\omega, t) = \frac{1}{2\pi} \int_{-\infty}^{\infty} \mathrm{e}^{\mathrm{i}\omega t} R_X(t, \tau) \mathrm{d}\tau \tag{1.57}$$

It has been observed, however, that the nonnegativity of the power spectrum can not always be preserved in the above model (Priestley 1981).

1.5 Stochastic differential equations

1.5.1 Markov processes

As it was said at the beginning of the present chapter, a random process is completely described by the joint probability density function of all the states of the process. For a process observed at $N-$ instants such density function

$$f(\boldsymbol{x}_1, t_1; \boldsymbol{x}_2, t_2; \ldots \boldsymbol{x}_N, t_N) \tag{1.58}$$

can be obtained as the derivative of the distribution function (see equation 1.2). For a discrete-valued process this statement requires the so-called conditions of *consistency* and *symmetry* to be satisfied (Soong and Grigoriu 1993). The first implies that marginal distributions can be consistently obtained by integration from those of higher dimension; the second imposes the condition that the distribution function remains invariant under any permutation of indexes $1, \ldots, N$.

In terms of these joint densities it is possible to define conditional probabilities of the kind

$$f(\boldsymbol{x}_n, t_n; \ldots \boldsymbol{x}_N, t_N | \boldsymbol{x}_1, t_1; \ldots \boldsymbol{x}_{n-1}, t_{n-1}) =$$

$$\frac{f(\boldsymbol{x}_1, t_1; \boldsymbol{x}_2, t_2; \ldots; \boldsymbol{x}_N, t_N)}{f(\boldsymbol{x}_1, t_1; \ldots \boldsymbol{x}_{n-1}, t_{n-1})} \tag{1.59}$$

which express the probability of obtaining future states of the process given the knowledge of its past, provided that

$$t_1 \leq t_2 \ldots \leq t_n \ldots \leq t_N$$

As has been said in section 1.1, the general probabilistic decription (Eq. 1.1) can be simplified for *Markovian processes*, i.e. those in which any state n is completely determined (in probabilistic sense) by its most recent predecessor:

$$f(\boldsymbol{x}_n, t_n | \boldsymbol{x}_1, t_1 \ldots \boldsymbol{x}_{n-1}, t_{n-1}) = f(\boldsymbol{x}_n, t_n | \boldsymbol{x}_{n-1}, t_{n-1}) \tag{1.61}$$

The joint density function corresponding to all states of a Markov process can then be expressed in terms of elementary conditional probabilities relating the passage from one state to the next, i. e.

$$f(\boldsymbol{x}_1, t_1; \boldsymbol{x}_2, t_2; \ldots \boldsymbol{x}_N, t_N) = f(\boldsymbol{x}_1, t_1) f(\boldsymbol{x}_2, t_2 | \boldsymbol{x}_1, t_1)$$

$$\ldots f(\boldsymbol{x}_n, t_n | \boldsymbol{x}_{n-1}, t_{n-1}) \tag{1.62}$$

On the basis of these equations it is possible to demonstrate that

$$f(\boldsymbol{x}_3, t_3 | \boldsymbol{x}_1, t_1) = \int_{-\infty}^{\infty} f(\boldsymbol{x}_3, t_3 | \boldsymbol{x}_2, t_2) f(\boldsymbol{x}_2, t_2 | \boldsymbol{x}_1, t_1) \mathrm{d}\boldsymbol{x}_2 \tag{1.63}$$

which is known as the *Smoluchovski - Chapman - Kolmogorov equation.* It simply describes the flow of probability from one state to another through an intermediate state. This explains the denomination of *transition probability densities* given to the density functions involved in the equation. Another consequence of the Markov property is that the probability at any state can be obtained as

$$f(\boldsymbol{x}_2, t_2) = \int_{-\infty}^{\infty} f(\boldsymbol{x}_2, t_2; \boldsymbol{x}_1, t_1) f(\boldsymbol{x}_1, t_1) \mathrm{d}\boldsymbol{x}_1 \tag{1.64}$$

It must be observed that according to their definition Markov processes are only physically realizable in the discrete case. In fact, an entity such as a *continuous Markov process* is a mathematical idealization, because at the infinitesimal scale it is difficult to accept the Markov assumption. However, when turning back to the macroscopic scale it is undoubtful that many physical process can be regarded as Markovian.

1.5.2 Brownian motion and Wiener Process

An important example of a Markov process is the *Brownian motion*, which is the irregular trajectory of small particles in a fluid, investigated by Robert Brown in the ninteenth century. The solution of this problem by Albert Einstein in 1905 gave birth to the field of Statistical Mechanics, and the rigorous probabilistic treatment of the subject by Norbert Wiener in 1923 explains why the Brownian motion of physicists is known as *Wiener process* in mathematics. In essence, the Brownian motion is the combined effect of viscous forces and molecular collisions upon a small particle inside a fluid. From a probabilistic point of view what matters is that if $B(t)$ is the position of the particle in the one dimensional space at time $t \geq 0$, the probability distribution of the the increment $\Delta B(t_1, t_2) = B(t_1) - B(t_2)$ is Gaussian with zero mean and a variance given by

$$\mathrm{E}[\{\Delta B(t_1, t_2)\}^2] = 2D|t_1 - t_2| \tag{1.65}$$

provided that the particle is at rest at $t = 0$ with probability one (Einstein 1956). In this equation D is called *diffussion constant* and is given by

$$D = \frac{kT}{6\pi\eta a} \tag{1.66}$$

where k is Boltzmann's constant, T is the absolute temperature, η the viscosity of the fluid and a the diameter of the particle. An important property of the Wiener process is that the increments of the type $\Delta B(t_{n-1}, t_n)$ are mutually independent and, being Gaussian, they are also uncorrelated, so that the increments of the process are orthogonal (see section 1.3.2). Moreover, it can be shown that the process has continuous samples with probability one. In fact, since the Brownian increment is a Gaussian process,

$$\lim_{h\to 0} P[|B(t+h) - B(t)| < \epsilon] = \lim_{h\to 0}\Big[1 - 2\Phi\Big(-\frac{\epsilon}{\sqrt{2Dh}}\Big)\Big] = 1 \tag{1.67}$$

in which $\Phi(\cdot)$ is the standard Gaussian distribution function. However,

$$\lim_{h\to 0} P\Big[\Big|\frac{|B(t+h) - B(t)|}{h}\Big| > \epsilon\Big] = \lim_{h\to 0}\Big[2\Phi\Big(-\frac{\epsilon h}{\sqrt{2Dh}}\Big)\Big] = 1 \tag{1.68}$$

which means that the Wiener realizations are not differentiable with probability one. This renders mean square integration unapplicable to this process and, as a consequence, a special mathematical formalism is required to its treatment. Figure 1.3 illustrates three approximate realizations of a Wiener process. The great variability of their paths is evident.

Wiener process is very useful in the development of stochastic differential equations due to its formal relationship with Gaussian white noise. In fact, the auto-correlation function of the Wiener process can be shown to be (Ibrahim 1985)

$$R_B(t, s) = 2D\min(t, s) \tag{1.69}$$

while its mean is zero. Its derivative, then, would also have zero mean as is that of its derivative. Further, despite the Wiener process is not m.s. differentiable,

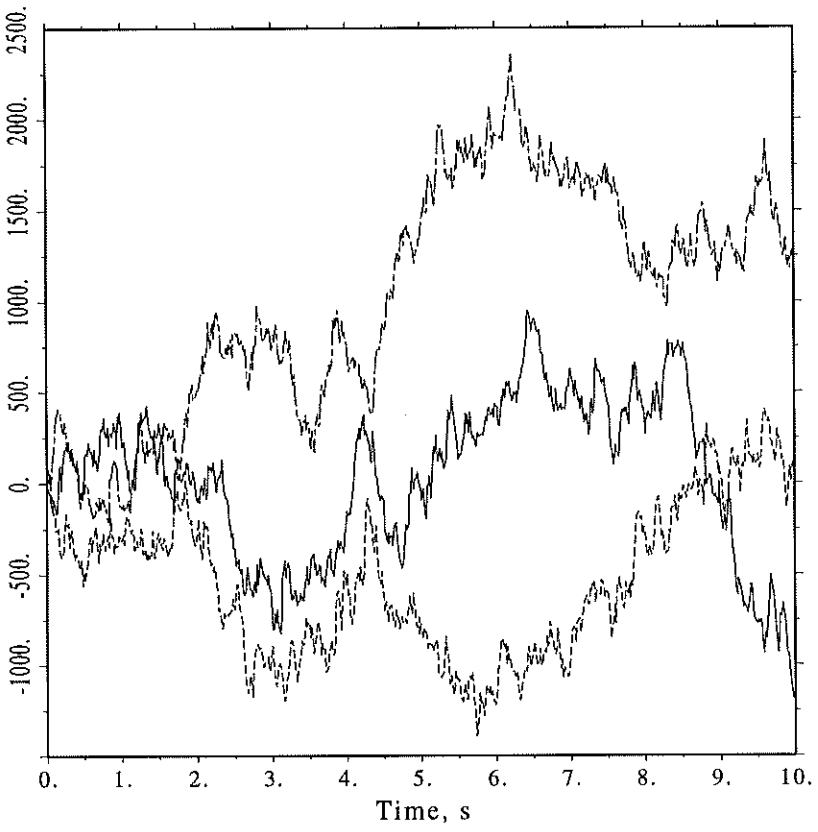

Figure 1.3 Realizations of a Wiener process

the auto-covariance function of the derivative process $\dot{B}(t)$ can be readily obtained. In fact, considering equation (1.14) and taking into account that the process has zero mean, its autocovariance is given by

$$\Sigma_{\dot{B}}(t,s) = \frac{\partial^2 R_X(t,s)}{\partial t \partial s} \tag{1.70}$$

according to (1.29). Thus, from (1.69)

$$\Sigma_{\dot{B}}(t,s) = 2D\frac{\partial^2 \min(t,s)}{\partial t \partial s} = 2D\frac{\partial H(t-s)}{\partial t} = 2D\delta(t-s) \tag{1.71}$$

where $H(\cdot)$ and $\delta(\cdot)$ are respectively the Heaviside unit step and Dirac delta functions. Since the Gaussian property is preserved under the operations of integration and derivation, it is concluded that the derivative of the Wiener process, if it were, would have the probabilistic structure of Gaussian white noise. Then it is possible to write, formally,

$$W(t) \doteq \frac{\mathrm{d}B(t)}{\mathrm{d}t} \tag{1.72}$$

1.5.3 Diffusion processes

A Markov process $X(t)$ with transition density $f(y,t|x,s)$ is called *diffusion process* if the following limits exists for all $\epsilon > 0$:

$$\lim_{t\to s} \frac{1}{t-s} \int_{|y-x|>\epsilon} f(y,t|x,s)\mathrm{d}y = 0 \tag{1.73}$$

$$\lim_{t\to s} \frac{1}{t-s} \int_{|y-x|\leq\epsilon} (y-x) f(y,t|x,s)\mathrm{d}y = \theta(x,s) \tag{1.74}$$

$$\lim_{t\to s} \frac{1}{t-s} \int_{|y-x|\leq\epsilon} (y-x)^2 f(y,t|x,s)\mathrm{d}y = \psi^2(x,s) \tag{1.75}$$

The first limit expresses the prevention of sudden jumps and hence it can also be interpreted in the sense that process $X(t)$ has continuous samples with probability one. On the other hand, functions $\theta(x,s)$ and $\psi^2(x,s)$ correspond to the local mean and spread of the process, as can be seen from the analogy of their definition to that of conventional moments. For this reason they are called, respectively, *drift* and *diffusion* functions. In stochastic differential equations play the role of convection and diffusion terms in the theory of fluid flow. For a short interval $t-s$ the above equations imply that the evolution of the process inside it is characterized by a systematic component

$$\mathrm{E}[X(t) - X(s)|X(s) = x] = \theta(x,s)(t-s) + o(t-s) \tag{1.76}$$

and a scattering component

$$\mathrm{E}[\{X(t) - X(s)\}^2|X(s) = x] = \psi^2(x,s)(t-s) + o(t-s) \tag{1.77}$$

The evolution from s to t can be formulated as

$$X(t) - X(s) \approx \theta(x,s)(t-s) + \psi(x,s)Z \tag{1.78}$$

where function Z must be such that the above expectations are satisfied. In fact, if Z is such that it has zero mean and variance $t-s$, the application of the expectation operator to the first two moments of the above equation will give the same values previously obtained if terms of order $o(t-s)$ are neglected. This means that a suitable function Z is the increment of a Wiener process

$$Z \equiv \Delta B = B(t) - B(s) \tag{1.79}$$

of unit strenght $2D = 1$ (*standard Wiener process*). Squeezing all increments in (1.78) to the infinitesimal level yields the standard formulation of *stochastic differential equations*

$$\mathrm{d}X(t) = \theta(X(t),t)\mathrm{d}t + \psi(X(t),t)\mathrm{d}B(t) \tag{1.80}$$

in which $B(t)$ is the standard Wiener process with stationary increments $\mathrm{d}B(t)$ that obeys a Gaussian distribution with zero mean and variance $\mathrm{d}t$ (see equation 1.65). For vector processes one can form a system of $N-$stochastic differential equations

$$\mathrm{d}\boldsymbol{X}(t) = \boldsymbol{\Theta}(\boldsymbol{X}(t),t)\mathrm{d}t + \boldsymbol{\Psi}(\boldsymbol{X}(t),t)\mathrm{d}\boldsymbol{B}(t) \tag{1.81}$$

where $\boldsymbol{\Theta}$ is a $N-$dimensional vector of drift functions, $\boldsymbol{\Psi}$ is a $N \times R$ diffusion matrix and $\boldsymbol{B}(t)$ is a vector of unit-strength, uncorrelated Wiener processes, that is,

$$\mathrm{E}[\mathrm{d}\boldsymbol{B}(t)] = \boldsymbol{0}$$

$$\mathrm{E}[\mathrm{d}\boldsymbol{B}(t)\mathrm{d}\boldsymbol{B}^{\mathrm{T}}(t)] = \boldsymbol{I}\mathrm{d}t \tag{1.82}$$

where $\boldsymbol{I}$ is the identity matrix. If the strength of the vector Wiener process $\boldsymbol{B}(t)$ is different from the identity matrix, i.e.,

$$\mathrm{E}[\mathrm{d}\boldsymbol{B}(t)\mathrm{d}\boldsymbol{B}^{\mathrm{T}}(t)] = \boldsymbol{\Gamma}(t)\mathrm{d}t \tag{1.83}$$

then matrix $\boldsymbol{\Psi}(\boldsymbol{X}(t),t)$ can be modified to $\boldsymbol{\Psi}(\boldsymbol{X}(t),t)\boldsymbol{\Gamma}^{\frac{1}{2}}(t)$ so as to produce a standard Wiener process as input. Here $\boldsymbol{\Gamma}^{\frac{1}{2}}(t)$ is defined by

$$\boldsymbol{\Gamma}^{\frac{1}{2}}(t)[\boldsymbol{\Gamma}^{\frac{1}{2}}(t)]^{\mathrm{T}} = \boldsymbol{\Gamma}(t) \tag{1.84}$$

1.5.4 Ito and Stratonovitch integrals

The difference between ordinary and stochastic differential equations lies in the presence of the Wiener term, whose particular mathematical features require special analytical and numerical techniques for achieving a solution. In fact, consider the formal solution of equation (1.80)

$$X(t) = X(t_0) + \int_{t_0}^{t} \theta(X(s), s)\mathrm{d}s + \int_{t_0}^{t} \psi(X(s), s)\mathrm{d}B(s) \tag{1.85}$$

The first integral can be treated as a conventional m.s. Riemann integral for every realization of $X(t)$, because the process has continuous samples with probability one, as it has already been shown. On the other hand, the second integral cannot be treated as m.s. Riemann-Stieltjes integral because of the unbounded variation of the Wiener process in any finite interval. It can in fact be demonstrated (Kloeden and Platten 1992) that, for any partition of the Wiener process of N points such that $t_0 \leq t_1 \leq t_2 \ldots \leq t_n = t$,

$$\sum_{k=1}^{n} |B(t_k) - B(t_{k-1})| \to \infty \tag{1.86}$$

It is also not difficult to demonstrate the *Lévy oscillation property*, namely, that

$$\text{m.s.} \lim_{\Delta_n \to 0} \sum_{k=1}^{n} [B(t_k) - B(t_{k-1})]^2 = t - t_0 \tag{1.87}$$

where $\Delta_n = \max(t_k - t_{k-1})$. This equation justifies the conventional use of the equivalence

$$[\mathrm{d}B(t)]^2 \doteq \mathrm{d}t \tag{1.88}$$

Let us define intermediate points τ_k inside each interval $[t_{k-1}, t_k)$ as it was previously done in the derivation of m.s. Riemann-Stieltjes integrals. The *stochastic integral* of a function of time $g(t)$, given by

$$I = \int_{t_0}^{t} g(s)\mathrm{d}B(s) \tag{1.89}$$

is defined as the m.s. limit of the partial sums

$$I_n = \sum g(\tau_k)[B(t_k) - B(t_{k-1})] \tag{1.90}$$

It is not difficult to see that the value of the integral will depend on the choice of points τ_k. If, for instance, $g(t) = B(t)$, the naive application of ordinary calculus leads to

$$\int_{t_0}^{t} B(s)\mathrm{d}B(s) = \frac{1}{2}[B^2(t) - B^2(t_0)] \tag{1.91}$$

On the other hand, the calculation of the m.s. limit of the partial sums gives the result

$$\frac{1}{2}[B^2(t) - B^2(t_0)] - \frac{t - t_0}{2} \tag{1.92}$$

if the intermediate points are selected as

$$\tau_k = t_{k-1} \tag{1.93}$$

and the same result of ordinary calculus (1.91) if

$$\tau_k = \frac{t_k + t_{k-1}}{2} \tag{1.94}$$

The first choice corresponds to the *Ito integral* while the second to the *Stratonovitch integral.* They lead to different mathematical results concerning integration, averages and stochastic differential equations. These developments, as well as those concerning the relationship between their respective Ito and Stratonovitch versions lie beyond the scope of this sketch. In what follows mention will be done only of some standard results of stochastic calculus, which are of importance for future developments.

1.5.5 The Ito formula

Let us assume that in equation (1.89) the second integral is interpreted in the Ito sense. Then, a unique solution of the stochastic differential equation can be obtained if the drift and diffusion functions satisfy the following conditions:

1. *Lipschitz's condition:*

$$|\theta(x, s) - \theta(y, s)| + |\psi(x, s) - \psi(y, s)| \leq k|x - y| \tag{1.95}$$

for any states x, y of the process, $t_0 \leq s \leq t$ and k is a constant.

2. *Growth condition*:

$$|\theta(x,s)|^2 + |\psi(x,s)|^2 \leq k^2|1+|x|^2| \tag{1.96}$$

It can be shown that the solution of the Ito differential equation will be a Markov process (Gardiner 1985). An important tool for its solution is the *Ito formula*. For a differentiable function $h(X(t),t)$ it states that (arguments omitted)

$$\mathrm{d}h = \Big[\frac{\partial h}{\partial t} + \theta\frac{\partial h}{\partial x} + \frac{1}{2}\psi^2\frac{\partial^2 h}{\partial x^2}\Big]\mathrm{d}t + \psi\frac{\partial h}{\partial x}\mathrm{d}B \tag{1.97}$$

which can be derived by expanding function $h(\cdot)$ in Taylor series up to second order terms, substituting the result into equation (1.80) and using the symbolic notation $\mathrm{d}B^2 = \mathrm{d}t$ introduced previously. Notice that the result differs from the one of ordinary calculus in the term $\mathrm{d}B$, which is $\sim \mathrm{d}t^{\frac{1}{2}}$ and hence cannot be neglected. In the general case of a function $h(\boldsymbol{X},t)$ of a $N-$ dimensional vector stochastic process $\boldsymbol{X}(t)$ we have

$$\mathrm{d}h = \Big[\frac{\partial h}{\partial t} + \sum_{i=1}^{N}\Theta_i(\boldsymbol{x},t)\frac{\partial h}{\partial x_i} + \frac{1}{2}\sum_{r=1}^{R}\sum_{i,j=1}^{N}\Psi_{ir}(\boldsymbol{x},t)\Psi_{jr}(\boldsymbol{x},t)\frac{\partial^2 h}{\partial x_i \partial x_j}\Big]\mathrm{d}t + \sum_{r=1}^{R}\sum_{i=1}^{N}\Psi_{ir}(\boldsymbol{x},t)\frac{\partial h}{\partial x_i}\mathrm{d}B_r \tag{1.98}$$

If, for example, function $h(\cdot)$ is sequentially set equal to some given powers of process $X(t)$ (or of the elements of $\boldsymbol{X}(t)$), a system of stochastic differential equations can be obtained after replacement of these functions into the Ito formula. This system can then be converted to a system of ordinary differential equations of moments by applying the expectation operator to the result and taking into account that $\mathrm{E}[\mathrm{d}B_r] = 0$ as said in the foregoing. This will be done in chapters 4 to 7 in the context of the structural dynamics problems which are the subject of the present work.

1.5.6 The Fokker-Planck and Kolmogorov equations

A final development in the theory of stochastic calculus that is necessary to mention in this chapter is that concerning two ordinary partial differential (the *Fokker-Planck* and *Kolmogorov*) equations, which describe the evolution of the conditional probability density $f(\boldsymbol{x},t|\boldsymbol{x}_0,t_0)$ of a Markov process starting from

initial conditions (x_0, t_0). They can be derived from the general Ito stochastic differential equation (Soong 1973). Let us particularize for a one dimensional system and consider an arbitrary function of the response $h(X(t))$. Applying the expectation operator to the corresponding Ito formula and ommitting arguments we have

$$\frac{\mathrm{d}}{\mathrm{d}t}\mathrm{E}[h] = \mathrm{E}\Big[\theta\frac{\partial h}{\partial x} + \frac{1}{2}\psi^2\frac{\partial^2 h}{\partial x^2}\Big] \tag{1.99}$$

in which it has been taken into account that $\mathrm{d}B$ has zero mean and that $h(\cdot)$ is not an explicit function of time. This equation is equivalent to

$$\frac{\mathrm{d}}{\mathrm{d}t}\int_{-\infty}^{\infty} h(x)f(x,t|x_0,t_0)\mathrm{d}x = \int_{-\infty}^{\infty}\Big[\theta\frac{\partial h}{\partial x} + \frac{1}{2}\psi^2\frac{\partial^2 h}{\partial x^2}\Big]f(x,t|x_0,t_0)\mathrm{d}x \tag{1.100}$$

where $f(x,t|x_0,t_0)$ is the conditional density of the state $X(t)$ given that $X(t_0) = x_0$. Integrating by parts and considering the boundary conditions

$$f(x,t|x_0,t_0) \to 0$$

$$\frac{\partial f(x,t|x_0,t_0)}{\partial x} \to 0 \tag{1.101}$$

as $x \to \pm\infty$ we obtain

$$\int_{-\infty}^{\infty} h(x)\frac{\partial f}{\partial x}\mathrm{d}x = \int_{-\infty}^{\infty}\Big[-\frac{\partial}{\partial x}[\theta(x,t)f] + \frac{1}{2}\frac{\partial^2 h}{\partial x^2}[\psi^2(x,t)f]\Big]\times h(x)\mathrm{d}x \tag{1.102}$$

Since $h(\cdot)$ is arbitrary, the final result is

$$\frac{\partial f}{\partial x} = -\frac{\partial}{\partial x}[\theta(x,t)f] + \frac{1}{2}\frac{\partial^2 h}{\partial x^2}[\psi^2(x,t)f] \tag{1.103}$$

which is called the *Fokker-Planck* equation. It expresses the variation of the conditional probability density $f(\cdot)$ in terms of the current state and time (see figure 1.4). In the general multidimensional case it has the form

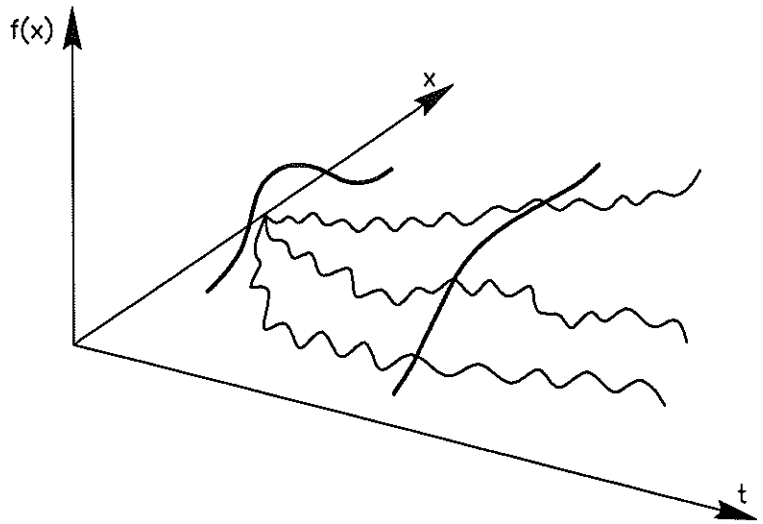

Figure 1.4 Evolution of the probability density function

$$\frac{\partial f}{\partial t} = -\sum_{i=1}^{N} \frac{\partial[\Theta_i(\boldsymbol{x},t)f]}{\partial x_i} +$$

$$\frac{1}{2}\sum_{r=1}^{R}\sum_{i,j=1}^{N} \frac{\partial^2[\Psi_{ir}(\boldsymbol{x},t)\Psi_{jr}(\boldsymbol{x},t)f]}{\partial x_i \partial x_j} \tag{1.104}$$

This equation satisfies the initial condition

$$f(\boldsymbol{x},t_0|\boldsymbol{x}_0,t_0) = \delta(\boldsymbol{x}-\boldsymbol{x}_0) \tag{1.105}$$

which expresses the certainty about the initial state of the system $\boldsymbol{x} = \boldsymbol{x}_0$ at $t = t_0$. In the *Kolmogorov equation*, which can be derived similarly, the derivatives are referred to the initial conditions, i.e.

$$\frac{\partial f}{\partial t_0} = -\sum_{i=1}^{N} \Theta_i(\boldsymbol{x}_o,t_o)\frac{\partial h}{\partial x_{oi}} -$$

$$\frac{1}{2}\sum_{r=1}^{R}\sum_{i,j=1}^{N} \Psi_{ir}(\boldsymbol{x}_o,t_o)\Psi_{jr}(\boldsymbol{x}_o,t_o)\frac{\partial^2 f(\boldsymbol{x},t)}{\partial x_{oi}\partial x_{oj}} \tag{1.106}$$

which explains its alternative name of *backward equation* in contrast to that of *forward equation* associated to the previous one. Note that while the repeated application of the Ito formula leads to a system of differential equations of moments, these equations lead directly to the joint probability density function at any time instant. Its solution, however, is only possible in some restricted, low dimensional cases (Risken 1989; Soize 1993).

Chapter 2

Stochastic models of the seismic excitation

2.1 Introduction

Earthquakes are random in double sense. In fact, not only their ocurrence is stochastic in time but also the trajectory of the spatial ground motion itself exhibits an erratic pattern. This explains why, besides other structural actions, such as wind forces and ocean waves, they have been examined from the stochastic point of view in structural engineering along the last decades.

This chapter deals with the modelling of the seismic action in stochastic terms. Three aspects of the subject will be covered, namely, the stationary and nonstationary models as such, the estimation of their parameters from real records and the digital simulation of earthquake accelerograms for structural dynamics analyses. The later constitute a prerequisite for Monte Carlo simulation, which will be intensively used in the following chapters as a reference for judging the accuracy of several analytical methods which will be discussed.

2.2 Stationary models

The first proposals of stochastic models of the seismic action considered that for structural analysis it would be sufficient to analyse the effect of the most important part of a record corresponding to the shear waves, which normally are larger in amplitude than the compressive and surface ones. Accordingly this portion was described as a stationary process (Newmark and Rosenblueth 1971). This consideration was largely based on records such as the Imperial Valley (El Centro, 1940) (figure 2.1) in which it can be observed an initial ascending part, a subsequent short interval of high amplitude waves and finally a large zone of waves of decreasing amplitude. The periodogram of this signal is shown in figure 2.2. It can seen that in its most important sector there is

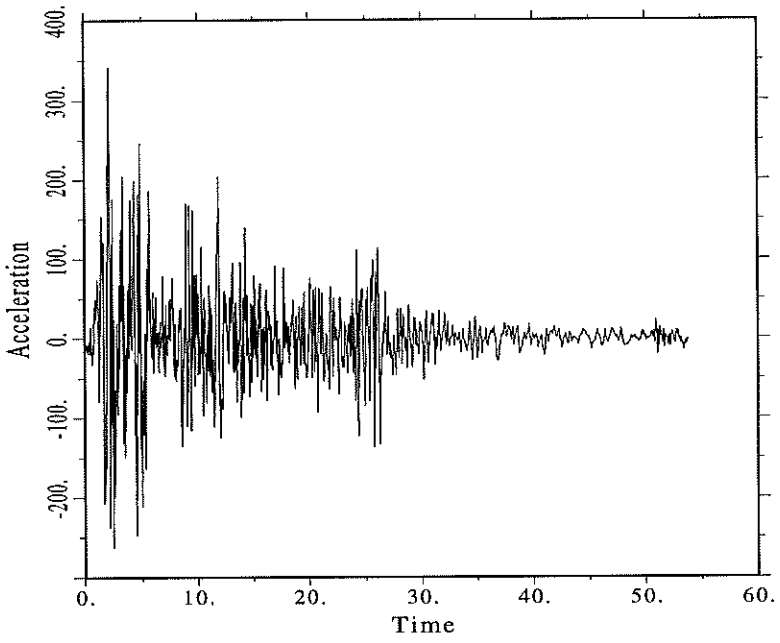

Figure 2.1 Record of El Centro earthquake (units: s, cm/s^2)

an oscillation about 100cm^2/s^3, which suggests that a roughly adequate model of the earthquake is a band limited Gaussian white noise (Bycroft 1960). In subsequent years more sophisticated stationary models of the strong motion phase were proposed. Among them attention will be given mainly in the present work to filter models due to the fact that they can be easily integrated into the equations of structural dynamics - a desirable feature that is absent in other spectral models, which are mainly oriented to purely seismological applications. The filter models will be described in more detail in what follows.

2.2.1 The Kanai-Tajimi model

The Kanai-Tajimi model of seismic horizontal acceleration, M^{KT}, is defined as

$$M^{\mathrm{KT}} = 2\,\nu_{\mathrm{g}}\omega_{\mathrm{g}}\dot{U}_{\mathrm{g}} + \omega_{\mathrm{g}}^{2}U_{\mathrm{g}} \tag{2.1}$$

where U_{g} is the response of a second order filter to a white noise $W(t)$:

$$\ddot{U}_{\mathrm{g}} + 2\,\nu_{\mathrm{g}}\omega_{\mathrm{g}}\dot{U}_{\mathrm{g}} + \omega_{\mathrm{g}}^{2}U_{\mathrm{g}} = -W(t) \tag{2.2}$$

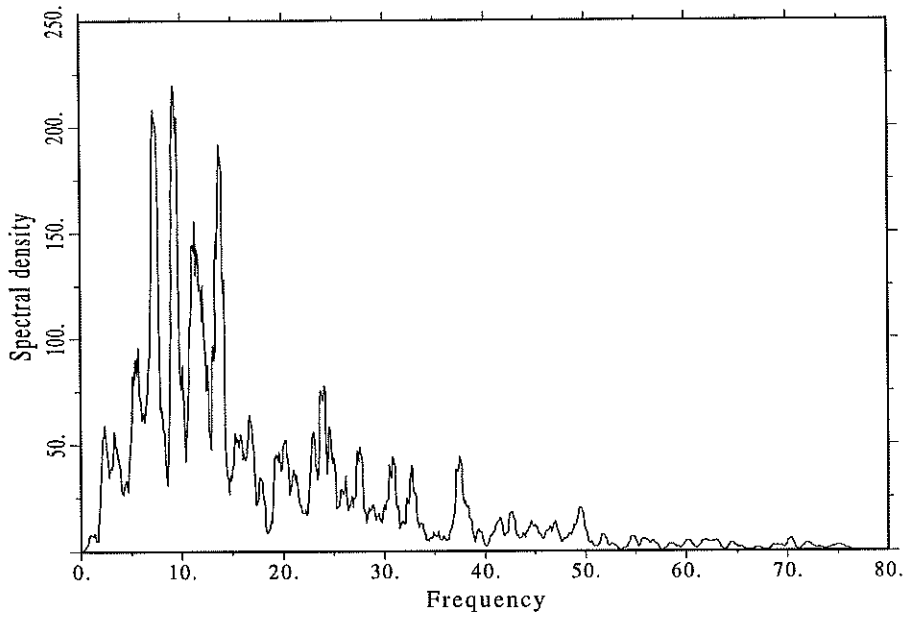

Figure 2.2 Power spectrum of El Centro earthquake (units: rad/s, cm^2/s^3)

The model is determined by the power spectral density of the noise G_W as well as by parameters ν_g and ω_g. Even though they are commonly associated to local soil conditions, they are also influenced by other factors, such as earthquake magnitude, hypocentral distance and others. (Lai 1982; Kameda and Nojima 1988; Sawada *et al.* 1992).

Applying the Laplace transform to both sides of the above equation it can be shown that the transfer function of the compound movement M^{KT} is

$$H(i\omega) = \frac{\omega_g^2 + i2\nu_g\omega_g\omega}{\omega_g^2 - \omega^2 + i2\nu_g\omega_g\omega} \tag{2.3}$$

and then its power spectral density is given by

$$G_M(\omega)^{KT} = |H(i\omega)|^2 G_W = \frac{\omega_g^4 + 4\nu_g^2\omega_g^2\omega^2}{(\omega_g^2 - \omega^2)^2 + 4\nu_g^2\omega_g^2\omega^2} G_W \tag{2.4}$$

The variance of the process, given by the integral of the power spectral density over the whole frequency axis, is

$$\sigma_M^2 = \pi \frac{\omega_g (1 + 4\nu_g^2)}{4\nu_g} G_W \tag{2.5}$$

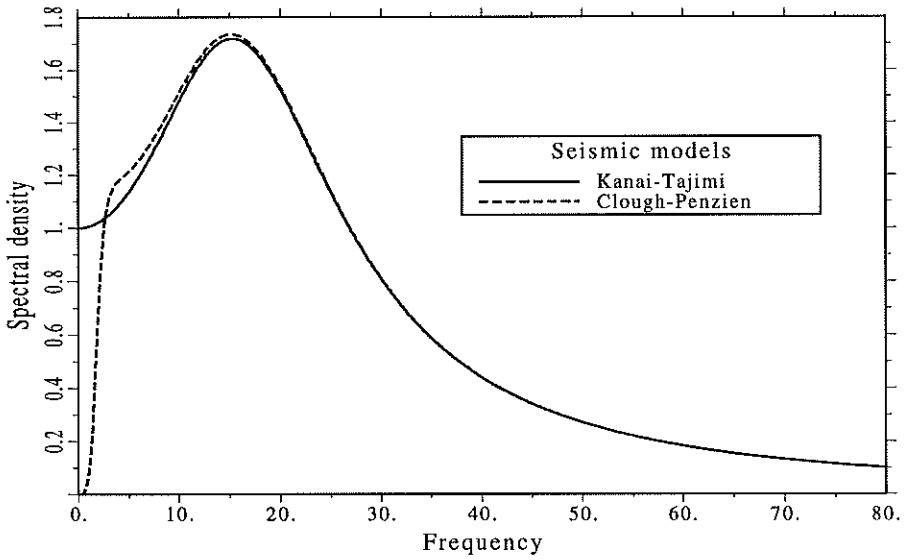

Figure 2.3 Filter models of seismic power spectrum (units: rad/s, cm^2/s^3)

In figure 2.3 the power spectrum of a Kanai-Tajimi type is plotted together with that corresponding to the Clough-Penzien model which is introduced in the following paragraph. The filter parameters are $\omega_g = 19$ rad/s and $\nu_g = 0.65$. They give the spectrum a similar overall shape to that of the power spectrum of the El Centro record (figure 2.2).

2.2.2 The Clough-Penzien model

The main drawback of the Kanai - Tajimi model lies in its assigning a non zero spectral value to the zero frequency, which is not in agreement with the observed null energy at that point (see figure 2.2). While this feature does not represent a serious error in the analysis of systems of low to high frequency, it can lead to large errors for the analysis of nonlinear structures. In such cases the use of the Clough-Penzien filter added to the above model is more adequate. This filter drastically reduces the ordinates of the K-T spectrum at very low

frequencies, while preserving the values at larger ones. (Clough and Penzien 1993). The dynamics of the additional filter is governed by the conventional linear equation

$$\ddot{U}_f + 2\nu_f\omega_f\dot{U}_f + \omega_f^2 U_f = -M^{KT} \tag{2.6}$$

where the parameters ν_f and ω_f must be selected for the purpose at hand. The model is defined as the acceleration response of the filter, i.e.,

$$M^{CP} = \ddot{U}_f = -2\nu_f\omega_f\dot{U}_f - \omega_f^2 U_f - 2\nu_g\omega_g\dot{U}_g - \omega_g^2 U_g \tag{2.7}$$

and hence its power spectral density is given by

$$G_M(\omega)^{CP} = \frac{\omega^4}{(\omega_f^2 - \omega^2)^2 + 4\nu_f^2\omega_f^2\omega^2} \times \frac{\omega_g^4 + 4\nu_g^2\omega_g^2\omega^2}{(\omega_g^2 - \omega^2)^2 + 4\nu_g^2\omega_g^2\omega^2} G_W \tag{2.8}$$

Finally, the variance of the process is

$$\sigma_M^2 = \pi\frac{A(\omega)}{2B(\omega)} G_W \tag{2.9}$$

where

$$A(\omega) = \omega_g^4(\nu_g\omega_f + \nu_f\omega_g) + 4\nu_g^2\omega_g^2[\nu_g\omega_f^3 + \nu_f\omega_g^3 + 4\nu_g\nu_f\omega_g\omega_f(\nu_g\omega_f + \nu_f\omega_g)]$$

and

$$B(\omega) = 2\nu_g\nu_f[(\omega_g^2 - \omega_f^2)^2 + 4\omega_g^2\omega_f^2(\nu_g^2 + \nu_f^2) + 4\nu_g\nu_f\omega_g\omega_f(\omega_g^2 + \omega_f^2)] \tag{2.10}$$

In figure 2.3 the Clough-Penzien model has been plotted using $\omega_f = 2\,\text{rad/s}$ and $\nu_g = 0.6$. The whole set of four parameters have been derived by Yeh (1989) from the El Centro record (figure 2.1).

2.2.3 Seismological models

The research performed by Boore and coworkers along the last two decades constitute an important step for providing engineering models of the seismic motion well rooted in the modern theory of seismology (Boore and Joyner 1982; Boore 1986; Boore and Atkinson 1987). In fact, the aim of these proposals is to estimate the Fourier amplitude spectrum, $\tilde{M}(\omega)$, on the basis of physical parameters of the earthquake corresponding to the energy radiation at the source and atenuation with distance. The power spectral density can then be estimated as a periodogram using the strong motion phase duration (see equation 1.44).

Tipically, a seismological model of the Fourier transform $\tilde{M}(\omega)$ is made up with the hypothesized source, attenuation and amplification spectra in addition to a scaling constant related to source parameters. Among the several formulations of them existing in the literature we have chosen a version addressed to structural dynamics applications (Faravelli 1988a):

$$\tilde{M}(\omega) = C\tilde{M}_{\mathrm{s}}(\omega)\tilde{M}_{\mathrm{c}}(\omega)\tilde{M}_{\mathrm{m}}(\omega)\tilde{M}_{\mathrm{a}}(\omega) \tag{2.11}$$

Here C is a scaling factor given by

$$C = \frac{R_{\theta\phi}FV}{4\pi\rho\beta^3 R} \tag{2.12}$$

where $R_{\theta\phi}$ is the *radiation pattern*, which expresses the spatial directivity of the energy radiation at the source; F is the amplification due to free surface (tipically $F = 2$); V is a factor that accounts for the partition of energy into two orthogonal directions for calculation purposes (so that it is usually taken as $1/\sqrt{2}$); ρ is the density of the medium, β the shear wave velocity and R the hypocentral distance. The several spectra contained in equation (2.11) correspond to the following factors:

1. The energy at the source:

$$\tilde{M}_{\mathrm{s}}(\omega) = \frac{M_0\omega_{\mathrm{s}}^2}{1 + \left(\frac{\omega_{\mathrm{s}}}{\omega}\right)^2} \tag{2.13}$$

in which M_0 is the seismic moment and ω_{s} the angular corner frequency. A correcting factor suggested to apply to this spectrum to European earthquakes is (Faravelli 1988b)

$$\tilde{M}_{\mathrm{c}}(\omega) = \frac{\alpha}{\sqrt{1 + \left(\frac{\omega}{\omega_{\mathrm{c}}}\right)^2}} \tag{2.14}$$

where α and f_{c} are empirical parameters.

2. The amplification of the waves when entering into the soil domain:

$$\tilde{M}_{\mathrm{m}}(\omega) = \frac{2}{1 + \left(\frac{\omega_{\mathrm{m}}}{\omega}\right)^2} \tag{2.15}$$

in which ω_{m} is a reference frequency.

3. The attenuation with distance:

$$\tilde{M}_{\mathrm{a}}(\omega) = C_{\mathrm{a}} \sqrt{1 + \left(\frac{\omega}{\omega_{\mathrm{a}}}\right)^2} \tag{2.16}$$

where ω_{a} is a cut-off frequency and C_{a} an attenuation factor which is an exponential function of frequency and hypocentral distance.

2.3 Nonstationary models

It has for long being recognized that earthquake records are highly nonstationary. This is due to the differences in frequency and arrival time of their component waves. The seismic action can be stochastically modelled as a nonstationary random process in two forms:

1. As a uniformly modulated process, i.e. a stationary process transformed to a one which is nonstationary only in amplitude. The transfomation is performed through a deterministic function $\xi(t)$, whose parameters are estimated from actual records (see equation 1.55).

2. As a process with a evolutionary power spectral density, that is, as one which not only varies in amplitude but also in the frequency content along the time (see equation 1.52). The estimation of the governing parameters from extant records is, of course, more involved than in the previous case. Let us consider these models in more detail.

2.3.1 Models with uniform modulation

Let $M(t)$ be a Gaussian stationary random process with one-sided power spectral density $G_M(\omega)$. Due to the linearity of the functions that govern the dynamics of the above models it can be identified with their respective signals M^{KT} or M^{CP} when the filters are excited by a Gaussian white noise. A realization $a(t)$ of the process $A(t)$ corresponding to the ground motion acceleration with uniform modulation would then be given by

$$a(t) = \xi(t)m(t) \tag{2.17}$$

where $a(t)$ is the simulated acceleration of the ground and $\xi(t)$ is a deterministic function which defines the variation of the amplitude in time. According to the theory of nonstationary processes sketched in the first chapter, the power spectral density of the compound process $A(t)$ will be

$$G_A(\omega, t) = \xi(t)^2 G_M(\omega) \tag{2.18}$$

The following are the most commonly used modulating functions among the several that can be found in the literature:

1. Shinozuka and Sato (1967)

The mathematical expression of this funtion is

$$\xi(t) = \frac{1}{c}(\mathrm{e}^{-at} - \mathrm{e}^{-bt}) \tag{2.19}$$

where a, b and c are parameters. The value of c can be chosen to give the maximum of the function a unit value, so that the parameters will be independent of the amplitude of the desired record or stochastic model. This yields

$$c = \max(\mathrm{e}^{-at} - \mathrm{e}^{-bt}) = \left[\left(\frac{a}{b}\right)^{\frac{a}{b-a}} - \left(\frac{a}{b}\right)^{\frac{b}{b-a}}\right] \tag{2.20}$$

Alternatively it can be set according to energy criteria as will be explained later. Figure 2.4 shows two modulating functions of this type which correspond qualitatively to earthquakes with short and long effective durations.

2. Amin and Ang (1966)

The distinguishing feature of this function is that it is defined by three branches that mimic the respective phases of the ground motion, i.e. those

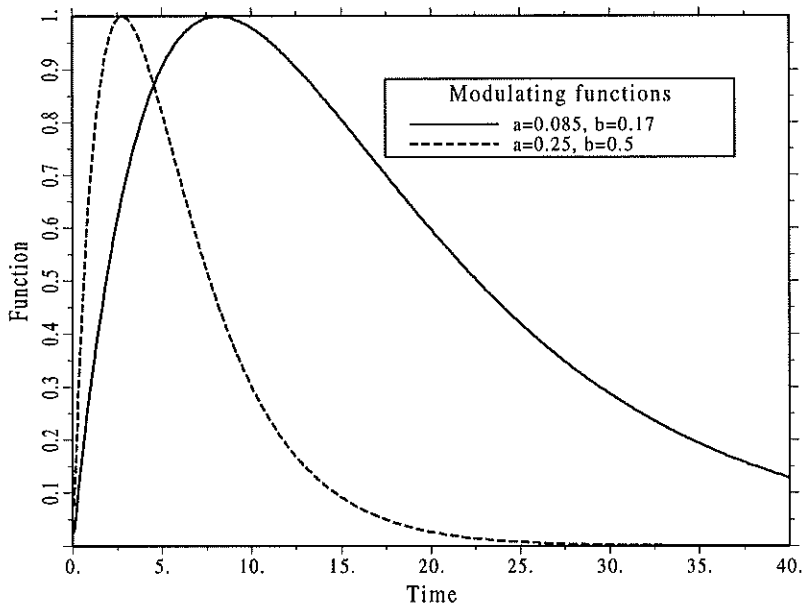

Figure 2.4 Shinozuka-Sato modulating functions

corresponding to the raising, strong motion and withering phases. Its expression is

$$\xi(t) = \begin{cases} \frac{t}{t_1}, & t \leq t_1 \\ 1, & t_1 \leq t \leq t_2 \\ \mathrm{e}^{-c(t-t_2)}, & t_2 \leq t \end{cases} \tag{2.21}$$

where c is a parameter, t_1 corresponds approximately to the arriving time of shear waves and the diference $t_2 - t_1$ can be associated to the duration of the strong motion phase.

3. Yeh and Wen (1990)

   This function is given by

$$\xi^2(t) = \frac{at^{-b}\exp(-ct)}{d + t^e} \tag{2.22}$$

where a, b, c, d and e are parameters.

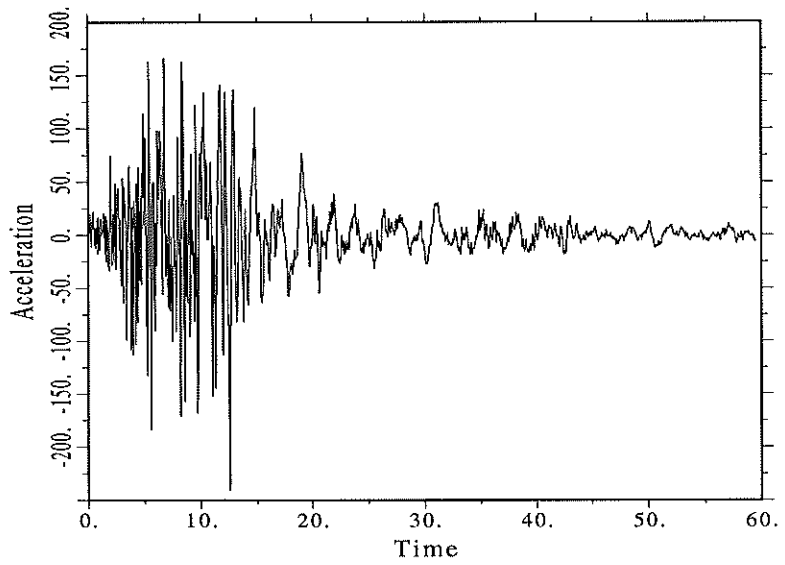

Figure 2.5 Record of Orion Boulevard earthquake (units: s, cm/s^2)

2.3.2 Evolutive models

On the basis of the purely theoretical physics of earthquakes it can be expected that a record obtained at free surface will exhibit a evolutionary nature. By this expression it is meant that both the amplitude as well as the dominant frequencies vary with time. This behaviour is due to the different velocity and energy of the several waves that compose the motion and their multiple reflections, refractions and difractions. The evolution of the frequencies appears clearly in some records such as the San Fernando (Orion Boulevard, 1971) accelerogram depicted in figure 2.5, in which one can distinguish the zones corresponding respectively to high frequency, low amplitude P waves, lower frequency and very high amplitude S waves, and very low frequency and intermediate amplitude surface waves. Cases with such a clear evolution as the one shown in the figure are somewhat rare. In the vast majority of records the evolutive appearance does not take place due to the effects of distance (in near source earthquakes the frequencies are still chaotically merged while at long distance high frequency waves damp out) or it is more or less blurred by the multiple distortions the waves endure along their travel. In the Tokachi-oki (1968) record depicted in figure 2.6, for instance, the low frequency waves appear in the last portion of the record merged with high frequency ones, while waves of the lowest frequency dominate the central portion.

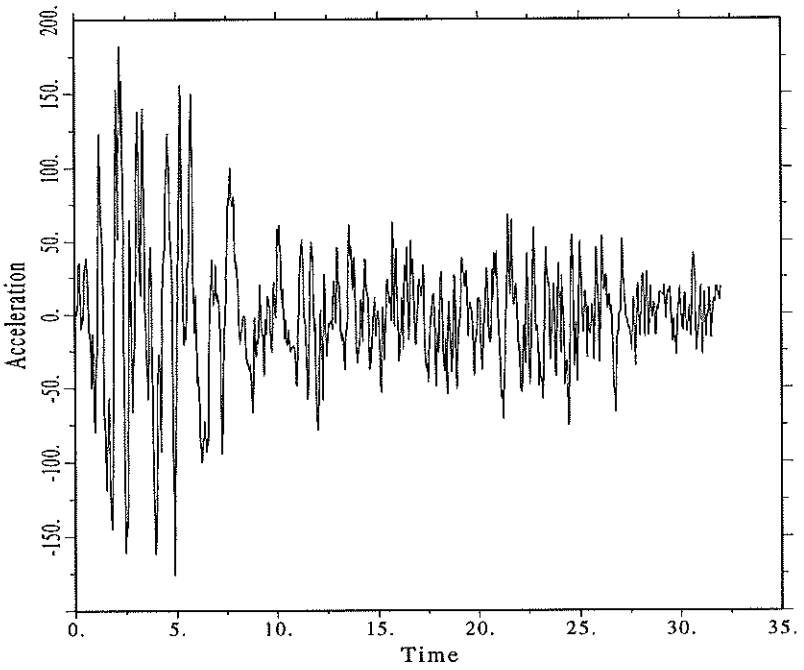

Figure 2.6 Record of Tokachi-oki earthquake (units: s, cm/s^2)

Several models have been proposed for the spectral analysis of the earthquake action with inclusion of the evolutive behaviour. Some of them are based of the theory of evolutionary spectra developped by Priestley (Priestley 1981), a brief account of which has been given in the first chapter. The above discussed process with uniform modulation is, in fact, a particular case of such a model, in which the modulating function $\xi(\omega, t)$ is only a function of time, $\xi(t)$. The function $\xi(\omega, t)$ has been estimated to the Mexico 1985 earthquake record by (Grigoriu *et al.*, 1988) be dividing the earthquake record into the three typical zones already mentioned. Other proposal is that by Spanos *et al.* (1992) who propose the use of the energy of single linear systems as a measure of the evolutive density of the input. Beck and Papadimitrou (1993) developped a Bayesian approach for the fitting of an evolutive Kanai-Tajimi model to earthquake records; similar approaches have been proposed by Fan and Ahmadi (1990), Kameda and Nojima (1988) and others. Finally, interesting evolutive seismological models have been presented by Faravelli (1988b) and Carli (1992, 1995).

In the present research, a model called *instantaneous spectrum* (Yeh and Wen 1990) has been selected for analysing the behaviour of base isolated build-

ings in chapter 8. It is based in the concept of frequency modulation which is common in communication engineering and the Bendat and Piersol nonstationary representation (equations 1.56 and 1.57). Since the modulation can be applied to any stationary model it is especially suitable for structural dynamics purposes when used in connection with seismic filters. For that reason it has been preferred over other proposals for the analyses reported in chapter 8.

As has been pointed out in chapter 1, any stationary process has a spectral respresentation of the form

$$X(\kappa) = \int_{-\infty}^{\infty} \exp(\mathrm{i}\omega\kappa)\mathrm{d}Z(\omega) \tag{2.23}$$

in which $Z(\omega)$ is a zero-mean, complex-valued stochastic process with orthogonal increments, i.e.

$$\mathrm{E}[\mathrm{d}Z(\omega_1)\mathrm{d}Z(\omega_2)] = 0 \tag{2.24}$$

for $\omega_1 \neq \omega_2$, and

$$\mathrm{E}[\,|\mathrm{d}Z(\omega)|^2] = S_X(\omega)\mathrm{d}\omega \tag{2.25}$$

where $S_X(\omega)$ is the power spectral density of $X(\kappa)$. Now let the argument of the process $X(\kappa)$ be a continuous, strictly increasing function of time. A new process can be created in the form

$$Y(t) = X(\kappa(t)) \tag{2.26}$$

for which an instantaneous autocorrelation function can be expressed as (see equation 1.56)

$$R_Y(t,\tau) = \mathrm{E}[X(t+\frac{\tau}{2})X(t-\frac{\tau}{2})] =$$

$$\int_{-\infty}^{\infty}\int_{-\infty}^{\infty} \exp\Big(\mathrm{i}\omega_1\kappa(t+\frac{\tau}{2}) - \mathrm{i}\omega_2\kappa(t-\frac{\tau}{2})\Big)\mathrm{E}[\mathrm{d}Z(\omega_1)\mathrm{d}Z(\omega_2)] \tag{2.27}$$

which, taking into account the properties of the process $Z(\omega)$, reduces to

$$R_Y(t,\tau) = \int_{-\infty}^{\infty} \exp(\mathrm{i}\,\omega\,\tau\dot{\kappa}(t))S_X(\omega)\mathrm{d}\omega \tag{2.28}$$

for infinitesimal τ. Making the change of variable $\bar{\omega} = \dot{\kappa}(t)\omega$ the following equation is finally obtained:

$$R_Y(t,\tau) = \int_{-\infty}^{\infty} \exp(\mathrm{i}\,\bar{\omega}\tau)\frac{1}{\dot{\kappa}(t)} S_X(\frac{\bar{\omega}}{\dot{\kappa}(t)})\mathrm{d}\bar{\omega} \tag{2.29}$$

This constitutes the Wiener-Khintchine relationship of process $Y(t)$. The condition imposed on the function $\kappa(t)$ (namely, of being a strictly increasing function) stems from the need of having a positive spectral density, which in turn requires a positive derivative $\dot{\kappa}(t)$ in the above equation. With this condition the main criticisim raised against the Bendat and Piersol model mentioned at section 1.4 is overcome. A function that satisfies this requirement and that is closely related to the frequency evolution of the earthquake record is the total number of zero crossings of the signal up to the current time. Hence, the expression proposed in (Yeh and Wen 1990) for the frequency moldulating function is

$$\kappa(t) = \frac{n(t)}{\dot{n}(t_s)} \tag{2.30}$$

where $n(t)$ is a polynomial function of time fitted to the actual function of accumulated zero crossings of the record and t_s is the time where the strong motion starts. The one-sided, evolutionary spectral density of the modulated process $Y(t) = X(\kappa(t))$ is then

$$G_Y(\omega,t)^{\mathrm{YW}} = \frac{1}{\dot{\kappa}(t)} G_X(\frac{\omega}{\dot{\kappa}(t)}) \tag{2.31}$$

The application of an amplitude modulation function $\xi(t)$ will then lead to a complete nonstationarity of process $A(t)$, which is thus given by

$$A(t) = \xi(t)Y(t) = \xi(t)X(\kappa(t)) \tag{2.32}$$

If the parameters of $\xi(t)$ are adjusted in such a way that the variance of the stationary process $X(\kappa)$ be unity, the energy of the composed process $A(t)$ will be controlled exclusively by the amplitude modulating function. This is due to the fact that the variance of $Y(t)$ given by

$$\int_{-\infty}^{\infty} G_Y(\omega,t)^{\mathrm{YW}}\mathrm{d}\omega = \int_{-\infty}^{\infty} \frac{1}{\dot{\kappa}(t)} G_X(\frac{\omega}{\dot{\kappa}(t)})\mathrm{d}\omega \tag{2.33}$$

will not vary with time, as can be demonstrated by making the change of variable $\theta = \omega/\dot{\kappa}(t)$ in the preceding equation. The expresion of the evolutionary spectral density of the resulting nonstationary process $A(t)$ is then

$$G_A(\omega,t)^{\mathrm{YW}} = \xi(t)^2 \frac{1}{\dot{\kappa}(t)} G_X\left(\frac{\omega}{\dot{\kappa}(t)}\right) \tag{2.34}$$

Perhaps the main advantage of this model for structural dynamics purposes is its versatility for modelling the seismic action by filters. In fact, let us consider the following equation describing the motion of a linear filter excited by a ground acceleration $y(t)$ on a fictitious time axis κ:

$$x''(\kappa) + 2\,\nu\omega x'(\kappa) + \omega^2 x(\kappa) = -y(\kappa) \tag{2.35}$$

where the commas stand for derivatives with respect to the dummy time variable κ. Making the later a function of real time $\kappa = \kappa(t)$ and applying the chain rule yields

$$\dot{x} = \frac{\mathrm{d}x}{\mathrm{d}t} = \frac{\mathrm{d}x}{\mathrm{d}\kappa}\frac{\mathrm{d}\kappa}{\mathrm{d}t} = x'\dot{\kappa} \tag{2.36}$$

which implies that

$$x' = \frac{\dot{x}}{\dot{\kappa}} \tag{2.37}$$

Then,

$$\ddot{x} = \frac{\mathrm{d}\dot{x}}{\mathrm{d}t} = \frac{\mathrm{d}x'}{\mathrm{d}\kappa}\frac{\mathrm{d}\kappa}{\mathrm{d}t}\dot{\kappa} + \frac{\mathrm{d}^2\kappa}{\mathrm{d}t^2}x' \tag{2.38}$$

which is equivalent to

$$\ddot{x} = x''\dot{\kappa}^2 + \ddot{\kappa}x' \tag{2.39}$$

Hence

$$x'' = (\ddot{x} - \frac{\ddot{\kappa}}{\dot{\kappa}}\dot{x})\frac{1}{\dot{\kappa}^2} \tag{2.40}$$

Replacing these expressions into equation (2.35) the final form of the dynamical equation of the filter in terms of $\kappa(t)$ is

$$\ddot{x} + (2\,\nu\omega\dot{\kappa} - \frac{\ddot{\kappa}}{\dot{\kappa}})\dot{x} + \omega^2\dot{\kappa}^2 x = -\dot{\kappa}^2 y(\kappa(t)) \tag{2.41}$$

On these basis it is possible to introduce frequency modulation into the conventional Kanai-Tajimi or Clough-Penzien filters. In the first case one has

$$\ddot{U}_g + (2\,\nu_g\omega_g\dot{\kappa} - \frac{\ddot{\kappa}}{\dot{\kappa}})\dot{U}_g + \omega_g^{\,2}\dot{\kappa}^{\,2}U_g = -\dot{\kappa}^{\,2}\xi(t)W(\kappa(t)) \tag{2.42}$$

where the amplitude function $\xi(t)$ has been applied to the noise $W(\kappa(t))$. In the second case one has, in addition,

$$\ddot{U}_f + (2\,\nu_f\omega_f\dot{\kappa} - \frac{\ddot{\kappa}}{\dot{\kappa}})\dot{U}_f + \omega_f^{\,2}\dot{\kappa}^{\,2}U_f = -2\,\nu_g\omega_g\dot{\kappa}\dot{U}_g - \omega_g^{\,2}\dot{\kappa}^{\,2}U_g \tag{2.43}$$

According to equations (1.55), (2.34) and (2.41), the underlying modulated white noise has an evolutionary spectral density given by

$$G_W(\omega,t)^{\mathrm{YW}} = \frac{1}{\dot{\kappa}(t)}\pi\xi^{\,2}(t)\dot{\kappa}^{\,4}(t)G_W(\frac{\omega}{\dot{\kappa}(t)}) = \pi\xi^{\,2}(t)\dot{\kappa}^{\,3}(t)G_W \tag{2.44}$$

where G_W is the one-sided density of the unmodulated white noise. On the other hand, the expression of the ground acceleration in the Kanai-Tajimi model (equation 2.1) becomes

$$M^{\mathrm{KT}} = \frac{1}{\dot{\kappa}^{\,2}}(2\,\nu_g\omega_g\dot{\kappa}\dot{U}_g + \omega_g^{\,2}\kappa^{\,2}U_g) = \frac{2\,\nu_g\omega_g}{\dot{\kappa}}\dot{U}_g + \omega_g^{\,2}U_g \tag{2.45}$$

The corresponding equation of the Clough-Penzien filter is

$$M^{\mathrm{CP}} = \frac{2\,\nu_f\omega_f}{\dot{\kappa}}\dot{U}_f + \omega_f^{\,2}U_f + \frac{2\,\nu_g\omega_g}{\dot{\kappa}}\dot{U}_g + \omega_g^{\,2}U_g \tag{2.46}$$

2.4 Estimation of the evolutionary spectral parameters

This paragraph is devoted to the estimation of the parameters of the functions used for a stochastic description of earthquake motions on the basis of single acceleration records. The emphasis will lie on the model of instantaneous spectrum which has been adopted in the analyses of the subsequent chapters of this work.

2.4.1 Estimation of the power spectral density

As in many physical stochastic problems, the estimation of spectral characteristics of an earthquake record must be done after a single realization of the underlying random process. This motivates the conventional resort to the hypothesis of ergodicity (see section 1.3.4), which allows to assume that the probabilistic measures obtained on the time axis are equal to those that could have been obtained from an ensemble of realizations if it were available.

The estimation of the power spectral density from a single earthquake record faces the additional problem of the strong nonstationarity of such type of signals. Since the emphasis of earthquake engineering has mainly been placed on the maximum structural responses, and these can be expected to be reached in the strong motion phase in most cases, it has been common practice to perform the spectral analyses on this portion of the accelerogram, which can be treated as a stationary signal.

To this purpose, one of the most popular methods for defining the duration of that phase and, consequently, for estimating the power spectral density of the record is due to Vanmarcke and Lai (1980). The estimator proposed is

$$\hat{G}_A(\omega) = \frac{|\tilde{A}(\omega)|^2}{\pi s} \tag{2.47}$$

where $\tilde{A}(\omega)$ is the Fourier transform of the ground acceleration $a(t)$ and s is an approximation of the duration of the strong motion phase of the event — an interval in which the motion can be considered as stationary as said before. Its expression is derived on the basis of the theory of level crossing of stochastic processes as

$$s = 2\ln\left(\frac{2s}{T_s}\right)\frac{E_\infty}{\max(a(t))}, \qquad s \geq 1.36T_s \tag{2.48}$$

and

$$s = 2\frac{E_\infty}{\max(a(t))}, \qquad s \leq 1.36T_s \tag{2.49}$$

where T_s the dominant period of the strong motion waves and E_∞ is the energy of the record measured as

$$E_\infty = \int_0^\infty a^2(t)\,\mathrm{d}t \tag{2.49}$$

As said in chapter 1, the high variance inherent to the periodogram (2.47) can be reduced by using spectral windows (Oppenheim and Schaffer 1989; Priestley 1981). Although, in earthquake engineering it is also usual to apply other techniques, such as moving-average smoothing of the periodogram or averaging of N segmental periodograms of the record (Soong and Grigoriu 1993):

$$\hat{G}_A(\omega) = \frac{1}{s}\sum_{n=1}^{N} |\tilde{A}_n(\omega)|^2 \tag{2.51}$$

with

$$\tilde{A}_n(\omega) = \frac{1}{\pi}\int_0^{\frac{s}{N}} a_n(t)\mathrm{e}^{-\mathrm{i}\omega t}\mathrm{d}t \tag{2.52}$$

The development of evolutionary models and the observation that omitting the ascending and decaying phases of the motion can lead to underestimation of nonlinear responses and damage indeces have fostered the use of a more rigorous technique of analysing the spectral characteristics of earthquake records, consisting in the transformation of the nonstationary signal into a stationary one of the same total duration, t_∞. This transformation implies, of course, that an adequate nonstationary model have been fitted to the signal. In a later paragraph this technique will be described for the particular case of the instantaneous spectrum, which has been used to derive stochastic models of some records that will be employed in subsequent chapters.

2.4.2 Estimation of amplitude modulating functions

The parameters of the amplitude functions $\xi(t)$ are usually determined on the basis of the energy of the record (equation 2.50). Its total value is proportional to the well-known *Arias intensity* which is widely used as a measure of seismic damage potential. It is also related to the Fourier amplitude transform according to Parseval's theorem:

$$\int_0^\infty a^2(t)\mathrm{d}t = \frac{1}{\pi}\int_0^\infty |\tilde{A}(\omega)|^2 \mathrm{d}\omega \tag{2.53}$$

In uniformly modulated as well as in instantaneous spectrum models one has

$$A(t) = \xi(t)M(t) \tag{2.54}$$

and hence

$$\sigma_A^2(t) = \xi^2(t)\sigma_M^2(t) \tag{2.55}$$

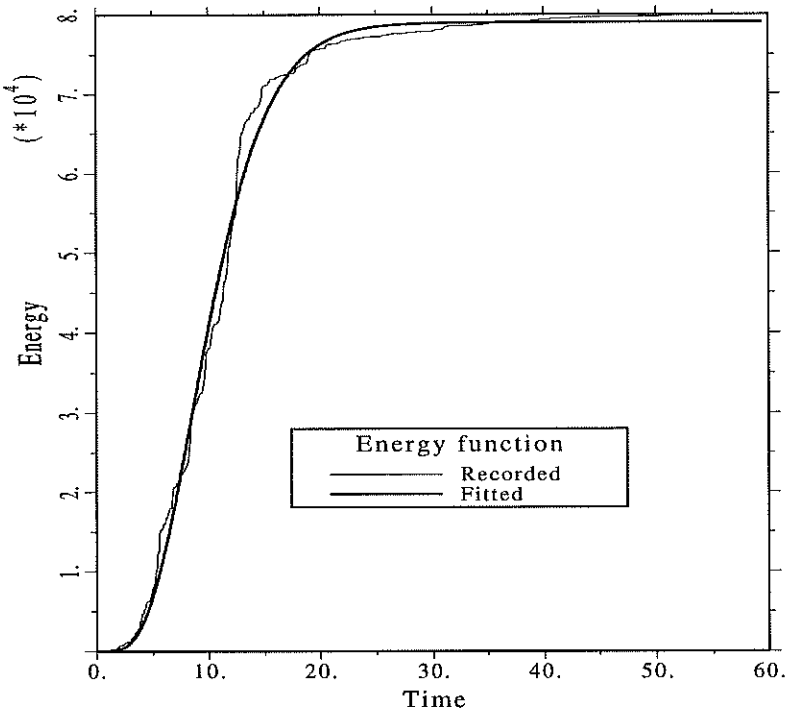

Figure 2.7 Energy functions of Orion earthquake (units: s, cm^2/s^3)

since $\xi(t)$ is deterministic and $M(t)$ has zero mean. The expected value of energy is then

$$\mathrm{E}[E(t)] = \int_0^t \xi^2(t)\mathrm{E}[M^2(t)]\mathrm{d}t \tag{2.56}$$

Since the relative distribution of energy between $\xi(t)$ and $M(t)$ is arbitrary, it is always possible to set $\mathrm{E}[M^2(t)] \equiv 1$ so that the expected energy will be completely controlled by $\xi(t)$:

$$\mathrm{E}[E(t)] = \int_0^t \xi^2(t)\mathrm{d}t \tag{2.57}$$

The identification of the parameters of any amplitude modulating function can then be done by obliging the equivalence of the energies associated to the function and original record, i.e.,

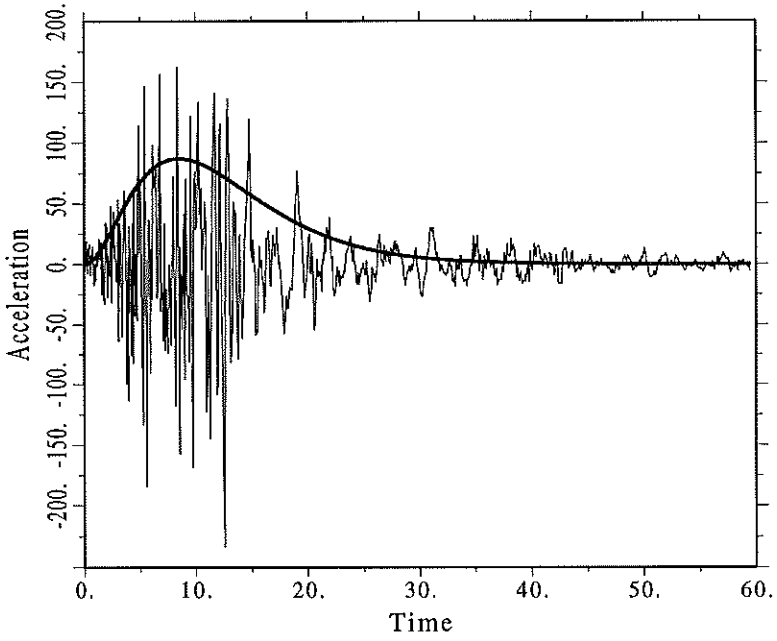

Figure 2.8 Record and Yeh-Wen modulating function of Orion earthquake (units: s, cm/s^2)

$$\int_0^t \xi^2(t)\mathrm{d}t \equiv \int_0^t a^2(t)\mathrm{d}t \tag{2.58}$$

To that purpose it is necessary to make use of algorithms of nonlinear indentification (Bard 1974)

Figure 2.7 shows a comparison of the energies associated to the record and to the fitted Yeh-Wen (2.22) and given energy functions of the Orion earthquake. The parameters of the model, which were obtained by means of the Levenberg-Marquart algorithm (Press *et al.*, 1992), are $a = 0.5577\text{E}02$, $b = 0.3214\text{E}02$, $c = 0.5093\text{E}00$, $d = 0.0$ and $e = 0.2782\text{E}02$. It can be seen the good agreement existing between both curves. The record is drawn again in figure 2.8 together with the fitted $\xi(t)$ function.

2.4.3 Modelling of instantaneous spectrum

Besides the fitting of an amplitude function $\xi(t)$ the construction of an instantaneous spectrum model requires the folowing steps:

1. To fit a model of the frequency modulating function $\kappa(t)$.

2. To transform the nonstationary signal into a stationary one using the fitted functions of amplitude and frequency.

3. To calculate the stationary power spectral density and to build a smooth model that reproduce its essential features.

As has been said previously, the frequency function can be derived from a $M-$order polynomial function fitted to the zero crossings of the record, that is,

$$\hat{\kappa}(t) = \frac{n(t)}{\dot{n}(t_s)} \tag{2.59}$$

with

$$n(t) = \sum_{i=1}^{M} r_i t^i \tag{2.60}$$

The time t_s, corresponding to the beginning of the strong motion phase, can be estimated by visual inspection as the first inflection point of the energy function $E(t)$ (see figure 2.7).

Figures 2.9 and 2.10 illustrate the regression of a model to the zero crossings of the El Centro and Orion records, respectively. The regression has been performed on a linear combination of Legendre polynomials due to the fact that their orthogonality makes minimum the least square error (Boas 1983). The corresponding parameters, as well as those of other records, are collected in table 2.1. Comparing figures 2.1 and 2.5, it can be observed that the evolution from high to low frequency waves is stronger in the Orion than in the El Centro record. The SMART record has been selected as an example of an intermediate situation. Their fitted $\kappa(t)$ functions will be used in the analyses of chapter 8. Figure 11 shows two snapshots of the Clough-Penzien evolutive spectral density of figure 2.3 using the fitted Orion $\kappa(t)$ function with $\xi(t) = 1$.

The next step is the transformation of the original nonstationary signal into a stationary one. This can be accomplished in two phases. First, the variation of amplitudes is removed by dividing the signal by the fitted amplitude function, i.e.,

$$m_1(t) = \frac{a(t)}{\xi(t)} \tag{2.61}$$

Then, the resulting signal is mapped in the modified time axis represented by the frequency modulating function,

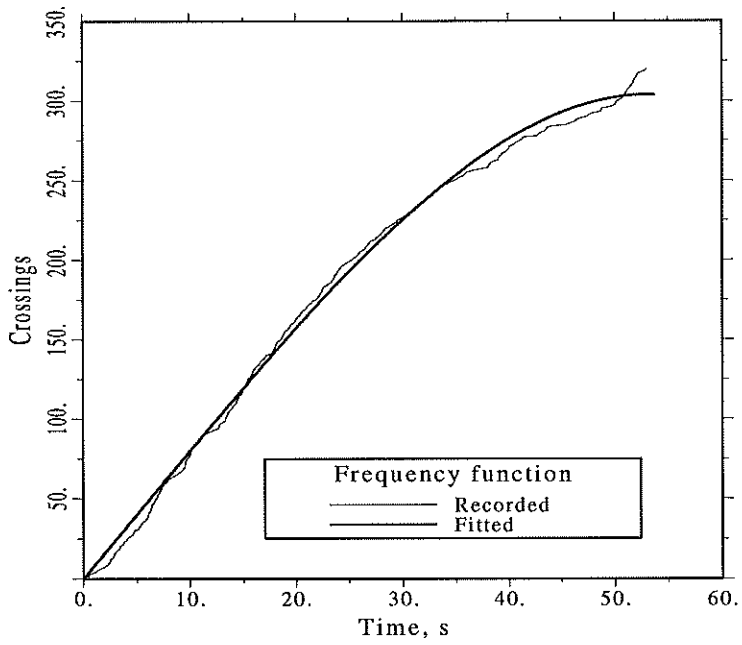

Figure 2.9 Frequency modulating function of El Centro earthquake

Table 2.1 Parameters of fitted frecuency modulating function

Earthquake record	r_1	r_2	r_3	t_s	$\dot{n}(t_s)$
Imperial Valley	0.7826 e 01	0.2733 e -01	-0.1260 e -02	2.0	0.7921 e 01
SMART 45	0.9806 e 01	-0.1980 e 00	0.1833 e -02	7.5	0.7145 e 01
San Fernando	0.9585 e 01	-0.2291 e 00	0.2298 e -02	2.5	0.8148 e 01

$$m(t) = m_1(\kappa(t)) \tag{2.62}$$

This end signal can be used for estimating the power spectral density using the total duration in equation (2.47). The fitting of a filter model will be commented in the following paragraph.

2.4.4 Estimation of parameters of filter models

Lai (1982) and Faravelli (1988a) have proposed the estimation of the parameters of simple and composed Kanai-Tajimi filters by minimizing the error

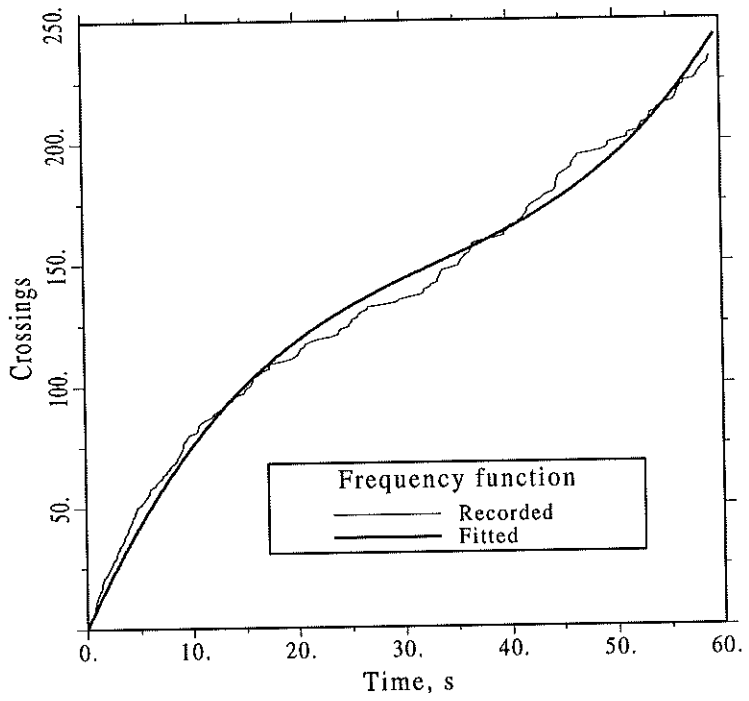

Figure 2.10 Frequency modulating function of Orion earthquake

existing the first spectral moments of the model to those of the signal. The spectral moments are defined as

$$\lambda_j = \int_0^\infty \omega^j G(\omega) \mathrm{d}\omega \tag{2.63}$$

Since the Kanai-Tajimi filter is defined by three parameters, it is necessary to solve the same number of nonlinear constraints simultaneously, which correspond to the spectral moments of order 0, 1 and 2. The procedure is facilitated by the availability of closed expressions for the spectral moments of this model derived by Faravelli (1988a). The procedure becomes more involved for higher order models such as the Clough-Penzien or Boore-type filters for which explicit expressions of the moments are difficult to obtain. Since these models reproduce more realistically the power spectrum, there is no alternative than to fit them by nonlinear identification techniques.

An important statistical study on the shape of the power spectral density based on U.S. records was performed by Moayyad and Mohraz (1982). The

authors grouped the records into three cathegories corresponding to different types of soils, namely hard, middle and soft and averaged the normalized spectra. Sues *et al.* (1985) fitted the Kanai-Tajimi model to the resulting averages. The results are collected in Table 2.2.

Table 2.2 Kanai-Tajimi model parameters (after Sues *et al.* 1983)

Ground condition	ω_g	ν_g
Soft	10.9	0.96
Intermediate	16.5	0.80
Hard	16.9	0.94

It is important to observe that when fitting the Kanai-Tajimi model to individual earthquakes much lower values of ν_g are tipically obtained in comparison to those shown in the table. In fact, Lai (1982) has found that the ν_g values are concentrated around 0.32 with moderate dispersion, irrespective of seismological or geothecnical conditions. This means that the high values stemming from the study by Moayyad and Mohraz (1982) suppose that the earthquake records have a wider band of frequencies than the mean one. This can be interpreted as a consequence of classifying the records by their associated soil conditions without regard to seismological variables such as magnitude and epicentral distance, which have an important influence on the value of the dominant frequencies. As a result, spectra of earthquakes origined at different seismological conditions are merged by the sole reason of their geothecnical similarity, which in turn implies that the averages display non realistic bandwidths.

2.5 Simulation of earthquake accelerograms

The synthetic simulation of stochastic processes and, specifically of earthquake accelerograms has been an active area of research since the advenance of fast computers. At present there is a wide spectrum of algorithms to that purpose. The choice among them depends on the available information, the characteristics to be given to the signal and the computational efficiency and accuracy (Nigam and Narayanan 1994).

In the present work use will be made of the algorithms that are exposed in the sequel, which correspond to Gaussian processes. This restriction is due to the fact that zero mean Gaussian random variables are completely defined by second order statistical information. Since the latter is indirectly given by the power spectral density of the process, it will be granted that upon such basis the synthetic realizations will correspond to the Gaussian probabilistic model.

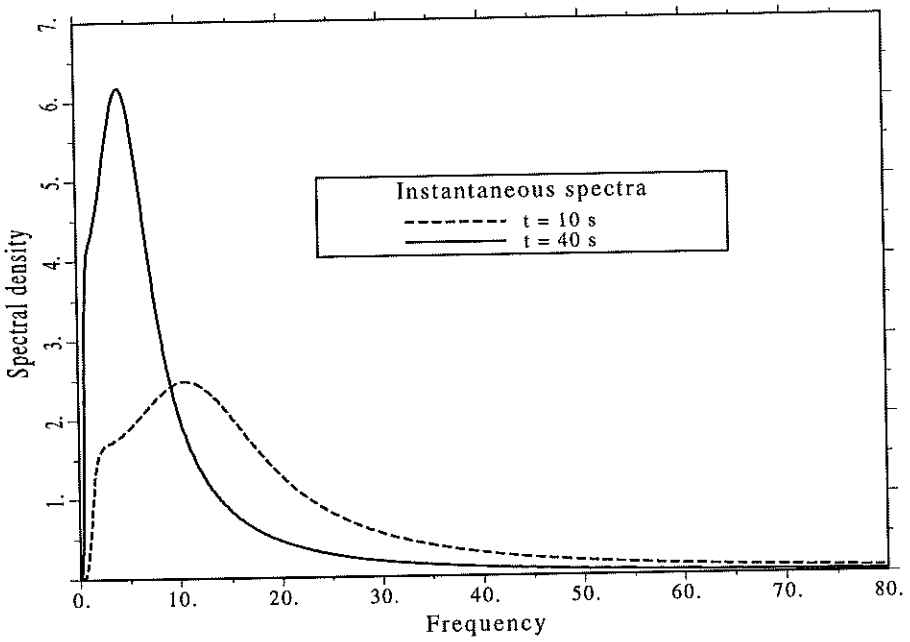

Figure 2.11 Evoutive Clough-Penzien spectral density (units: rad/s, cm^2/s^3)

This is not valid in case of non-Gaussian processes which require higher order spectral information.

2.5.1 Simulation of filtered white noise

There are, in general, two ways of performing this kind of synthetic simulation. The first consists in generating a realization of a white noise process, $w(t)$ (cf. chapter 1) and then calculating the response of the filters by solving the equations of structural dynamics, namely

$$\mathrm{L}[x,t] = w(t) \tag{2.64}$$

where $\mathrm{L}[\cdot]$ is the mathematical operator of the filter. The second technique relies on the availability of the mathematical or empirical expression of the power spectral density function of the process, $S_X(\omega)$. The realizations can be generated by the algorithm (Shinozuka 1987):

$$x(t) = \sum_{j=1}^{M} 2\sqrt{S_X(\omega_j)\Delta\omega}\cos(\omega_j t + \zeta_j) \tag{2.65}$$

where the spectral density has been discretized into M frequencies, which have an associated random phase angle ζ_j uniformly distributed between 0 and 2π. Evidently,

$$\Delta\omega = \frac{\omega_{\max}}{M} \tag{2.66}$$

where $\omega_{\max}$ is the maximum frequency given to the signal, selected on seismological as well as structural considerations. The frequencies ω_j are allocated either in the middle of each interval or randomly inside it. The algorithm is based on the spectral representation of stochastic processes sketched in chapter 1. In particular (see equation 1.36) the total variance computed on the simulated realizations

$$x(t) = \sum_{j=1}^{M} Z_j \cos(\omega_j t + \zeta_j) \tag{2.67}$$

is

$$\sigma_X^2 = \frac{1}{2}\sum Z_j^2 \tag{2.68}$$

On the other hand, the variance is also given by

$$\sigma_X^2 = \int_{-\infty}^{\infty} S_X(\omega)\mathrm{d}\omega \tag{2.69}$$

Accordingly, one can set amplitudes Z_j as

$$Z_j \equiv 2\sqrt{S_X(\omega_j)\Delta\omega} \tag{2.70}$$

It can be demonstrated that the density function of the signals $x(t)$ obtained this way tend to that of the process $X(t)$ as $M \to \infty$ (Shinozuka 1987). By expressing the cosine function in equation (2.65) as the real part of a complex exponential, the simulation can be carried out much more efficiently by means of the fast Fourier transform algorithm (Shinozuka and Lenoe 1976). In fact, equation (2.65) can be put in the form

$$x(t) = \Re\left\{\sum_{j=1}^{M} 2\sqrt{S_X(\omega_j)\Delta\omega}\exp(\mathrm{i}\zeta_j) \times \exp(\mathrm{i}\omega_j t)\right\} \tag{2.71}$$

which indicates that $x(t)$ can be calculated as the real part ($\Re(\cdot)$) of the discrete Fourier transform of the complex set

$$\{2\sqrt{S_X(\omega_j)\Delta\omega}\exp(\mathrm{i}\zeta_j)\} \tag{2.72}$$

2.5.2 Simulation of nonstationary accelerograms

The simulation of zero mean, nonstationary Gaussian processes characterized by a time-variant power spectral density $S_X(\omega_j, t)$, can be performed by a simple modification of the above algorithm:

$$x(t) = \sum_{j=1}^{M} 2\sqrt{S_X(\omega_j, t)\Delta\omega}\cos(\omega_j t + \zeta_j) \tag{2.73}$$

In the particular case of processes modelled according to Priestley's evolutive model, i.e.

$$S_X(\omega, t) = |\xi(t, \omega)|^2 S_Y(\omega) \tag{2.74}$$

one has

$$x(t) = |\xi(t, \omega)| \sum_{j=1}^{M} 2\sqrt{S_Y(\omega_j)\Delta\omega}\cos(\omega_j t + \zeta_j) \tag{2.75}$$

which in case of uniformly modulated processes reduces to

$$x(t) = \xi(t) \sum_{j=1}^{M} 2\sqrt{S_Y(\omega_j)\Delta\omega}\cos(\omega_j t + \zeta_j) \tag{2.76}$$

The simulation of accelerograms according to the instantaneous spectrum model can be done by solving the equations of motion of the time varying filters excited by the synthetic realizations of the driving white noise (equations 2.42 and 2.43).

Chapter 3

Second order stochastic analysis of nonlinear systems

3.1 Introduction

Let us consider a nonlinear dynamical system subject to a random external excitation:

$$\boldsymbol{h}(\ddot{\boldsymbol{X}}, \dot{\boldsymbol{X}}, \boldsymbol{X}) = \boldsymbol{P}(t) \tag{3.1}$$

Here $\boldsymbol{h}(\cdot)$ denotes a nonlinear vector function of its arguments and $\boldsymbol{P}(t)$ is the excitation. This chapter deals with the second order stochastic analysis of nonlinear systems. The main part of the chapter deals with *method of stochastic equivalent linearization*, which allows the estimation of first and second order statistical moments of the response vector of nonlinear deterministic structures subject to random vibration. This method, indeed, is not the only one available to such purpose (see, for example, Nigam 1983; Roberts and Spanos 1990; Soong and Grigoriu 1993; Lin and Cai 1995; Lutes and Sarkani 1997). For instance, the *method of perturbation* seeks the statistics of the response $\boldsymbol{X}$ of the system by power series expansions of all the terms involved in equation (3.1). It, however, can only be applied with good accuracy to weakly nonlinear systems, that is, those whose departure from linearity is slight. A similar restriction applies to the method known as *stochastic averaging*, which proceeds by searching some functions of the amplitude and phase of an harmonics which is the solution of the associated free vibration problem. Besides the restriction of applying to weak nonlinearities, both methods also pose computational difficulties when dealing with large nonlinear systems. Obviously, any of the methods for calculating higher order stochastic response that are the subject of chapter 7 provide the first and second order information as a bye-product. But as can be seen there, the application of such methods to large structural systems is also very limited.

In contrast to the methods of perturbation and stochastic averaging, the method of stochastic equivalent linearization can be applied to large structural systems exhibiting strong nonlinear response. The present chapter begins with a formal summary of the theory of second-order, random vibration analysis of linear systems, as this provide a basis for the calculation of the response of the nonlinear hysteretic models which are dealt with in the next chapter. The method of stochastic equivalent linearization is then exposed for the general case of nonlinear dynamical structures, after which the simplifications stemming from the assumption of Gaussianity of the response random processes are introduced. The chapter follows with a brief exposition of a method which exploits the second order information provided by stochastic linearization to the assessment of the reliability of nonlinear systems under nonstationary conditions, when it is measured as the probability of exceedance of maximum allowable displacements. Finally, the last section deals with an approximate method for considering the uncertainty of the structural or load model parameters on global response measures, which has been proposed by some authors as an attempt for overcoming the deterministic definition of such models in conventional random vibration analysis. The method, which is based on the Taylor expansion of the covariance response about the mean of the parameter set, is applied in chapter 8 to the analysis of base isolated buildings.

3.2 Second order analysis of linear systems

3.2.1 State space formulation

As is well known, the dynamics of a linear structure of N degrees of freedom with mass, viscous damping and stiffness matrices denoted by $\boldsymbol{M}$, $\boldsymbol{C}$ and $\boldsymbol{K}$ respectively is given by (Clough and Penzien 1993)

$$\boldsymbol{M}\ddot{\boldsymbol{x}}(t) + \boldsymbol{C}\dot{\boldsymbol{x}}(t) + \boldsymbol{K}\boldsymbol{x}(t) = \boldsymbol{p}(t) \tag{3.2}$$

in which $\boldsymbol{x}, \dot{\boldsymbol{x}}$ and $\ddot{\boldsymbol{x}}$ are displacement, velocity and acceleration vectors, respectively. With the aim of calculating the statistical second order response of the structure, it is convenient to express the above system of equations in state space form. That is, by collecting the displacement and velocity responses in the state vector $\boldsymbol{q}^{\mathrm{T}}(t) = [\boldsymbol{x}^{\mathrm{T}}(t), \dot{\boldsymbol{x}}^{\mathrm{T}}(t)]$, the original system of N second order differential equations is transformed into the following system of $2N$ first order differential equations:

$$\dot{\boldsymbol{q}}(t) = \boldsymbol{A}\boldsymbol{q}(t) + \boldsymbol{f}(t) \tag{3.3}$$

$\boldsymbol{A}$ is the so-called *system matrix* given by

$$\boldsymbol{A} = \begin{pmatrix} \mathbf{0} & \boldsymbol{I} \\ -\boldsymbol{M}^{-1}\boldsymbol{K} & -\boldsymbol{M}^{-1}\boldsymbol{C} \end{pmatrix} \tag{3.4}$$

and the vector of external loads is then

$$\boldsymbol{f}(t) = \begin{pmatrix} \mathbf{0} \\ -\boldsymbol{M}^{-1}\boldsymbol{p}(t) \end{pmatrix} \tag{3.5}$$

3.2.2 Mean and covariance evolution

Let us now derive the differential equations governing the evolution of the first and second order moments of the random response of a linear structure, when excited by a external load defined as a stochastic process $\boldsymbol{P}(t)$. Under this stochastic point of view equation (3.3) is written as

$$\dot{\boldsymbol{Q}}(t) = \boldsymbol{A}\boldsymbol{Q}(t) + \boldsymbol{F}(t) \tag{3.6}$$

The application of the expected value operator $\mathrm{E}[\cdot]$ to this equation gives the evolution of the vector of mean responses

$$\dot{\boldsymbol{\mu}}(t) = \boldsymbol{A}\boldsymbol{\mu}(t) + \boldsymbol{\mu}_{\boldsymbol{F}}(t) \tag{3.7}$$

which for the stationary case simplifies to

$$\boldsymbol{\mu} = -\boldsymbol{A}^{-1}\boldsymbol{\mu}_{\boldsymbol{F}} \tag{3.8}$$

For the sake of simplicity in the derivation of the covariance evolution, let us assume that the excitation and, consequently, the response have zero mean. The time derivative covariance matrix, given in such case by

$$\boldsymbol{\Sigma}(t) = \mathrm{E}[\boldsymbol{Q}(t)\boldsymbol{Q}(t)^{\mathrm{T}}] \tag{3.9}$$

is

$$\begin{aligned} \dot{\boldsymbol{\Sigma}}(t) &= \frac{\mathrm{d}}{\mathrm{d}t}\mathrm{E}[\boldsymbol{Q}(t)\boldsymbol{Q}^{\mathrm{T}}(t)] \\ &= \mathrm{E}[\{\boldsymbol{A}\boldsymbol{Q}(t) + \boldsymbol{F}(t)\}\boldsymbol{Q}^{\mathrm{T}}(t)] + \mathrm{E}[\boldsymbol{Q}(t)\{\boldsymbol{A}\boldsymbol{Q}(t) + \boldsymbol{F}(t)\}^{\mathrm{T}}] \end{aligned} \tag{3.10}$$

which leads to

$$\dot{\boldsymbol{\Sigma}}(t) = \boldsymbol{A}\mathrm{E}[\boldsymbol{Q}(t)\boldsymbol{Q}^{\mathrm{T}}(t)] + \mathrm{E}[\boldsymbol{Q}(t)\boldsymbol{Q}^{\mathrm{T}}(t)]\boldsymbol{A}^{\mathrm{T}} + \mathrm{E}[\boldsymbol{F}(t)\boldsymbol{Q}^{\mathrm{T}}(t) + \boldsymbol{Q}(t)\boldsymbol{F}^{\mathrm{T}}(t)] \quad (3.11)$$

that is,

$$\dot{\boldsymbol{\Sigma}}(t) = \boldsymbol{A}\boldsymbol{\Sigma}(t) + \boldsymbol{\Sigma}(t)\boldsymbol{A}^{\mathrm{T}} + \mathrm{E}[\boldsymbol{F}(t)\boldsymbol{Q}^{\mathrm{T}}(t) + \boldsymbol{Q}(t)\boldsymbol{F}^{\mathrm{T}}(t)] \quad (3.12)$$

Let the external excitation in equation (3.2) be modelled as a modulated white noise, i.e.,

$$\boldsymbol{P}(t) = \boldsymbol{\xi}(t)\boldsymbol{W}(t) \quad (3.13)$$

where $\boldsymbol{W}(t)$ is a vector of stationary white noises and $\boldsymbol{\xi}(t)$ a vector of deterministic functions that modulate the instensity in time, thus giving $\boldsymbol{P}(t)$ a non-stationary character. We will now derive the value of the last term in equation (3.12). For simplicity a single-degree-of-freedom system will be considered:

$$m\ddot{X}(t) + c\dot{X}(t) + kX(t) = \xi(t)W(t) \quad (3.14)$$

Here m, c and k are the mass, damping and stiffness constants. The intensity of the white noise $W(t)$ is $2\pi S_W$. The above equation can be written in the form of a stochastic differential equation,

$$\mathrm{d}\begin{pmatrix} X(t) \\ \dot{X}(t) \end{pmatrix} = \begin{pmatrix} \dot{X}(t) \\ -m^{-1}kX - m^{-1}c\dot{X} \end{pmatrix}\mathrm{d}t + \begin{pmatrix} 0 \\ m^{-1}\xi(t)\sqrt{2\pi S_W} \end{pmatrix}\mathrm{d}B \quad (3.15)$$

Applying the Ito formula (1.98) on the function

$$h(X, \dot{X}) = X^p \dot{X}^q \quad (3.16)$$

and then the expectation operator $\mathrm{E}[\cdot]$, the following general differential equation is obtained:

$$\dot{\mu}_{p,q}(X, \dot{X}) = p\mu_{p-1,q+1}(X, \dot{X}) - qm^{-1}k\mu_{p+1,q-1}(X, \dot{X}) -$$

$$qm^{-1}c\mu_{p,q}(X, \dot{X}) + \frac{1}{2}m^{-2}\xi(t)^2 2\pi S_W q(q-1)\mu_{p,q-2}(X, \dot{X}) \quad (3.17)$$

For the set of values $(p, q) = (2, 0), (1, 1), (0, 2)$ it is easy to see that the first three terms of the right hand side of this equation generate the terms $\boldsymbol{A}\boldsymbol{\Sigma}(t) + \boldsymbol{\Sigma}(t)\boldsymbol{A}^{\mathrm{T}}$ in equation (3.12). Accordingly, the unsolved expectation is

$$\mathrm{E}[\boldsymbol{F}(t)\boldsymbol{Q}^{\mathrm{T}}(t) + \boldsymbol{Q}(t)\boldsymbol{F}^{\mathrm{T}}(t)] = 2\pi \begin{pmatrix} 0 & 0 \\ 0 & m^{-2}\xi(t)^2 S_W \end{pmatrix} \tag{3.18}$$

Generalizing to the multidimensional case we have

$$\mathrm{E}[\boldsymbol{F}(t)\boldsymbol{Q}^{\mathrm{T}}(t) + \boldsymbol{Q}(t)\boldsymbol{F}^{\mathrm{T}}(t)] = 2\pi \begin{pmatrix} \mathbf{0} & \mathbf{0} \\ \mathbf{0} & \boldsymbol{M}^{-1}\boldsymbol{\xi}(t)\boldsymbol{S}_W\boldsymbol{\xi}^{\mathrm{T}}(t)\boldsymbol{M}^{-1} \end{pmatrix} \tag{3.19}$$

Turning back to the equation (3.12) we arrive to the final expression that governs the evolution of the covariance response of a linear structure excited by a vector shot noise of intensity $\boldsymbol{S}_W$:

$$\dot{\boldsymbol{\Sigma}}(t) = \boldsymbol{A}\boldsymbol{\Sigma}(t) + \boldsymbol{\Sigma}(t)\boldsymbol{A}^{\mathrm{T}} + 2\pi\boldsymbol{S}_{\boldsymbol{F}}(t) \tag{3.20}$$

where

$$\boldsymbol{S}_{\boldsymbol{F}}(t) = 2\pi \begin{pmatrix} \mathbf{0} & \mathbf{0} \\ \mathbf{0} & \boldsymbol{M}^{-1}\boldsymbol{\xi}(t)\boldsymbol{S}_W\boldsymbol{\xi}^{\mathrm{T}}(t)\boldsymbol{M}^{-1} \end{pmatrix} \tag{3.21}$$

It can be demonstrated that this equation also applies to the case of nonzero mean random excitation (Cunha 1990; Soong and Grigoriu 1993).

In the stationary case the covariance matrix does not vary with time and then we have the following algebraic equation

$$\boldsymbol{A}\boldsymbol{\Sigma} + \boldsymbol{\Sigma}\boldsymbol{A}^{\mathrm{T}} + \boldsymbol{S}_{\boldsymbol{F}} = \mathbf{0} \tag{3.22}$$

which has the same appearance as the Lyapounov equation arising in the study of chaos and bifurcation of nonlinear systems.

Finally, it is important to note that in many instances the random external forces are modelled as linear combinations of the responses of linear filters to white or shot noises. In that case, the equation of motion in state space form is

$$\dot{\boldsymbol{q}}(t) = \boldsymbol{A}\boldsymbol{q}(t) + \boldsymbol{B}\boldsymbol{q}_{\mathrm{f}}(t) \tag{3.23}$$

where $\boldsymbol{B}$ is a matrix of the coefficients of the linear combinations of the responses $\boldsymbol{q}_{\mathrm{f}}$ of the filters. The dynamics of the latter is governed by

$$\dot{\boldsymbol{q}}_{\mathrm{f}}(t) = \boldsymbol{D}\boldsymbol{q}_{\mathrm{f}}(t) + \boldsymbol{p}(t) \tag{3.24}$$

in which the vector of forces $\boldsymbol{p}$ can asume any of the forms mentioned in the preceeding, i.e. white or shot noise. Since the above equations have the same

linear structure, both systems can be grouped into a single one describing the dynamics of the enhanced state vector $\boldsymbol{q}^{\mathrm{T}}(t) = [\boldsymbol{x}^{\mathrm{T}}(t), \dot{\boldsymbol{x}}^{\mathrm{T}}(t), \boldsymbol{q}_{\mathrm{f}}^{\mathrm{T}}(t)]$; the structural matrices are assembled accordingly.

3.3 The method of stochastic equivalent linearization

3.3.1 Basic formulation

Let the motion of a nonlinear structural system excited by random forces be described by the nonlinear equation

$$\boldsymbol{h}(\ddot{\boldsymbol{X}}, \dot{\boldsymbol{X}}, \boldsymbol{X}) = \boldsymbol{P} \tag{3.25}$$

where the time argument has been omitted for simplicity. In the case of hysteretic systems is commonly assumed that the function $\boldsymbol{h}(\cdot)$ is antisymmetric, i.e.,

$$\boldsymbol{h}(\ddot{\boldsymbol{X}}, \dot{\boldsymbol{X}}, \boldsymbol{X}) = -\boldsymbol{h}(-\ddot{\boldsymbol{X}}, -\dot{\boldsymbol{X}}, -\boldsymbol{X}) \tag{3.26}$$

For the random vibration problem this assumption implies that the function has a zero mean.

The method of stochastic equivalent linearization, when applied to structural dynamics problems, proposes the substitution of the above nonlinear equation by the following linear one

$$\boldsymbol{M}_{\mathrm{e}}\ddot{\boldsymbol{X}} - \boldsymbol{C}_{\mathrm{e}}\dot{\boldsymbol{X}} - \boldsymbol{K}_{\mathrm{e}}\boldsymbol{X} = \boldsymbol{P} \tag{3.27}$$

In this equation $\boldsymbol{M}_{\mathrm{e}}, \boldsymbol{C}_{\mathrm{e}}$ and $\boldsymbol{K}_{\mathrm{e}}$ are the equivalent mass, viscous damping and stiffness matrices which are in general time -varying. The error of this equation is

$$\boldsymbol{\epsilon} = \boldsymbol{h}(\ddot{\boldsymbol{X}}, \dot{\boldsymbol{X}}, \boldsymbol{X}) - \boldsymbol{M}_{\mathrm{e}}\ddot{\boldsymbol{X}} - \boldsymbol{C}_{\mathrm{e}}\dot{\boldsymbol{X}} - \boldsymbol{K}_{\mathrm{e}}\boldsymbol{X} \tag{3.28}$$

and the most common strategy for the calculation of the equivalent matrices is the minimization of the expected value of its square norm

$$\mathrm{E}[\boldsymbol{\epsilon}\boldsymbol{\epsilon}^{\mathrm{T}}] \rightarrow \text{minimum} \tag{3.29}$$

which is equivalent to

$$\sum_{i=1}^{N} \mathrm{E}[\epsilon_i^2] \tag{3.30}$$

due to the linearity property of the expectation operator. The terms of the above summation are

$$\epsilon_i = h_i(\ddot{\boldsymbol{X}}, \dot{\boldsymbol{X}}, \boldsymbol{X}) - \sum_{j=1}^{N} m_{ij}^{\mathrm{e}} \ddot{X}_j - \sum_{j=1}^{N} c_{ij}^{\mathrm{e}} \dot{X}_j - \sum_{j=1}^{N} k_{ij}^{\mathrm{e}} X_j \tag{3.31}$$

in which $h_i(\cdot)$ is the $i-$th component of the function $\boldsymbol{h}(\cdot)$, while $m_{ij}^{\mathrm{e}}, c_{ij}^{\mathrm{e}}$ and k_{ij}^{e} are the elements of matrices $\boldsymbol{M}_{\mathrm{e}}, \boldsymbol{C}_{\mathrm{e}}$ and $\boldsymbol{K}_{\mathrm{e}}$ respectively. Since the terms of the above summation are positive the minimization of the total error is equivalent to the minimization of each of them. Hence, it can be concluded that the conditions allowing the determination of the equivalent matrices are the following:

$$\frac{\partial \mathrm{E}[\epsilon_i^2]}{\partial m_{ij}^{\mathrm{e}}} = 2\mathrm{E}\left[\epsilon_i \frac{\partial \epsilon_i}{\partial m_{ij}^{\mathrm{e}}}\right] = 0 \tag{3.32a}$$

$$\frac{\partial \mathrm{E}[\epsilon_i^2]}{\partial c_{ij}^{\mathrm{e}}} = 2\mathrm{E}\left[\epsilon_i \frac{\partial \epsilon_i}{\partial c_{ij}^{\mathrm{e}}}\right] = 0 \tag{3.32b}$$

$$\frac{\partial \mathrm{E}[\epsilon_i^2]}{\partial k_{ij}^{\mathrm{e}}} = 2\mathrm{E}\left[\epsilon_i \frac{\partial \epsilon_i}{\partial k_{ij}^{\mathrm{e}}}\right] = 0 \tag{3.32c}$$

Substituting these expressions in equation (3.29) and invoking the linearity property of the expectation operator we arrive to the set

$$\sum_{l=1}^{N} m_{il}^{\mathrm{e}} \mathrm{E}[\ddot{X}_l \ddot{X}_j] + \sum_{l=1}^{N} c_{il}^{\mathrm{e}} \mathrm{E}[\dot{X}_l \ddot{X}_j] + \sum_{l=1}^{N} k_{il}^{\mathrm{e}} \mathrm{E}[X_l \ddot{X}_j] = \mathrm{E}[\ddot{X}_j h_i(\ddot{\boldsymbol{X}}, \dot{\boldsymbol{X}}, \boldsymbol{X})] \tag{3.33a}$$

$$\sum_{l=1}^{N} m_{il}^{\mathrm{e}} \mathrm{E}[\ddot{X}_l \dot{X}_j] + \sum_{l=1}^{N} c_{il}^{\mathrm{e}} \mathrm{E}[\dot{X}_l \dot{X}_j] + \sum_{l=1}^{N} k_{il}^{\mathrm{e}} \mathrm{E}[X_l \dot{X}_j] = \mathrm{E}[\dot{X}_j h_i(\ddot{\boldsymbol{X}}, \dot{\boldsymbol{X}}, \boldsymbol{X})] \tag{3.33b}$$

$$\sum_{l=1}^{N} m_{il}^{\mathrm{e}} \mathrm{E}[\ddot{X}_l X_j] + \sum_{l=1}^{N} c_{il}^{\mathrm{e}} \mathrm{E}[\dot{X}_l X_j] + \sum_{l=1}^{N} k_{il}^{\mathrm{e}} \mathrm{E}[X_l X_j] = \mathrm{E}[X_j h_i(\ddot{\boldsymbol{X}}, \dot{\boldsymbol{X}}, \boldsymbol{X})] \tag{3.33c}$$

Collecting terms we have

$$\boldsymbol{M}_{\mathrm{e}}\mathrm{E}[\ddot{\boldsymbol{X}}\ddot{\boldsymbol{X}}^{\mathrm{T}}] + \boldsymbol{C}_{\mathrm{e}}\mathrm{E}[\dot{\boldsymbol{X}}\ddot{\boldsymbol{X}}^{\mathrm{T}}] + \boldsymbol{K}_{\mathrm{e}}\mathrm{E}[\boldsymbol{X}\ddot{\boldsymbol{X}}^{\mathrm{T}}] = \mathrm{E}[\boldsymbol{h}(\ddot{\boldsymbol{X}}, \dot{\boldsymbol{X}}, \boldsymbol{X})\ddot{\boldsymbol{X}}^{\mathrm{T}}] \qquad (3.34a)$$

$$\boldsymbol{M}_{\mathrm{e}}\mathrm{E}[\ddot{\boldsymbol{X}}\dot{\boldsymbol{X}}^{\mathrm{T}}] + \boldsymbol{C}_{\mathrm{e}}\mathrm{E}[\dot{\boldsymbol{X}}\dot{\boldsymbol{X}}^{\mathrm{T}}] + \boldsymbol{K}_{\mathrm{e}}\mathrm{E}[\boldsymbol{X}\dot{\boldsymbol{X}}^{\mathrm{T}}] = \mathrm{E}[\boldsymbol{h}(\ddot{\boldsymbol{X}}, \dot{\boldsymbol{X}}, \boldsymbol{X})\dot{\boldsymbol{X}}^{\mathrm{T}}] \qquad (3.34b)$$

$$\boldsymbol{M}_{\mathrm{e}}\mathrm{E}[\ddot{\boldsymbol{X}}\boldsymbol{X}^{\mathrm{T}}] + \boldsymbol{C}_{\mathrm{e}}\mathrm{E}[\dot{\boldsymbol{X}}\boldsymbol{X}^{\mathrm{T}}] + \boldsymbol{K}_{\mathrm{e}}\mathrm{E}[\boldsymbol{X}\boldsymbol{X}^{\mathrm{T}}] = \mathrm{E}[\boldsymbol{h}(\ddot{\boldsymbol{X}}, \dot{\boldsymbol{X}}, \boldsymbol{X})\boldsymbol{X}^{\mathrm{T}}] \qquad (3.34c)$$

Denoting by $\boldsymbol{Q}$ and $\boldsymbol{H}_{\mathrm{e}}$ the response and equivalent structural matrices given respectively by

$$\boldsymbol{Q}^{\mathrm{T}} = [\ddot{\boldsymbol{X}}^{\mathrm{T}}, \dot{\boldsymbol{X}}^{\mathrm{T}}, \boldsymbol{X}^{\mathrm{T}}], \qquad \boldsymbol{H}_{\mathrm{e}} = [\boldsymbol{M}_{\mathrm{e}}, \boldsymbol{C}_{\mathrm{e}}, \boldsymbol{K}_{\mathrm{e}}] \qquad (3.35)$$

the above expressions can be condensed into the following matrix equation:

$$\mathrm{E}[\boldsymbol{Q}\boldsymbol{Q}^{\mathrm{T}}]\boldsymbol{H}_{\mathrm{e}}^{\mathrm{T}} = \mathrm{E}[\boldsymbol{Q}\boldsymbol{h}^{\mathrm{T}}(\boldsymbol{Q})] \qquad (3.36)$$

which is the fundamental equation of the method. Notice that the equivalent structure matrix is a function of the covariance response as well as the expected value of the product of the state vector and the nonlinear function. Such a complicated structure can be greatly simplified if one assumes that the state vector obeys a Gaussian distribution, as detailed in section 3.3.3.

The equations leading to the minimization of the error correspond to the necessary conditions for the calculation of the equivalent structural matrices. It is possible to demonstrate that these conditions are also sufficient to that purpose by applying a perturbation to the resulting equivalent system (Roberts and Spanos 1990). Let then a new structural system be defined as

$$\bar{m}_{ij}^{\mathrm{e}} = m_{ij}^{\mathrm{e}} + \Delta m_{ij}^{\mathrm{e}} \qquad (3.37a)$$

$$\bar{c}_{ij}^{\mathrm{e}} = c_{ij}^{\mathrm{e}} + \Delta c_{ij}^{\mathrm{e}} \qquad (3.37b)$$

$$\bar{k}_{ij}^{\mathrm{e}} = k_{ij}^{\mathrm{e}} + \Delta k_{ij}^{\mathrm{e}} \qquad (3.37c)$$

Since the polynomial expression of the square error is of second order, the derivatives of order higher than two vanish. For this reason the following Taylor expansion of the square error about the equivalent system is exact:

$$\mathrm{E}[\bar{\epsilon}_i^2] = \mathrm{E}[\epsilon_i^2] + \sum_{j=1}^{N} \left\{ \frac{\partial \mathrm{E}[\epsilon_i^2]}{\partial m_{ij}^{\mathrm{e}}} \Delta m_{ij}^{\mathrm{e}} + \frac{\partial \mathrm{E}[\epsilon_i^2]}{\partial c_{ij}^{\mathrm{e}}} \Delta c_{ij}^{\mathrm{e}} + \frac{\partial \mathrm{E}[\epsilon_i^2]}{\partial k_{ij}^{\mathrm{e}}} \Delta k_{ij}^{\mathrm{e}} \right\} +$$

$$\frac{1}{2} \sum_{k,l=1}^{N} \frac{\partial^2 \mathrm{E}[\epsilon_i^2]}{\partial m_{ik}^{\mathrm{e}} \partial m_{il}^{\mathrm{e}}} \Delta m_{ik}^{\mathrm{e}} \Delta m_{il}^{\mathrm{e}} + \frac{\partial^2 \mathrm{E}[\epsilon_i^2]}{\partial c_{ik}^{\mathrm{e}} \partial c_{il}^{\mathrm{e}}} \Delta c_{ik}^{\mathrm{e}} \Delta c_{il}^{\mathrm{e}} +$$

$$\frac{\partial^2 \mathrm{E}[\epsilon_i^2]}{\partial k_{ik}^{\mathrm{e}} \partial k_{il}^{\mathrm{e}}} \Delta k_{ik}^{\mathrm{e}} \Delta k_{il}^{\mathrm{e}} + \frac{\partial^2 \mathrm{E}[\epsilon_i^2]}{\partial m_{ik}^{\mathrm{e}} \partial c_{il}^{\mathrm{e}}} \Delta m_{ik}^{\mathrm{e}} \Delta c_{il}^{\mathrm{e}} +$$

$$\frac{\partial^2 \mathrm{E}[\epsilon_i^2]}{\partial m_{ik}^{\mathrm{e}} \partial k_{il}^{\mathrm{e}}} \Delta m_{ik}^{\mathrm{e}} \Delta k_{il}^{\mathrm{e}} + \frac{\partial^2 \mathrm{E}[\epsilon_i^2]}{\partial c_{ik}^{\mathrm{e}} \partial k_{il}^{\mathrm{e}}} \Delta c_{ik}^{\mathrm{e}} \Delta k_{il}^{\mathrm{e}} \tag{3.38}$$

Taking into account the conditions (3.32) the above expression simplifies to

$$\mathrm{E}[\bar{\epsilon}_i^2] = \mathrm{E}[\epsilon_i^2] + \frac{1}{2}\mathrm{E}\Big\{ \Big[\sum_{j=1}^{N} \ddot{X}_j \Delta m_{ij}^{\mathrm{e}} + \dot{X}_j \Delta c_{ij}^{\mathrm{e}} + X_j \Delta k_{ij}^{\mathrm{e}} \Big]^2 \Big\} \tag{3.39}$$

in which the last term in the right hand side is always greater or equal to zero. Hence it can be concluded that

$$\mathrm{E}[\bar{\epsilon}_i^2] \geq \mathrm{E}[\epsilon_i^2] \tag{3.40}$$

which means that the error corresponding to the linear system obtained by the minimization procedure is less than or equal to that corresponding to any other system. This is not, of course, a statement about the accuracy of the method but only on the existence of a minimum of the error.

3.3.2 Historical development

The method of stochastic equivalent linearization has its roots in the work of Krylov and Bogoliubov (1943) on deterministic linearization and it first appears in papers by Caughey (1963), Iwan (1973) and others in a probabilistic formulation. It was soon evident that the method was the most suitable for random vibration analysis of large nonlinear structures among the existing techniques for such purpose (Iwan and Yang 1972). A great impulse to practical applications of the method was given by a paper of Atalik and Utku (1976) which demonstrated that the assumption of a Gaussian behavior of all the state variables greatly simplified the computation of the linearization coefficients, as it

will be seen in the next paragraph. A later paper by Faravelli *et al.* (1988), demonstrated that the Gaussian density is the only for which such a simplification is valid. Mathematical questions such as the existence and uniqueness of the solutions have already been discussed (Spanos and Iwan 1978). A monograph by Roberts and Spanos (1990) on computational techniques in nonlinear stochastic dynamics shows that this is the one with the clearest appeal to the practical analysis of large structures among them.

Much of the interest received by the method for practical applications is due to the introduction of an smooth and versatile model of hysteresis by Bouc (1967) and its posterior development by Wen (1976), Baber and Wen (1979), Casciati (1987a), Noori *et al.*, (1991), Chen and Ahmadi (1994), Foliente *et al.* (1996) and others. This class of models opened the way to the application of the method in many areas of structural dynamics such as vibration of frames (Baber and Wen 1981; Baber 1985, 1986) reinforced and concrete structures (Wen and Eliopoulos 1994; Noori *et al.* 1991; Sues *et al.* 1988), soil liquefaction (Pires *et al.* 1983), three dimensional frames (Casciati and Faravelli 1988), base isolation devices (Constantinou and Tadjbaksh 1985) and active control (Yang *et al.* 1994) among others. The extension of this hysteretic model from the one dimensional force-displacement space to the bidimensional one (Park *et al.* 1986; Casciati and Faravelli 1988) and also to stress-strain space (Casciati 1989; Pradlwarter and Li 1991) allowed the application of the method to structures modelled by hysteretic spatial frames and planar finite elements. Complex modal decomposition was introduced to minimize the computational labour required when applying the method to such complex large structural systems (Chang 1985; Faravelli *et al.* 1988; Simulescu *et al.* 1989).

The smooth hysteretic model has also found its way in nonlinear stochastic dynamics not only because of its versatility but also for the possibility of calculating the linearization matrices in explicit form. This is rarely possible for other hysteretic oscillators, such as elasto-plastic, bilinear, origin-oriented, etc, which together with the smooth one can be grouped under the label of *Markovian*, after Li and Katsukura (1990). Some of this classical models have been studied by the method of equivalent linearization by Kimura *et al.* (1994) among others.

The accuracy ot the method with respect to exact known results or to those obtained by Monte Carlo simulations has also been investigated. Generally speaking, it can be said that the size of the errors depends on many factors, such as oscillator's type and parameters, type of calculation (i.e., stationary or nonstationary), excitation level, etc. (Robert and Spanos 1990). For the specific case of the smooth hysteretic model it has been found that, under the assumption of joint Gaussian behaviour, the method estimates with reasonably

good accuracy the response in stationary analyses, but underestimates the displacement responses in nonstationary cases (Baber and Wen 1979; Iwan and Paparizos 1988). Given the importance of displacement estimations in design, attempts to overcome this situation has been proposed (Wen and Yeh 1989; Park 1992; Pradlwarter *et al.* 1988; Pradlwarter and Schuëller 1992). The method proposed by the author (Hurtado and Barbat 1996a) is studied from the point of view of accuracy in the chapter 5 after a detailed analysis of the nature and source of the errors when using the assumption of Gaussianity.

Finally, it must be said that alternative ways of linearization to the classical one that was exposed in the previous paragraph have been investigated. Among them the following are worth mentioning: the energy approach (Elishakoff and Colombi 1993), in which linearization is not perfomed on response but on energy error; higher order linearization (Naess and Johnsen 1991) which pursues the approximation to the nonlinear system by raising the order of the error norm; statistical quadratization (Donley and Spanos 1991), which is based on the use of Volterra series; linearization based on the crossing rate of the response process (Casciati *et al.*, 1993) or on the search of the system that best solves the Fokker-Planck equation (Polidori and Beck 1996). It must be said, however, that most of these recent developments in this field are not applicable to Markovian hysteretic oscillators, or only to limited situations in which they are involved, due to the fact that these models are built up at the very brim of mathematical discontinuity. The same comment applies to the methods for estimating the probability flow and evolution which are the subject of the chapter 7.

3.3.3 The hypothesis of Gaussian behaviour

An important property of the Gaussian density function has proven to be useful for calculating the expectations in equation (3.36). If a vectorial variable $\boldsymbol{Q}$ has a normal density, then it can be shown that the following property holds (Atalik and Utku 1976)

$$\mathrm{E}[\boldsymbol{Q}\boldsymbol{h}^{\mathrm{T}}(\boldsymbol{Q})] = \mathrm{E}[\boldsymbol{Q}\boldsymbol{Q}^{\mathrm{T}}]\,\mathrm{E}[\boldsymbol{\nabla}_{\boldsymbol{Q}}^{\mathrm{T}}\boldsymbol{h}(\boldsymbol{Q})] \tag{3.41}$$

under the following conditions:

1. $\boldsymbol{Q}$ is a jointly Gaussian vector with zero mean.
2. Function $\boldsymbol{h}(\boldsymbol{Q})$ has first partial derivatives with respect to the elements of vector $\boldsymbol{Q}$.
3. The inequality

$$|\boldsymbol{h}(\boldsymbol{Q})| < k \exp\left(\sum_{i=1}^{N} Q_i^{\delta}\right), \qquad \delta < 2 \tag{3.42}$$

holds for some arbitrary k. In Faravelli *et al.* (1988) it is demonstrated that these are also necessary conditions for the validity of equation (3.41). It must be observed that most nonlinear fuctions found in structural dynamics satisfy these requirements.

The main advantage arising form the supposition of normality of all the variables is that the calculation of the joint expectation of the responses $\boldsymbol{Q}$ and nonlinear forces $\boldsymbol{h}$ can be splitted into two parts corresponding to each of those terms. Substitution of (3.41) into (3.36) yields

$$\mathrm{E}[\boldsymbol{Q}\boldsymbol{Q}^{\mathrm{T}}]\boldsymbol{H}_{\mathrm{e}}^{\mathrm{T}} = \mathrm{E}[\boldsymbol{Q}\boldsymbol{Q}^{\mathrm{T}}]\,\mathrm{E}[\boldsymbol{\nabla}^{\mathrm{T}}\boldsymbol{h}(\boldsymbol{Q})] \tag{3.43}$$

which means that

$$\boldsymbol{H}_{\mathrm{e}}^{\mathrm{T}} = \mathrm{E}[\boldsymbol{\nabla}^{\mathrm{T}}\boldsymbol{h}(\boldsymbol{Q})] \tag{3.44}$$

if the inverse of the covariance matrix exists. This in turn requires that the state variables are not linearly dependent; otherwise, it is always possible to remove the redundant equations to obtain an equivalent system of reduced dimension. The particular expresions of the equivalent dynamic matrices are therefore the following:

$$m_{ij}^{\mathrm{e}} = \mathrm{E}\left[\frac{\partial h_i(\ddot{\boldsymbol{X}}, \dot{\boldsymbol{X}}, \boldsymbol{X})}{\partial \ddot{X}_j}\right] \tag{3.45a}$$

$$c_{ij}^{\mathrm{e}} = \mathrm{E}\left[\frac{\partial h_i(\ddot{\boldsymbol{X}}, \dot{\boldsymbol{X}}, \boldsymbol{X})}{\partial \dot{X}_j}\right] \tag{3.45b}$$

$$k_{ij}^{\mathrm{e}} = \mathrm{E}\left[\frac{\partial h_i(\ddot{\boldsymbol{X}}, \dot{\boldsymbol{X}}, \boldsymbol{X})}{\partial X_j}\right] \tag{3.45c}$$

3.3.4 Solution of the overall moment differential equations

The system matrix being already linearized, the evolution of the covariance matrix can then be calculated by solving the differential equation (3.20), which is here put in the form

$$\dot{\boldsymbol{\Sigma}}(t) = \boldsymbol{A}_{\mathrm{e}}(t)\boldsymbol{\Sigma}(t) + \boldsymbol{\Sigma}(t)\boldsymbol{A}_{\mathrm{e}}^{\mathrm{T}}(t) + 2\pi \boldsymbol{S}_{F}(t) \tag{3.46}$$

The system matrix has been denoted as $\boldsymbol{A}_{\mathrm{e}}(t)$ to indicate the equivalent linear nature of some or all of its elements. Notice that unlike the linear case the system matrix $\boldsymbol{A}_{\mathrm{e}}$ is now time-dependent because the linearized matrices $\boldsymbol{M}_{\mathrm{e}}, \boldsymbol{C}_{\mathrm{e}}$ and $\boldsymbol{K}_{\mathrm{e}}$ require the knowledge of expectations of the responses which are themselves functions of the system matrix as shown by the last equation. This interdependence between the system and the responses is a characteristic feature of nonlinear systems, as is well known. The calculation of the covariance evolution by means of the above equation will be called *direct method* to distinguish it from the *complex modal method* discussed in chapter 6. In the stationary case one has to solve the algebraic system

$$\boldsymbol{A}_{\mathrm{e}}\boldsymbol{\Sigma} + \boldsymbol{\Sigma}\boldsymbol{A}_{\mathrm{e}}^{\mathrm{T}} + 2\pi \boldsymbol{S}_{F} = \boldsymbol{0} \tag{3.47}$$

Taking into consideration the symmetry of the covariance matrix the last equation can be transformed into a system of linear equations of dimension $2N$, where N is the size of the system matrix. Alternatively, the algorithms proposed by Bartels and Stewart (1972) or Beavers and Denmann (1975) can be applied. However, Casciati *et al.* (1986) and Casciati and Venini (1994) report large overestimations of the response in the application of the former to nearly elatoplastic hysteretic systems and the impossibility of reaching a solution for purely elastoplastic ones.

Note that in the stationary problem it is necessary to iterate the value of the equivalent matrices for arriving at the solution. In nonstationary analysis the equivalent matrices obtained in a time step are used for calculating the mean and covariance matrices at the next, so that iteration is not required. Conventional algorithms for solving systems of differential equations such as Runge - Kutta, Adams - Moulton, etc. can be used without difficulty.

3.4 Reliability assessment based on second order information

By the expression *reliability assessment* it is generally meant the estimation of the probability that a system does not exceed a response level considered as critical for its performance. It is well known that a distinghising feature of the Gaussian over other probability density functions lies in the fact that

it is completely specified by first and second order moment information. This means that the reliability of a Gaussian system under any situation could be easily and exactly assessed on such basis. The random response of nonlinear systems is, however, non Gaussian even when excited by Gaussian forces. As a consequence, their reliability can only be estimated approximately if only first and second order information is available.

In random vibration theory many methods have been proposed to this purpose (see, e.g., Soong and Grigoriu 1993). In the present section a method due to Yang and Liu (1981) for the assessment of the probability distribution of maximum responses will be briefly summarized. The method constitutes a solid basis for estimating the performance and reliability of linear or nonlinear structural systems subject to nonstationary random loads.

Let X_{m} denote the maximum of a random variable X. Yang and Liu postulate the following Gumbel-type distribution function for a maximum ocurring between time instants t_1 and t_2 :

$$F(x_{\mathrm{m}}, t_1, t_2) = \exp\left[-\exp(-K^{\eta-1}(\frac{x_{\mathrm{m}}}{\epsilon} - K))\right] \tag{3.48}$$

where the parameters η and ϵ depend on the time instants t_1 and t_2 and the first two moments of the peaks ocurring in that interval. The latter are given by

$$\mu_{\mathrm{P}}(t_1, t_2) = \sqrt{\frac{\pi}{2}} \frac{1}{t_2 - t_1} \int_{t_1}^{t_2} \sigma_X(t)\mathrm{d}t \tag{3.49}$$

$$\sigma_{\mathrm{P}}^2(t_1, t_2) = \frac{\sqrt{2}}{t_2 - t_1} \int_{t_1}^{t_2} \sigma_X^2(t)\mathrm{d}t \tag{3.50}$$

where $\sigma_X(t)$ is the standard deviation of X. On the other hand, η and ϵ can be obtained by solving the following system of nonlinear equations:

$$\frac{\sigma_{\mathrm{P}}(t_1, t_2)}{\mu_{\mathrm{P}}(t_1, t_2)} = \frac{\left[\Gamma(\frac{2}{\eta} + 1) - \Gamma^2(\frac{1}{\eta} + 1)\right]^{\frac{1}{2}}}{\Gamma(\frac{1}{\eta} + 1)} \tag{3.51}$$

$$\mu_{\mathrm{P}}(t_1, t_2) = \epsilon \eta^{\frac{1}{\eta}} \Gamma(\frac{1}{\eta} + 1) \tag{3.52}$$

where $\Gamma(\cdot)$ is the Gamma function. The value of K is expressed in terms of the time-varying zero upcrossing rate of the process $\lambda^{\uparrow}(t)$, i.e. the mean rate at which the process crosses the time axis with positive slope:

$$K = \left[\eta \ln \int_{t_1}^{t_2} 2\lambda^{\uparrow}(t)\mathrm{d}t\right]^{\frac{1}{\eta}} \tag{3.53}$$

It has been reported that the use of the zero upcrossing rate of Gaussian processes gives satisfactory results. The latter is given by

$$\lambda^{\uparrow}(t) = \frac{\sigma_{\dot{X}}(t)\sqrt{1-\rho_{X\dot{X}}(t)^2}}{2\pi\sigma_X(t)} \tag{3.54}$$

where $\sigma_{\dot{X}}(t)$ is the standard deviation of the time derivative of X and $\rho_{X\dot{X}}$ the correlation coefficient of X and $\dot{X}$, as given by the second order analysis. Note that since the postulated distribution of the maximum is Gumbel, the mean and standard deviation of the maximum are

$$\mu_{X_{\mathrm{m}}}(t) = (K + 0.577K^{1-\eta})\epsilon \tag{3.55}$$

$$\sigma_{X_{\mathrm{m}}}(t) = \frac{\pi\epsilon}{\sqrt{6}K^{1-\eta}} \tag{3.56}$$

3.5 Consideration of model uncertainties

Classical random vibration analysis deals with deterministic structures subject to random external or parametric excitations. It is desirable, however, to enhance the scope of the second order analysis to include the effect of the uncertainties of the parameters defining the excitation or the structural models on some measures of the overall stochastic structural response, such as maximum displacement, damage indexes, etc.

Some aproaches have been proposed for an analysis of this type. For instance the *response surface method* (Box and Draper 1987; Casciati and Faravelli 1991) could be applied in this case. It consists in the realization of some planned numerical experiments, each one with combinations of some prescribed values of the uncertain quantities, and the fitting of an adequate function to the response of interest. For instance, a single numerical experiment would consist in the estimation of a expected maximum response, $\mathrm{E}[U]$ by means of the method of stochastic equivalent linearization using certain values of the excitation and

structural model parameters. Fitting a non linear surface by least-squares to the pairs $(\mathrm{E}[U], \boldsymbol{\theta})$, where $\boldsymbol{\theta}$ is the set of uncertain parameters, the resulting analytical relationship will serve as an indication on the sensitivity of each model parameter on the maximum displacement.

Another approach, directly linked to method of stochastic equivalent linearization has been proposed by Sues *et al.* (1985) and applied to specific situations by Socha (1986) and Socha and Zasucha (1991). It is based on the so-called *first order sensitivity method*, which has its roots on Taylor expansion of a certain vector variable $\boldsymbol{v}$ in the vicinity of the mean value of a vector of parameters $\boldsymbol{\theta}$, truncated at the first derivative:

$$\boldsymbol{v} = \boldsymbol{v}\Big|_{\boldsymbol{\mu}_{\boldsymbol{\theta}}} + \frac{\partial \boldsymbol{v}}{\partial \boldsymbol{\theta}}(\boldsymbol{\theta} - \boldsymbol{\mu}_{\boldsymbol{\theta}}) \tag{3.57}$$

Multiplying the above equation by its transpose and applying the expectation operator yields the following equation for the covariance of the variable:

$$\mathrm{E}[\boldsymbol{v}\boldsymbol{v}^{\mathrm{T}}] = \mathrm{E}[\boldsymbol{v}\boldsymbol{v}^{\mathrm{T}}]\Big|_{\boldsymbol{\mu}_{\boldsymbol{\theta}}} + \frac{\partial \boldsymbol{v}}{\partial \boldsymbol{\theta}}\mathrm{E}[\boldsymbol{\theta}\,\boldsymbol{\theta}^{\mathrm{T}}](\frac{\partial \boldsymbol{v}}{\partial \boldsymbol{\theta}})^{\mathrm{T}} \tag{3.58}$$

while the mean value of $\boldsymbol{v}$ corresponds simply to the result obtained using the mean value of $\boldsymbol{\theta}$, $\boldsymbol{\mu}_{\boldsymbol{\theta}}$, as can be seen by taking averages on equation (3.57).

This approach constitutes the fundamentals of the *perturbation method* widely used in the field of stochastic finite elements (Kleiber and Hien 1992). In the frame of random vibration analysis of structures by means of the equivalent linearization method, the perturbation technique can be used to analyse the sensitivity of the variance of the displacement with respect to the model parameters. The evolution of the covariance of the linearized state vector $\boldsymbol{Q}$ is governed by the differential equation

$$\dot{\boldsymbol{\Sigma}} = \boldsymbol{A}_{\mathrm{e}}\boldsymbol{\Sigma} + \boldsymbol{\Sigma}\boldsymbol{A}_{\mathrm{e}}^{\mathrm{T}} + \boldsymbol{S}_{\boldsymbol{F}} \tag{3.59}$$

Deriving this equation with respect to $\boldsymbol{\theta}$ the following equation for the evolution of the covariance sensitivity is obtained (Socha 1986) :

$$\frac{\partial \dot{\boldsymbol{\Sigma}}}{\partial \boldsymbol{\theta}} = \frac{\partial \boldsymbol{A}_{\mathrm{e}}}{\partial \boldsymbol{\theta}}\boldsymbol{\Sigma} + \boldsymbol{A}_{\mathrm{e}}\frac{\partial \boldsymbol{\Sigma}}{\partial \boldsymbol{\theta}} + \frac{\partial \boldsymbol{\Sigma}}{\partial \boldsymbol{\theta}}\boldsymbol{A}_{\mathrm{e}}^{\mathrm{T}} + \boldsymbol{\Sigma}\frac{\partial \boldsymbol{A}_{\mathrm{e}}^{\mathrm{T}}}{\partial \boldsymbol{\theta}} + 2\pi\frac{\partial \boldsymbol{S}_{\boldsymbol{F}}}{\partial \boldsymbol{\theta}} \tag{3.60}$$

which in the stationary case reduces to

$$\frac{\partial \boldsymbol{A}_{\mathrm{e}}}{\partial \boldsymbol{\theta}}\boldsymbol{\Sigma} + \boldsymbol{A}_{\mathrm{e}}\frac{\partial \boldsymbol{\Sigma}}{\partial \boldsymbol{\theta}} + \frac{\partial \boldsymbol{\Sigma}}{\partial \boldsymbol{\theta}}\boldsymbol{A}_{\mathrm{e}}^{\mathrm{T}} + \boldsymbol{\Sigma}\frac{\partial \boldsymbol{A}_{\mathrm{e}}^{\mathrm{T}}}{\partial \boldsymbol{\theta}} + 2\pi\frac{\partial \boldsymbol{S}_{\boldsymbol{F}}}{\partial \boldsymbol{\theta}} = \boldsymbol{0} \tag{3.61}$$

As can be observed in the above equation, for the computation of the evolution of the covariance sensitivity at time t the covariance itself must be known at the current time so that the two systems must be solved in parallel. Also, the calculation requires the knowledge of the derivatives of the elements of the linearized system matrix $\boldsymbol{A}_{\mathrm{e}}$ with respect to $\boldsymbol{\theta}$. The latter will be derived in chapter 5 for the specific case of the smooth hysteretic model linearized by the proposed non Gaussian approach.

Chapter 4

Gaussian linearization of hysteretic structures

4.1 Introduction

After presenting the basic concepts and equations of the method of stochastic equivalent linearization in the preceding chapter, the specific problems of its application to the estimation of the stochastic response of hysteretic structures when making use of the hypothesis of Gaussian behaviour will be dealt with in the present chapter. The emphasis will lie on the nonstationary analysis of a class of such systems inasmuch as higher errors are found in this class of problems than in stationary ones when using such hypothesis.

The chapter begins with a formal presentation of the hysteretic model which will be used in the rest of this work. The stochastic linearization of this model as resulting from the application of the assumption of Gaussianity is then derived and discussed. It is shown that, depending on the combination of load and system parameters in the case at hand, it can lead either to satisfactory or to quite erroneous results when compared to those afforded by Monte Carlo simulation. It must be observed that this is a theme on which there are opposite views published in the technical literature. While in some publications it is argued that the Gaussian method leads to moderate errors other report very large ones. This chapter is thus partly purported to shed light on this error scenario. Taking as reference the results of Monte Carlo simulation comparisons will be made of the results given by the conventional (Gaussian) method. The numerical study will show that there are situations in which the conventional method is reasonably accurate while in others errors as large as 300% are common.

4.2 Smooth Markovian models of hysteresis

The analysis of random vibration of structures performed in state space requires the formulation of the equations of motion in the form

$$\dot{\boldsymbol{Q}}(t) = \boldsymbol{g}(\boldsymbol{Q}; t) + \boldsymbol{F}(t) \tag{4.1}$$

where $\boldsymbol{Q}(t)$ is the state vector, $\boldsymbol{g}(\cdot)$ is a vector nonlinear function and $\boldsymbol{F}(t)$ is the external excitation. The Euler approximation of the derivative gives

$$\boldsymbol{Q}(t_{k+1}) = \boldsymbol{Q}(t_k) + h[\boldsymbol{g}(\boldsymbol{Q}; t_k) + \boldsymbol{F}(t_k)] \tag{4.2}$$

This formulation justifies the denomination of *Markovian* given to some hysteretic models presented in state space form, because the probabilistic description of any state can be completely derived from the knowledge of that corresponding to the preceeding time instant. (Li and Katsukura 1990; Rahman and Grigoriu 1994) For example, consider a bilinear system of mass, damping and stiffness constants denoted as m, c and k subject to a external excitation $p(t)$:

$$m\ddot{x}(t) + c\dot{x}(t) + \alpha k x(t) + (1-\alpha)kz = p(t) \tag{4.3}$$

Here α is a coefficient related to the post-yielding stiffness and z a function that controls the hysteretic behaviour. A Markovian decription of the latter has been proposed by Kobori *et al.* (1977) in a normalized space as

$$\dot{z} = \dot{x}[1 - H(\dot{x})H(z-1) - H(-\dot{x})H(-z-1)] \tag{4.4}$$

where $H(\cdot)$ is the Heaviside function, i.e.,

$$H(x) = \begin{cases} 0, & \text{if} \quad x < 0 \\ 1, & \text{if} \quad x \geq 0 \end{cases} \tag{4.5}$$

Similar but more involved piece-wise formulations have been proposed for other hysteretic models such as origin-oriented, peak-oriented, stiffness degrading, etc. (Rahman and Grigoriu 1994). Evidently, such piece-wise models are characterized by strong changes imposed by the Heaviside function. Therefore, the resulting hysteretic loops do not have the smooth appearance observed in laboratory tests of many structural materials. Furthemore, piece-wise models are difficult to extend to the case of biaxial hysteretic vibration. These reasons have fostered the development of some Markovian hysteretic models which use

smoother functions so that the resulting loops have a more realistic and elegant appearance. Such models are known as *smooth endochronic models.* They essentially are developments of an initial proposal by Bouc (1967).

In the present research smooth endocronic models have been preferred over piece-wise ones for several reasons. In first lieu, the estimations of the response statistics of the latter by equivalent linearization are by far more inaccurate when compared with Monte Carlo simulations than those of the former (Roberts and Spanos 1990). Also, when dealing with piece-wise models use must be made of functions of a lower order of continuity which pose numerical or mathematical difficulties when treated in a probabilistic frame. This is specially true for higher order methods such as those examined in chapter 7. Finally, the computation of the linearization matrices for piece-wise systems is more involved since they are not given by closed expressions as in the case of smooth models. Indeed, this is a desirable feature in nonstationary analyses of large structures.

4.2.1 Non degrading model

Instead of equation (4.4), the equation of the hysteretic component is in this case (Wen 1976)

$$\dot{z} = A\dot{x} - \beta|\dot{x}||z|^{n-1}z - \gamma\dot{x}|z|^{n} \tag{4.6}$$

where A, n, β and γ are parameters that define the size and shape of the hysteresis loops. More specifically A is related with the initial stiffness of the system as well as with the maximum level of the restoring force; n controls the smoothness of the transition from elastic to plastic behaviour in the (z, x) space, in such a way that the smaller n, the smoother the transition. A bilinear model corresponds to $n \to \infty$ and for modelling a perfectly elasto-plastic transition the condition $\alpha = 0$ must be added. On the other hand β represents the energy dissipation level, tending to zero for little dissipation. In fact, a null value of β corresponds to elastic behaviour. Finally γ defines the softening or hardening of the system together with β; the first condition corresponds to $\beta+\gamma > 0$ while the second to $\beta + \gamma \leq 0$. For the analyses that follow it is important to observe that in softening systems there is however a tendency to hardening when $\gamma < 0, |\gamma| < \beta$. Figure 4.1 illustrate the softening loops corresponding to cases in which the hardening tendency is absent $(\beta/\gamma = 1)$ and present $(\beta/\gamma = -2)$ for a system subject to a negatively damped harmonic force.

The softening case will be given more attention in this work because it is more usually found in earthquake engineering. The smooth endochronic model has mainly been applied to softening materials, i. e. those exhibiting saturation of the restoring force when deformation increases. An expression for the maxi-

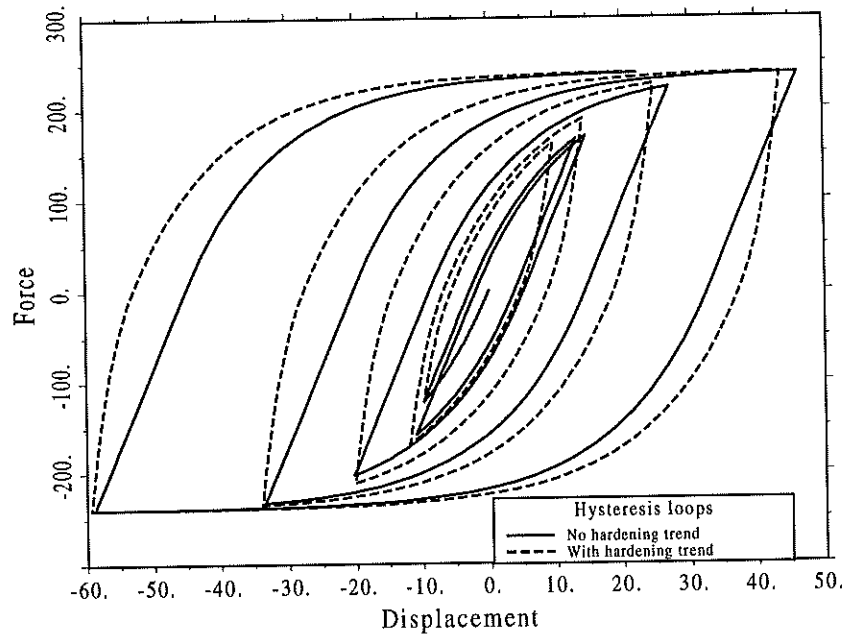

Figure 4.1 Hysteresis loops for softening systems with $\beta/\gamma = 1$ and $\beta/\gamma = -2$)

mum value reached by the auxiliary variable z, z_u, can be derived by setting to zero the derivative of z with respect to x:

$$\frac{dz}{d\dot{x}} = A - \beta\frac{|\dot{x}|}{\dot{x}}|z|^{n-1}z - \gamma|z|^n = 0 \tag{4.7}$$

For positive $\dot{x}$ and z the solution is

$$z_u = \left(\frac{A}{\beta+\gamma}\right)^{\frac{1}{n}} \tag{4.8}$$

which gives the following expression for the maximum achievable restoring force (or *strength*):

$$h_u = (1-\alpha)k\left(\frac{A}{\beta+\gamma}\right)^{\frac{1}{n}} \tag{4.9}$$

On the other hand, the initial stiffness k_0 of the system can be obtained by derivation, i.e.

$$k_0 = \left(\frac{\partial g}{\partial x}\right)_0 = \alpha k + (1-\alpha)k\left(\frac{\partial z}{\partial x}\right)_0 \tag{4.10}$$

or

$$k_0 = \alpha k + (1-\alpha)kA \tag{4.11}$$

Aditionally, the post-yielding stiffness for softening systems is

$$k_{\mathrm{f}} = \left(\frac{\partial g}{\partial x}\right)_{z_{\mathrm{u}}} = \alpha k + (1-\alpha)k\left(\frac{\partial z}{\partial x}\right)_{z_{\mathrm{u}}} \tag{4.12}$$

or

$$k_{\mathrm{f}} = \alpha k \tag{4.13}$$

The above equations allow the identification of the model parameters on the basis of experimental results (Sues *et al.* 1988).

The original derivation of this model is due to Bouc (1967). It did not included parameter n which was added by Wen (1976) for enhancing the applicability of the model to some common materials. Further refinements of the model have been proposed. Worth mentioning are those due to Baber and Wen (1981), who extended the model to include energy-based stiffness and strength degradation; the proposals by Noori *et al.* (1991) and Foliente *et al.* (1995), who included new terms to model also the phenomenon of pinching observed in reinforced concrete and masonry structures; the extension to the biaxial case proposed by Park *et al.* (1986) and Casciati and Faravelli (1988), which greatly contributed to the analysis of deterministic or random vibrations of spatial frames or base isolation devices under bidirectional excitations; and the proposals for modelling a hysteretic continuum and the formulation of the corresponding finite element strategy for its numerical analysis (Chang 1985; Casciati 1989; Simulescu *et al.* 1989). Some applications of different versions of the model in a random vibration context have been mentioned in the preceding chapter.

On the other hand, the model has been examined from the point of view of plasticity theory by several authors. Casciati and Faravelli (1991) have disclosed the connections between this model and the *endochronic theory of plasticity* whose main characteristic is that it makes no use of the concept of yield surface (Khan and Huang 1995). Also, the authors have pointed out the major drawback of the smooth model, which consists in the local violations of the

so-called *Drucker stability postulate* according to which the difference between the net work performed by external forces during the cycle of adding and removing stress is nonnegative (Shames and Cozzarelli 1992). The violation of this principle has been observed in the smooth endochronic model when the restoring force does not change sign. The main consequence of this violation from the external point of view is the appearance of some negative energy cycles which entails the introduction of an artificial plastic drift (Thyagarajan and Iwan 1990) (see figure 4.2).

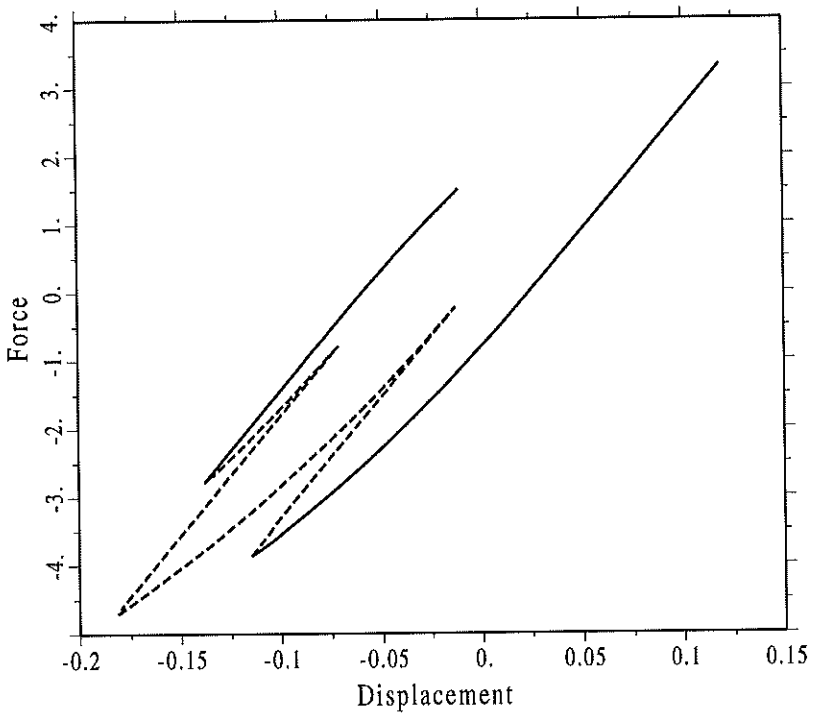

Figure 4.2 Artificial drift of the smooth endochronic system

An improved version of the model that attempts to reduce the effect of this drawback has been proposed by Casciati (1987a) in the form

$$\dot{z} = A\dot{x} - \beta|\dot{x}||z|^{n-1}z - \gamma\dot{x}|z|^{n} - (\epsilon|\dot{x}||z|^{\kappa-1} + \epsilon\dot{x}|z|^{\kappa}) \qquad (4.14)$$

where ϵ and κ are parameters. It has been argued, however, that for from the point of view of random vibrations the additional drift has minor relevance

(Wen 1991) and that the comparison of both models under stationary random vibration shows no significant discrepancies (Casciati and Faravelli 1991).

4.2.2 Degrading model

The above model has been extended to the case of systems exhibiting stiffness or strength degradation, which have been related with the dissipated energy or with the maximum deformation reached in previous states. The former type has been included into the endochronic model by Baber and Wen (1979) while an approach to the incorporate the latter was proposed by Sues *et al* (1988). In the present paragraph we will consider only the first case. An infinitesimal of the dissipated energy is

$$\mathrm{d}\varepsilon = (1-\alpha)kz\,\mathrm{d}x = (1-\alpha)kz\dot{x}\,\mathrm{d}t \tag{4.15}$$

which means that its evolution is governed by the following differential equation:

$$\dot{\varepsilon} = (1-\alpha)kz\dot{x} \tag{4.16}$$

According to equations 4.8 and 4.11 the strength of the system is controlled by A, n, β and γ while the contribution of the hysteretic component z to the initial stiffness is determined by A. If n is mantained constant along the deformation history (a reasonable assumption, since the hysteretic loops tend to exhibit a similar transition from elastic to plastic states, the level of degradation notwithstanding), the strength reduction will be controlled only by A, β and γ. In addition, if the energy-dependent variation of β and γ is collected into a single factor $\nu(\varepsilon)$, the value of the latter will have the meaning of a strength reduction only, while a factor $\eta(\varepsilon)$ affecting A, β and γ will produce strength as well as stiffness reduction. According to this reasoning, Baber and Wen (1981) proposed the following energy-based degrading model:

$$\dot{z} = \frac{A(\varepsilon)\dot{x} - \nu(\varepsilon)(\beta|\dot{x}||z|^{n-1} - \gamma\dot{x}|z|^{n})}{\eta(\varepsilon)} \tag{4.17}$$

If it is assumed that hysteretic energy changes slowly with time (an assumption valid even in case of strong earthquakes), it can additionally be supposed that functions $A(\varepsilon), \nu(\varepsilon)$ and $\eta(\varepsilon)$ vary also slowly in a monotonic manner, which suggests the adoption of the following first-order approximation of the evolution of the energy-dependent parameters:

$$A(\varepsilon) \approx \mu_A = A_0 - \delta_A\mu_\varepsilon \tag{4.18a}$$

$$\nu(\varepsilon) \approx \mu_\nu = \nu_0 + \delta_\nu \mu_\varepsilon \tag{4.18b}$$

$$\eta(\varepsilon) \approx \mu_\eta = \eta_0 + \delta_\eta \mu_\varepsilon \tag{4.18c}$$

In the above equation μ_A, μ_ν, μ_η and μ_ε are the mean values of the respective variables and δ_A, δ_ν and δ_η are parameters. As a rule ν_0 and η_0 are set equal to one.

4.3 Gaussian stochastic linearization

Having outlined the basic formulation of the method of stochastic equivalent linearization and its methods of solution in the preceding chapter we will devote the present paragraph to derive the expressions of the linearization coefficients of the Bouc-Wen hysteretic model.

Let us consider the case of a single degree of freedom structure whose restoring force is of the Bouc - Wen endochronic type. The results of the linearization can be readily used for larger structures such as buildings modelled as shear beams or frames with plastic hinges at the ends of the members (Casciati and Faravelli 1991). The equation of motion of such a system is

$$m\ddot{X} + c\dot{X} + \alpha k X + (1-\alpha) k Z = P(t) \tag{4.19}$$

where the nonlinear random variable Z is the solution of the following differential equation

$$\dot{Z} = h(\dot{X}, Z) = A\dot{X} - \beta|\dot{X}||Z|^{n-1} Z - \gamma \dot{X}|Z|^n \tag{4.20}$$

An stochastically equivalent equation will be looked for in the form

$$\dot{Z} = s_e X + c_e \dot{X} + k_e Z \tag{4.21}$$

where s_e, c_e and k_e are coefficients which are to be obtained by minimizing the expected value of the square of the error

$$\epsilon = h(\dot{X}, Z) - (s_e X + c_e \dot{X} + k_e X) \tag{4.22}$$

By proceeding in a similar fashion as it was done in the general formulation of the method and admitting the hypothesis of (marginal and joint) Gaussian behavior of all variables, the coefficients, making use of equation (3.44) are given by

$$s_e = \mathrm{E}\left[\frac{\partial h}{\partial X}\right] \tag{4.23a}$$

$$c_e = \mathrm{E}\left[\frac{\partial h}{\partial \dot{X}}\right] = \mathrm{E}\left[A - \beta\frac{\partial|\dot{X}|}{\partial \dot{X}}|Z|^{n-1}Z - \gamma|Z|^n\right] \tag{4.23b}$$

$$k_e = \mathrm{E}\left[\frac{\partial h}{\partial Z}\right] = \mathrm{E}[-\beta|\dot{X}|\frac{\partial}{\partial Z}|Z|^{n-1}Z - \gamma\dot{X}\frac{\partial}{\partial Z}|Z|^n\Big] \tag{4.23c}$$

Using the expressions of the one- and two-dimensional zero mean Gaussian density functions

$$\varphi_{\dot{X}}(\dot{x}) = \frac{1}{\sqrt{2\pi}\sigma_{\dot{X}}}\exp\Big(-\frac{\dot{x}^2}{2\sigma_{\dot{X}}^2}\Big) \tag{4.24a}$$

$$\varphi_{\dot{X}Z}(\dot{x},z) = \frac{1}{2\pi\sigma_{\dot{X}}\sigma_Z\sqrt{1-\rho_{\dot{X}Z}^2}}\exp\left(-\frac{1}{2(1-\rho_{\dot{X}Z}^2)}\left\{\frac{\dot{x}^2}{\sigma_{\dot{X}}^2} - \frac{2\rho_{\dot{X}Z}\dot{x}z}{\sigma_{\dot{X}}\sigma_Z} + \frac{z^2}{\sigma_Z^2}\right\}\right) \tag{4.24b}$$

and carrying out the derivatives and expectations, the following result is arrived at (Casciati and Faravelli 1991):

$$s_e = 0 \tag{4.25a}$$

$$c_e = A - \beta F_1 - \gamma F_2 \tag{4.25b}$$

$$k_e = -\beta F_3 - \gamma F_4 \tag{4.25c}$$

where the coefficients F_i, $i = 1, 2, 3, 4$ are given by

$$F_1 = \frac{\sigma_Z^n}{\pi}\Gamma\Big(\frac{n+2}{2}\Big)2^{n/2}I_s \tag{4.26a}$$

$$F_2 = \frac{\sigma_Z^n}{\sqrt{\pi}}\Gamma\Big(\frac{n+1}{2}\Big)2^{n/2} \tag{4.26b}$$

$$F_3 = \frac{n\sigma_{\dot{X}}\sigma_Z^{n-1}}{\pi}\Gamma\Big(\frac{n+2}{2}\Big)2^{n/2}\Big(2(1-\rho_{\dot{X}Z}^2)^{\frac{n+1}{2}} + \rho_{\dot{X}Z}I_s\Big) \tag{4.26c}$$

$$F_4 = \frac{n\rho_{\dot{X}Z}\sigma_{\dot{X}}\sigma_Z^{n-1}}{\sqrt{\pi}}\Gamma\left(\frac{n+1}{2}\right)2^{n/2} \tag{4.26d}$$

with

$$I_s = 2\int_{\ell}^{\pi/2} \sin^n\theta \mathrm{d}\theta \tag{4.27}$$

$$\ell = \tan^{-1}\left(\frac{\sqrt{1-\rho_{\dot{X}Z}^2}}{\rho_{\dot{X}Z}}\right) \tag{4.28}$$

It must be noted that no closed expressions such as these can be obtained for piece-wise hysteretic models, in whose case the linearization coefficients are tipically expressed through integrals that should be solved at each time step in nonstationary analyses (Roberts and Spanos 1990). In the more general case of the degrading uniaxial model proposed by Baber and Wen (1979), the equation of the dynamics of the hysteretic component reads

$$\dot{Z} = \frac{A\dot{X} - \nu(\beta|\dot{X}||Z|^{n-1}Z - \gamma\dot{X}|Z|^n)}{\eta} \tag{4.29}$$

and the linearization coefficients, calculated according to the Gaussian assumption can be obtained as

$$c_e = \mathrm{E}\left[\frac{1}{\eta}\left[\frac{\partial A}{\partial \dot{X}}\dot{X} + A - \frac{\partial \nu}{\partial \dot{X}}(\beta|\dot{X}||Z|^{n-1}Z + \gamma\dot{X}|Z|^n) - \nu(\beta\frac{\partial|\dot{X}|}{\partial\dot{X}}|Z|^{n-1}Z + \right.\right.$$

$$\left.\left.\gamma|Z|^n)\right] - \frac{\partial\eta}{\partial\dot{X}}\left[\frac{A\dot{X} - \nu(\beta|\dot{X}||Z|^{n-1}Z + \gamma\dot{X}|Z|^n}{\eta^2}\right]\right] \tag{4.30a}$$

$$k_e = \mathrm{E}\left[\frac{1}{\eta}\left[\frac{\partial A}{\partial Z}\dot{X} - \frac{\partial \nu}{\partial Z}(\beta|\dot{X}||Z|^{n-1}Z + \gamma\dot{X}|Z|^n) - \nu(\beta|\dot{X}|\frac{\partial}{\partial Z}(|Z|^{n-1}Z) + \right.\right.$$

$$\left.\left.\gamma|\dot{X}|\frac{\partial}{\partial Z}(|Z|^n))\right] - \frac{\partial\eta}{\partial Z}\left[\frac{A\dot{X} - \nu(\beta|\dot{X}||Z|^{n-1}Z + \gamma\dot{X}|Z|^n}{\eta^2}\right]\right] \tag{4.30b}$$

These expressions are more difficult to solve in explicit form than those of the nondegrading case due to the presence of the expectations of partial derivatives of the parameters that control the degradation, i.e., A, ν y η. Nevertheless, if it is assumed that these parameters exhibit a low variation with time (which corresponds to the physical fact that degradation takes place in a slow manner and is represented by little values of δ_A, δ_ν and δ_η) their mean values μ_A, μ_ν y μ_η can be used in each time step of the calculation instead of their actual values. In that case the non linear component of the hysteretic system evolves according to the following approximate equation

$$\dot{Z} \approx \frac{\mu_A \dot{X} - \mu_\nu(\beta|\dot{X}||Z|^{n-1}Z - \gamma\dot{X}|Z|^n)}{\mu_\eta} \tag{4.31}$$

whose linearization leads to

$$c_e = \frac{\mu_A - \mu_\nu(\beta F_1 + \gamma F_2)}{\mu_\eta} \tag{4.32a}$$

$$k_e = \frac{-\mu_\nu(\beta F_3 + \gamma F_4)}{\mu_\eta} \tag{4.32b}$$

where functions F_i, $i = 1, 2, 3, 4$ are given by equations (4.26) while the mean values of the degrading parameters can be calculated as functions of the mean dissipated energy by equations (4.18).

4.4 Error sources

The stochastic linearization of the hysteretic system exposed above hinges upon the assumption of Gaussian behaviour of all the variables of the model. It has been pointed out that such hypothesis leads in some cases to reasonably good estimations of the second order response when compared with the results of Monte Carlo simulation, which can be considered as the best approximation to the true probabilistic measure of the response. Such is the case, for example, of the calculation of stationary response of structures subject to filtered or unfiltered white noise (Baber and Wen 1981; Roberts and Spanos 1990). In other instances, however, large discrepancies can be found between the Monte Carlo results and those of the conventional method based on the assumption of Gaussianity (Pradlwarter and Schuëller 1991; Park 1992). The errors concern mainly the nonstationary estimation of displacement statistics which is one of the most important variables in practical design. The standard deviation of velocities and hysteretic forces, as well as the covariances are reasonably well

estimated. The following is a description of the error sources in the estimation of displacement statistics based on the published literature on the subject as well as on the author's own experience.

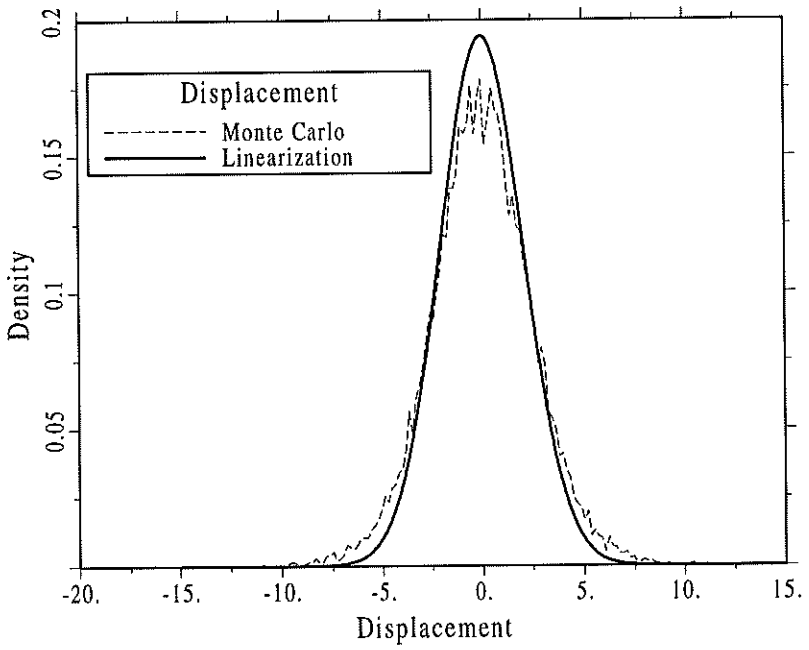

Figure 4.3 Density function of displacement response

4.4.1 Probability density assumption

The most evident cause of error lies in the assumption of Gaussianity of all the variables as such. Figures 4.3 to 4.5 ilustrate the probability density functions of the displacement, velocity and restoring force of a strongly nonlinear uniaxial hysteretic system subject to white noise calculated by Monte Carlo simulation (10,000 samples) together with the corresponding Gaussian densities depicted with the information obtained by stochastic linearization with Gaussian assumption. It can be seen that while Gaussianity is reasonably admissible for displacement and velocity, as far as only second order information is concerned, it is clearly inadequate for the hysteretic component Z. In fact, when vibrating in the nonlinear range the hysteretic component of a softening system

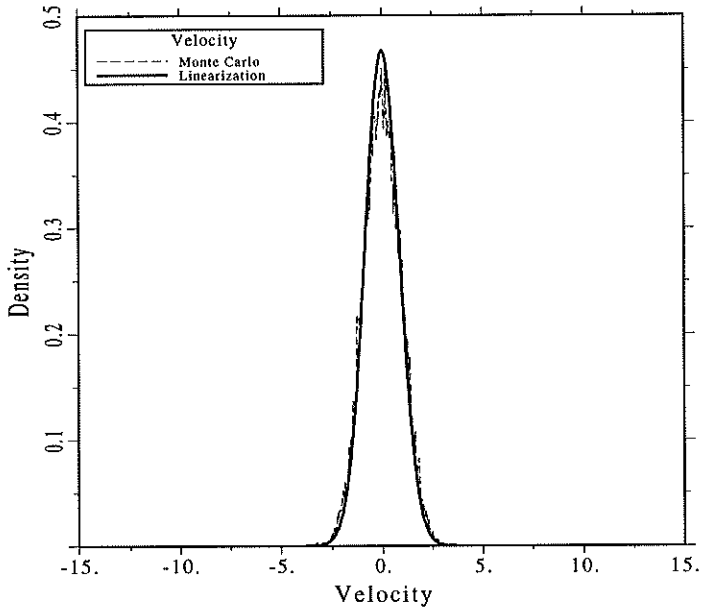

Figure 4.4 Density function of velocity response

equals its maximum z_u for large periods of time with the consequence that the density function presents a concentration at its maximum, as shown in figure 4.5.

4.4.2 Drift motion

A second – and perhaps, the most important – cause of errors lies in the tendency of some hysteretic systems to drift, that is, to exhibit an erratic trend to vibrate temporaly in one of the two sides of the displacement axis so that the hysteretic loops have the appearance shown in figure 4.6. Therefore, drift consitutes an underlying low-frequency motion that can be thought of as a Brownian motion of the kind of that illustrated by figure 1.3 (Iwan and Paparizos 1988). For random vibration analyses this trend implies that local non zero mean vibration occurs and, consequently, the power spectral density of the displacement response exhibits a large peak at zero frequency (Iwan and Paparizos 1988; Donley and Spanos 1991). This makes highly inaccurate the reliability assessment of the structure in the stationary state, which is based on

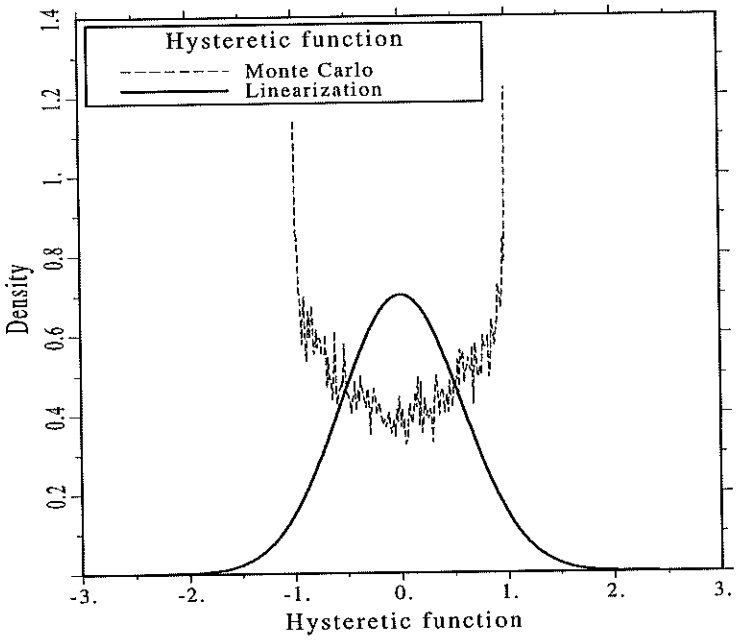

Figure 4.5 Density function of Z

the power spectrum of the response. For piece-wise or smooth hysteretic models this phenomenon is the stronger, the lower the value of α, i.e., the nearer the system is to the perfectly elasto-plastic case (Park 1992). The typical shape of the displacement response of a hysteretic system with low and high α when subject to unmodulated excitation are those illustrated by figure 4.7. It can be seen that while the latter achieves rapidly a stationary state, the displacement of the former increases monotonically. However, the size of the errors of the Gaussian method brought about by drift are tightly linked to the excitation spectrum as explained in the following.

4.4.3 Excitation model

The response estimates derived from the assumption of Gaussianity are also greatly influenced by the type of power spectrum and its associated evolutionary features. In fact, for purely white noise low frequency waves will tend to produce drift irrespective of the hardening ratio α, whose slope, at least, is reasonably well detected by the Gaussian method. In contrast, when low-cut filters are introduced (as in the Clough-Penzien or Iwan-Paparizos seismic models) the Gaussian method becomes unable to detect the system's drift, and consequently

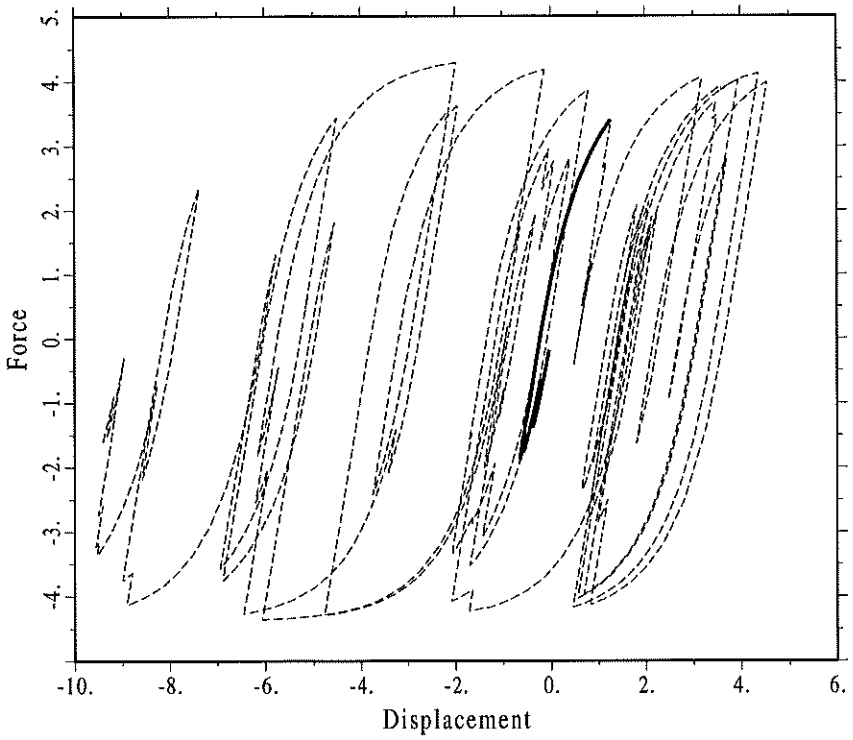

Figure 4.6 Drift of a system with null yield ratio

the errors in the displacement estimation grow as far as the excitation remains in stationary state. This is illustrated by comparing figures 4.8 and 4.9 which correspond respectively to an hysteretic system with drift-enforcing, null value of α subject to white noise and Clough-Penzien excitations. It can be seen that under purely white excitation the Gaussian method gives qualitatively better results than in the Clough-Penzien case, at which the method does not follow the displacement trajectory anymore. When a modulating function is introduced in connection to the Clough-Penzien filter, as a realistic model of seismic action, the errors can be as large as 300 percent, as figure 4.10 shows. Notice that in cases like this the Gaussian method not only fails in capturing the peak value but also in assessing the correct shape of the response. As a matter of fact, since the Gaussian method is unable to trace the drift errance in such cases, it becomes entirely governed by the modulating function, as made evident by the vivid resemblance of the shape of the response to that of the modulating function shown in figure 2.4 (long duration case) which was used in this analysis. Note that for many materials, such as reinforced concrete,

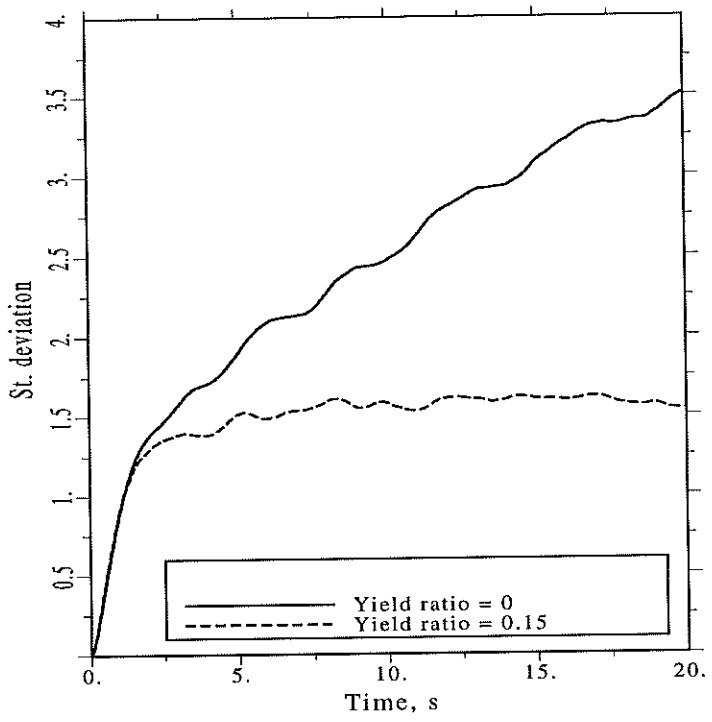

Figure 4.7 Effect of yield ratio on displacement drift

steel (Sues *et al.* 1988) or soil (Pires *et al.* 1983) very low values of α have been proposed, so that some amount of drift can be expected in their response. Inasmuch as the reliability assessment is based on the whole evolution of the level crossing rate (see chapter 3), the importance of estimating correctly the whole evolution of the response moments needs not to be emphasized.

The reason for such a different sensitivity of the method with respect to drift under white noise or Clough-Penzien excitations lies in the search of an equivalent linear system as such. In fact, for a linearized Bouc-Wen SDOF system having the dynamics

$$\ddot{x} + 2\bar{\nu}\bar{\omega}\dot{x} + \alpha\bar{\omega}^2 x + (1-\alpha)\bar{\omega}^2 z = a \tag{4.33a}$$

$$\dot{z} = c_e\dot{x} + k_e z \tag{4.33b}$$

where $a(t)$ is a white noise of acceleration units, the squared modulus of the transfer function of the displacement is

$$|H_X(\mathrm{i}\omega)^{\mathrm{W}}|^2 = \frac{1}{\left(-\omega^2 + \alpha\bar{\omega}^2 + \frac{(1-\alpha)\bar{\omega}^2\omega^2 c_e}{\omega^2+k_e}\right)^2 + \left(2\bar{\nu}\bar{\omega}\omega - \frac{(1-\alpha)\bar{\omega}^2\omega c_e k_e}{\omega^2+k_e}\right)^2} \tag{4.34}$$

Therefore, the power spectral density of the displacement is given by

$$G_X(\omega) = |H_X^{\mathrm{W}}(\mathrm{i}\omega)|^2 G_W \tag{4.35}$$

It can be seen that

$$G_X(\omega) \to \frac{G_W}{\alpha^2\bar{\omega}^4} \tag{4.36}$$

as $\omega \to 0$. This explains why the linearized system is able to detect the low-frequency drift motion to some extent. On the other hand, when $a(t)$ is modelled according to the Clough-Penzien spectrum, we have

$$G_X(\omega) = |H_X^{\mathrm{W}}(\mathrm{i}\omega)|^2 |H^{\mathrm{CP}}(\mathrm{i}\omega)|^2 G_W \tag{4.37}$$

where the modulus of the transfer function of the Clough-Penzien filter is given by equation (2.8):

$$|H^{\mathrm{CP}}(\mathrm{i}\omega)|^2 = \frac{\omega^4}{(\omega_f^2 - \omega^2)^2 + 4\nu_f^2\omega_f^2\omega^2} \times \frac{\omega_g^4 + 4\nu_g^2\omega_g^2\omega^2}{(\omega_g^2 - \omega^2)^2 + 4\nu_g^2\omega_g^2\omega^2} \tag{4.38}$$

It can be observed that unlike the white noise case the displacement power spectrum will always tend to zero along with the frequency. This has the important consequence that when subject to the Clough-Penzien excitation the linearized system will always filter away the low frequency responses, the values of the model or excitation parameters notwithstanding. Together with the increasing importance of drift as $\alpha \to 0$, this points out that, in practical cases, the highest errors of the method of stochastic linearization occur for excitation models with low-cut filters and null post-yield ratio, as that of figure 4.10.

Since the above has been demonstrated to be a drawback of linearization as such, a clear way of overcoming it would be the application of equivalent non-linearization techniques (Lin and Cai 1995). However, in such case the practical appealing of the linearization techniques will be lost and, generally speaking, equivalent non-linearization is not practical for MDOF systems. To cope with

cases like this the only way for keeping in use linearization techniques is the employment of non Gaussian densities. In fact, since under Gaussian inputs linear sytems behave as Gaussian, the modification of this distribution for the response can be managed to compensate in some way for the drawbacks of the linearization as such. As will be shown in the next chapter, the proposed non Gaussian method accomplish this task reasonably well.

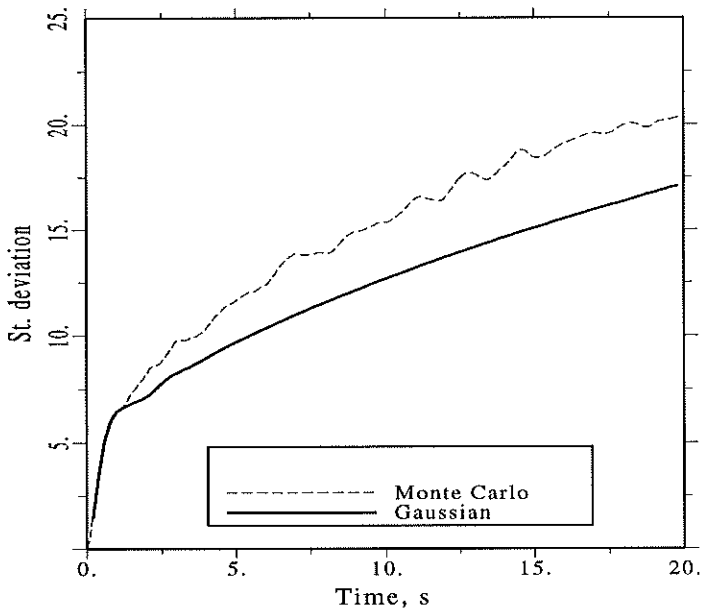

Figure 4.8 Gaussian response estimation under white noise excitation for $\alpha = 0$

4.4.4 Nonlinearity degree of the response

A third cause of errors is the level of nonlinearity of the response (Roberts and Spanos 1990). In fact, for very low or very large excitation levels (as measured by the power spectral density function of the input noise) the response of the hysteretic system is clearly narrow band, because the structure responses either in the linear or in the nonlinear ranges. When subject to a middle strenght excitation the response shows a larger width, with the consequence that the any assessment on the probability density of the displacement be it Gaussian or non-Gaussian is more uncertain. By stationary analyses that scan the physically relevant intensity range of white excitation it has been demonstrated, however, that this type of error affects mainly the response estimations of piece-wise

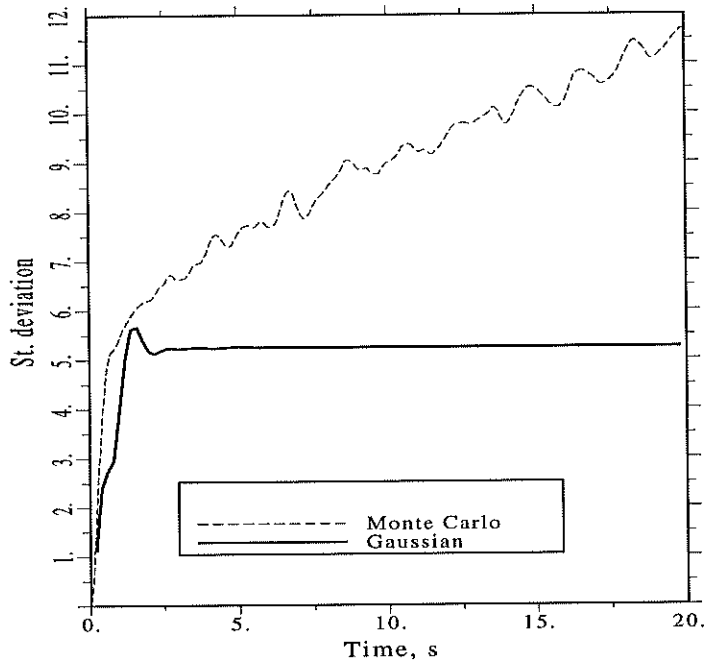

Figure 4.9 Gaussian response estimation under Clough-Penzien seismic excitation for $\alpha = 0$

rather than those of smooth hysteretic models, for which these errors seem to be of minor importance (Baber and Wen 1981; Roberts and Spanos 1990). Nevertheless, when nonstationarity is considered, this kind of errors reappear and, generally speaking, they are the larger, the higher the nonlinearity degree of the response. This issue will be illustrated in more detail by the numerical analyses of the next chapter.

For explaining the diverse accuracy of both stationary and nonstationary calculations it must be taken into account that (a), in the latter case the response is always wide-band and (b), their numerical procedures are rather different, the former proceeding by time-independent iteration and the latter by solving a system of differential equations in which the response at any instant depends on the whole estimated evolution. Accordingly, one could regard the nonstationary problem as one more dependent on the assumption of Gaussianity than the stationary one. Since Gaussianity means linearity in this context, due to the fact that the response of a linear system to Gaussian input is always Gaussian, it is clear that when the structural model in nonstationary calculation begins to depart from linearity it also departs from Gaussianity and thus

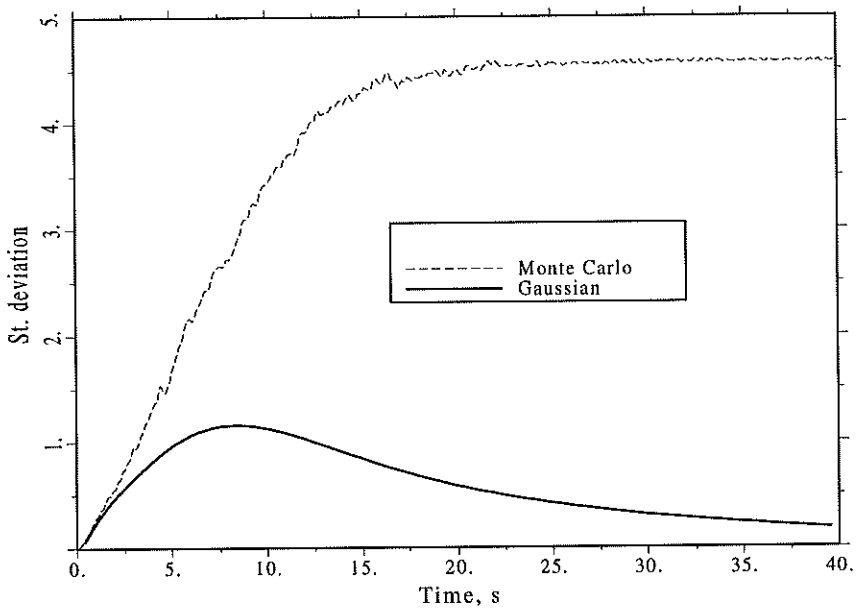

Figure 4.10 Gaussian response with modulated Clough-Penzien excitation ($\alpha = 0$)

the accuracy of future estimations under such hypothesis will depend on the degree of nonlinearity of the response.

4.4.5 Loop shape

Last but not least, the shape of the hysteretic loops, as defined by the model parameters has an important influence on the errors of the Gaussian method. As was said before softening behaviour takes place whenever $\beta+\gamma > 0$, but there is nonetheless an intrinsic tendency to hardening if $\gamma < 0, |\gamma| < \beta$ (see figure 4.1). Despite the overall response of the system seems not to be not seriously affected by such details from a deterministic point of view, it is intuitively clear that the loop shape imposes a different probability distribution for the variable Z. In the numerical analyses discussed at the next chapter it will be shown that, in fact, the hardening tendency has an important influence on the errors brought about by the Gaussian assumption. In particular, in the present research it has been found that the underestimation of the displacement response when using such an assumption is lower is systems with hardening tendency than in the opposite case under white excitation. It is important to note that the confussion regarding the accuracy of the conventional Gaussian method of

stochastic linearization when applied to hysteretic systems is partly due to the fact that the influence of the loop shape has been overlooked. Softening models with hardening tendency has been proposed for reinforced concrete (Sues *et al.* 1988), lead-rubber isolation devices (Constantinou *et al.* 1985) and bridge rubber bearings (Li *et al.*, 1994). Purely softening systems, i.e. those without hardening tendency have been proposed for steel (Sues *et al.* 1988), clay and sand (Pires *et al.* 1983) and lead-rubber bearings (Yang *et al.* 1992a, b).

The above error sources work together in producing a single discrepancy between Monte Carlo and analytical results derived from the Gaussian assumption in each specific case, so that the determination of their proportions, with the aim of correcting the Gaussian results by empirical factors, would require an extensive and tedious parametric study before applying them. A more direct approach is presented in the next chapter.

Chapter 5

Non-Gaussian linearization of hysteretic structures

5.1 Introduction

The objective of this chapter is to introduce a non-Gaussian approach aimed at obtaining better response estimations than those given by the Gaussian one without significant increase of the light computational effort required by the latter. To such purpose the proposed method makes use of mixed Gauss-Dirac density functions, in which the Dirac pulses play the role of weigths that modify the linearization coefficients obtained at each step in dependence of the current degree of response nonlinearity. The derivation of the method as well as the numerical study shows that it not only is superior over the conventional Gaussian approach but also over some proposals which are either not so accurate or are much more involved from the computational viewpoint.

5.2 Proposed non-Gaussian linearization approach

It has been demonstrated that if the true multidimensional density function of the vectorial response $\boldsymbol{Q}$ were used in the linearization procedure (equation 3.36) the estimated responses by stochastic linearization would be exact (Roberts and Spanos 1990). Since such an information is not available beforehand and, if it were, the determination of second order responses by stochastic linearization would be superfluous, it is necessary to devise methods for estimating the joint density function as closer to the true one as possible. Attempts in this direction have been undertaken by some researchers. For instance, Pradlwarter and Schuëller (1991) have proposed the use of a nonlinear transformation of the density of the hysteretic component, together with the application of the Nataf method (Nataf 1963) to estimate the joint density functions required to calculate the linearization coefficients. Since the target density of the hysteretic

component is not known in advance the realization of some Monte Carlo simulations is proposed to fill this gap. In case of real structural systems the latter device will, of course, largely increase the computational effort. However, when the nonlinear trasformation is not applied the method still produces important errors in the estimation of displacements (Pradlwarter and Schuëller 1992). On the other hand Kimura *et al.* (1994) proposed the use of a truncated Gaussian density combined with Dirac pulses to simulate the effect of the concentration at the maximum values of the hysteretic component as mentioned before. The method proposed here is a variant of this approach. Instead of truncating the Gaussian density, it is combined with the Dirac pulses in its entire form both in the marginal and joint situations. The advantages derived from such an approach over the last mentioned proposal will be explicited in the folllowing paragraph. The basics of the algorithm as well as the preliminary experiences in its use appeared in Hurtado and Barbat (1996a).

Before entering in a detailed exposition of the proposed approach mention must be done of a different way of upgrading the statistics deriving from the Gaussian assumption, which consists in the use of empirical factors and equations. An important method of this kind is due to Park (1992), who proposed the use of some coefficients obtained through intensive Monte Carlo simulations. A similar approach was adopted by Yeh (1989) to the specific case of hysteretic spatial buildings modelled as shear beams. The accuracy of Park's method will ocassionally be tested in the numerical analyses.

5.2.1 Non-Gaussian densities

As mentioned in the preceding, the concentration of values of the hysteretic restoring force in the vicinity of its maximum z_u suggests the use of a mixed density of the type

$$f_Z(z) = (1-2p)\varphi_Z(z) + p\delta(z-z_u) + p\delta(z+z_u) \tag{5.1}$$

where p is a weighting coefficient. Note that the Dirac pulses play the role of a correcting mass intended to modify the second statistical moment, which is equivalent to area's moment of inertia. Besides, the value of the coefficient p is selected in such a way that it give the best approximation to the Monte Carlo results in standard cases.

The calculation of the linearization matrices requires the knowledge of joint density functions of the pairs (X,Z) and $(\dot{X},Z)$. Denoting by V either of X or $\dot{X}$, they are succintly expressed as

$$f_{VZ}(v,z) = (1-2p)\varphi_{VZ}(v,z) + p\delta(z-z_u)\varphi_V(v) + p\delta(z+z_u)\varphi_V(v) \tag{5.2}$$

in such a way that the integration with respect to x or $\dot{x}$ will give the marginal density of the hysteretic component (equation 5.1). On the other hand, taking into account the aforesaid about the first error source of the conventional method, variables X and $\dot{X}$ can be assumed to remain jointly Gaussian. Note that for separating the contributions of the Gaussian and Dirac parts a dummy splitting of their density functions is needed, i.e.

$$f_V(v) = (1-2p)\varphi_V(v) + 2p\varphi_V(v) \tag{5.3a}$$

$$f_{X\dot{X}}(x,z) = (1-2p)\varphi_{X\dot{X}}(x,\dot{x}) + 2p\varphi_{X\dot{X}}(x,\dot{x}) \tag{5.3b}$$

Note also that the linearity of the above assumed densities and the use of the entire Gaussian densities allow making use of the Gaussian coefficients, whose closed-form expressions are an important prerogative of this model in most of its versions.

5.2.2 Consistency requirements

It is important ot observe that p is constrained by an upper bound. In fact, any density function must satisfy the so-called *Pearson criterion* (Tikhonov 1982; Johnson *et al.* 1994),

$$\frac{\mu_4}{\mu_2} \geq \frac{\mu_3^2}{\mu_2^3} + 1 \tag{5.4}$$

where μ_i is the central moment of order i. Notice that for symmetric densities $\mu_3 = 0$ and for the Gaussian distribution in particular $\mu_4 = 3\mu_2^2$. Taking moments with the proposed non-Gaussian density function and substituting these expressions into the preceding equation yields the following upper bound to the weighting coefficient:

$$p \leq \frac{1}{3 - \frac{z_u^4}{\sigma_Z^4}} \tag{5.5}$$

Note that $p \to 0$ for low levels of response (as defined by $\sigma_Z \to 0$), while $p \to 1/3$ for intense responses ($\sigma_Z \to \infty$). Also note that there is no lower bound. This means that p can be a bounded positive number or a negative one. In fact, negative p values have been found to be more adequate for improving the

accuracy of the linearization method applied to the hysteretic models studied herein.

Also, inasmuch as the Gaussian function is completely determined by moments of the first two orders, additional consistency requirements must be satisfied by the latter. In particular, using equation (5.33) the variance of the hysteretic variable Z is

$$\mathrm{E}[Z^2] = (1-2p)\sigma_Z^2 + 2p\,z_u^2 \tag{5.6}$$

so that the linearization coefficients must be calculated using

$$\sigma_Z^2 = \frac{\mathrm{E}[Z^2] - 2pz_u^2}{(1-2p)} \tag{5.7a}$$

Similarly, the following relationships are obtained:

$$\sigma_{XZ} = \frac{\mathrm{E}[XZ]}{(1-2p)} \tag{5.7b}$$

$$\sigma_V^2 = \mathrm{E}[X^2] \tag{5.7c}$$

$$\sigma_{X\dot{X}} = \mathrm{E}[X\dot{X}] \tag{5.7d}$$

where V stands for X or $\dot{X}$ and the expectations are obtained from the solution of the covariance response. Note that for satysfying these consistency requirements when using truncated Gaussian densities, as in the approach by Kimura *et al.* (1994), a system of nonlinear equations must be solved in order to find these covariances at each time step.

5.2.3 Linearization coefficients

Substituting equations (5.1) to (5.3) into (3.36) yields the folowing vector of linearization coefficients:

$$\boldsymbol{H}_e^{\mathrm{T}} = [s_e,\ c_e,\ k_e] = (1-2p)\ [s_g,\ c_g,\ k_g] + 2p\ [s_d,\ c_d,\ k_d]\boldsymbol{\Pi}^{-1} \tag{5.8}$$

Here the subindexes 'g' and 'd' denote Gaussian and Dirac parts, respectively, and in the general MDOF case the 3×3 matrix $\boldsymbol{\Pi}$ is built up with the elements of the covariance response $\boldsymbol{\Sigma}$ corresponding to the degree of freedom at hand, i.e.

$$\boldsymbol{\Pi} = \mathrm{E}\begin{pmatrix} X^2 & X\dot{X} & XZ \\ \dot{X}X & \dot{X}^2 & \dot{X}Z \\ ZX & Z\dot{X} & Z^2 \end{pmatrix} \tag{5.9}$$

The calculation of the Dirac linearization coefficients yields

$$s_{\mathrm{d}} = \sigma_{X\dot{X}}(A - \gamma z_{\mathrm{u}}^n) \tag{5.10a}$$

$$c_{\mathrm{d}} = \sigma_{\dot{X}}^2(A - \gamma z_{\mathrm{u}}^n) \tag{5.10b}$$

$$k_{\mathrm{d}} = -\sigma_{\dot{X}}\beta z_{\mathrm{u}}^{n+1}\sqrt{\frac{2}{\pi}} \tag{5.10c}$$

while those corresponding to the Gaussian part are given by equation (4.25); in both cases use must be made of the consistency requirements (5.7). Note that the new additional coefficients are given in closed form, while their evaluation in the approach by Kimura *et al.* (1994) requires the calculation of several double integrals at each step. Notice also that the method is readily applicable to degrading systems under the condition that the values

$$\bar{A} = \frac{\mu_A}{\mu_\eta} \tag{5.11a}$$

$$\bar{\beta} = \beta\frac{\mu_\nu}{\mu_\eta} \tag{5.11b}$$

$$\bar{\gamma} = \gamma\frac{\mu_\nu}{\mu_\eta} \tag{5.11c}$$

be used instead of A, β and γ, respectively.

5.2.4 Weighting coefficient

The application of the present approach requires the assignation of a weighting coefficient p for the Dirac and Gaussian parts. Since the response in the elastic range is Gaussian, the coefficient could be put in relationship with the portion of the area of the Gaussian density $\varphi_Z(z)$ lying beyond the limiting value z_{u}, due to the fact that this portion is an indirect measure of the error in modelling the nonlinearity of the stochastic response using Gaussian density. Several alternatives for the coefficient p were tested, namely, those based on the dissipated energy ε as well as on the excess of probability mass,

$$p = r \int_{-\infty}^{z_u} \varphi_Z(z)\mathrm{d}z = r\Phi_Z(-z_u) \tag{5.12}$$

variance,

$$p = \frac{r}{\sigma_Z^2} \int_{z_u}^{\infty} z^2 \varphi_Z(z)\mathrm{d}z = \frac{r}{\sqrt{\pi}} \Gamma^c\left(1.5, \frac{z_u^2}{2\sigma_Z^2}\right) \tag{5.13}$$

kurtosis,

$$p = \frac{r}{3\sigma_Z^4} \int_{z_u}^{\infty} z^4 \varphi_Z(z)\mathrm{d}z = \frac{2r}{3\sqrt{\pi}} \Gamma^c\left(2.5, \frac{z_u^2}{2\sigma_Z^2}\right) \tag{5.14}$$

and averages between them. In the preceding equations r is constant whose value is determined on empirical basis and $\Gamma^c(a,x)$ is the complementary incomplete Gamma function,

$$\Gamma^c(a,x) = \int_x^{\infty} y^{a-1} e^{-y} \mathrm{d}y \tag{5.15}$$

After many numerical analyses performed with this algorithm, varying load and model parameters, it was found that the excess-mass criterion were the most stable in the sense that its associated coefficient r was the least influenced by the several conditions imposed on the random vibration of the hysteretic system, such as response level, type of excitation, nonstationarity, etc. This coefficient will be discussed in more detail in the numerical study that follows.

5.3 Numerical study

In order to demonstrate the adequacy of the proposed approach to give good estimates of the stochastic response several numerical analyses were performed on a family of Bouc - Wen oscillators subject to different types of excitations. The parameters of the system and loads were succesively varied in order to gain insight into the factors most influential on the errors of the conventional method and the ability of the present approach to improve the estimations.

The structural mass was set equal to unity and no viscous damping was considered. Two very different types of excitations were used, namely white noise base acceleration with one-sided, constant power spectral density $G_W = 2S_W = 288\,\mathrm{cm}^2/\mathrm{s}^3$, and the Clough - Penzien double filter described in chapter

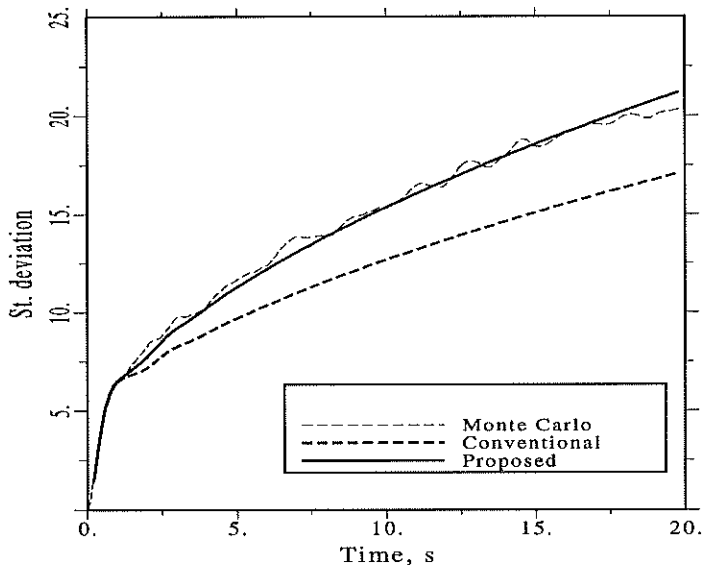

Figure 5.1 Displacement response under white noise. $T = 1.5$, $R = 10$, $\alpha = 0$

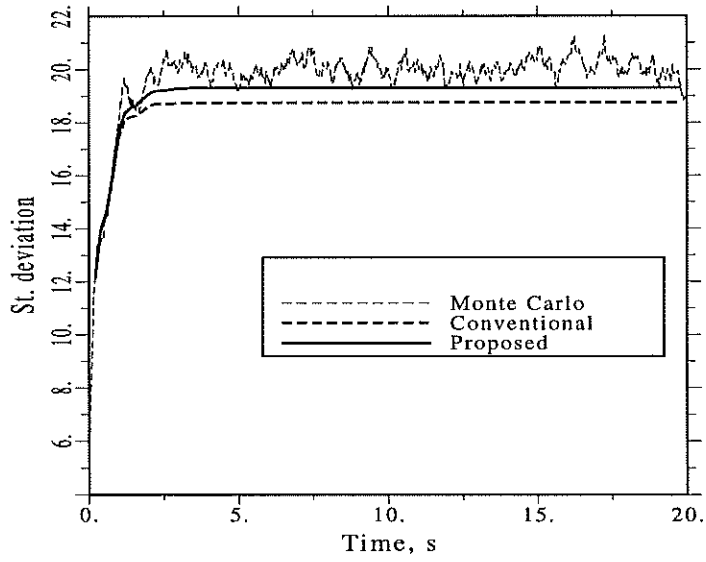

Figure 5.2 Velocity response under white noise. $T = 1.5$, $R = 10$, $\alpha = 0$

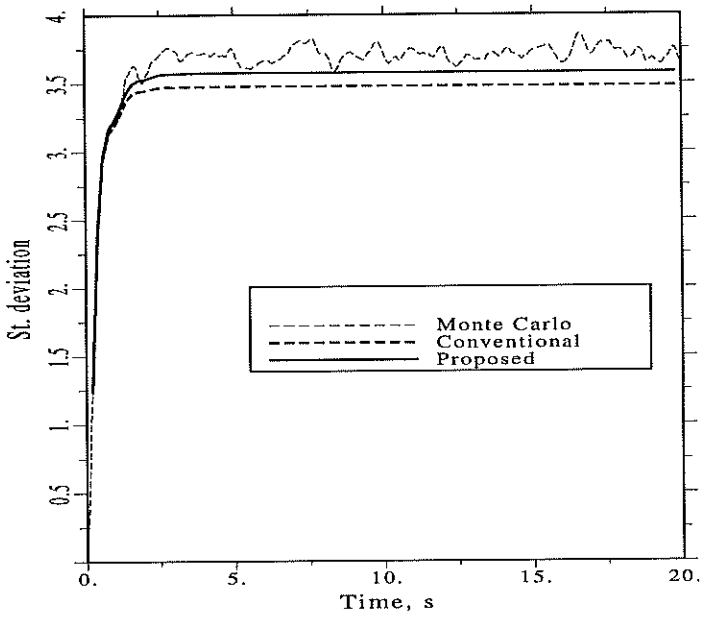

Figure 5.3 Z response under white noise. $T = 1.5$, $R = 10$, $\alpha = 0$

2. The parameters ω_g and ν_g selected to the study correspond to the intermediate soil condition, as given by Table 2.2. The parameters of the low-cut filter were set equal to $\omega_f = 2\,\text{rad/s}$ and $\nu_f = 0.65$ for all cases. Both unmodulated and modulated excitations were considered. The modulating function used was that proposed by Shinozuka and Sato (1967) (equation 2.19) with parameters $a = 0.085$ and $b = 0.17$, which correspond to an earthquake with long effective duration.

For modeling several degrees of nonlinear behavior it was decided to keep constant the excitation intensity and to vary instead the value of the restoring force h_u. To do this n was set equal to unity as well as A, in which case parameter k will represent the initial stiffness of the system, while the sum $\beta + \gamma$ was varied according to the intended degree of nonlinearity of system's response in the form

$$\beta + \gamma = \frac{(1-\alpha)Rk}{100\sqrt{S_W}} \tag{5.16}$$

Here R is a prescribed measure of the degree of energy dissipation that plays a similar role as the elastic spectrum reducing factors in deterministic earthquake-resistant design. Values of R equal to 2.5 up to 10 were chosen to reflect situa-

tions from low to severe nonlinearity of the response. For analyzing the influence of system's natural frequency, the initial stiffness k was calculated so as to give the structure initial periods in the range $T = 0.25$ to 2.5 s. Finally, the study was performed on softening systems without and with hardening tendency. The ratios $\beta/\gamma = 1$ and $\beta/\gamma = -2, \gamma < 0$ were chosen as representative of such cases.

It is evident that the above experimental design samples soberly and adequately the variety of situations on which the Bouc - Wen model is used. The following are the main conclusions drawn from the multiple analyses performed on the two type of cases studied.

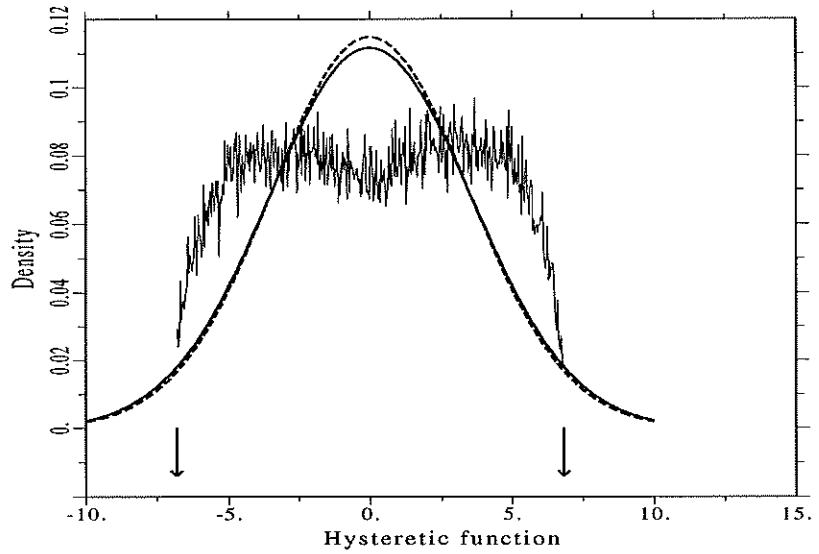

Figure 5.4 Density functions of Z

5.3.1 Softening systems with no hardening tendency

The most common situation found in the bibliographic research about the use of the Bouc - Wen hysteretic model corresponds to $\beta + \gamma > 0, \beta/\gamma = 1$, in which the hardening tendency is completely absent.

The influence of the structural period on the magnitude of errors of the conventional and proposed approaches will be discussed first. Figure 5.1 illustrates the response of a middle period system with $R = 10$ and $\alpha = 0.0$ to white noise. These parameters have been chosen so as to produce the highest possible error resulting from the Gaussian assumption when the system is subject to white noise, inasmuch as the error is the higher, the stronger the nonlinear behaviour

and the lower the value of α. A value of $r = -0.5$ was used. It can be observed that the proposed approach yields a better estimation The results corresponding to the standard deviation of velocity $\dot{X}$ and hysteretic function Z of the middle period system are depicted in figures 5.2 and 5.3. Even though both are satisfactorily estimated by the Gaussian approach, the results obtained by the proposed method are somewhat closer to the Monte Carlo curves. In the sequel only the results corresponding to displacement's standard deviation will be discussed.

Figure 5.4 shows a comparison between the density functions of Z of this example as postulated by conventional and proposed approaches and as calculated by Monte Carlo (50,000 samples). It can be seen that the introduction of the Dirac pulses has no other effect than to serve as a balancing mass for second order calculations, and that they will never be useful as a means of approximating the true density when combined with the Gaussian. Also, the figure justifies the somewhat surprising option for negative p values mentioned before, as it is evident that the effect is to flat the peak and raise the tails of the Gaussian function just as much as needed for second order agreement with the empirical density function.

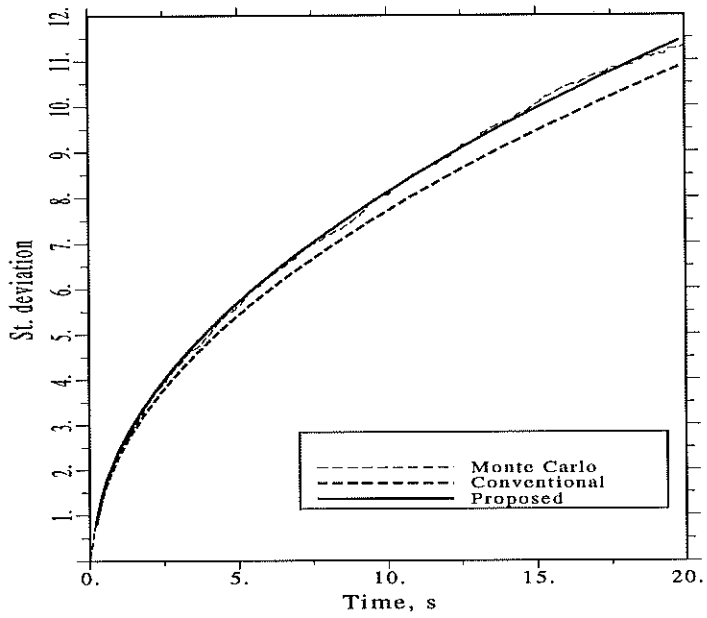

Figure 5.5 Displacement response under white noise. $T = 0.3$, $R = 10$, $\alpha = 0$

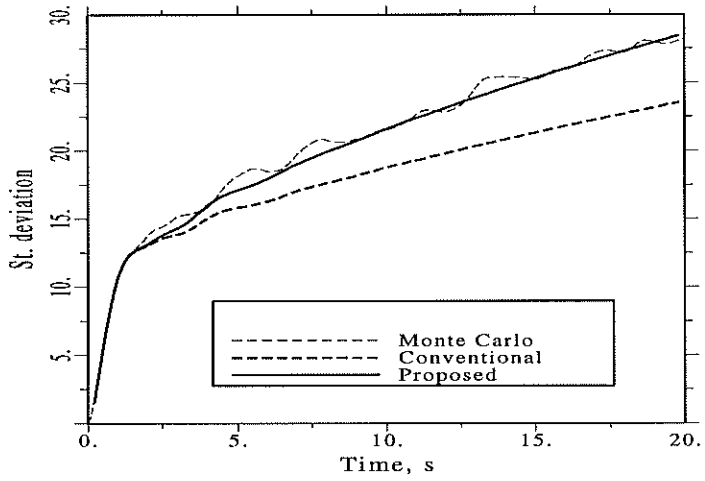

Figure 5.6 Displacement response under white noise. $T = 3.0$, $R = 10$, $\alpha = 0$

The results corresponding to systems with low and high periods (figures 5.5 and 5.6) indicate that the correction is achieved independently of the natural frequency. This feature of the proposed approach was observed in many additional analyses as well as the independency of coefficient r on the post-yielding ratio α, which is one of the main causes of errors stemming from the assumption of Gaussianity as explicited above. This is illustrated by figure 5.7, which corresponds to the same system as that of figure 5.1 with a large post-yielding stiffness ($\alpha = 0.15$).

For seismic analyses purposes it has been observed that the use of adequate spectrum models, i.e. those characterized by zero energy at null frequency, makes the Gaussian method unable to detect the drift of the system described above. The results displayed in figures 5.8 and 5.9 correspond to systems subject to the Clough-Penzien spectrum with $\alpha = 0$ and $\alpha = 0.15$, respectively. A period $T = 0.4$ was used in both cases in order to subject the system to a nearly-to-resonance state. The assessment made in chapter 4 about the effect of low-cut filters on the Gaussian method can be verified. Also, the superiority of the proposed approach in this important respect is evident, as it is able to detect the drift trend, due to the fact that the alteration of Gaussianism is an indirect way of overcoming the effects of the supression of low frequency response by the transfer function of the equivalent linear system when excited by the Clough-Penzien spectrum, as shown in the previous chapter. However, it can be observed that the start of the correcting effect of the Dirac pulses takes place

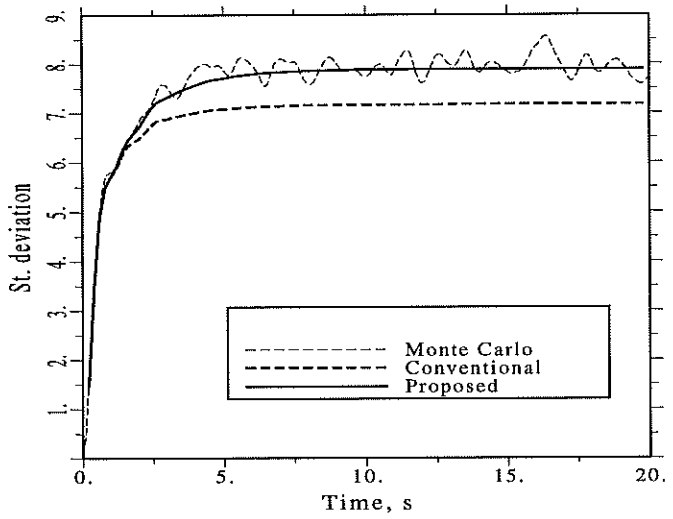

Figure 5.7 Displacement response under white noise. $T = 1.5$, $R = 10$, $\alpha = 0.15$

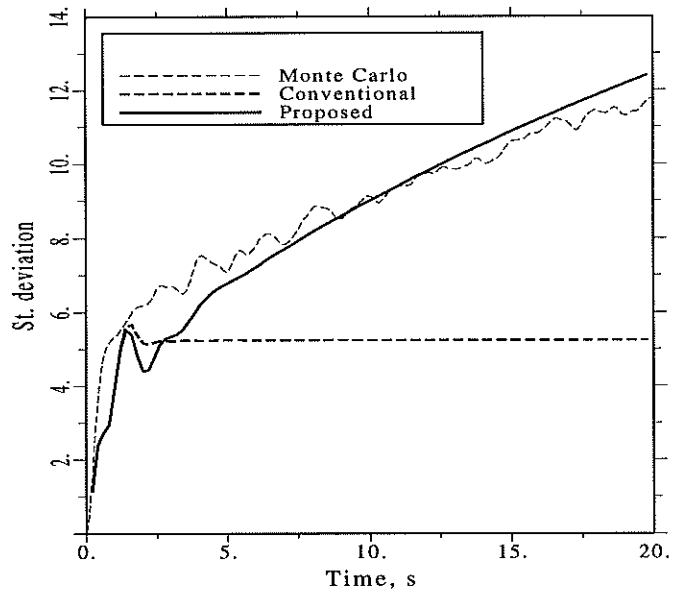

Figure 5.8 Displacement response under Clough-Penzien excitation. $T = 0.4$, $\alpha = 0$

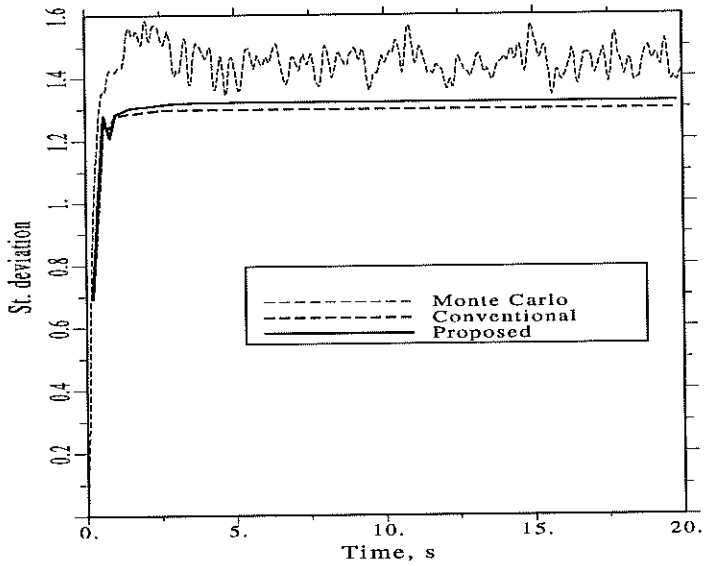

Figure 5.9 Displacement response under Clough-Penzien excitation. $T = 0.4$, $\alpha = 0.15$

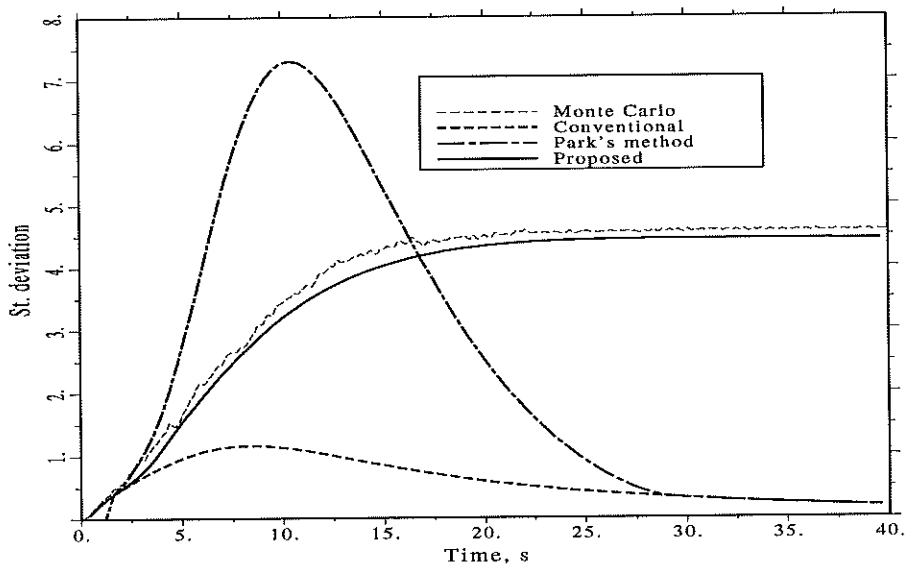

Figure 5.10 Displacement response under modulated Clough-Penzien excitation. $\alpha = 0$

later than the somewhat abrupt switching of the drift errance. As a result the drift path of the Monte Carlo and proposed estimations are different in shape. Nevertheless, the delay is much less pronounced when smooth amplitude modulating functions are used, as is common practice in seismic random vibration analysis. This is illustrated by figure 5.10, which adds to the results depicted in figure 4.10 the estimation afforded by the proposed method. It can be observed that the error of the proposed approach is negligible for practical purposes. On the other hand, while the Gaussian estimation mimics the modulating function for the reasons explained above, the standard deviation evolution calculated by the proposed technique is rather close to the right one.

The figure also displays the results obtained by the correction method proposed by Park (1992). Unlike the present approach, which combines new analytical linearization coefficients with the empiricism required for finding an adequate r value, Park's method attempts to upgrade the results given by the conventional method on purely empirical basis. The method considers two types of errors of the Gaussian approach, namely, what the author calls *stationary error*, i.e. the type of systematic, constant error of the conventional approach appearing for example in figure 5.9 which can be attributed to the assumption of Gaussian probability densities, and the second, *nonstationary error*, which corresponds to drift. It must be observed that the coefficients have been empirically derived for the rather specific situation of (a), a seismic excitation modeled by the Iwan-Paparizos spectrum, which in the nomenclature of chapter 2 corresponds to the acceleration

$$M^{\mathrm{IP}} = 2\nu_{\mathrm{g}}\omega_{\mathrm{g}}\dot{U}_{\mathrm{g}} \tag{5.17}$$

and (b), a prescribed amplitude modulating function which acts on a hysteretic system with initial frequency equal to that corresponding to the peak of the spectrum. As a result, it is expected that the empirical method give erroneous estimations in a case different from those used for its calibration, such as that of figure 5.10. In fact, the peak of the standard deviation of the displacement is largely overestimated. Moreover, insofar as Park's method attempts to modify a posteriori the results given by the Gaussian method by a multiplying factor, the erroneous shape of the latter is mantained.

As was said before, the errors of the Gaussian method diminish when the post-yield ratio α increases due to the implied reduction of drift. This is illustrated by figure 5.11, which corresponds to a system with a natural frequency equal to that of the hard soil conditions of Table 2.3 and $\alpha = 0.05$. The estimation given by Park's method in this case are also far from the Monte Carlo results, while the agreement of the latter with the proposed approach is again excellent.

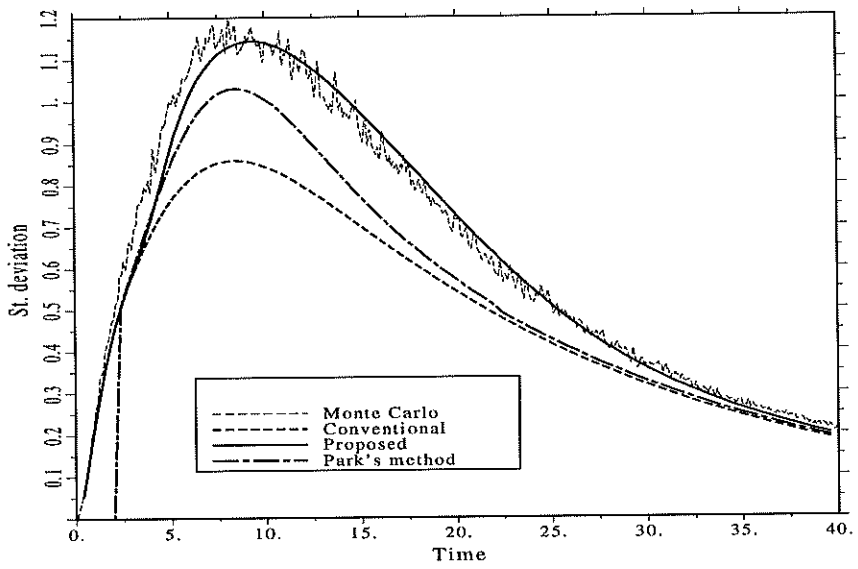

Figure 5.11 Displacement response under modulated Clough-Penzien excitation. $\alpha = 0.05$

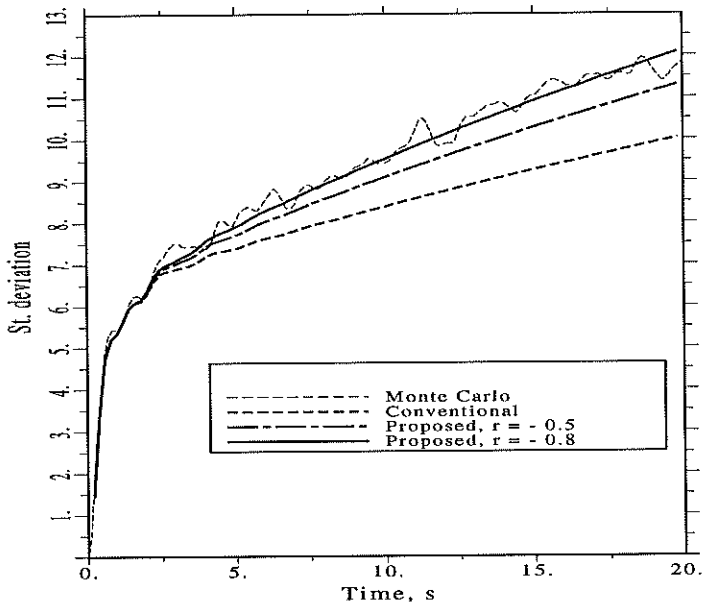

Figure 5.12 Displacement response under white noise. $T = 1.5$, $R = 5$, $\alpha = 0$

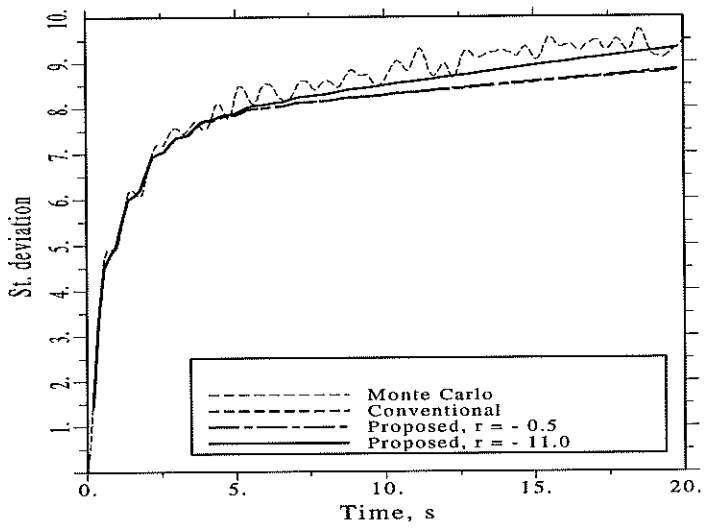

Figure 5.13 Displacement response under white noise. $T = 1.5$, $R = 2.5$, $\alpha = 0$

The cases analysed so far correspond to large incursions in the nonlinear range, as reflected by the factor $R = 10$. For lower degrees of nonlinear behaviour less concentration of Z values near its maximum and hence a different probability density can be expected. As a result, the effectivity of the Dirac pulses in that case could decrease when using the same r as before so that it must be increased in absolute terms. However, as the elastic response level is approached, the error of the Gaussian estimations diminish drastically, an thus one could expect that the estimations given by both methods approach to each other and to the Monte Carlo results at those levels. These intuitive reflections are confirmed by figures 5.12 and 5.13, which correspond to $R = 5$ and $R = 2.5$ respectively. A period T equal to 1.5 s was used in both cases. It is noted that in the first case the same r value used before leads to estimations which are somewhat unconservative but anyway better than those stemming from the assumption of Gaussianity. On the other hand the approximation of the responses predicted by both methods to those given by Monte Carlo as R decreases is evident. The figures also display the results obtained using $r = -0.8$ and $r = -11$, respectively. Closer estimations to the exact ones can be observed. In general, the empirical curve for the $-r$ coefficient depicted in figure 5.14 can be used for obtaining more accurate estimations of the displacement response of this type of system for low degrees of nonlinear behaviour. The coefficient has been put in relation to a sort of ductility ratio given by

$$q = \frac{\sigma_{0.5}}{x_y} \tag{5.18}$$

where x_y is the yield displacement of the system and $\sigma_{0.5}$ is the standard deviation of the displacement obtained with $r = -0.5$ at the maximum response level when subject to unmodulated white noise. The dots displayed in the figure have been obtained by iterating until the moment when the proposed approach and Monte Carlo gave close results. The equation of the empirical curve is

$$-r = \begin{cases} 32.082 - 61.823q & q \leq 0.5 \\ 0.5184 + \mathrm{e}^{0.445q} + \mathrm{e}^{-1.183q^2} & q > 0.5 \end{cases} \tag{5.19}$$

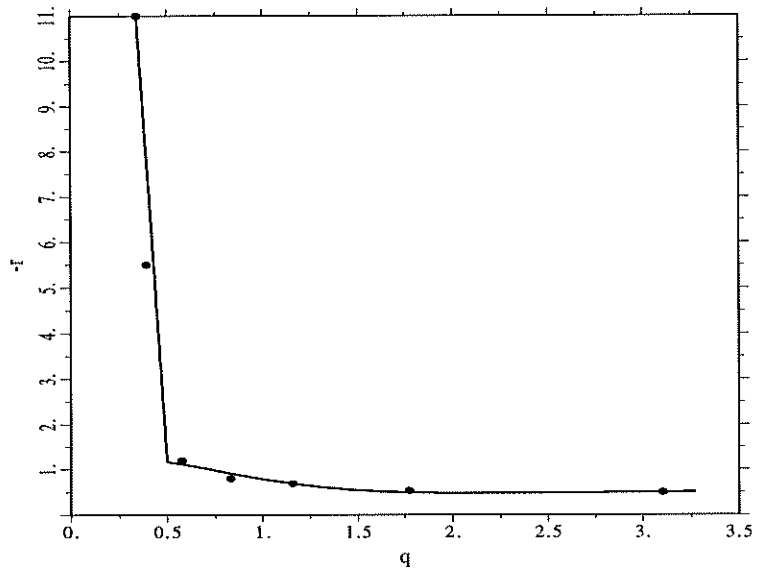

Figure 5.14 Empirical curve of $-r$ for $\beta/\gamma = 1$

It can be seen in the figure that the standard value of -0.5 is adequate for a wide range of the ductility factor q. Thus, for the analysis of multidegree-of-freedom hysteretic systems subject to random excitations, it can be safely applied to the degrees of freedom showing moderate to large energy dissipation. However, for those hysteretic degrees of freedom showing small incursions in the nonlinear range there would be a need of analysing the structure using the reference value in order to calculate an upgraded one. Nevertheless, complications

can be avoided if use is made of the standard value of -0.5 for the entire structure, due to the following reasons: first, such degrees of freedom are of lower importance insofar as their contribution to the overall probability of failure is small; second, the underestimation of the displacement results for such degrees of freedom is slight in percent when compared to that ocurring at high levels of response nonlinearity due to their proximity to the elastic response.

5.3.2 Softening systems with hardening tendency

As said in the preceding, a negative γ, such that $\beta+\gamma > 0$ (softening condition) and $|\gamma| < \beta$ imposes a tendency to hardening. Consequently, the frequency distribution of Z and the errors arising from the assumption of Gaussianity will be different from those resulting from positive γ. As an example, let us consider the case $\beta/\gamma = -2, \gamma < 0$. The agreement of the proposed approach with the simulation results is shown figure 5.15, which corresponds to a system akin to that of figure 5.10 with the only change of $\beta/\gamma = -2, \gamma < 0$, calculated with $r = -0.22$, which appeared to be suitable to this type of system. No regression curve for r has been calculated in this case.

Generally speaking, it can be concluded that the estimations reached with the proposed approach are always better than those given by the classical method and the empirical correction approach proposed by Park (1992). Also, the method is computationally much simpler than the proposal of Kimura *et al* (1994) as well as than other methods which are based on non linear transformations and/or on-line Monte Carlo simulations (Pradlwarter and Schuëller 1990). Its practical application only requires to find an adequate r value for each type of system, as defined by the doublet n and β/γ ratio.

5.4 Sensitivities of the linearized model

This chapter ends with the derivation of the sensitivities of the elements of the covariance matrix $\boldsymbol{A}_{\mathrm{e}}$ with respect to the any parameter θ of the excitation or structural models, which are necessary to apply the perturbation approach introduced in chapter 3 for considering the effect of parameter uncertainty on the overall measures of structural response. The derivation will be carried out in the general frame of the non Gaussian method of stochastic linearization introduced herein.

Most of the derivatives of the elements of matrix $\boldsymbol{A}_{\mathrm{e}}$ are trivial except those corresponding to the linearization coefficients. Deriving equation (5.8) with respect θ yields

$$\frac{\partial \boldsymbol{H}_{\mathrm{e}}^{\mathrm{T}}}{\partial \theta} = \frac{\partial}{\partial \theta}[s_{\mathrm{e}},\ c_{\mathrm{e}},\ k_{\mathrm{e}}] = (1-2p)\ \frac{\partial}{\partial \theta}[s_{\mathrm{g}},\ c_{\mathrm{g}},\ k_{\mathrm{g}}]$$

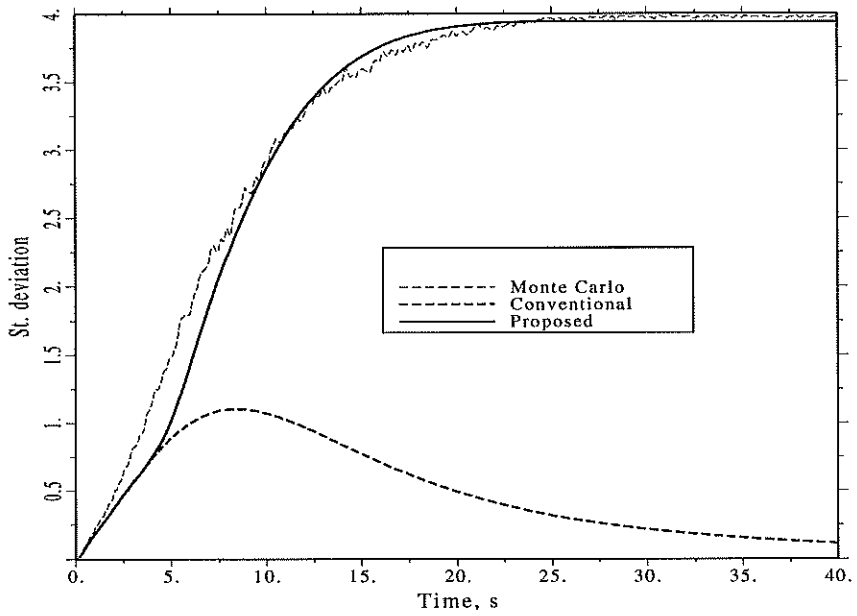

Figure 5.15 Displacement response of a system with $\beta/\gamma = -2$ under C-P excitation

$$+2p\left\{\frac{\partial}{\partial\theta}[s_{\mathrm{d}},\ c_{\mathrm{d}},\ k_{\mathrm{d}}]\boldsymbol{\Pi}^{-1}+[s_{\mathrm{d}},\ c_{\mathrm{d}},\ k_{\mathrm{d}}]\frac{\partial\boldsymbol{\Pi}^{-1}}{\partial\theta}\right\} \tag{5.20}$$

where the weighting coefficient p has been considered constant. The derivatives of the Gaussian part are (Sues *et al.* 1985)

$$\frac{\partial s_{\mathrm{g}}}{\partial\theta}=0 \tag{5.21a}$$

$$\frac{\partial c_{\mathrm{g}}}{\partial\theta}=\frac{\partial A}{\partial\theta}-\Big(\beta\frac{\partial F_1}{\partial\theta}+\frac{\partial\beta}{\partial\theta}F_1+\gamma\frac{\partial F_2}{\partial\theta}+\frac{\partial\gamma}{\partial\theta}F_2\Big) \tag{5.21b}$$

$$\frac{\partial k_{\mathrm{g}}}{\partial\theta}=-\Big(\beta\frac{\partial F_3}{\partial\theta}+\frac{\partial\beta}{\partial\theta}F_3+\gamma\frac{\partial F_4}{\partial\theta}+\frac{\partial\gamma}{\partial\theta}F_4\Big) \tag{5.21c}$$

where the derivatives of the functions $F_i, i=1,2,3,4$ required in the above equations, with respect to any model parameter different from n, are given by

$$\frac{\partial F_1}{\partial\theta}=\frac{2^{\frac{n}{2}}}{\pi}\Gamma\Big(\frac{n+2}{2}\Big)\Big(\sigma_Z^{\,n}\frac{\partial I_{\mathrm{s}}}{\partial\theta}+n\sigma_Z^{\,n-1}\frac{\partial\sigma_Z}{\partial\theta}I_{\mathrm{s}}\Big) \tag{5.22a}$$

$$\frac{\partial F_2}{\partial \theta} = \frac{2^{\frac{n}{2}}}{\sqrt{\pi}}\Gamma(\frac{n+1}{2})n\sigma_Z^{n-1}\frac{\partial \sigma_Z}{\partial \theta} \tag{5.22b}$$

$$\frac{\partial F_3}{\partial \theta} = \frac{2^{\frac{n}{2}}n}{\pi}\Gamma(\frac{n+2}{2})\Big(\sigma_{\dot{X}}(n-1)\sigma_Z^{n-2}\frac{\partial \sigma_Z}{\partial \theta} + \frac{\partial \sigma_{\dot{X}}}{\partial \theta}\sigma_Z^{n-1}\Big)$$

$$\Big[2\frac{(1-\rho_{\dot{X}Z}^2)^{\frac{n+1}{2}}}{n} + \rho_{\dot{X}Z}I_s\Big] + \frac{n\sigma_Z^{n-1}\sigma_{\dot{X}}}{\pi}\Gamma(\frac{n+2}{2})2^{\frac{n}{2}}$$

$$\Big(-\frac{n+1}{n}(1-\rho_{\dot{X}Z}^2)^{\frac{n-1}{2}}2\rho_{\dot{X}Z}\frac{\partial \rho_{\dot{X}Z}}{\partial \theta} + \rho_{\dot{X}Z}\frac{\partial I_s}{\partial \theta} + \frac{\partial \rho_{\dot{X}Z}}{\partial \theta}I_s \tag{5.22c}$$

$$\frac{\partial F_4}{\partial \theta} = \frac{2^{\frac{n}{2}}n}{\sqrt{\pi}}\Gamma(\frac{n+1}{2})\Big(\rho_{\dot{X}Z}\sigma_{\dot{X}}(n-1)\sigma_Z^{n-2}\frac{\partial \sigma_Z}{\partial \theta} +$$

$$\rho_{\dot{X}Z}\frac{\partial \sigma_{\dot{X}}}{\partial \theta}\sigma_Z^{n-1} + \frac{\partial \rho_{\dot{X}Z}}{\partial \theta}\sigma_{\dot{X}}\sigma_Z^{n-1}\Big) \tag{5.22d}$$

with

$$\frac{\partial \sigma_Z}{\partial \theta} = \frac{1}{2\sigma_Z}\frac{\partial \mathrm{E}[Z^2]}{\partial \theta} \tag{5.23}$$

$$\frac{\partial \sigma_{\dot{X}}}{\partial \theta} = \frac{1}{2\sigma_{\dot{X}}}\frac{\partial \mathrm{E}[\dot{X}^2]}{\partial \theta} \tag{5.24}$$

$$\frac{\partial \rho_{\dot{X}Z}}{\partial \theta} = \frac{1}{\sqrt{\mathrm{E}[\dot{X}^2]\mathrm{E}[Z^2]}}\frac{\partial \mathrm{E}[\dot{X}Z]}{\partial \theta} - \frac{\rho_{\dot{X}Z}(\mathrm{E}[\dot{X}^2]\frac{\partial \mathrm{E}[Z^2]}{\partial \theta} + \frac{\partial \mathrm{E}[\dot{X}^2]}{\partial \theta}\mathrm{E}[Z^2]}{2\mathrm{E}[\dot{X}^2]\mathrm{E}[Z^2]}$$

$$\frac{\partial I_s}{\partial \theta} = -2\sin^n \ell \frac{\partial \ell}{\partial \theta} \tag{5.25}$$

$$\frac{\partial \ell}{\partial \theta} = -\frac{1}{\sqrt{1-\rho_{\dot{X}Z}^2}}\frac{\partial \rho_{\dot{X}Z}}{\partial \theta} \tag{5.26}$$

In case the selected structural parameter θ is the strength of the hysteretic model h_u, given by

$$h_u = (1-\alpha)k\Big(\frac{A}{\beta+\gamma}\Big)^{\frac{1}{n}} \tag{5.27}$$

it is convenient to calculate the covariance sensitivity with respect to A and then applying the chain rule,

$$\frac{\partial \boldsymbol{\Sigma}}{\partial h_u} = \frac{\partial \boldsymbol{\Sigma}}{\partial A}\frac{\partial A}{\partial h_u} \tag{5.28}$$

with

$$\frac{\partial A}{\partial h_u} = \frac{nA}{(1-\alpha)k}\Big(\frac{A}{\beta+\gamma}\Big)^{-\frac{1}{n}} \tag{5.29}$$

On the other hand, the derivatives of the Dirac coefficients (5.10) are

$$\frac{\partial s_d}{\partial \theta} = \frac{\partial \sigma_{X\dot{X}}}{\partial \theta}(A-\gamma z_u^n) + \sigma_{X\dot{X}}\Big(\frac{\partial A}{\partial \theta} - \frac{\partial \gamma}{\partial \theta} z_u^n - n\gamma z_u^{n-1}\frac{\partial z_u}{\partial \theta}\Big) \tag{5.30a}$$

$$\frac{\partial c_d}{\partial \theta} = \frac{\partial \sigma_{\dot{X}}^2}{\partial \theta}(A-\gamma z_u^n) + \sigma_{\dot{X}}^2\Big(\frac{\partial A}{\partial \theta} - \frac{\partial \gamma}{\partial \theta} z_u^n - n\gamma z_u^{n-1}\frac{\partial z_u}{\partial \theta}\Big) \tag{5.30b}$$

$$\frac{\partial k_d}{\partial \theta} = -\sqrt{\frac{2}{\pi}}\Big(\sigma_{\dot{X}}\Big[\frac{\partial \beta}{\partial \theta} z_u^{n+1} + \beta(n+1)z_u^n\frac{\partial z_u}{\partial \theta}\Big] + \frac{\partial \sigma_{\dot{X}}}{\partial \theta}\beta z_u^{n+1}\Big) \tag{5.30c}$$

Finally, the derivatives of the elements of matrix $\boldsymbol{\Pi}^{-1}$ in equation (5.20) can be obtained by making use of the rule for derivating the inverse of a matrix, i.e.

$$\frac{\partial \boldsymbol{\Pi}^{-1}}{\partial \theta} = -\boldsymbol{\Pi}^{-1}\frac{\partial \boldsymbol{\Pi}}{\partial \theta}\boldsymbol{\Pi}^{-1} \tag{5.31}$$

where the elements of $\partial \boldsymbol{\Pi}/\partial\theta$ are entries of $\partial \boldsymbol{\Sigma}/\partial\theta$. This method will be applied in chapter 8 for determining the influence of strength uncertainty of lead-rubber bearing devices on the maximum displacement of base isolated buildings.

Chapter 6

Nonstationary analysis using complex modal decomposition

6.1 Introduction

Complex modal decomposition has been proposed to extend the application of the method of stochastic equivalent linearization to large structural systems for which the dimension of the state vector is so large that the direct solution of the resulting set of differential equations by algorithms such as Runge-Kutta or Adams-Moulton can be very slow. Such is the case when dealing with frames with nonlinear behaviour of plastic hinges located at member ends or when using finite element techniques on hysteretic continua for which the smooth hysteretic endochronic model is formulated in the stress-strain space.

In principle, the modal treatment of random vibration depends on the aim of the calculation, namely, stationary or nonstationary analysis. In this chapter the solution of the mean and covariance differential equations by means of complex modal decomposition is addressed, with the emphasis placed on nonstationary solutions. After a short summary of some basic notions concerning the state space analysis of linear systems, an well known algorithm proposed by different authors is discussed. It is shown that this classical algorithm is characterized by an unadmissible numerical instability when dealing with non stationary response. More specifically, it is demonstrated that the estimated moments depend dramatically on the time step chosen for solving the system of equations according to a roughly proportional law. This simply means that the estimations obtained by this method are of no use unless there would be a hint on the right time step needed for the current calculation. Since this would require the realization of a Monte Carlo analysis, the application of method of stochastic linearization would be superfluous in that case. It is demonstrated here that this instability is due to the fact that the method proceeds by direct

integration of the equations of motion as in the solution of linear systems. A new procedure intended to to overcome this difficulty (that makes this complex modal approach almost useless) is then introduced. Briefly, the solution for the modal responses is sought by differential equations rather than by direct integration. As a consequence, some exponential functions, which are related with the the so-called *state transition matrix* and that are the ultimate cause for the numerical instability, no longer appear. It is demonstrated that the proposed method is mathematically equivalent to the direct method of solving the covariance equation (3.46) so that it can be connected either with Gaussian or the proposed non Gaussian linearization schemes for hysteretic systems at will.

6.2 State space solution of linear systems

In the beginning of the chapter 3 the state space formulation of linear systems was introduced. The following lines summarize some basic developments about the solution of linear state space equations which are required for later derivations.

As said in chapter 3, the dynamics of a linear system can be written in state space form as

$$\dot{\boldsymbol{q}}(t) = \boldsymbol{A}\boldsymbol{q}(t) + \boldsymbol{f}(t) = \boldsymbol{0} \tag{6.1}$$

In case of free vibration, i. e., when $\boldsymbol{f}(t) = \boldsymbol{0}$, we have

$$\dot{\boldsymbol{q}}(t) = \boldsymbol{A}\boldsymbol{q}(t) \tag{6.2}$$

whose solution, according to the theory of linear systems (e.g. Szidarovski 1993), is given by

$$\boldsymbol{q}(t) = \exp(\boldsymbol{A}t) \tag{6.3}$$

where the exponential function of the system matrix is defined as

$$\exp(\boldsymbol{A}(t)) = \boldsymbol{I} + \boldsymbol{A}t + \frac{1}{2!}(\boldsymbol{A}t)^2 + \frac{1}{3!}(\boldsymbol{A}t)^3 + \cdots \tag{6.4}$$

The calculation of this function is simplified by solving previously the eigenproblem

$$\boldsymbol{A}\boldsymbol{R} = \boldsymbol{\Lambda}\boldsymbol{R} \tag{6.5}$$

where $\boldsymbol{R}$ and $\boldsymbol{\Lambda}$ are the matrices of rigth eigenvectors and eigenvalues, respectively, which due to the asymmetry of matrix $\boldsymbol{A}$ are in general complex. It can also be shown that

$$\exp(\boldsymbol{A}(t)) = \boldsymbol{R}\exp(\boldsymbol{\Lambda}t)\boldsymbol{R} \tag{6.6}$$

which is simpler to evaluate than equation (6.4) due to the diagonal structure of the matrix $\boldsymbol{\Lambda}$. The general solution of (6.1) is

$$\boldsymbol{q}(t) = \exp(\boldsymbol{A}t)\boldsymbol{q}(0) + \int_0^t \exp(\boldsymbol{A}(t-\tau))\boldsymbol{f}(\tau)\mathrm{d}\tau \tag{6.7}$$

which in case of quiescent initial conditions reduces to

$$\boldsymbol{q}(t) = \int_0^t \exp(\boldsymbol{A}(t-\tau))\boldsymbol{f}(\tau)\mathrm{d}\tau \tag{6.8a}$$

or

$$\boldsymbol{q}(t) = \int_0^t \exp(\boldsymbol{A}(t))\boldsymbol{f}(t-\tau)\mathrm{d}\tau \tag{6.8b}$$

These equations show that the matrix $\exp(\boldsymbol{A}t)$ plays in the time domain the role of a transfer matrix commonly appearing in the frequency domain analysis of linear systems. For this reason it is usually called *state transition matrix.*

6.3 Classical complex modal algorithm

The solution of the differential equation of the covariance matrix (3.46) can imply a high computational effort when dealing with large structural systems. For such cases it has been proposed to perform an eigenvalue decomposition of the equations of motion and to use only the most significant modes in the calculation of the response. For linear systems a commonly applied technique consists in the solution of the eigenproblem of the homogeneous version of equation (3.2) by doing certain assumptions on the viscous damping matrix. When working in state space those assumptions are no longer needed, but the eigenvalues and eigenvectors of the system matrix will in general be complex.

The advantages of the complex eigendecomposition of matrices have been exploited in the context of the method of stochastic linearization in several ways. Some of them apply exclusively to stationary calculations (Roberts and Spanos 1990; Pradlwarter and Schuëller 1992; Casciati *et al.* 1994). The method discussed herein has been proposed to nonstationary analyses by different authors

(Chang 1985; Simulescu *et al.* 1989; Pradlwarter and Schuëller 1991; Pradlwarter and Li 1991). It is rooted in the theory of linear systems outlined above. The following is a detailed exposition of the essential features of the algorithm which are common to the different proposals just quoted.

For the equation of motion of the linearized system in state space the following transformation can be applied:

$$\boldsymbol{Q} = \boldsymbol{R}\boldsymbol{\Xi} \tag{6.9}$$

where $\boldsymbol{R}$ is the matrix of right eigenvalues of the system matrix $\boldsymbol{A}_\mathrm{e}$ and $\boldsymbol{\Xi}$ is the generalized modal coordinate. Replacing this equation into (6.1) we obtain

$$\dot{\boldsymbol{\Xi}} = \boldsymbol{R}^{-1}\boldsymbol{A}_\mathrm{e}\,\boldsymbol{R}\boldsymbol{\Xi} + \boldsymbol{R}^{-1}\boldsymbol{F} \tag{6.10}$$

which can be simplified by considering the statement of the eigenproblem

$$\boldsymbol{A}_\mathrm{e}\boldsymbol{R} = \boldsymbol{R}\boldsymbol{\Lambda} \tag{6.11}$$

where $\boldsymbol{\Lambda}$ is the diagonal matrix of complex eigenvalues. The corresponding left eigenproblem is

$$\boldsymbol{A}_\mathrm{e}^\mathrm{T}\boldsymbol{L} = \boldsymbol{L}\boldsymbol{\Lambda} \tag{6.12}$$

Applying the normalization

$$\boldsymbol{I} = \boldsymbol{L}^\mathrm{T}\boldsymbol{R} \tag{6.13}$$

which implies that

$$\boldsymbol{\Lambda} = \boldsymbol{L}^\mathrm{T}\boldsymbol{A}_\mathrm{e}\boldsymbol{R} \tag{6.14}$$

the equation of motion in modal coordinates becomes

$$\dot{\boldsymbol{\Xi}} = \boldsymbol{\Lambda}\boldsymbol{\Xi} + \boldsymbol{\Psi} \tag{6.15}$$

with the modal external forces defined as

$$\boldsymbol{\Psi} = \boldsymbol{R}^{-1}\boldsymbol{F} \tag{6.16}$$

or

$$\boldsymbol{\Psi} = \boldsymbol{L}^{\mathrm{T}}\boldsymbol{F} \tag{6.17}$$

according to the normalization condition. In the sequel we will assume that the excitation and, consequently, the responses have zero mean. Defining

$$\boldsymbol{\Gamma} = \{\Gamma_{ij}\} = \left\{\mathrm{E}[\Xi_i \Xi_j^{\mathrm{C}}]\right\} \tag{6.18}$$

the relationship between modal and global covariance matrices is

$$\boldsymbol{\Sigma} = \boldsymbol{R}\boldsymbol{\Gamma}\boldsymbol{R}^{\mathrm{CT}} \tag{6.19}$$

For nonlinear systems analysed by the stochastic linearization technique the application of the above equations, which are valid exclusively for linear systems, requires that the system matrix $\boldsymbol{A}_{\mathrm{e}}$ be assumed to remain constant inside each time step (t_k, t_{k+1}). The dynamics of the $i-$th element of the state vector will then be expressed as

$$\dot{\Xi}_i(\tau) = \lambda_i \Xi_i(\tau) + \Phi_i(\tau) \tag{6.20}$$

where Φ_i is the $i-$th generalized force corresponding to the same row of $\boldsymbol{\Psi}$ and $0 \leq \tau \leq h = t_{k+1} - t_k$. Let us particularize for an excitation of the form

$$\boldsymbol{F} = \boldsymbol{J}N(t) \tag{6.21}$$

where $\boldsymbol{J}$ is a vector of constants that can be assembled by the considering the equilibrium equations of the structure and filter systems and $N(t)$ is in general a modulated stationary process. Denoting by $\boldsymbol{M}_i$ the $i-$th row of any matrix $\boldsymbol{M}$, $\Phi_i(\tau)$ can be expressed as

$$\Phi_i(\tau) = \boldsymbol{L}_i^{\mathrm{T}}\boldsymbol{F}(t_k + \tau) = l_i N(t_k + \tau) \tag{6.22}$$

where

$$l_i = \boldsymbol{L}_i^{\mathrm{T}}\boldsymbol{J} \tag{6.23}$$

is the participation factor of the $i-$th mode. On the basis of linear system theory sketched above the solution of the above differential equation can be put in the form

$$\Xi_i(\tau) = \exp(\lambda_i \tau)\Xi_i(\mathrm{o}) + \int_0^\tau \exp(\lambda_i[\tau - v])l_i N(t_k + v)\mathrm{d}v \tag{6.24}$$

The covariance matrix of the state vector is

$$\boldsymbol{\Sigma}(t_k + \tau) = \Re\left(\mathrm{E}[\boldsymbol{Q}(t_k + \tau)\boldsymbol{Q}(t_k + \tau)^{\mathrm{CT}}]\right) \tag{6.25}$$

where the symbol $\Re(\cdot)$ stands for the real part of its argument. According to the modal transformation it can be related to the covariance of the generalized coordinate as

$$\boldsymbol{\Sigma}(t_k + \tau) = \Re\left(\boldsymbol{R}\boldsymbol{\Gamma}(\tau)\boldsymbol{R}^{\mathrm{CT}}\right) \tag{6.26}$$

where $\boldsymbol{\Gamma}(\tau)$ is the covariance of the modal coordinates at time τ. Taking into account equation (6.24) and setting $\tau = h$, its terms can be expanded as follows:

$$\Gamma_{ij}(h) = \mathrm{E}[\Xi_i(h)\Xi_j^{\mathrm{C}}(h)] \approx \mathrm{E}\Big[\{\exp(\lambda_i h)\Xi_i(\mathrm{o})$$

$$+ \int_0^h \exp(\lambda_i[h - v_1])\Phi_i(t_k + v_1)\mathrm{d}v_1\}\{\exp(\lambda_j^{\mathrm{C}} h)\Xi_j^{\mathrm{C}}(\mathrm{o})$$

$$+ \int_0^h \exp(\lambda_j^{\mathrm{C}}[h - v_2])\Phi_j^{\mathrm{C}}(t_k + v_2)\mathrm{d}v_2\}\Big] \tag{6.27}$$

Carrying out the multiplications and expectations, the final expression of the elementary covariance becomes

$$\Gamma_{ij}(h) = \exp([\lambda_i + \lambda_j^{\mathrm{C}}]h)\Big\{\mathrm{E}[\Xi_i(\mathrm{o})\Xi_j^{\mathrm{C}}(\mathrm{o})]$$

$$+ \int_0^h \int_0^h \exp(-\lambda_i v_1 - \lambda_j^{\mathrm{C}} v_2) l_i l_j^{\mathrm{C}} \mathrm{E}[N(t_k + v_1)N(t_k + v_2)]\mathrm{d}v_1\mathrm{d}v_2\Big\} \tag{6.28}$$

In making the above product the cross terms involving $\Xi_i(\mathrm{o})\,\Phi_j^{\mathrm{C}}(t_k + v_2)$ and $\Xi_j^{\mathrm{C}}(\mathrm{o})\,\Phi_i(t_k + v_1)$ have been disregarded as the initial value of the generalized coordinate is poorly correlated with later values of the excitation. Since $N(t)$ has been assumed to be of the form

$$N(t) = \xi(t)U(t) \tag{6.29}$$

where $\xi(t)$ is a slowly varying deterministic function and $U(t)$ is a stationary process, the above result can be expressed as

$$\Gamma_{ij}(h) = \exp([\lambda_i + \lambda_j^{\mathrm{C}}]h)\Big\{\mathrm{E}[\Xi_i(0)\Xi_j^{\mathrm{C}}(0)]$$

$$+\xi^2(t_k + \frac{h}{2})l_i l_j^{\mathrm{C}} \int_0^h \int_0^h \exp(-\lambda_i v_1 - \lambda_j^{\mathrm{C}} v_2) R_U(v_2 - v_1)\mathrm{d}v_1\mathrm{d}v_2\Big\} \qquad (6.30a)$$

where $R_U(v_2 - v_1)$ is the autocorrelation function of process $U(t)$. In the preceding equation it has been assumed that function $\xi(t)$ varies so slowly that it can be driven out from the integral and set equal to its value at the half of the interval of integration. For the specific case of unmodulated white noise the above integral can be explicited in closed form

$$\Gamma_{ij}(h) = \exp([\lambda_i + \lambda_j^{\mathrm{C}}]h)\Gamma_{ij}(0) + \frac{2\pi S_W l_i l_j^{\mathrm{C}}}{\lambda_i + \lambda_j^{\mathrm{C}}}[\exp([\lambda_i + \lambda_j^{\mathrm{C}}]h - 1] \qquad (6.30b)$$

Since the system matrix contains the linearization coefficients, which in turn depend on the eigenvalues and eigenvectors of the system matrix, an iterative solution is required at each time step. Note that the eigenproblem must be solved again at the next step. Therefore, in order to make the method competitive with the direct approach (equation 3.46) efficient techniques for eigenvalue search based on the current available information should be devised, taking into account that from iteration to iteration and from step to step only the linearization coefficients change. The Taylor approach proposed by Casciati *et al.* (1994) is an important contribution in this direction.

For performing the iterations it must be remembered that the system matrix $\boldsymbol{A}_{\mathrm{e}}$ is assumed to remain constant inside the step. However, different linearization coefficients will result from using the response values corresponding to its beginning and end. Therefore, the final expression of the system matrix at the $k-$th step can be set to be equal to their average (Pradlwarter and Schuëller 1991). The iteration inside each interval can then be performed according to the following scheme:

1. Assume as initial value of the matrix at the current step the final value at the preceding,

$$^1\boldsymbol{A}_{\mathrm{e}}(t_k) = \boldsymbol{A}_{\mathrm{e}}(t_{k-1}) \qquad (6.31)$$

where the rear superindex denotes iteration.

2. After solving the equation for the covariance, the linearization coefficients corresponding to the end of the $k-$ step can be calculated. Denoting it by ${}^{i}\boldsymbol{A}_{\mathrm{e}}(t_{k+1}), i = 1, 2, \ldots$ the new value of the system matrix is

$$ {}^{i+1}\boldsymbol{A}_{\mathrm{e}}(t_k) = \frac{1}{2}({}^{i}\boldsymbol{A}_{\mathrm{e}}(t_k) + {}^{i}\boldsymbol{A}_{\mathrm{e}}(t_{k+1})) \tag{6.32} $$

3. Repeat step 2 until an acceptable convergence in $\boldsymbol{\Sigma}(t_k)$ is achieved.

On the other hand, a restriction could be imposed on the discontinuous variation of the system matrix in order that the mean and covariance responses be in agreement with the necessary continuity of the vector $\boldsymbol{q}$. This requires that

$$ \boldsymbol{q}(t_k^-) = \boldsymbol{q}(t_k^+) \tag{6.33} $$

so that

$$ \boldsymbol{R}(t_{k-1})\boldsymbol{\Xi}(t_k^-) = \boldsymbol{R}(t_k)\boldsymbol{\Xi}(t_k^+) \tag{6.34} $$

Applying the expectation operator and taking into account the normalization conditions (equations 6.13 and 6.14) the following expression is obtained:

$$ \boldsymbol{\Gamma}(t_k^+) = \{\boldsymbol{L}^{\mathrm{T}}(t_k)\boldsymbol{R}(t_{k-1})\}\boldsymbol{\Gamma}(t_k^-)\{\boldsymbol{L}^{\mathrm{T}}(t_k)\boldsymbol{R}(t_{k-1})\}^{\mathrm{T}} \tag{6.35} $$

Considering equation (6.13), it can be noticed that this is a very mild condition indeed. However, it has been found that albeit not essential, its introduction entails numerical difficulties in many cases. Therefore, in the analyses that follow it has not been imposed.

As an example, let us consider the case of a single degree of freedom structure whose restoring force is of the Bouc - Wen endochronic type, whose motion is governed by the classical differential equation

$$ m\ddot{X} + c\dot{X} + \alpha kX + (1-\alpha)kZ = -mN(t) \tag{6.36} $$

in which m, c and k are mass, damping and stiffness constants. The model parameters for the example are $m = 0.933$, $c = 0.573$, $k = 35.2$, $\alpha = 0.15$, $A = 1$, $\beta = \gamma = 2$ and $n = 1$. The excitation $N(t)$ is equal to the product of a Gaussian white noise $W(t)$ with autocorrelation function $2\pi S_W \delta(v_2 - v_1)$ and a Shinozuka-Sato modulating function (equation 2.19) with parameters $a = 0.25, b = 0.5$. The noise intensity has been set equal to 0.1.

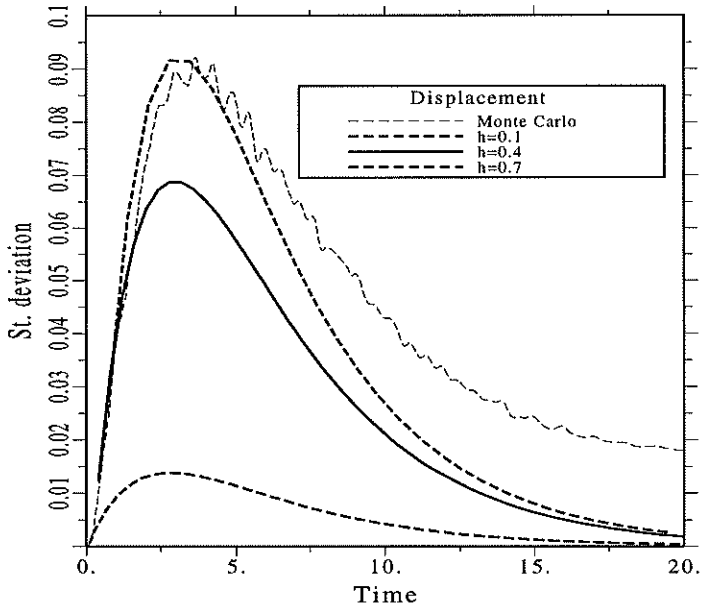

Figure 6.1 Displacement response by conventional complex modal method using different time steps

Figures 6.1 and 6.2 show respectively the standard deviation of the displacement X and velocity $\dot{X}$ obtained by this classical algorithm using three different values of the time step h. They are depicted together with those corresponding to 1,000 Monte Carlo simulations. It can be observed that the estimation depends so largely on the selected time step h that it is unreliable for practical use. Up to the author's knowledge, however, this critical drawback of the complex modal algorithm has neither been discussed nor overcome in the specialized literature.

Seemingly, the reason for this numerical instability lies in the presence of an exponential function. In fact, for white noise excitation $U(t) = W(t)$, the derivative of the modal covariance can be estimated from (7.30b) as

$$\dot{\Gamma}_{ij}(h) \approx \frac{\Gamma_{ij}(h) - \Gamma_{ij}(0)}{h} = \frac{\Gamma_{ij}(0) + b}{h}(\exp([\lambda_i + \lambda_j^{\mathrm{C}}]h - 1) \qquad (6.37a)$$

where b is a complex constant equal in this case to

$$b = \frac{2\pi S_W l_i l_j^{\mathrm{C}} \xi^2(t_k + \frac{h}{2})}{\lambda_i + \lambda_j^{\mathrm{C}}} \qquad (6.37b)$$

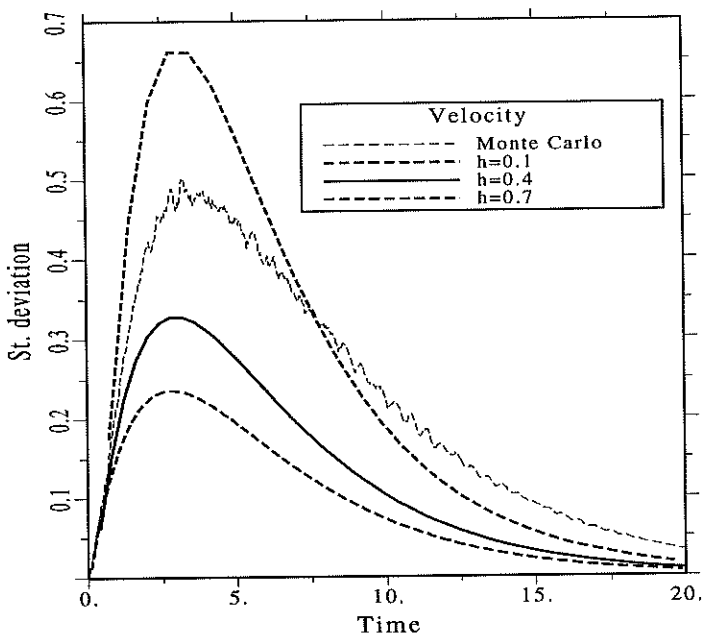

Figure 6.2 Velocity response by conventional complex modal method using different time steps

Equation (6.37a) makes evident that the exponential function causes a strong nonlinear dependence of the variation of the modal covariance on the time step h, so that the selection of the later determines the evolution of the modal covariance altogether.

6.4 Proposed complex modal algorithm

In this section an algorithm that circumvents the above nonlinear dependency on the time interval is developped. As for using the direct method (equation 3.46), it requires that the excitation be modeled in terms of white noise. In particular, it can be either a unmodulated or uniformly modulated white noise or also a white noise with frequency and amplitude modulation passed through time invariant or time variant filters.

Let us define

$$G_{ij} = \Xi_i \Xi_j^{\mathrm{C}} \tag{6.38}$$

The evolution of the two factors entering in the above expression (see equations 6.20) can be cast as a bidimensional system of Ito stochastic differential equations, i.e.,

$$\mathrm{d}\begin{pmatrix} \Xi_i \\ \Xi_j^{\mathrm{C}} \end{pmatrix} = \begin{pmatrix} \lambda_i \Xi_i \\ \lambda_j^{\mathrm{C}} \Xi_j^{\mathrm{C}} \end{pmatrix} \mathrm{d}t + \begin{pmatrix} l_i \\ l_j^{\mathrm{C}} \end{pmatrix} \mathrm{d}B(t) \tag{6.39}$$

where $B(t)$ is a Wiener processes with properties

$$\mathrm{E}[\mathrm{d}B(t)] = 0 \tag{6.40}$$

$$\mathrm{E}[\{\mathrm{d}B(t)\}^2] = \sqrt{2\pi S_W}\xi(t)\mathrm{d}t \tag{6.41}$$

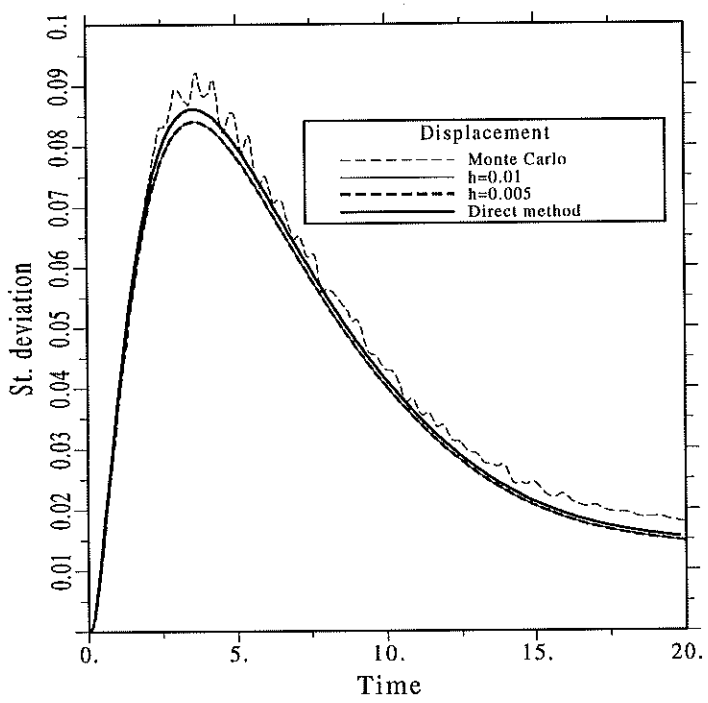

Figure 6.3 Displacement response by proposed complex modal method using different time steps ($S_W = 0.1$)

The Ito formula for this case reads

$$\mathrm{d}G_{ij} = \left\{ \lambda_i \Xi_i \Xi_j^{\mathrm{C}} + \lambda_j^{\mathrm{C}} \Xi_j^{\mathrm{C}} \Xi_i + 2\pi S_W \xi^2(t) l_i l_j^{\mathrm{C}} \right\} \mathrm{d}t +$$

$$\sqrt{2\pi S_W}\xi(t)(l_i \Xi_j^{\mathrm{C}} + l_j^{\mathrm{C}} \Xi_i)\mathrm{d}B(t) \tag{6.42}$$

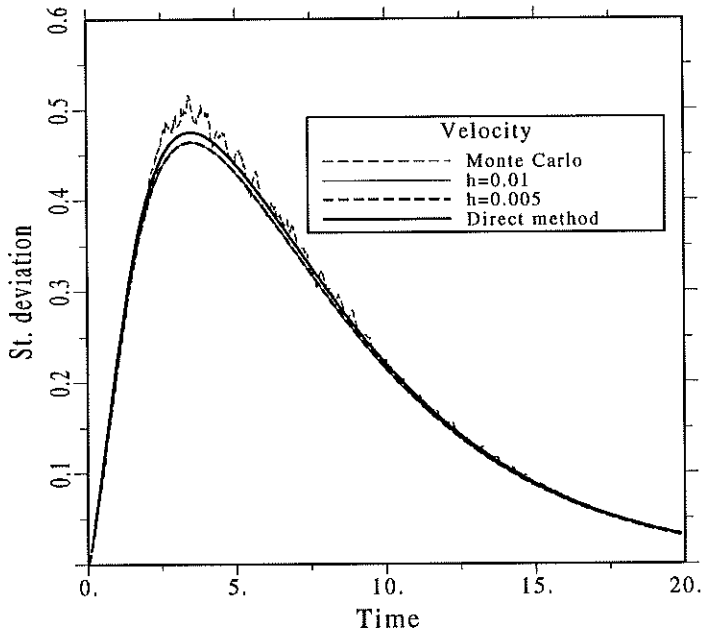

Figure 6.4 Velocity response by proposed complex modal method using different time steps ($S_w = 0.1$)

Taking expectations we finally obtain

$$\dot{\Gamma}_{ij}(t) = (\lambda_i + \lambda_j^c)\Gamma_{ij}(t) + 2\pi S_W \xi^2(t) l_i l_j^c, \qquad t_k \leq t \leq t_{k+1} \tag{6.43}$$

Notice that there is no need of approximating the modulating function by its mean value in this case, as it was required in deriving equation (6.30). It can be seen that in contrast to equation (6.37a) the above derivative of the modal covariance does not depend on the time interval. Thus, the results obtained by this method are expected to be no longer beset by the numerical instability exhibited by those calculated with the classical algorithm. In fact, despite equation (6.30b) is the exact mathematical solution of equation (6.43) when $\xi(t) = 1$, its numerical use for a step-by-step calculation involves exponential functions that introduce a strong nonlinear dependence on the time step h. Therefore, equation (6.43) points out the right way of solving numerically the nonstationary complex modal analysis, despite the mathematical exactness of the integral solution.

On the other hand, they should be similar to those obtained by the direct method, due to the equivalence between both approaches. Such an equivalence

can be easily demonstrated. In fact, taking time derivatives in equation (6.26) one obtains

$$\dot{\boldsymbol{\Sigma}}(t_k+\tau)=\Re\left\{\dot{\boldsymbol{R}}\boldsymbol{\Gamma}(\tau)\boldsymbol{R}^{\mathrm{CT}}+\boldsymbol{R}\boldsymbol{\Gamma}(\tau)\dot{\boldsymbol{R}}^{\mathrm{CT}}+\boldsymbol{R}\dot{\boldsymbol{\Gamma}}(\tau)\boldsymbol{R}^{\mathrm{CT}}\right\} \tag{6.44}$$

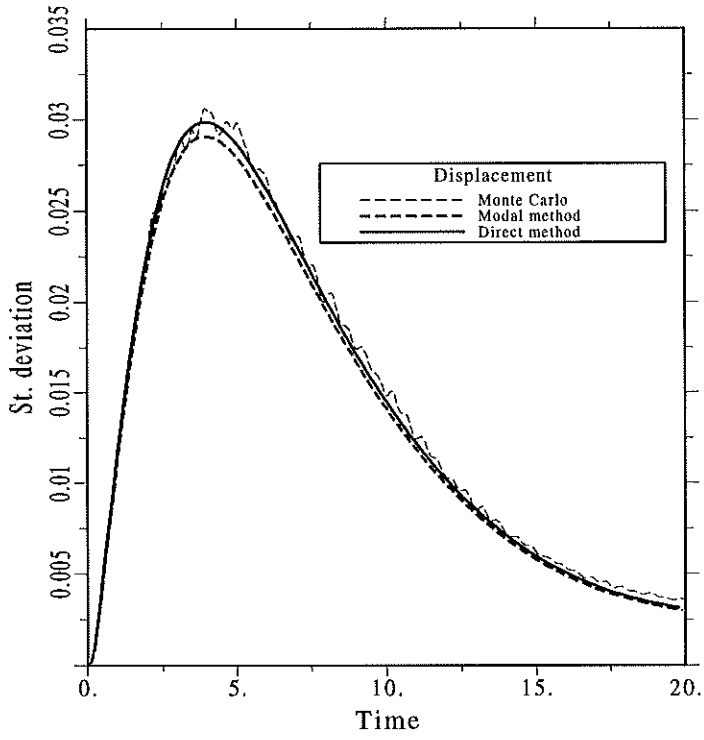

Figure 6.5 Displacement responses ($S_w = 0.01$).

Considering that the system matrix is assumed constant inside the (t_k, t_k+h), the first two terms of the right hand side of the above equation vanish in that interval. The substitution of the resulting expression and of equation (6.26) into equation (3.46) yields

$$\dot{\boldsymbol{\Sigma}}(t_k+\tau)=\Re\left\{\boldsymbol{R}\dot{\boldsymbol{\Gamma}}(\tau)\boldsymbol{R}^{\mathrm{CT}}\right\}=\boldsymbol{A}_{\mathrm{e}}\Re\left(\boldsymbol{R}\boldsymbol{\Gamma}(\tau)\boldsymbol{R}^{\mathrm{CT}}\right)+$$

$$\Re\left(\boldsymbol{R}\boldsymbol{\Gamma}(\tau)\boldsymbol{R}^{\mathrm{CT}}\right)\boldsymbol{A}_{\mathrm{e}}^{\mathrm{T}}+2\pi\boldsymbol{S}_{\boldsymbol{F}} \tag{6.45}$$

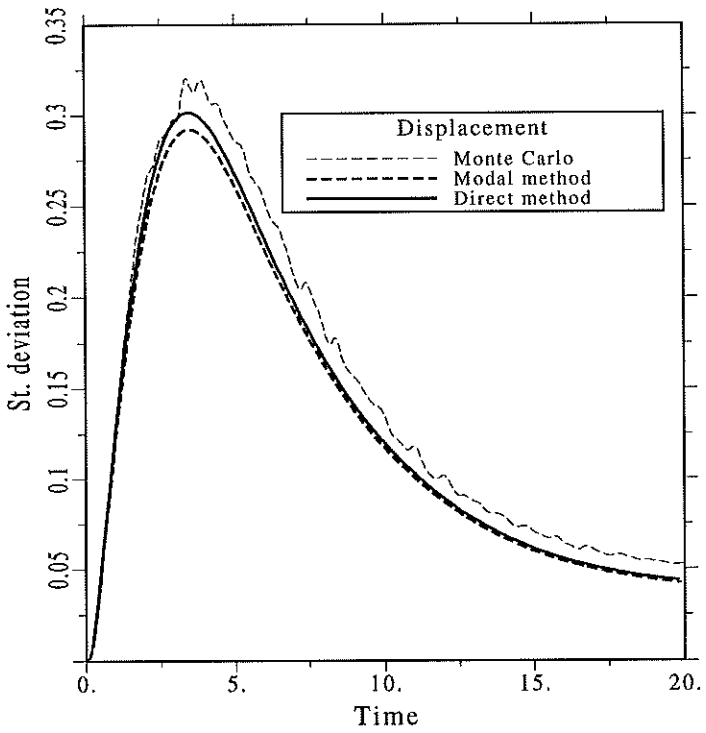

Figure 6.6 Displacement responses ($S_w = 1.0$).

Pre- and postmultiplying by $\boldsymbol{R}^{-1}$ and $\boldsymbol{R}^{-\mathrm{CT}}$ and taking into account the normalization and orthogonality conditions the following equation is obtained:

$$\dot{\boldsymbol{\Gamma}} = \boldsymbol{\Lambda\Gamma} + \boldsymbol{\Gamma\Lambda}^{\mathrm{C}} + 2\pi \boldsymbol{L}^{\mathrm{T}} \boldsymbol{S}_F \boldsymbol{L}^{\mathrm{C}} \tag{6.46}$$

which is the matrix expression of the componentwise equation (6.43).

The numerical stability of the proposed approach is illustrated by figure 6.3, which depicts the same Monte Carlo curve of figure 6.1 along with the estimation from the present approach using two different values of the time step h. All complex modes have been used in the calculation. It is seen that the two results of the proposed approach are undistinguishable from each other. The figure also shows the results obtained by the direct method. The minor differences between the proposed complex modal and direct approaches can be attributed to the rather different ways of solving the dynamic equations in the two procedures (Notice that the direct method does not require iteration). The corresponding results for the velocity of this system are depicted in figure 6.4.

Further analyses were conducted on the same system using a lower and a higher white noise intensities ($S_W = 0.01$ and $S_W = 1$) in order to test the numerical robustness and accuracy of the algorithm in a wide range of response nonlinearity. In fact, such excitations correspond respectively to slight and high degrees of nonlinear behavior of the example system, while that with $S = 0.1$ corresponds to an intermediate situation. Figures 6.5 and 6.6 compare the displacement results obtained by the proposed complex modal algorithm and those by direct method and Monte Carlo.

Notice that the method proposed in the foregoing chapter for calculating the linearization coefficients can be plugged into this algorithm without difficulty. Gaussian linearization coefficients, however, have been used in the above examples in all which they lead to good response estimations due to the high value of α.

Chapter 7

Higher order stochastic response of hysteretic structures

7.1 Introduction

In the preceding chapters the applicability of the method of stochastic equivalent linearization for estimating the first two statistical moments of the response of hysteretic structures was discussed. Despite such information seems to supply only a rough description of the probabilistic behaviour of such systems when subject to random external or parametric excitations, it is nevertheless quite useful for an approximate reliability assessment of the structure as explicited in chapter 3. However, a deeper insight into the system's stochastic behaviour is even possible by making use of the Markov methods summarized in chapter 1, which would eventually lead to an estimation of the (stationary or evolutive) probability density function of the response.

This chapter is devoted to a discussion on the feasability of the application of existing Markov methods for calculating the probability functions of the response variables of hysteretic systems. It begins with a short account of the classical *closure techniques* which are based on the moment equations generated by the Ito formula. It is shown that when using these methods for hysteretic systems some assumptions and/or simplifications are required. This is also valid for using the *Taylor method* proposed by DiPaola *et al.* 1995. The only methods readily applicable to any nonlinear system are the *finite element solution of the Fokker-Plank equation*, on which substantial research has been conducted in the last years, and the *method of maximum entropy* recently proposed by Trębicki and Sobczyk (1996). Since an enormous computational effort is envisaged in applying the former method to the simplest hysteretic oscillator, the main attention has been focussed on the latter in the present research.

The maximum entropy method is much less expensive then the finite ele-

ment approach due to the fact that it decouples the Fokker-Planck equation by means of the moment equations generated by the application of the Ito formula, as closure methods do. With respect to the latter, however, it has the added advantage of exploting a sound physical principle that has proven to be very useful in information theory as well as in other areas (Kapur 1989). Nevertheless, it is shown that the method is so weak from the numerical point of view that the calculation breaks down even at low levels of nonlinearity when using conventional numerical methods. After a discussion on the causes of such failures a somewhat heterodox numerical integration algorithm is proposed. It is demonstrated that with its aid a solution can be achieved even in case of strong nonlinear behaviour of the hysteretic oscillator considered in the present work and, in general, of nonlinear structural systems.

7.2 Closure methods

Let us recall the theory of stochastic systems sketched in chapter 1. The set of stochastic differential equations for a $N-$dimensional system subject to Gaussian white noise $W(t)$ reads

$$\mathrm{d}\boldsymbol{X}(t) = \boldsymbol{\Theta}(\boldsymbol{X}(t), t)\mathrm{d}t + \boldsymbol{\Psi}(\boldsymbol{X}(t), t)\mathrm{d}\boldsymbol{B}(t) \tag{7.1}$$

where $\boldsymbol{X}$ is the state vector of the system, $\boldsymbol{B}(t)$ is a vector of R uncorrelated Wiener processes, $\boldsymbol{\Theta}$ is a $N-$dimensional vector of drift functions and $\boldsymbol{\Psi}$ is a $N \times R$ diffusion matrix.

For a function differentiable function $h(\boldsymbol{X})$ the Ito formula states that

$$\mathrm{d}h = \Big[\frac{\partial h}{\partial t} + \sum_{i=1}^{N} \Theta_i(\boldsymbol{X}, t)\frac{\partial h}{\partial X_i} + \frac{1}{2}\sum_{r=1}^{R}\sum_{i,k=1}^{N} \Psi_{ir}(\boldsymbol{X}, t)\Psi_{kr}(\boldsymbol{X}, t)\frac{\partial^2 h}{\partial X_i \partial X_k}\Big]\mathrm{d}t + \sum_{r=1}^{R}\sum_{i=1}^{N} \Psi_{ir}(\boldsymbol{X}, t)\frac{\partial h}{\partial X_i}\mathrm{d}B_r \tag{7.2}$$

Set function $h(\boldsymbol{X})$ equal to

$$h(\boldsymbol{X}) = X_1^{j_1} X_2^{j_2} \ldots X_N^{j_N} \tag{7.3}$$

For the sake of simplicity in the notation, the exponents $j_i, i = 1, 2, \ldots, N$ can be considered as elements of the multi-index vector

$$\boldsymbol{j} = [j_1, j_2, \ldots, j_N] \tag{7.4}$$

whose sum of elements

$$|\boldsymbol{j}| = j_1 + j_2 + \ldots + j_N \tag{7.5}$$

indicates the order of the moment being evaluated. Consider a dynamical system whose nonlinearities have a polynomial form. For instance, in the Duffing system the equation of motion is

$$\ddot{Y}(t) + \beta\dot{Y}(t) + \omega^2 Y(t) + \epsilon\omega^2 Y^3(t) = W(t) \tag{7.6}$$

Taking into account that

$$\mathrm{E}[\mathrm{d}\boldsymbol{B}(t)] = \boldsymbol{0} \tag{7.7}$$

and that function $h(\cdot)$ is not an explicit function of time, it can be easily shown that the application of the expectation operator to the Ito formula for such a system yields the following set of moment equations:

$$\dot{\boldsymbol{\mu}}_J = \boldsymbol{g}_J[\boldsymbol{\mu}_1, \boldsymbol{\mu}_2, \ldots], \qquad J = 1, 2, \ldots \tag{7.8}$$

Here $\boldsymbol{\mu}_J$ denotes the vector of all moments $\mu_{\boldsymbol{j}}$ for which $|\boldsymbol{j}| = J$ and $\boldsymbol{g}_J$ are vector linear functions. For example, writting the equation of motion of the above Duffing oscillator in the standard form of stochastic differential equations and applying the Ito formula to the function

$$h(\boldsymbol{X}) = X_1^{j_1} X_2^{j_2} \tag{7.9}$$

where $X_1 = Y$ and $X_2 = \dot{Y}$, the set of moment equations reads

$$\dot{\mu}_{|\boldsymbol{j}|}(j_1, j_2) = j_1\mu_{|\boldsymbol{j}|}(j_1 - 1, j_2 + 1) - \omega^2 j_2\mu_{|\boldsymbol{j}|}(j_1 + 1, j_2 - 1) - \epsilon\omega^2 j_2 \times$$

$$\mu_{|\boldsymbol{j}|+2}(j_1 + 3, j_2 - 1) - \beta j_2\mu_{|\boldsymbol{j}|}(j_1, j_2) + \frac{\pi G_W}{2} j_2(j_2 - 1)\mu_{|\boldsymbol{j}|-2}(j_1, j_2 - 2) \tag{7.10}$$

where the arguments of the moments are the powers of the state variables and G_W is the one-sided power spectral density of the white noise $W(t)$. It can be seen that in the above general differential equation moments of higher order than the currently evaluated are involved, thus rendering the problem indeterminate. In order to arrive at a solution several *closure techniques* have been proposed. Essentialy they consist in expressing higher order moments as function of lower

order ones, thus allowing the closure of the system of equations. The most important closure techniques are the following:

1. *Central moment closure.*
   It consists in assuming that the central moments of an order higher than a certain J are zero, so that they can be discarded from the moment equations.

2. *Gaussian closure.*
   In this case it is assumed that the the response of the system $\boldsymbol{X}(t)$ obeys a Gaussian distribution at any time t. This opens up the possibility of expressing the higher order moments as functions of lower order ones using well known formulas for the Gaussian distribution (Soong and Grigoriu 1993).

3. *Cumulant or quasi-moment closure.*
   This technique is based on the fact that cumulants and quasi-moments provide information of lower importance the higher their order. Therefore, by means of the relationships linking moments and cumulants (or moments and quasimoments) it is possible to obtain the desired dependency of higher on lower order moments by neglecting the cumulants or quasi-moments of order higher than a certain maximum value (Muscolino 1993; Lutes and Sarkani 1997).

Let us now consider the case of a single mass, uniaxial endochronic hysteretic system of the Bouc-Wen type subject to a white ground acceleration $W(t)$. The equation of motion of the system is

$$m\ddot{Y} + c\dot{Y} + \alpha kY + (1-\alpha)kZ = -mW(t) \tag{7.11}$$

where the dynamics of the nonlinear hysteretic component is governed by the following differential equation:

$$\dot{Z} = \zeta(\dot{Y}, Z) = A\dot{Y} - \beta|\dot{Y}||Z|^{n-1}Z - \gamma\dot{Y}|Z|^n \tag{7.12}$$

The state vector and the drift and diffusion matrices have the following expressions:

$$\boldsymbol{X} = \begin{pmatrix} Y \\ \dot{Y} \\ Z \end{pmatrix} \tag{7.13}$$

$$\boldsymbol{\theta}(\boldsymbol{X}(t), t) = \begin{pmatrix} \dot{Y} \\ -m^{-1}\{\alpha kY + c\dot{Y} + (1-\alpha)kZ\} \\ \zeta(\dot{Y}, Z) \end{pmatrix} \tag{7.14}$$

$$\boldsymbol{\Psi}(\boldsymbol{X}(t),t) = \begin{pmatrix} 0 \\ \sqrt{\pi G_W} \\ 0 \end{pmatrix} \tag{7.15}$$

Set function $h(\cdot)$ as the following power function:

$$h(\boldsymbol{X}) = Y^{j_1}\dot{Y}^{j_2}Z^{j_3} \tag{7.16}$$

where the exponents j_i, $i = 1,2,3$ can be regarded as elements of the multi-index vector

$$\boldsymbol{j} = [j_1, j_2, j_3] \tag{7.17}$$

Proceeding in the same way as before, the following system of moment equations is finally obtained:

$$\dot{\mu}_{|\boldsymbol{j}|}(j_1,j_2,j_3) = j_1\mu_{|\boldsymbol{j}|}(j_1-1,j_2+1,j_3)$$

$$-\frac{\alpha k}{m}j_2\mu_{|\boldsymbol{j}|}(j_1+1,j_2-1,j_3) - \frac{c}{m}j_2\mu_{|\boldsymbol{j}|}(j_1,j_2,j_3)$$

$$-\frac{(1-\alpha)k}{m}j_2\mu_{|\boldsymbol{j}|}(j_1,j_2-1,j_3+1) + j_3\mathrm{E}[\zeta(\dot{X},Z)X^{j_1}\dot{X}^{j_2}Z^{j_3-1}]+$$

$$\frac{\pi G_W}{2}j_2(j_2-1)\mu_{|\boldsymbol{j}|-2}(j_1,j_2-2,j_3) \tag{7.18}$$

It must be taken into account that for antisymmetric hysteretic systems, i.e. those for which the restoring force $g(X,\dot{X},Z)$ has the property

$$g(X,\dot{X},Z) = -g(-X,-\dot{X},-Z) \tag{7.19}$$

moments of odd $|\boldsymbol{j}|$ are zero for zero mean random excitation.

Unlike the polynomial case, the above system of differential equations is not characterized by its lack of closure but only by the presence of expectations whose calculation requires the knowledge of the joint probability density function. Since this information is not available beforehand, the employment of closure techniques would not be sufficient to solve the system of moment equations unless the required probability density function be inferred from the current moment values invoking auxiliary assumptions or principles.

An approximate method for applying closure techniques to the the specific case of bilinear hysteretic oscillator was proposed by Nielsen *et al.* (1990a, 1990b). They substitute the hysteretic equation for Z (4.1) by a third order polynomial in $\dot{X}$ and Z whose coefficients are calculated by least-square minimization of the expected error in a similar fashion as it is routinely done when using the method of equivalent linearization. Since this task requires the calculation of some expectations, a probability density function in the form of a truncated Gram-Charlier expansion combined with Dirac pulses is postulated. The coefficients of the modified expansion are obtained from the current values of the moments, which in turn are given by the solution of the moment equations. Then the cumulant closure technique is applied on the new system of equations having now the general appearance of equation (7.8).

It is evident that this method requires the assumption of a density function, as in the method of stochastic linearization. In this case the assumed density is a modification of an expansion which otherwise leads directly to the characteristic function. Clearly, this modification is imposed by the large departure from Gaussianity of the restoring force component of hysteretic systems, because the Dirac pulses play here the same role they do in the linearization approach proposed in chapter 5. Further, the nonlinear system must be approximated by a polynomial in order to apply the closure techniques. No solution for the stationary multidimensional density function of the Bouc-Wen hysteretic model calculated by this method is known to the author.

7.3 The method of Taylor cumulants

A method for solving a system stochastic differential equations that leads directly to an estimate of the probability density function was reported by DiPaola *et al.* (1995). The method is based on the Taylor expansion of either the multidimensional density function of the state vector $\boldsymbol{X}(t)$ or its logarithm. After substituting into the Fokker-Planck equation the first alternative gives a system of differential equations of the so-called *Taylor moments* while the second produces the system of *Taylor cumulants.*

Of these two alternatives only the second will be summarized here. Let the multidimensional density function of the vector process $\boldsymbol{X}(t)$ be expanded as

$$f(\boldsymbol{x};t) = \exp\left(\lambda_0 + \sum_{i=1}^{N} \lambda_1[X_i]x_i + \sum_{i,k=1}^{N} \frac{1}{2!}\lambda_2[X_iX_k]x_ix_k + \ldots\right) \tag{7.20}$$

where the coefficients of the expansion can be shown to be given by the following equation:

$$\lambda_{|j|}[X_1^{j_1} X_2^{j_2} \dots X_N^{j_N}] = \frac{\partial^{|j|} \ln f(x;t)}{\partial x_1^{j_1} \partial x_2^{j_2} \dots \partial x_N^{j_N}}\Big|_{x=0} \tag{7.21}$$

where $|j| = 1, 2, \dots$. In (7.20) λ_0 plays the role of a normalization constant. Substituting equations (7.20) and (7.21) into the Fokker-Planck equation

$$\frac{\partial f(x;t)}{\partial t} = -\sum_{i=1}^{N} \frac{\partial[\Theta_i(x;t) f(x;t)]}{\partial x_i} + \frac{1}{2} \sum_{i,m=1}^{N} \sum_{r=1}^{R} \frac{\partial^2[\Psi_{ir}(x;t)\Psi_{mr}(x,t) f(x;t)]}{\partial x_i \partial x_m} \tag{7.22}$$

the final form of the differential equation of the coefficient of order $|j|$ is obtained:

$$\dot{\lambda}_{|j|}[X_1^{j_1} X_2^{j_2} \dots X_N^{j_N}] = \sum_{i=1}^{N} a_{ij} + \sum_{i=1}^{N} \sum_{k_i=0}^{j_i} b_{ijk} \lambda_{|k|+1}[X_1^{k_1} X_2^{k_2} \dots X_N^{k_N} X_i]$$

$$+\frac{1}{2} \sum_{i,m=1}^{N} \sum_{r=1}^{R} \sum_{k_i=0}^{j_i} \Psi_{ir}(x,t)\Psi_{mr}(x,t) \Big\{ \lambda_{|j|+2}[X_1^{j_1} X_2^{j_2} \dots X_N^{j_N} X_i X_m]$$

$$+c_{jk} \lambda_{|k|+1}[X_1^{k_1} X_2^{k_2} \dots X_N^{k_N} X_i] \lambda_{|j|+1-|k|}[X_1^{j_1-k_1} X_2^{j_2-k_2} \dots X_N^{j_N-k_N} X_m] \Big\} \tag{7.23}$$

where

$$a_{ij} = -\frac{\partial^{|j|+1} \Theta_i(x;t)}{\partial x_1^{j_1} \partial x_2^{j_2} \dots \partial x_N^{j_N} \partial x_i}\Big|_{x=0} \tag{7.24}$$

$$b_{ijk} = -\binom{j_1}{k_1}\binom{j_2}{k_2} \dots \binom{j_N}{k_N} \frac{\partial^{|j|-|k|} \Theta_i(x;t)}{\partial x_1^{j_1-k_1} \partial x_2^{j_2-k_2} \dots \partial x_N^{j_N-k_N}}\Big|_{x=0} \tag{7.25}$$

$$c_{jk} = \binom{j_1}{k_1}\binom{j_2}{k_2} \dots \binom{j_N}{k_N} \tag{7.26}$$

with the notation

$$\binom{m}{n} = \frac{m(m-1)\dots(m-n+1)}{n!} \tag{7.27}$$

This system of ordinary differential equations can then be solved by conventional strategies.

The direct application of this method to hysteretic systems is hampered by some mathematical difficulties. In fact, for both smooth and piece-wise hysteretic systems some derivatives needed in equation (7.23) are given in terms of Dirac functions from the very first orders, which make impossible even the calculation of the Taylor moments. It is evident that for such systems the only way of using this method would be by calculating equivalent polynomials as in the closure technique proposed by Nielsen *et al.* (1990a, 1990b). As in that case, no experience has been reported on its application to smooth hysteretic systems.

7.4 Finite element solution of the Fokker-Planck equation

As said in chapter 1, the Fokker-Planck equation provides a general method for solving stochastic dynamic problems that can be modelled as diffusion processes. This and related equations appear in physics and chemistry, so that most of the available solutions and methods have been worked out by scientists of such fields (cf. Risken 1989; Gardiner 1985). For the case of nonlinear structural mechanics it is important to note that explicit solutions have been obtained for limited types of simple oscillators in stationary response to which is devoted a monograph by Soize (1994).

In recent times approaches based on finite element techniques have been proposed (Langtagen 1991; Spencer and Bergman 1993; Shiau and Wu 1996; Bergman and Spencer 1997). It must be observed that the number of independent variables in the Fokker-Planck equation is equal to the size of the state vector, N, which is just the very size of the finite elements required for the solution. This means that for a polynomial nonlinear oscillator 2D elements for the state variables of displacement and velocity are required, while for the simplest hysteretic oscillator (equation 7.11) 3D elements will be needed due to the presence of variable Z. It is evident that even the solution of these simple problems in the nonstationary case implies a very large computational effort.

In general, finite element approaches treat the problem as a convection-diffusion equation of the type appearing in fluid dynamics, whose terms correspond to the drift and difussion terms in probability flow. Using a classical finite element approach, the probability density function is discretized in the form

$$f(\boldsymbol{x},t) \approx \sum_{i=1}^{M_e} N_i(\boldsymbol{x}) f_i(t) \tag{7.28}$$

where M_e is the number of nodes per element, N_i are the shape functions and f_i the discrete probability densities. Replacing this equation into (7.22) one eventually obtains a problem in the form

$$\boldsymbol{C}\dot{\boldsymbol{p}} + \boldsymbol{K}\boldsymbol{p} = \boldsymbol{0} \tag{7.29}$$

where $\boldsymbol{C}$ and $\boldsymbol{K}$ are matrices whose entries are determined by the numerical approach (Galerkin, streamline/upwind, etc.). For solving the dynamics of such convection-diffusion problems specific numerical treatment is required (Zienckiewics and Taylor 1995). In particular the Crank-Nicholson method has been applied in most of the few attempts for solving the above system in 2D cases.

A further difficulty found in the finite element solution of the Fokker -Planck equation is that one has to deal with infinite domains. To solve it the use of Hermite polynomial expansions (Langtangen 1991) or adaptive grid generation (Shiau and Wu 1996) have been proposed. Up to the author's knowledge, however, for the Bouc-Wen hysteretic oscillator no finite element solution of the probability density function has yet been reported. But, at first sight, the application of finite element techniques for orders higher than 2 is discouraging, because of the need of dealing with high dimensional finite elements for the analysis of a flow problem over an infinite domain. In the research presented here the method of maximum entropy has been preferred to such an attempt because it has two distinct advantages over the finite element strategies: First, its basic stuff is not a single equation as Fokker-Planck's but the set of moment equations, which play in this context a similar role as the generalized equations resulting from eigendecomposition in linear dynamics. Second, the moment information at any time instant is gathered by an additional physical principle which restores the decoupled multidimensional density function. It will be discussed to a larger lenght than the previous methods in the next section.

7.5 The method of maximum entropy

A general method for solving systems of differential equations of moments based on the principle of maximum entropy, has recently been proposed (Trębicki and Sobczyk 1996; Sobczyk 1997). It is an extension to the nonstationary case of a previous proposal formulated by the same authors for stationary analyses (Sobczyk and Trębicki 1990). Its main advantage over the closure techniques described in section 7.2 is that it leads directly to an approximation of

the probability density function of the state vector without symplifying assumptions. At first sight it seems to be of unlimited applicability and its accuracy has been demonstrated by several examples in the quoted papers. However, it will be shown in this section that despite its sound physical basis the method is very weak from a numerical point of view, so that it is difficult to arrive at a solution when using conventional numerical techniques.

The first section of this paragraph is devoted to a brief summary of the method, which is in general useful for solving systems of stochastic differential equations in many fields. After that introduction, the mentioned numerical difficulties in its application will be examined. This discussion is followed by the exposition of a proposed procedure that helps to arrive at a solution in many cases, based on the use of multidimensional Fourier transforms. The numerical examples demonstrate the accuracy of the method for assessing the stationary probability function of the response of nonlinear oscillators as well as the upgrading of the numerical stability of the method when using the proposed integration technique.

7.5.1 Basic algorithm

The principle of maximum entropy, as formulated in the frame of classical theory of probability and mathematical statistics, states that under some constraints (generally given in the form of moments of a $N-$dimensional state vector $\boldsymbol{x}$ or their differential equations) the density function $p(\boldsymbol{x})$ that must be chosen is the one that maximizes the entropy functional

$$H[f] = -\int f(\boldsymbol{x},t)\ln f(\boldsymbol{x},t)\mathrm{d}\boldsymbol{x} \tag{7.30}$$

where the integral spans the entire real space. (Kapur 1989; Dmitriev 1991; Gzyl 1995). The constraints (which are more adequately called *prior information* in this context) can be given in the form of moments, that is

$$\mu_{\boldsymbol{i}}(t) = \int M_{\boldsymbol{i}}(\boldsymbol{x},t)\mathrm{d}\boldsymbol{x} = \int m_{\boldsymbol{i}}(\boldsymbol{x})f(\boldsymbol{x},t)\mathrm{d}\boldsymbol{x} \tag{7.31}$$

where $\boldsymbol{i}$ denotes the multi-index $[i_1, i_2, \cdots i_N]$ and $m_{\boldsymbol{i}}(\cdot)$ is the moment kernel $m_{\boldsymbol{i}}(\boldsymbol{x}) = x_1^{i_1}x_2^{i_2}...x_L^{i_N}$ For want of a better name, the product $M_{\boldsymbol{i}}(\boldsymbol{x},t) = m_{\boldsymbol{i}}(\boldsymbol{x})f(\boldsymbol{x},t)$ will be called "weighted moment kernel" in what follows. According to the aforesaid, the probability density function must be obtained by maximizing the extended entropy functional

$$L[f] = H[f] - \lambda_0\Big\{\int f(\boldsymbol{x},t)\mathrm{d}\boldsymbol{x} - 1\Big\} - \sum_{|\boldsymbol{k}|=1}^{K} \lambda_{\boldsymbol{k}}\Big\{\int m_{\boldsymbol{k}}(\boldsymbol{x}) f(\boldsymbol{x},t)\mathrm{d}\boldsymbol{x} - \mu_{\boldsymbol{k}}(t)\Big\} \quad (7.32)$$

where λ_0 and $\lambda_{\boldsymbol{k}}$ are Lagrange multipliers corresponding to the constraints of unit hypervolume and moments, respectively. The result of the maximization of the functional is

$$f(\boldsymbol{x},t) = C_1^{-1}(t)\exp\Big(-\sum_{|\boldsymbol{k}|=1}^{K} \lambda_{\boldsymbol{k}} m_{\boldsymbol{k}}(\boldsymbol{x})\Big) \quad (7.33)$$

where K is the highest order of moment considered and $C_1(t)$ is a normalizing constant, i.e.,

$$C_1(t) = \int p_1(\boldsymbol{x},t)\mathrm{d}\boldsymbol{x} \quad (7.34a)$$

where

$$p_1(\boldsymbol{x},t) = \exp\Big(-\sum_{|\boldsymbol{k}|=1}^{K} \lambda_{\boldsymbol{k}} m_{\boldsymbol{k}}(\boldsymbol{x})\Big) \quad (7.34b)$$

Alternatively, the prior information can be the system of ordinary differential equations of moments, which are obtained by application of the Ito formula and the expectation operator to a system of stochastic differential equations describing the dynamics of the system as shown before. The former can be put in the form

$$\dot{\mu}_i(t) = \gamma_i(t) \quad (7.35)$$

or, alternatively, as

$$\frac{\mathrm{dE}[m_i(\boldsymbol{X},t)]}{\mathrm{d}t} = \mathrm{E}[g_i(\boldsymbol{X},t)] \quad (7.36)$$

in which

$$g_i(\boldsymbol{X},t) = \sum_{i=1}^{N} \Theta_i(\boldsymbol{X},t)\frac{\partial h}{\partial X_i} + \frac{1}{2}\sum_{r=1}^{R}\sum_{i,k=1}^{N} \Psi_{ir}(\boldsymbol{X},t)\Psi_{kr}(\boldsymbol{X},t)\frac{\partial^2 h}{\partial X_i \partial X_k}\Big] \quad (7.37)$$

Note that greek letters are employed here to indicate expected values, while latin ones denote the corresponding kernels. By taking the system (7.35) as prior information, the maximization of entropy gives the following estimate of the probability density function:

$$f(\boldsymbol{x},t) = C_2^{-1}(t)\exp\Big(-\sum_{|\boldsymbol{k}|=1}^{K}\lambda_{\boldsymbol{k}}g_{\boldsymbol{k}}(\boldsymbol{x})\Big) \tag{7.38}$$

with

$$C_2(t) = \int p_2(\boldsymbol{x},t)\mathrm{d}\boldsymbol{x} \tag{7.39a}$$

$$p_2(\boldsymbol{x},t) = \exp\Big(-\sum_{|\boldsymbol{k}|=1}^{K}\lambda_{\boldsymbol{k}}g_{\boldsymbol{k}}(\boldsymbol{x})\Big) \tag{7.39b}$$

Observing the dual definition of $\gamma_i(\boldsymbol{x})$, any of the above interpretations of the probability density function can be introduced into the following integrals:

$$\gamma_i(t) = \dot{\mu}_i(t) = \int m_i(\boldsymbol{x})\frac{\partial f(\boldsymbol{x},t)}{\partial t}\mathrm{d}\boldsymbol{x} \tag{7.40}$$

$$\gamma_i(t) = \mathrm{E}[g_i(\boldsymbol{X},t)] = \int g_i(\boldsymbol{x})f(\boldsymbol{x},t)\mathrm{d}\boldsymbol{x} \tag{7.41}$$

where the subindex a states for 1 or 2. If the first interpretation is followed, the evolution of the Lagrange coefficient is given by

$$\sum_{|\boldsymbol{k}|=1}^{K}[R_i(t)R_{\boldsymbol{k}}(t) - C_1(t)Q_{i\boldsymbol{k}}(t)]\dot{\lambda}_{\boldsymbol{k}}(t) = C_1(t)P_i(t) \tag{7.42}$$

which is obtained by substituting equation (7.33) into (7.40) and (7.41). In this equation

$$R_i(t) = \int m_i(\boldsymbol{x})p_1(\boldsymbol{x},t)\mathrm{d}\boldsymbol{x} \tag{7.43a}$$

$$P_i(t) = \int g_i(\boldsymbol{x})p_1(\boldsymbol{x},t)\mathrm{d}\boldsymbol{x} \tag{7.43b}$$

$$Q_{ik}(t) = \int m_i(\boldsymbol{x}) m_k(\boldsymbol{x}) p_1(\boldsymbol{x}, t) \mathrm{d}\boldsymbol{x} \tag{7.43c}$$

Under the second interpretation the corresponding system of algebraic equations is

$$\sum_{|\boldsymbol{k}|=1}^{K} [\bar{P}_i(t)\bar{R}_k(t) - C_2(t)\bar{Q}_{ik}(t)]\dot{\lambda}_k(t) = C_2(t)\bar{P}_i(t) \tag{7.44}$$

with

$$\bar{R}_i(t) = \int m_i(\boldsymbol{x}) p_2(\boldsymbol{x}, t) \mathrm{d}\boldsymbol{x} \tag{7.45a}$$

$$\bar{P}_i(t) = \int g_i(\boldsymbol{x}) p_2(\boldsymbol{x}, t) \mathrm{d}\boldsymbol{x} \tag{7.45b}$$

$$\bar{Q}_{ik}(t) = \int g_i(\boldsymbol{x}) m_k(\boldsymbol{x}) p_2(\boldsymbol{x}, t) \mathrm{d}\boldsymbol{x} \tag{7.45c}$$

In both cases the resulting operations can be put matrix form as

$$\boldsymbol{S}\dot{\boldsymbol{\lambda}} = \boldsymbol{b} \tag{7.46a}$$

This system can be solved by diferent strategies. Trębicki and Sobczyk (1996) propose the use of the simple Euler scheme to that purpose. This means that for the $l+1$ step the estimated $\boldsymbol{\lambda}(l+1)$ can be obtained from

$$\boldsymbol{S\lambda}(l+1) = \boldsymbol{b}h - \boldsymbol{S\lambda}(l) \tag{7.46b}$$

where h is the time increment. It is important to note that the use of more refined numerical methods for solving the ODE system (such as Runge-Kutta or Adams-Moulton) will largely increase the computational labour due to the need of calculating the integrals (7.43) or (7.45) and solving the system of algebraic equations (7.46) at each intermediate step.

It must be observed that the first interpretation of the maximum entropy density supposes the knowledge of the moments at each time instant. Trębicki and Sobczyk (1996) state that despite the latter are not being calculated explicitly in the algorithm, they can be assumed to be given indirectly by the solution of the resulting algebraic equations. Moreover, amid the two methods the first one has more practical appealing due to the following reasons: a) With

respect to the initial condition it is easier to start than the second one. This is due to the fact that the initial state of the probability density, which is usually a Dirac function corresponding to a deterministic original situation, can be modelled by a slim Gaussian function. That is, the initial condition (1.105) can be approximated by

$$f(\boldsymbol{x}, t_0|\boldsymbol{x}_0, t_0) = \delta(\boldsymbol{x} - \boldsymbol{x}_0) \approx (2\pi)^{-\frac{N}{2}} |\boldsymbol{\Sigma}|^{-\frac{1}{2}} \times$$

$$\exp[-\frac{1}{2}(\boldsymbol{x} - \boldsymbol{x}_0)^{\mathrm{T}} \boldsymbol{\Sigma}^{-1} (\boldsymbol{x} - \boldsymbol{x}_0)] \tag{7.47}$$

where the diagonal elements of the covariance matrix $\boldsymbol{\Sigma}$ must be as low as possible. Equating this Gaussian density to equation (7.33) one obtains a system from which the initial values of the Lagrange vector $\boldsymbol{A}$ can be easily calculated. This is rarely the case when applying the second method, because the powers of the exponential functions are the right hand sides of the system of differential equations. b) Matrix $\boldsymbol{Q}$ is symmetric while $\bar{\boldsymbol{Q}}$ is, in general, not and, also, some Q_{jk} coincide with some R_j. As a consequence, that the amount of integrals that is necessary to evaluate at each time step in the first method is smaller than in the second.

In what follows the numerical problems associated to the first method of maximum entropy will be examined. It will be shown that matrix $\boldsymbol{S}$ introduced in equation (7.46) is so badly conditioned that the use of conventional techniques of mutidimensional integration for calculating its elements (equations 7.43 and 7.45) lead to numerical collapse of the solution before reaching stationarity. A more accurate method for integration is proposed in the next section, which consists in calculating the integrals in the complex space as one-point Fourier transforms. In the numerical study it will be shown that this method leads to a solution in many (not all) cases. That is, even with such highly accurate method of multidimensional integration the method of maximum entropy (whose generality and sound physical roots make it quite alluring) cannot be unconditionally applied.

7.5.2 Numerical evaluation

The numerical analysis will be performed using the following nonlinear oscillators as examples:

1. *Duffing oscillator.* The equation of motion in this case is

$$\ddot{Y}(t) + \dot{Y}(t) + Y(t) + 2Y^3(t) = W(t) \tag{7.48}$$

where $W(t)$ is a Gaussian white noise with autocorrelation function $R_W(t_1, t_2) = \delta(t_2 - t_1)$

2. Coulomb oscillator. The governing equation of this highly nonlinear case is the following:

$$\ddot{Y}(t) + 0.4\pi\dot{Y}(t) + 4\pi^2 Y(t) + 0.98\,\mathrm{sgn}(\dot{Y}(t)) = W(t) \tag{7.49}$$

where the auto-correlation of the noise is $R_W(t_1, t_2) = 2\pi\delta(t_2 - t_1)$.

3. Van der Pol oscillator. This example has been studied by Donley and Spanos (1991) using Padé approximants. The corresponding equation of motion is

$$\ddot{Y}(t) + 0.2(-1 + 10Y^2(t))\dot{Y}(t) + Y(t) = W(t) \tag{7.50}$$

The excitation is defined in the same way as in the Duffing example.

4. Quadratic damping oscillator. The dynamics of this system is governed by the following equation:

$$\ddot{Y}(t) + 0.5|\dot{Y}(t)|\dot{Y}(t) + Y(t) = W(t) \tag{7.51}$$

with $R_W(t_1, t_2) = \delta(t_2 - t_1)$.

5. Bouc-Wen hysteretic oscillator.

$$\ddot{Y} + 0.2\omega\dot{Y} + \alpha\omega^2 Y + (1 - \alpha)\omega^2 Z = W(t) \tag{7.52}$$

where $\omega = 2\pi/3$ and Z is governed by the differential equation (7.12) with $\alpha = 0.1, A = 1, \beta = \gamma = 0.5$ and $n = 1$. The noise intensity was set at $S_W = 0.1$.

These examples were solved by the Euler integration scheme using Gauss-Legendre integration with 19 points per axis. The initial covariance matrix in equation (7.47) was built with diagonal values equal to 0.04 and zero off diagonal entries. The system of algebraic equations (7.46) was solved by LU-decomposition. The calculation in all cases collapsed at its beginnings by overflow when using single or double precision. In the later case the failure time instants were 1.46, 2.01, 0.95, 1.67 and 1.31 s for the five examples considered,

respectively, so that in not a case the system reached stationarity. Several attempts were made using a higher number of quadrature points and/or different strategies for solving the linear system of equations (7.46), such as the powerful Singular Value Decomposition without success.

Table 7.1 Singular values of the $\boldsymbol{S}$ matrix of the Duffing example

No.	Gauss-Legendre at $t = 1.45$ s	Gauss-Legendre at $t = 1.461$ s	Fourier at $t = 1.45$ s
1	8.2406	4.8789E+075	2.2734
2	1.4313	4.4579E+074	0.3877
3	0.4272	3.2306E+073	0.1731
4	0.1093	1.0732E+072	0.0592
5	0.0970	1.0574E+071	0.0385
6	0.0823	1.4512E+068	0.0285
7	0.0186	9.3698E+064	0.0111
8	0.0321	1.8100E+066	0.0076

It is easy to see that the algorithm is numerically weak in at least three aspects. First, the ill-conditioning of matrix $\boldsymbol{S}$. This is the most important factor contributing to the numerical collapses encountered in the analyses carried out. The best measure of ill conditioning of a matrix is given by its singular values, insofar as if the ratio of the largest to the lowest one (the so-called *condition number*) is greater than the reciprocal of the machine precision (roughly 10^{-6} for single and 10^{-12} for double) the matrix is said to be ill conditioned (Hämmerlin and Hoffmann, 1991; Press *et al.*, 1992). Table 7.1 shows the singular values of matrix $\boldsymbol{S}$ at two instants on the verge of the numerical breakdown in the Duffing's case, which has the most well-behaved nonlinear function among the five systems analysed. It is seen that the just before the collapse the range of the singular values range is 5.2 E10, which is wider than the required by single precision calculations, and at the next step it becomes greater than 1.0 E12, thus exceeding the double precision accuracy. Second, the location of the quadratures. As can be seen in any table on numerical integration by Gauss-Legendre quadratures (which is the most economical method for integrating any function) they allocate the integration points the closer to each other, the farther their distance from the origin. It has been observed that this feature represents a

further contribution to the numerical breakdown of the solution. In fact, when evaluating the density function and the weighted moment kernels, in which the values of the state variables are to be raised to high powers, the argument of the integrand's function can reach very large values at some points. The use of higher order precision did not remedy the situation. Needless to say that such a concentration of high values does not occur in uniformly discretized spaces such as those required by Simpson method or the herein proposed Fourier-based algorithm. A third cause could eventually be attributed to the use of the Euler integration scheme, which is reputed to be the the most unstable method for solving differential equations. However, even when using more accurate methods to such purpose such as fifth order Runge-Kutta no significant differences in the partial results calculated have been found; moreover, such a device did not help in overcoming the numerical breakdown of the solution.

In the next paragraph a method for numerical integration based on Fourier transforms is introduced. The solution of all the above examples has been possible with its aid due to its high accuracy.

7.5.3 Proposed Fourier integration algorithm

It is well known that if a $N-$dimensional integral is to be evaluated by a discretization of L points, the number of function evaluations is L^N. Thus, the practical use of the method of maximum entropy requieres efficient methods for performing such a large numerical task at each time step.

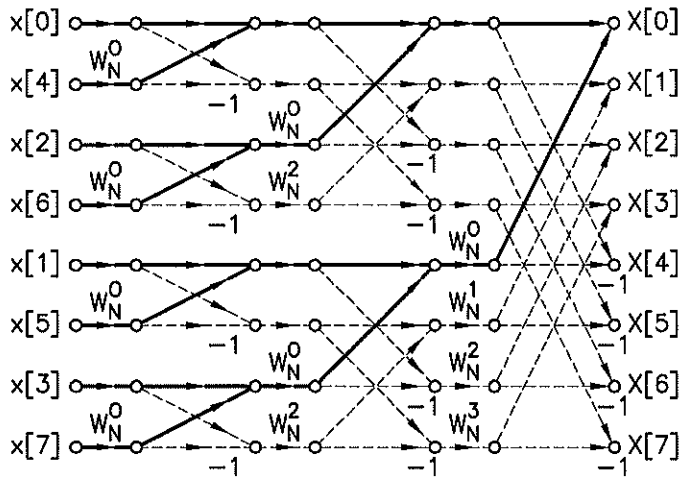

Figure 7.1 On the calculation of one-point Fourier transforms

Besides conventional methods for numerical integration, this labour can be faced by having resort to the characteristic function of the maximum entropy density. Dividing both sides of equation (7.42) by $C_1^2(t)$ it is easy to see that it can be recast in terms of moments, i.e.,

$$\sum_{|\boldsymbol{k}|=1}^{K} [\mu_{\boldsymbol{i}}(t)\mu_{\boldsymbol{k}}(t) - \mu_{\boldsymbol{i}+\boldsymbol{k}}(t)]\dot{\lambda}_{\boldsymbol{k}}(t) = \gamma_{\boldsymbol{i}}(t) \tag{7.53}$$

In passing, it can be seen from the above equation that if the highest order of moment to be evaluated is K, the maximum entropy method uses information of order $2K$, which explains the good accuracy achieved at low K orders as reported by Trębicki and Sobczyk (1996).

While the moments are defined as integrals of the product of the respective kernels by the density function, they can also be expressed as:

$$\mu_{\boldsymbol{i}} = (\frac{1}{\mathrm{i}})^{|\boldsymbol{i}|}\Big(\frac{\partial^{|\boldsymbol{i}|}\Omega(\boldsymbol{\theta})}{\partial^{i_1}\partial^{i_2}\ldots\partial^{i_L}}\Big)_{\boldsymbol{\theta}=\boldsymbol{0}} \tag{7.54}$$

where $\mathrm{i}^2 = -1$ and $\Omega(\boldsymbol{\theta})$ is the characteristic function defined as the Fourier transform of the density

$$\Omega(\boldsymbol{\theta}) = \int \exp(\mathrm{i}\boldsymbol{\theta}^{\mathrm{T}}\boldsymbol{x})\, f(\boldsymbol{x})\mathrm{d}\boldsymbol{x} \tag{7.55}$$

According to this definition the moment of order $\boldsymbol{i}$ can be calculated as the following one point Fourier transform of the weighted kernel functions:

$$\mu_{\boldsymbol{i}} = \Big(\int \exp(\mathrm{i}\boldsymbol{\theta}^{\mathrm{T}}\boldsymbol{x}) m_{\boldsymbol{i}}(\boldsymbol{x})\, f(\boldsymbol{x})\mathrm{d}\boldsymbol{x}\Big)_{\boldsymbol{\theta}=\boldsymbol{0}} \tag{7.56}$$

It is obvious that any integral spanning the whole real space can be estimated as the real part of the zero frequency value of the Fourier transform, provided the later exists. Hence, from a computational point of view the calculation of the elements of matrix $\boldsymbol{S}$ can be done by taking advantage of some properties of the Fourier transform. Specifically, the computer code written for these analyses takes into account the following facts:

1. The need of calculating one single transform point which corresponds to the zero "frequency". Figure 7.1 (adapted from Oppenheim and Schaffer 1989) illustrates by solid lines the operations needed for calculating such single point out of the many needed to compute the discrete Fourier transform

$$X[k] = \sum_{l=0}^{L-1} x[l] \mathrm{e}^{2\pi \mathrm{i} \frac{lk}{L}} \tag{7.57}$$

at $L = 8$ locations. The circles represent summation and the functions W_L^j are the weights $\exp(2\pi \mathrm{i} j/L)$ applied to the corresponding value. It is evident that the operations indicated dashed lines are superfluous in this case. This simplification of the calculation is needed to make the method competitive with other numerical strategies such as Gauss-Legendre quadratures in terms of computation time.

2. The reduction of the $N-$dimensional Fourier transform to a sum of L^{N-1} one dimensional, one point transforms, where L is a discretization order common to all dimensions. In fact the multidimensional continuous transform (equation 7.56) can be approximated by

$$\sum_{l_N=0}^{L_N-1} \cdots \sum_{l_1=0}^{L_1-1} \exp\Big(2\pi \mathrm{i}[\frac{l_1 k_1}{L_1} + \ldots + \frac{l_N k_N}{L_N}]\Big) M_i(l_1, ..., l_N) \cdot \prod_{n=1}^{N} \Delta_N \tag{7.58}$$

in which $L_1, \ldots, L_N$ are the number of discretization points of the weighted moment kernel on each axis, $k_1, \ldots, k_L$ are the coordinate points of a desired value of the transform, $M_i(\cdot)$ is the value of the i weighted moment kernel evaluated at the point of coordinates $(l_1, ..., l_N)$ and $\Delta_1, \ldots, \Delta_N$ are the discretization intervals. Since the moment integrals extend over the whole real space, there is no special reason for assigning a different number of discretization points to each axis, so that all of them can be made equal to a certain L. Also, by proceeding in this way, the value of all the $k_n, n = 1, 2, \ldots N$ corresponding to the zero frequency happen to be also mutually equal because the null frequency occupies the central position. If its corresponding coordinate is denoted by k, the single point multidimensional trannsform (7.56) can be estimated by

$$\sum_{|l|=0}^{N(L-1)} \exp\Big(2\pi \mathrm{i}(\frac{|l|k}{L})\Big) M_i(l_1, ..., l_N) \cdot \prod_{n=1}^{N} \Delta_n \tag{7.59}$$

A simple examination of this equation makes apparent that, by splitting the whole sum into segments according to the index that changes most rapidly, the calculation can be done by summing up L^{N-1} one dimensional, one point transforms. Symbolically, we have

$$\mathrm{FFT}(N,k) = \sum_{i=1}^{L^{N-1}} \mathrm{FFT}_i(1,k) \tag{7.60}$$

Table 7.2 illustrates the way the splitting must be done in a bidimensional case ($N = 2$) using $L = 4$ points so that $L^{N-1} = 4$. The elementary single point FFTs are calculated following the paths depicted in figure 7.1.

Table 7.2 Splitting of a one-point bidimensional Fourier transform (Equation 7.59)

Single FFT No.	l_1	l_2	$\|l\|$
1	0 1 2 3	0 0 0 0	0 1 2 3
2	0 1 2 3	1 1 1 1	1 2 3 4
3	0 1 2 3	2 2 2 2	2 3 4 5
4	0 1 2 3	3 3 3 3	3 4 5 6

3. The possibility of calculating two transforms at a time, due to the fact that the weighted moment kernels are real quantitites. This option represents an additional saving of computation time. A complex array can be built in such a way that its real and complex parts are filled up with the values of two different weighted kernel functions and the transform will return the corresponding moments simultaneously. This device makes use of the symmetry of the Fourier transform for both purely real and purely imaginary functions (Press *et al.* 1992).

Figure 7.2 shows the shape of a typical Fourier transform of an even weigthed moment kernel of a zero mean variable. It can be observed that the zero fre-

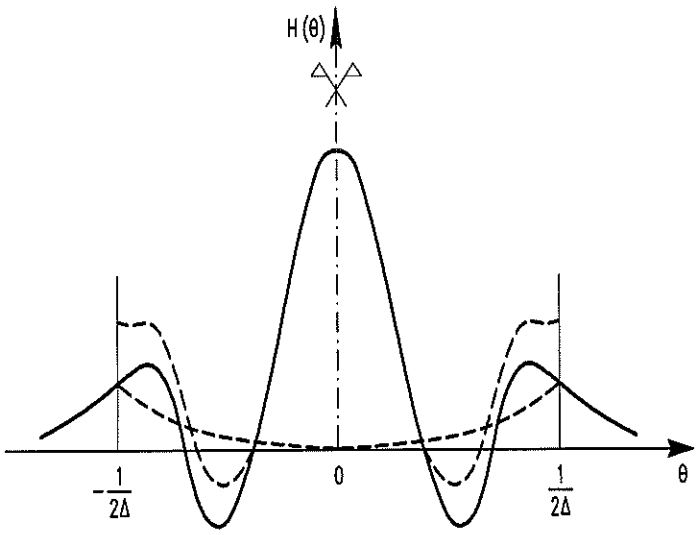

Figure 7.2 Aliasing in transforming a moment kernel

quency is the least affected by the so-called *aliasing* phenomenon, by which the transform values corresponding to frequencies above the critical Nyquist frequency are folded up and added to the values of the transform corresponding to frequencies lower than it. This means that the transforms can be calculated with a reduced number of points per axis with no serious risk to the accuracy of the algorithm.

Table 7.3 Integration of the normal density function (Equation 7.61)

Integration method	Number of points	Value	error, %
Fourier	8	0.9999978	0.00020
Gauss-Legendre	10	0.9998938	0.01062
Simpson	65	0.9999366	0.00634

Table 7.4 Integration of the normal kurtosis kernel (Equation 7.62)

Integration method	Number of points	Value	error, %
Fourier	8	2.998442	0.051
Gauss-Legendre	10	2.973016	0.899
Simpson	129	2.979467	0.684

Table 7.5 Integration of a 3D normal kurtosis kernel (Equation 7.63)

Method	Number of points per axis	Value	error, %
Fourier	8	26.12110	0.065
	16	26.99837	0.006
Gauss-Legendre	9	32.28138	19.561
	17	26.98895	0.041

Tables 7.3 and 7.4 compare the results obtained by the present algorithm with those calculated by Gauss-Legendre quadratures and adaptive Simpson rule (Press *et al.* 1992) for the case of the one dimensional integrals

$$I_1 = \frac{1}{\sqrt{2\pi}} \int \mathrm{e}^{-\frac{x^2}{2}} \mathrm{d}x = 1 \tag{7.61}$$

$$I_2 = \frac{1}{\sqrt{2\pi}} \int x^4 \mathrm{e}^{-\frac{x^2}{2}} \mathrm{d}x = 3 \tag{7.62}$$

which correspond respectively to the standard Gaussian function and a kurtosis kernel. It is observed that the proposed Fourier method is the most accurate of all and that it is as economical as the Gauss-Legendre's.

Since for a task of masive multidimensional integration (as that required by the method of maximum entropy) techniques like Simpson's or Romberg's represent a large computational burden, only the Gauss-Legendre's will be used as a reference for comparing the accuracy and efficacy of the proposed Fourier algorithm in the sequel. Table 7.5 shows a comparison of the evaluation of the normal kurtosis kernel in three dimensions:

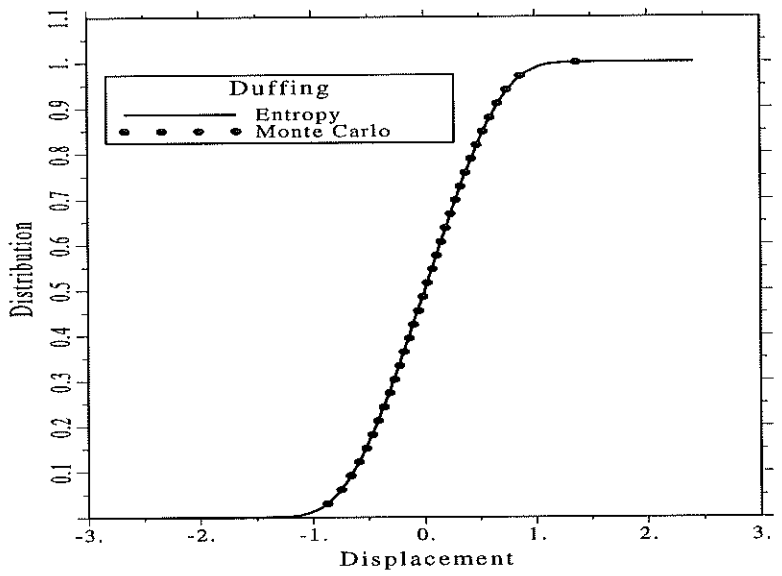

Figure 7.3 Displacement distribution of the Duffing oscillator

$$I_3 = \frac{1}{(2\pi)^{\frac{3}{2}}} \int\int\int x_1^4 x_2^4 x_3^4 \exp(-\frac{1}{2}[x_1^2 + x_2^2 + x_3^2])\mathrm{d}x_1\mathrm{d}x_2\mathrm{d}x_3 = 27 \qquad (7.63)$$

It is observed that the Fourier method converges faster to the target value than the Gauss-Legendre technique, due to the low sensitivity of the zero frequency transform to the aliasing phenomenon as said above. Also, its accuracy is at least one order of magnitude higher than Gauss-Legendre's when using a similar number of points. Thus, the accumulated error for a calculation of several seconds of response will be less when using the present approach, let alone the problem of the numerical instability which will be examine next.

The reason for the superior accuracy of the Fourier method over the other ones lies in the fact that the transform is linked to the integrand by an exact (albeit tricky) mathematical relationship. On the other hand, Simpson or similar rules are exact only for polynomial integrands of specific order and Gaussian quadratures give exact results only for integrands that can be expressed as a polynomial multiplied by the corresponding weighting function. Finally, the Fourier technique employs a regular discretization mesh that is less riskly in the frame of the maximum entropy method than the one used by Gauss-Legendre quadratures, as explained in the foregoing.

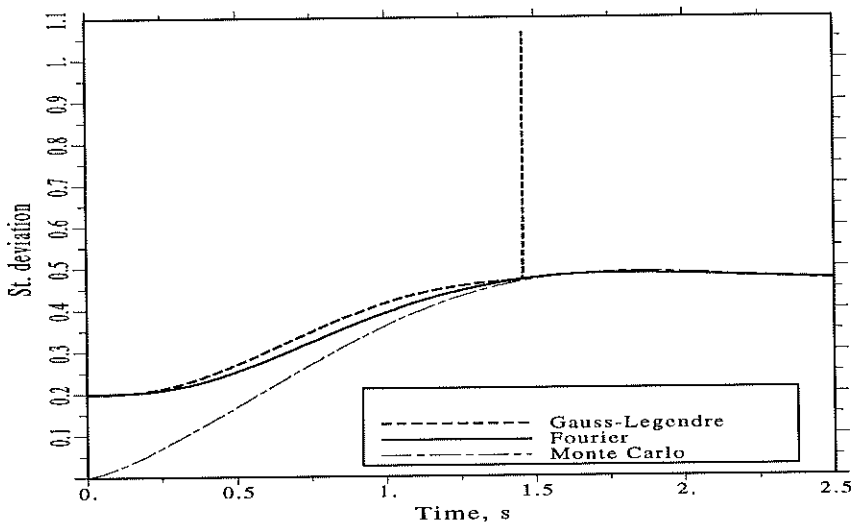

Figure 7.4 Evolution of the standard deviation the Duffing oscillator

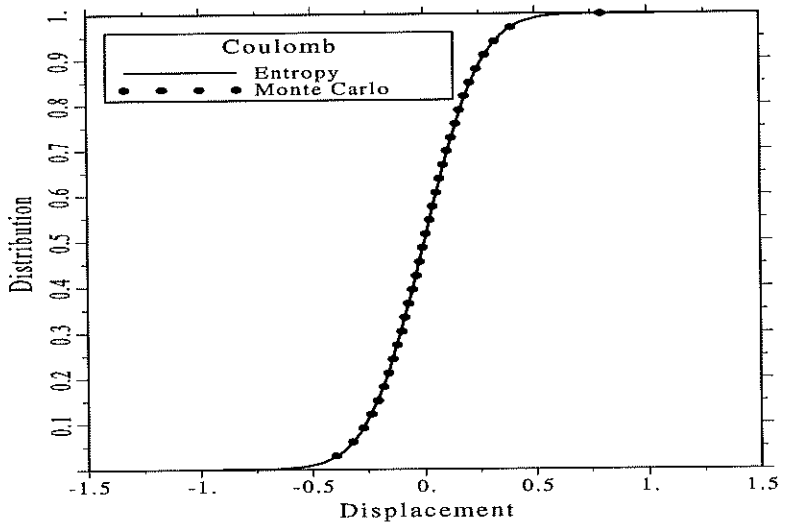

Figure 7.5 Displacement distribution of the Coulomb oscillator

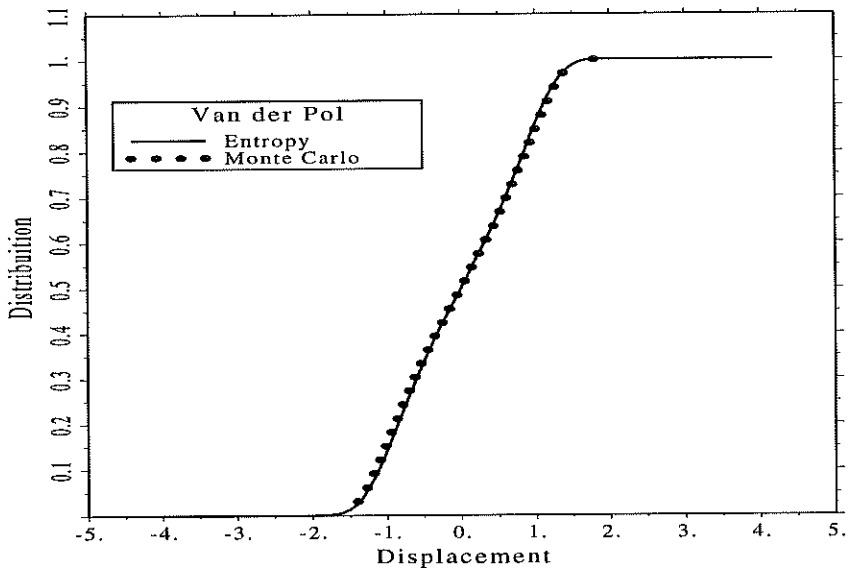

Figure 7.6 Displacement distribution of the Van der Pol oscillator

7.5.4 Numerical examples

The above method of integration was applied to the five examples presented above using 16 Fourier integration points and double precision. In all cases it was possible to calculate many seconds of response without numerical difficulties. A value of $K = 4$ was used in all cases. As expected, it was observed that the first method of maximum entropy does not estimate correctly the first seconds of the evolution of the probability function up to its stationary state due to the need of starting the calculation with a density different from the Dirac pulse. But when stationarity is finally reached the agreement is excellent, as is also the the estimation of the nonstationary evolution when compared with a Monte Carlo solution that includes the randomness of the initial velocity and position, as shown in the paper by Trębicki and Sobczyk (1996).

Figures 7.3 shows the results of the distribution function of the displacement of the Duffing oscillator as calculated by intensive Monte Carlo (50,000 samples) and maximum entropy approaches (both calculated at $t = 5$ s). On the other hand, figure 7.4 depicts the evolution of the displacement standard deviation of the same oscillator as calculated by Fourier and Gauss-Legendre integration techniques. The failure of the latter is evident. It can also be observed that the solutions follow different paths from the very beginning due to their diverse

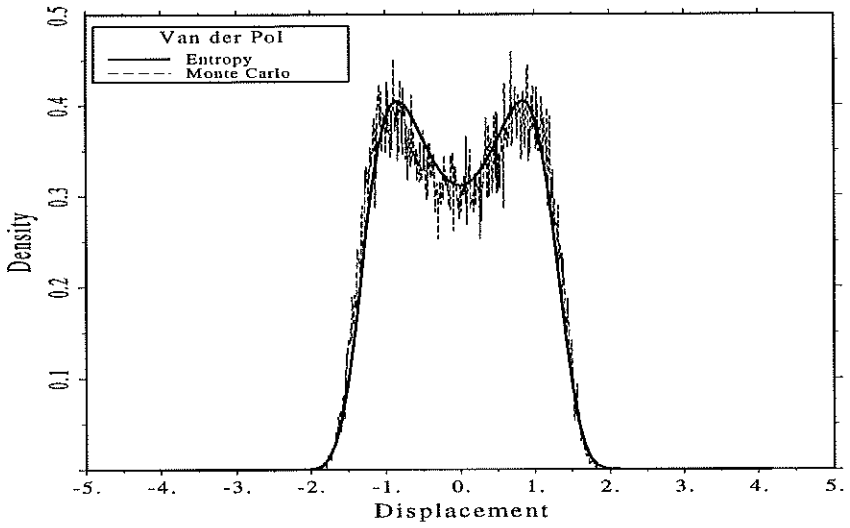

Figure 7.7 Displacement density of the Van der Pol oscillator

accuracy degrees.

Figures 7.5, 7.6 and 7.8 show the estimated probability functions of the displacement X of the Coulomb, Van der Pol and quadratic damping oscillators, respectively. In the second case the density function is depicted in figure 7.7. Together with figure 7.6, it suggests that a higher K is needed for improving accuracy in this case.

On the other hand, figure 7.9 shows the results of the Bouc-Wen case. As indicated in the figure, there was a need of calculating 40 seconds of response in order to find a close-to-stationarity state due to the effect of drift (see chapter 4) Figure 7.10 shows the evolution of the standard deviation as given by Monte Carlo and maximum entropy methods. It can be observed that the latter oscillates erratically at the first instants, which is an indirect measure of the inability of the method for estimating correctly the initial evolution of the probability functions for the above stated reason. However, after stabilizing, it shows a trend to converge from above to seemingly the same value to which the Monte Carlo result tends from below. It can also be observed that the maximum entropy method leads to a value similar to the assymptotic one faster than Monte Carlo. Taking into account that for calculating accurate density functions of the response a large number of Monte Carlo analyses are required, these remarks indicate that a good approximation to the stable result of the

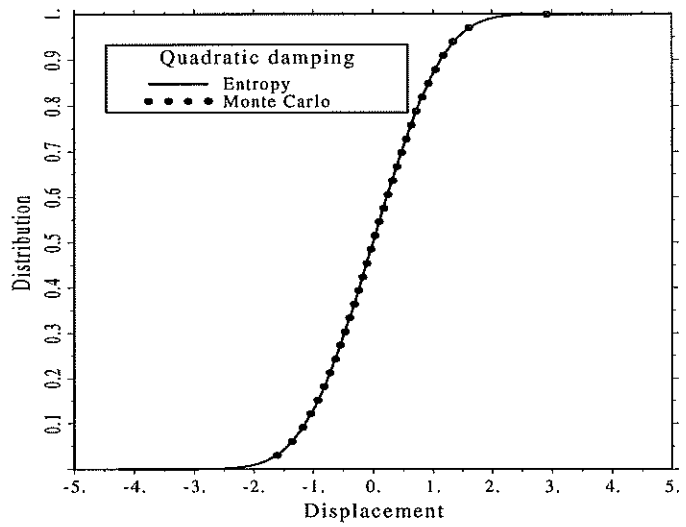

Figure 7.8 Displacement stationary distribution of the quadratic damping oscillator

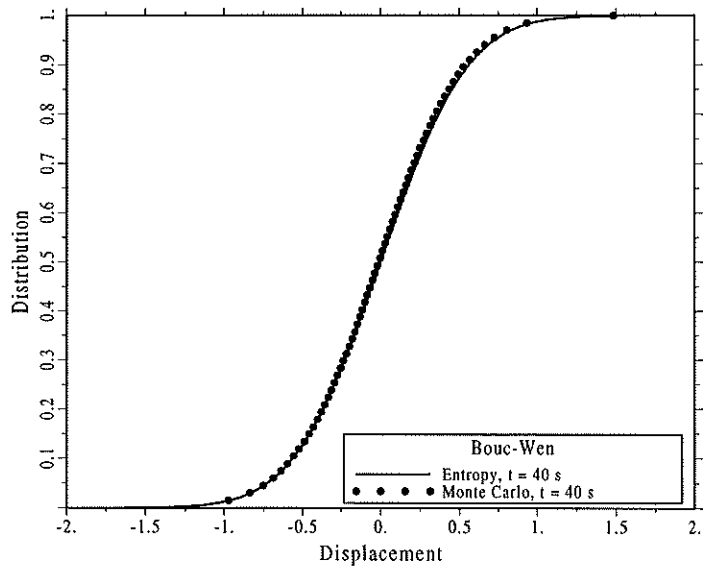

Figure 7.9 Displacement distribution of the Bouc-Wen oscillator ($S_W = 0.1$)

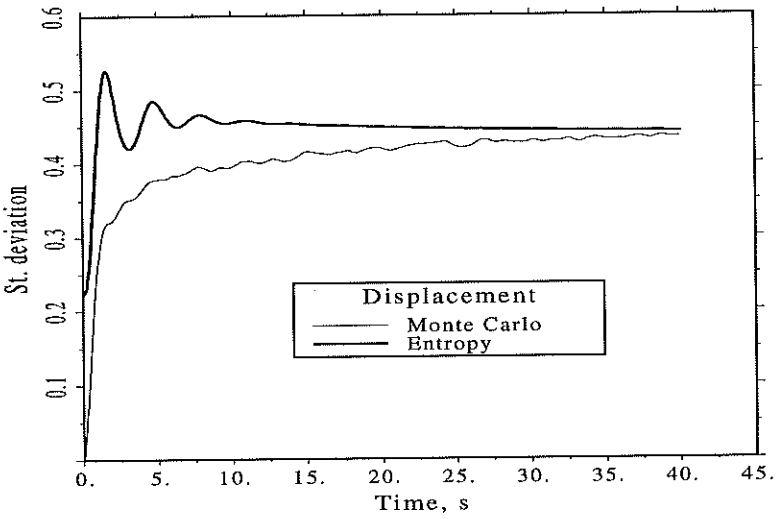

Figure 7.10 Evolution of the standard deviation of the Bouc-Wen oscillator ($S_w = 0.1$)

stationary probability function can be obtained by calculating a few seconds of response with the maximum entropy method at a very low computational cost.

Figure 7.11 shows the stationary joint X, Z stationary density function of the Bouc-Wen system as calculated by the method of maximum entropy. Its shape clearly indicates that the response reaches a moderate degree of nonlinearity under an excitation $S_W = 0.1$ because there is no concentration of Z values near the maximum $z_u = 1$ (see figure 4.5). In order to test the numerical stability of the method under a stronger excitation, a further analysis was performed with S_W ten times larger. Figure 7.12 displays the evolution of the joint density function of X and Z. It can be observed that, when the stationary state is finally reached, the function is bell shaped on the displacement axis while bimodal on the Z axis. This confirms that this case in fact corresponds to a severe nonlinear behaviour.

Finally, it should be pointed out that the better accuracy of Fourier integration has a reflect on the numerical stability of the entropy algorithm. This can be illustrated by comparing the singular values of the $\boldsymbol{S}$ matrix of the Duffing case obtained by the Fourier approach at the threshold of the Gauss-Legendre failure time (see Table 7.1). It is noticed that the range of singular values of the Fourier approach (299.6) is lower than that obtained in using Gauss-Legendre integration a little bit before its numerical breakdown (441.2). Since there is no

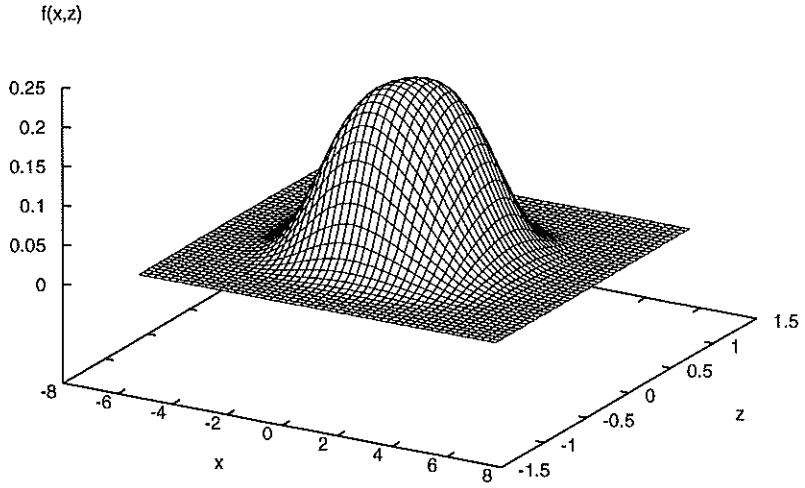

Figure 7.11 Joint density of displacement and hysteretic function. ($S_w = 0.1$)

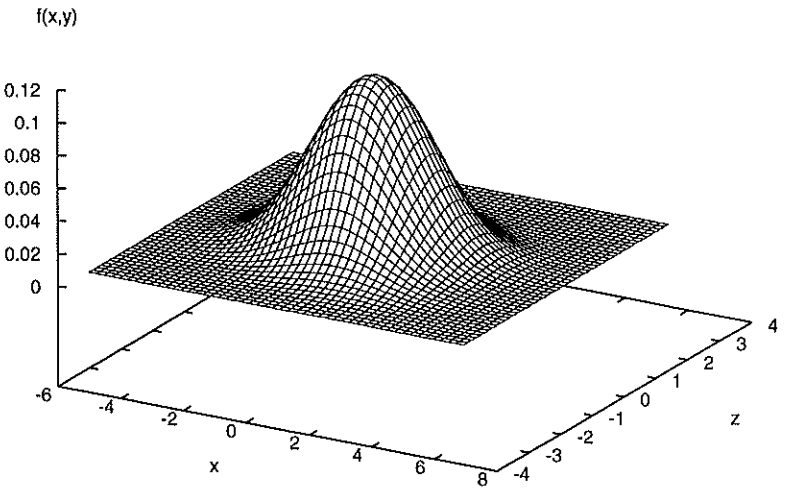

(*a*)

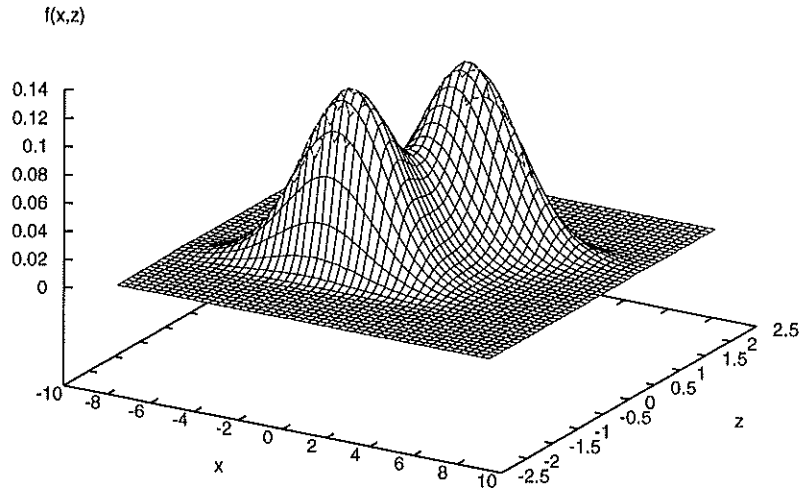

(*b*)

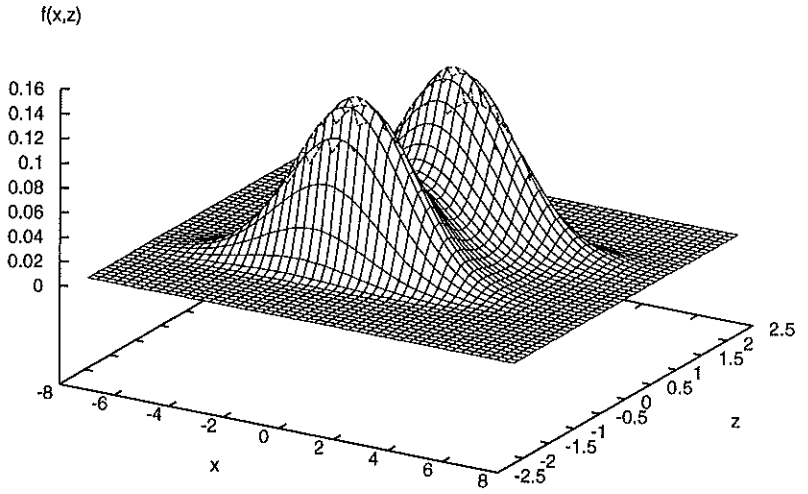

(*c*)

Figure 7.12 Joint density of displacement and hysteretic function ($S_w = 1.0$) at (*a*) $t = 0.5$ s, (*b*) $t = 1$ s, (*c*) $t = 5$ s

direct mathematical link between the accuracy of the integration and the conditioning of matrix $\boldsymbol{S}$, the superiority of the Fourier-based calculation can only be stated here on the empirical basis of the many cases analysed in the present research, some of which are included in this chapter. However, the achievement of a stationary solution by the Fourier approach can not be taken for granted, inasmuch as the calculation advances along the edge of numerical pitfalls burrowed by the ill-conditioning of matrix $\boldsymbol{S}$. In fact, despite the conditioning of $\boldsymbol{S}$ is in general better when use is made of the Fourier technique, some analyses performed on the Coulomb system failed. Perhaps the abrupt discontinuity of its restoring force function contributed to the breakdown.

Chapter 8

Seismic stochastic response of base isolated buildings

8.1 Introduction

It is well-known that current earthquake-resistant design aims at dissipating the input seismic energy in the form of nonlinear deformations when the structure is excited by strong ground motions. In the last years, intensive research has been conducted in the field of *seismic base isolation*, i.e. a technique purported to reducing the vibrations of buildings caused by earthquake ground motions. The building is supported on an additional slab which in turn rests on special devices which are intended to undergo very large displacements. The effect is to have the structure vibrating with a close-to-rigid-body motion. As illustrated by figure 8.1, the objective is to avoid the damage associated to the energy dissipation mechanism of conventional seismic design philosophy. (Barbat and Bozzo 1997).

Several types of devices have been developped for base isolation. The most spread of all are the *laminated rubber bearings*, which is formed by layers of neoprene and steel plates (Kelly 1993). The purpose of this system is to give the structure a large natural period such that low response accelerations can be expected. The *lead-rubber bearings* (Skinner *et al.* 1993) include in addition a lead cylinder which is intended to give some energy dissipation (figure 8.2). The *friction isolation system* was developped to dissipate the input seismic energy by friction at the base. A major disadvantage of this system lies in the possibility of having large residual displacements after the end of the ground motion. In the *friction pendulum system* this drawback is corrected by including an elastic restoring force in the form of a spherical base that grants the return to the original position (figure 8.3). Other proposals consist in combinations of the two leading principles, i.e. increase of the natural period or energy dissipation.

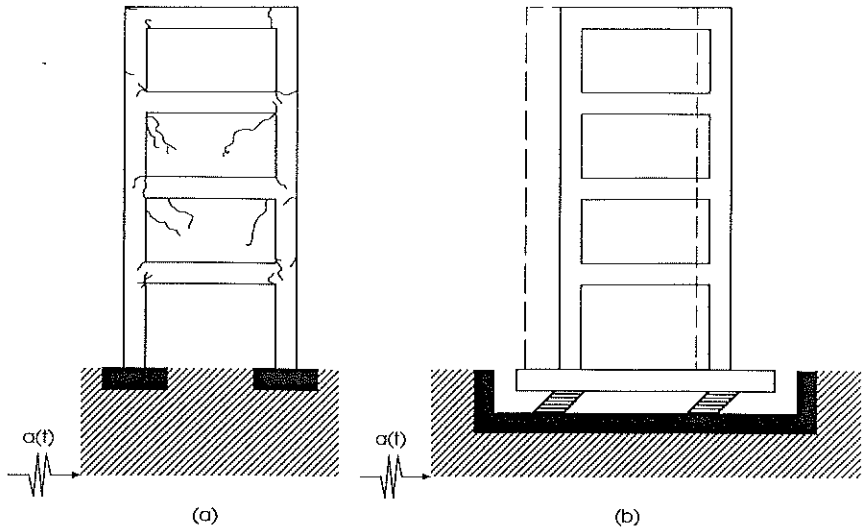

Figure 8.1 Seismic behaviour of conventional *(a)* and base isolated buildings *(b)*

As an application of the concepts and methods dealt with in the foregoing chapters, some issues of the seismic behaviour of two classes of base isolation proposals will be examined here. The selected systems are the lead-rubber bearings and the friction pendulum system, as they represent two of the most used seismic isolation appliances. However, some conclusions reached in this chapter apply to other systems as well.

8.2 Equivalent linearization of base isolation models

Before discussing the stochastic response of base isolated buildings as estimated by the method of stochastic linearization it is important to examine its accuracy when applied to some models of the base isolation devices under study considered as single mass systems.

8.2.1 Lead-rubber bearings

Lead-rubber bearings have been modelled by some authors using the Bouc-Wen hysteretic system (Constantinou *et al.* 1985, Lin *et al.* 1990a, b) The equation of motion of the single mass system shown in figure 8.2 is

$$m_{\mathrm{b}}\ddot{X} + c_{\mathrm{b}}\dot{X} + \alpha_{\mathrm{b}}k_{\mathrm{b}}X + (1-\alpha_{\mathrm{b}})k_{\mathrm{b}}Z = -mP(t) \tag{8.1}$$

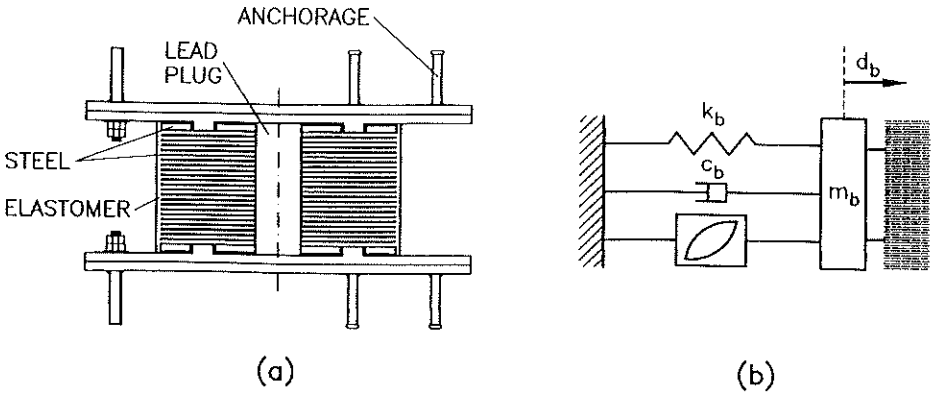

Figure 8.2 Lead core laminated rubber bearing. *(a)* Scheme. *(b)* Dynamic model

where m_b, c_b and k_b are the mass, damping and stiffness constants of the base system, $X = d_b$ the random base displacement and $P(t)$ the random excitation. The hysteretic component of the system can be described by the differential equation

$$\dot{Z} = \zeta(\dot{X}, Z) = A_b \dot{X} - \beta_b |\dot{X}||Z|^{n_b - 1} Z - \gamma_b \dot{X} |Z|^{n_b} \tag{8.2}$$

For all the numerical analyses of the present chapter we will adopt the following model parameters (Lin *et al.* 1990a): $A_b = 1.0, \beta_b = 1.4, \gamma_b = -0.54$ and $n_b = 1$. Figure 8.4 illustrates the hysteresis loops of the response of such system subject to a Gaussian white noise of intensity $S_W = 0.01\text{m}^2/\text{s}^3$, which corresponds to a strong excitation. It is evident that the parameters of the system compel to a close-to-linear behaviour in which the governing stiffness is that of the post-yielding branch. Therefore, the estimation of its statistics can be performed by stochastic linearization using the assumption of Gaussianity. In fact, as figure 8.5 points out, this hypothesis even leads to a slight overestimation of the response of this system. This trend has been confirmed in several additional

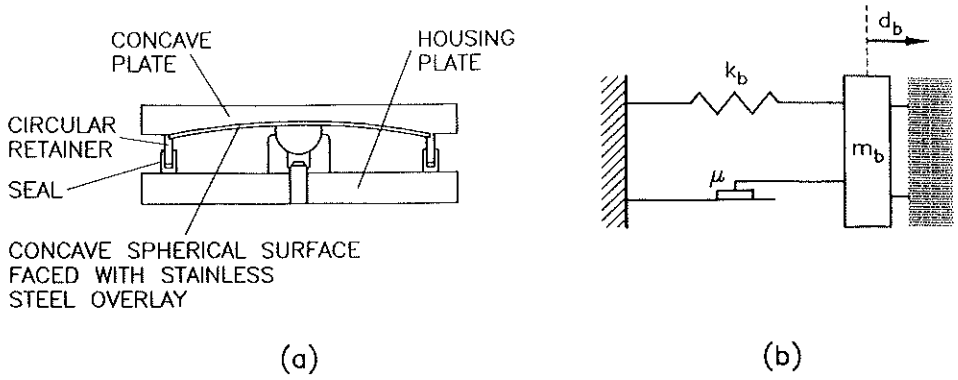

Figure 8.3 Frictional Pendulum System. *(a)* Scheme. *(b)* Dynamic model

analysis with different excitation types and intensities. As a consequence there is no need of employing the approach proposed in Chapter 5 to this case.

8.2.2 Friction pendulum systems

Friction forces are usually modelled as Coulomb systems. This means that for a structure described with the equation of motion

$$m_b \ddot{X} + c_b \dot{X} + h(\dot{X}) = P(t) \tag{8.3}$$

the restoring force is given by

$$h(\dot{X}) = \mu g m_b \operatorname{sgn}(\dot{X}) \tag{8.4}$$

where μ is the coefficient of friction, g the acceleration of gravity and $\operatorname{sgn}(\cdot)$ is the signum function defined as:

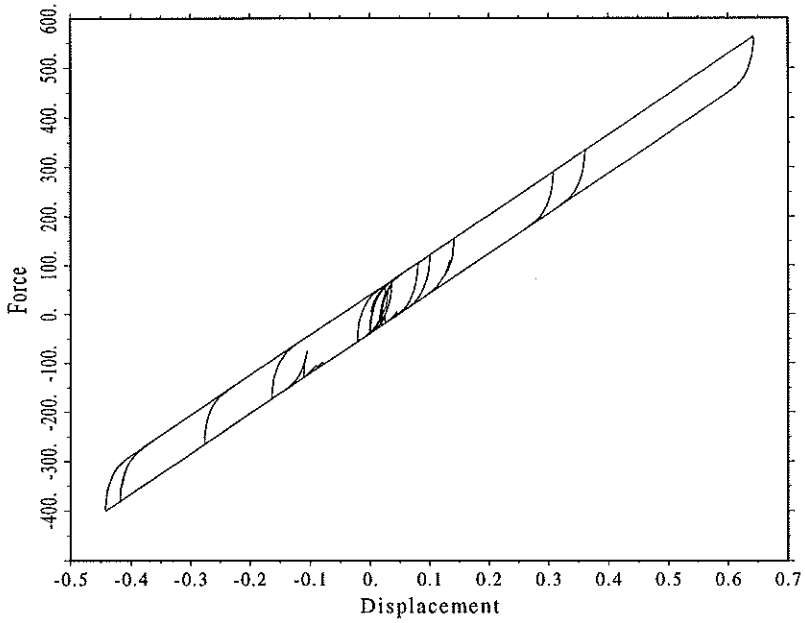

Figure 8.4 Typical force-displacement diagram of lead-rubber bearings

$$\operatorname{sgn}(X) = \begin{cases} -1, & X < 0 \\ 0, & X = 0 \\ 1, & X > 0 \end{cases} \tag{8.5}$$

Common friction coefficients found in base isolation systems are in the range of 0.05 to 0.15 (Barbat and Bozzo 1997). It has been recognized that this model represent a simplification of the actual relationship between restoring force and velocity, in that friction coefficients has been found to be somewhat velocity-dependent (Robert and Spanos 1990; Bozzo and Barbat 1995). Also, the equation of motion should be completed with the so-called *stick condition*, according to which sliding does not occur unless the absolute value of the reponse acceleration exceeds a threshold value given by $\mu g \operatorname{sgn}(\dot{X})$. However, from the point of view of random vibration the effect of these details is blurred by the large scattering of the earthquake action and the subsequent randomness of the structural response and therefore they are usually ignored in such type of studies (Fan and Ahmadi 1991).

In the friction pendulum system the equation of motion must be enlarged to include the restoring force associated to the pendulum, i.e.

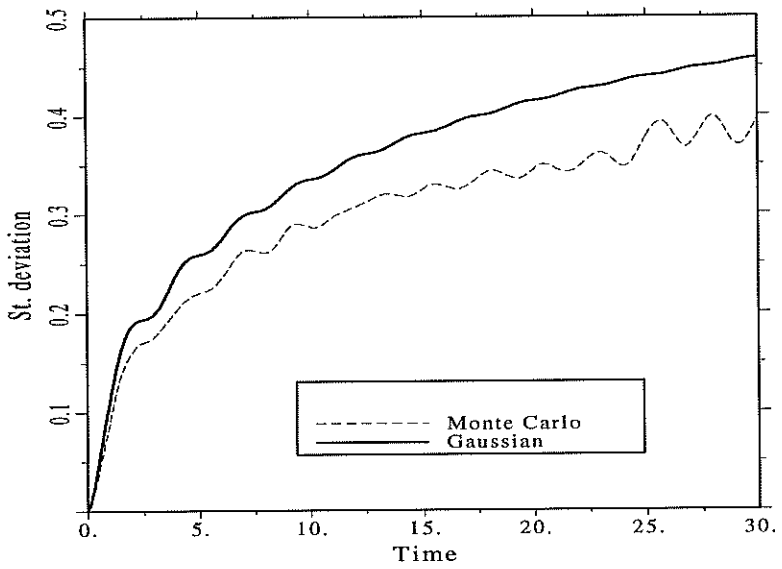

Figure 8.5 On the stochastic linearization of lead-rubber bearings

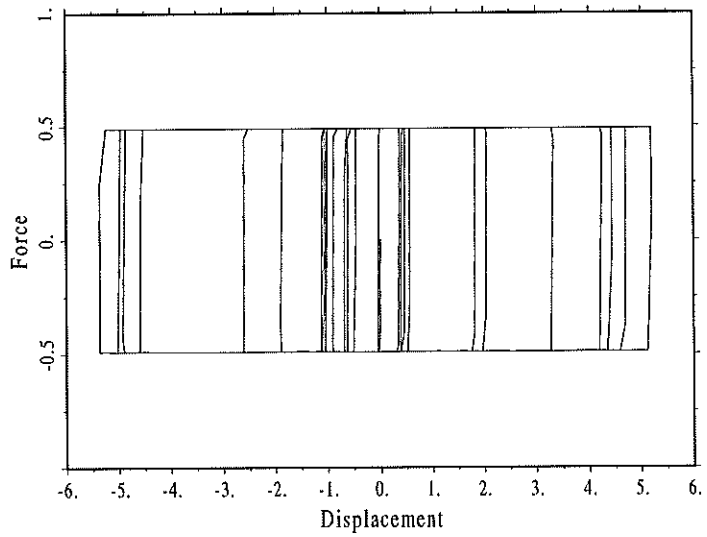

Figure 8.6 Frictional hysteresis loops with endochronic model

$$m_b\ddot{X} + c_b\dot{X} + k_bX + h(\dot{X}) = P(t) \tag{8.6}$$

where k_b can be determined after the period of the pendulum. The latter is usually set in the range from 2 to 3 s. The linearization technique can be easily applied to this equation by transforming the nonlinear force into a linear one in the form of an equivalent damping force

$$h(\dot{X}) = \mu_e\dot{X} \tag{8.7}$$

The classical result derived under the hypothesis of Gaussian behaviour is an equivalent damping coefficient equal to (Roberts and Spanos 1990)

$$\mu_e = \sqrt{\frac{2}{\pi}}\frac{\mu g m_b}{\sigma_{\dot{X}}} \tag{8.8}$$

It is not difficult to see that the direct use of the Coulomb formulation poses numerical difficulties to the solution of the equation of motion in deterministic analysis due to the presence of the signum function. As an alternative, it has been proposed the modelling of the frictional restoring force by means of the Bouc-Wen differential equation (Yang *et al.* 1992a, b). In this case one has

$$h(\dot{X}) = \mu g m_b V \tag{8.9}$$

where V is an auxiliary variable governed by

$$\dot{V} = \frac{1}{x_y}(A_b\dot{X} - \beta_b|\dot{X}||V|^{n_b-1}V - \gamma_b\dot{X}|V|^{n_b}) \tag{8.10}$$

Here x_y is a dummy yield displacement to which a very low value is assigned in order to obtain the typical rectangular hysteresis loops resulting from the signum function in equation (8.4) (see figure 8.6). Obviously, the above equation can be linearized in the same way as the Bouc-Wen auxiliary variable.

Figures 8.7 and 8.8 display the results of the analysis of a frictional oscillator with friction coefficients 0.05 and 0.15, respectively, subject to Gaussian white noise of intensity $S_W =$. The parameters m_b and k_b have been assigned to give the system a pendular period of 3 s. It can be seen that while the Gaussian linearization of the original Coulomb model (equation 8.7) largely underestimates the displacement response, in the endochronic formulation it leads to estimations that depend somewhat on the selected parameter n_b, but which are although undoubtly better. As seen in the figures, a value of $n_b = 1$ seems

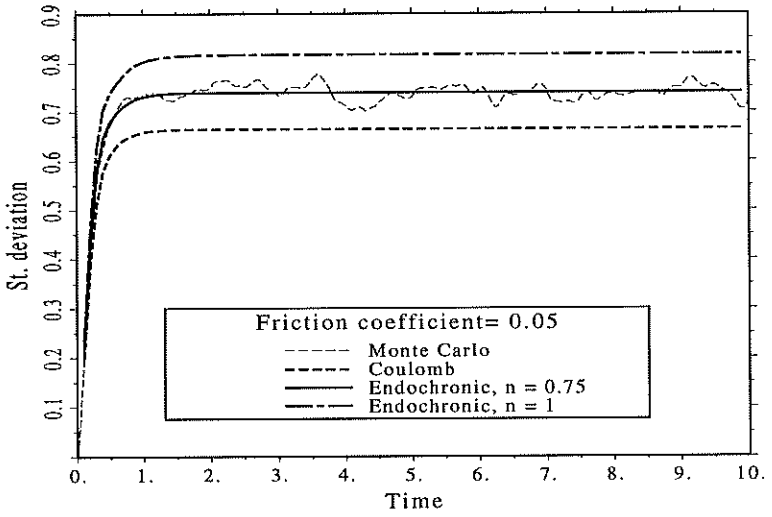

Figure 8.7 Stochastic linearization of friction pendulum system. $\mu = 0.05$

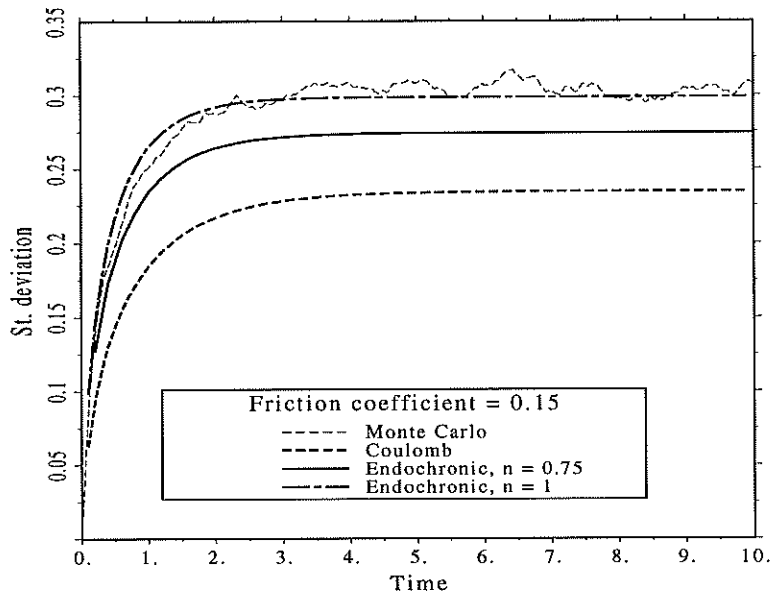

Figure 8.8 Stochastic linearization of friction pendulum system. $\mu = 0.15$

adequate in the range of interest. In the analyses that follow the endochronic formulation of the friction restoring forces will be preferred over the Coulomb one.

8.3 Structural model

In the present chapter a simplified structural model of the superstructure of base isolated buildings known as *shear beam* model has been adopted. In such model slabs are assumed to have an infinite stiffness so that the story flexibility equals that of the columns. Such a simplification, of course, implies that there are no rotations at column ends – an assumption that contradicts the real behaviour of building frames. However, beam flexibilities can be considered in an approximate manner in the value of the story stiffness by calculating the stiffness of equivalent, more flexible columns. Approximate formulas for such a simplification have been proposed.

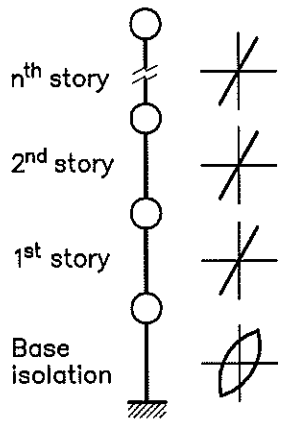

Figure 8.9 Shear beam model of base isolated buildings

The main consequence of the shear-beam simplification is that the whole building can be analysed as a string of masses interconnected by linear or non linear springs (figure 8.9). For the analysis of base isolated buildings the use of this model is more justified than in case of conventional ones due to the tendency of the superstructure to move as a rigid block when isolated at the base (Kelly 1993). Let us consider a shear-beam model with N hysteretic stories of the Bouc-Wen type, considering the base isolation layer as one of them. Linear layers can be modelled by setting its α equal to unity. Refering to figure 8.9,

for the $i-$th story, $i = \mathrm{b}, 1, 2, \ldots, N$ where $i = \mathrm{b}$ corresponds to the isolation layer, we have the following equation of motion:

$$m_i[\sum_{j=\mathrm{b}}^{i} \ddot{x}_j(t) + \ddot{x}_{\mathrm{g}}(t)] + c_i\dot{x}_i(t) - c_{i+1}x_{i+1}(t) + h_i(t) - h_{i-1}(t) = 0 \qquad (8.11)$$

where $\ddot{x}_{\mathrm{g}}(t)$ is the ground acceleration and $x_i(t)$ is the so-called *story drift* defined as the difference between sucessive story displacements,

$$x_i(t) = u_i(t) - u_{i-1}(t) \qquad (8.12)$$

Assembling the equilibrium equations for the entire building model, and changing from deterministic to stochastic notation, the following system of differential equations is obtained:

$$\boldsymbol{M}\ddot{\boldsymbol{X}}(t) + \boldsymbol{C}\dot{\boldsymbol{X}}(t) + \boldsymbol{K}\boldsymbol{X}(t) + \boldsymbol{G}\boldsymbol{Z}(t) = -\boldsymbol{N}\boldsymbol{J}\ddot{X}_{\mathrm{g}}(t) \qquad (8.13)$$

with

$$\boldsymbol{M} = \begin{pmatrix} m_{\mathrm{b}} & 0 & \ldots & 0 \\ m_{\mathrm{b}} & m_1 & \ldots & 0 \\ \vdots & \vdots & & \vdots \\ m_{\mathrm{b}} & m_1 & \ldots & m_N \end{pmatrix} \qquad (8.14a)$$

$$\boldsymbol{C} = \begin{pmatrix} c_{\mathrm{b}} & -c_1 & 0 & \ldots & 0 \\ 0 & c_1 & -c_2 & \ldots & 0 \\ \vdots & \vdots & \vdots & & \vdots \\ 0 & 0 & 0 & \ldots & c_N \end{pmatrix} \qquad (8.14b)$$

$$\boldsymbol{K} = \begin{pmatrix} \alpha_{\mathrm{b}}k_{\mathrm{b}} & -\alpha_1 k_1 & 0 & \ldots & 0 \\ 0 & \alpha_1 k_1 & -\alpha_2 k_2 & \ldots & 0 \\ \vdots & \vdots & \vdots & & \vdots \\ 0 & 0 & 0 & \ldots & \alpha_N k_N \end{pmatrix} \qquad (8.14c)$$

$$\boldsymbol{G} = \begin{pmatrix} (1-\alpha_{\mathrm{b}})k_{\mathrm{b}} & -(1-\alpha_1)k_1 & 0 & \ldots & 0 \\ 0 & (1-\alpha_1)k_1 & -(1-\alpha_2)k_2 & \ldots & 0 \\ \vdots & \vdots & \vdots & & \vdots \\ 0 & 0 & 0 & \ldots & (1-\alpha_N)k_N \end{pmatrix} \qquad (8.14d)$$

$$\boldsymbol{N} = \begin{pmatrix} m_{\mathrm{b}} & 0 & \dots & 0 \\ 0 & m_1 & \dots & 0 \\ \vdots & \vdots & & \vdots \\ 0 & 0 & \dots & m_N \end{pmatrix} \tag{8.14e}$$

and

$$\boldsymbol{J}^{\mathrm{T}} = [1, 1, \dots, 1] \tag{8.14f}$$

For frictional systems of the type considered here, the first diagonal term of matrices $\boldsymbol{K}$ and $\boldsymbol{G}$ are equal to k_{b} and $\mu g m_{\mathrm{t}}$ respectively, where m_{t} is the total mass gravitating over the isolation layer. The linearized equations of the hysteretic components of the restoring forces of the strings can be collected in vector form as

$$\dot{\boldsymbol{Z}}(t) = \boldsymbol{C}_{\mathrm{e}}\, \dot{\boldsymbol{X}}(t) + \boldsymbol{K}_{\mathrm{e}}\, \boldsymbol{Z}(t) \tag{8.15}$$

where $\boldsymbol{C}_{\mathrm{e}}$ and $\boldsymbol{K}_{\mathrm{e}}$ are diagonal matrices of the equivalent coefficients. In the analyses performed in this chapter the ground motion acceleration is exclusively modelled as a Clough-Penzien filter. In such case the state vector is

$$\boldsymbol{Q}^{\mathrm{T}}(t) = [\boldsymbol{X}(t), \dot{\boldsymbol{X}}(t), \boldsymbol{Z}(t), U_{\mathrm{g}}(t), \dot{U}_{\mathrm{g}}(t), U_{\mathrm{f}}(t), \dot{U}_{\mathrm{f}}(t)] \tag{8.16}$$

where the dynamics of the filter is governed by the equations (2.2) and (2.6) which are repeated here for convenient reference:

$$\ddot{U}_{\mathrm{g}}(t) + 2\,\nu_{\mathrm{g}}\omega_{\mathrm{g}}\dot{U}_{\mathrm{g}}(t) + \omega_{\mathrm{g}}^{2} U_{\mathrm{g}}(t) = -W(t) \tag{8.17a}$$

$$\ddot{U}_{\mathrm{f}}(t) + 2\,\nu_{\mathrm{f}}\omega_{\mathrm{f}}\dot{U}_{\mathrm{f}}(t) + \omega_{\mathrm{f}}^{2} U_{\mathrm{f}}(t) = -2\,\nu_{\mathrm{g}}\omega_{\mathrm{g}}\dot{U}_{\mathrm{g}}(t) - \omega_{\mathrm{g}}^{2} U_{\mathrm{g}}(t) \tag{8.17b}$$

where $W(t)$ is a Gaussian white noise of power spectral density S_W. These equations correspond to the following model for the random ground acceleration:

$$\ddot{X}_{\mathrm{g}} = \ddot{U}_{\mathrm{f}} = -2\,\nu_{\mathrm{f}}\omega_{\mathrm{f}}\dot{U}_{\mathrm{f}} - \omega_{\mathrm{f}}^{2} U_{\mathrm{f}} - 2\,\nu_{\mathrm{g}}\omega_{\mathrm{g}}\dot{U}_{\mathrm{g}} - \omega_{\mathrm{g}}^{2} U_{\mathrm{g}} \tag{8.18}$$

Finally, the differential equation for the linearized system is

$$\dot{\boldsymbol{Q}}(t) = \boldsymbol{A}_{\mathrm{e}}\, \boldsymbol{Q}(t) + \boldsymbol{F}(t) \tag{8.19}$$

with system matrix

$$\boldsymbol{A}_{\mathrm{e}} = \begin{pmatrix} \mathbf{0} & \boldsymbol{I} & \mathbf{0} & \mathbf{0} & \mathbf{0} & \mathbf{0} & \mathbf{0} \\ -\tilde{\boldsymbol{K}} & -\tilde{\boldsymbol{C}} & -\tilde{\boldsymbol{G}} & -\tilde{\boldsymbol{N}} \cdot \omega_{\mathrm{g}}^{2} & -\tilde{\boldsymbol{N}} \cdot 2\nu_{\mathrm{g}}\omega_{\mathrm{g}} & -\tilde{\boldsymbol{N}} \cdot \omega_{\mathrm{f}}^{2} & -\tilde{\boldsymbol{N}} \cdot 2\nu_{\mathrm{f}}\omega_{\mathrm{f}} \\ \mathbf{0} & \boldsymbol{C}_{\mathrm{e}} & \boldsymbol{K}_{\mathrm{e}} & \mathbf{0} & \mathbf{0} & \mathbf{0} & \mathbf{0} \\ \mathbf{0} & \mathbf{0} & \mathbf{0} & 0 & 1 & 0 & 0 \\ \mathbf{0} & \mathbf{0} & \mathbf{0} & -\omega_{\mathrm{g}}^{2} & -2\nu_{\mathrm{g}}\omega_{\mathrm{g}} & -\omega_{\mathrm{f}}^{2} & -2\nu_{\mathrm{f}}\omega_{\mathrm{f}} \\ \mathbf{0} & \mathbf{0} & \mathbf{0} & 0 & 0 & 0 & 1 \\ \mathbf{0} & \mathbf{0} & \mathbf{0} & 0 & 0 & -\omega_{\mathrm{f}}^{2} & -2\nu_{\mathrm{f}}\omega_{\mathrm{f}} \end{pmatrix} \tag{8.20a}$$

and excitation vector

$$\boldsymbol{F}(t) = \begin{pmatrix} 0 \\ \vdots \\ W(t) \end{pmatrix} \tag{8.20b}$$

In the above equations

$$\tilde{\boldsymbol{K}} = \boldsymbol{M}^{-1}\boldsymbol{K},\ \tilde{\boldsymbol{C}} = \boldsymbol{M}^{-1}\boldsymbol{C},\ \tilde{\boldsymbol{G}} = -\boldsymbol{M}^{-1}\boldsymbol{G},\ \tilde{\boldsymbol{N}} = \boldsymbol{M}^{-1}\boldsymbol{N}\boldsymbol{J} \tag{8.20c}$$

The evolution of the covariance matrix of the zero mean state vector $\boldsymbol{Q}$

$$\boldsymbol{\Sigma} = \mathrm{E}\{\boldsymbol{Q}\boldsymbol{Q}^{\mathrm{T}}\} \tag{8.21}$$

can be obtained by solving the differential equation (3.46)

$$\dot{\boldsymbol{\Sigma}} = \boldsymbol{A}_{\mathrm{e}}\boldsymbol{\Sigma} + \boldsymbol{\Sigma}\boldsymbol{A}_{\mathrm{e}}^{\mathrm{T}} + 2\pi\boldsymbol{S}_{\boldsymbol{F}} \tag{8.22}$$

where the entries of matrix $\boldsymbol{S}_{\boldsymbol{F}}$ are all zero with the exemption of the one in position (N, N) which is equal to $2\pi\xi^{2}(t)S_{W}$ in the uniformly modulated non stationary case, or to $2\pi\xi^{2}(t)\kappa^{3}(t)S_{W}$ if the instantaneous spectrum model is adopted. In the latter case it is necessary to make the following transformations in the system matrix:

$$-\tilde{\boldsymbol{N}} \cdot 2\nu_{\mathrm{h}}\omega_{\mathrm{h}} \rightarrow -\tilde{\boldsymbol{N}} \cdot 2\nu_{\mathrm{h}}\omega_{\mathrm{h}}/\dot{\kappa}(t) \tag{8.23a}$$

$$-\omega_{\mathrm{h}}^{2} \rightarrow -\omega_{\mathrm{h}}^{2}\dot{\kappa}(t)^{2} \tag{8.23b}$$

$$-2\nu_{\mathrm{h}}\omega_{\mathrm{h}} \rightarrow -2\nu_{\mathrm{h}}\omega_{\mathrm{h}}(\dot{\kappa}(t) + \ddot{\kappa}(t)/\dot{\kappa}(t)) \tag{8.23c}$$

where subindex h stands for either f or g.

8.4 Seismic random vibration of base isolated buildings

The introduction of base isolation is very recent. As a consequence, there is little experience on the actual response of buildings with passive or active base isolation to actual strong earthquakes. This makes more relevant the insight provided by random vibration analyses of such structures, due to the synthetic view they can afford.

Some research in this direction has been performed. A first attempt was done by Constantinou *et al.* (1985), who applied the classical method of stochastic equivalent linearization to analyse the response of some models of passive base isolated buildings. Lin *et al.* (1989) analysed various systems using as seismic model a Clough-Penzien filter fitted to a seismological model. The objective was to compare the response of the selected systems and to classify then according to their range of applicability. A similar study had been conducted by Lin *et al.* (1989). It is important to observe that in both studies the seismological model chosen corresponds to rock motions and the analyses were performed for stationary conditions. Thus the effect of local soil conditions is ignored as well as that of non stationary details of the seismic action. Finally, stochastic analysis of active base isolated building models have been performed by Yang *et al.* (1994) using the algorithm of optimal control.

The aim of the present section is to discuss the effect of some features of the seismic exctiation as well as other aspects of the stochastic modelling. Specifically, the issues examined are the following:

1. The influence of the nonstationary features of the seismic excitation.
2. The influence of seismic spectrum parameters.
3. The effect of structural nonlinearities.

In the numerical analyses, which are performed on two- and six-story buildings, use will be made of the structural parameters appearing in table 8.1. The stories are numbered from top to bottom in the table, so that the two-story case takes only the first two lines of the table. The mass of the isolation slab is $m_b = 450$ t and that of the stories is 345.6 t. The values are taken from Yang *et al.* (1992a).

8.4.1 Influence of nonstationary features of the seismic excitation

Even though a thourough parametric study on the subject of nonstationary seismic response of base isolated buildings is beyond the purpose of this section, the case studies presented herein will shed light on some important issues of their seismic response that are not reflected when analysing them in the stationary

Table 8.1 Structural parameters of the shear beam building models

Story No.	damping, c_i (kN·s/m)$\times 10^5$	stiffness, k_i (kN/m)
1	1.37	196
2	1.69	243
3	2.07	298
4	2.43	348
5	2.69	386
6	2.85	410

regime. The conclusions, then, will serve as a complement to those drawn in the quoted previous studies, most which have analysed the stochastic behaviour of base isolated buildings from a stationary point of view.

The main purpose of introducing flexible base isolation bearings in building design is to increase the natural period of the structure in order to reduce the acceleration response (Kelly 1993). This is due to the fact that typical earthquake acceleration spectra exhibit large ordinates at the low period range and a rough exponential decrease after a certain period. However, the introduction of high flexibility at the base of the building can make them quite vulnerable to earthquakes of a different spectral content, such as those filtered and amplified by very soft soils in which low frequency waves play the dominant role. In such cases the use of base isolation systems that increase the natural period is obviously discarded. Nevertheless, the behaviour of such building under normal high frequency earthquakes exhibiting some low frequency waves of high energy is worth an investigation.

In order to examine this issue, a two story building supported on 20 lead rubber bearings was subject to an earthquake excitation with the intermediate soil conditions of table 2.2. The nonstationarity in amplitude was defined by means of two Shinozuka and Sato (1967) functions (equation 2.19) corresponding to earthquakes with low and high effective durations. The parameters are $a = 0.25, b = 0.5$ on the one hand and $a = 0.085$ and $b = 0.17$ on the other. The building model was first analysed with amplitude modulation only and then with the three frequency modulation functions corresponding to El Centro, SMART No. 45 and Orion Boulevard records, whose parameters appear in table 2.1. As said in chapter 2, these records correspond respectively to situations in which there is a low, intermediate and high presence of low frequency surface waves at the end of them.

Figures 8.10 to 8.13 display the evolution of the standard deviation of the base isolation displacement and the drift of the second story of the building, subject to low and high effective duration earthquakes, respectively. It can be

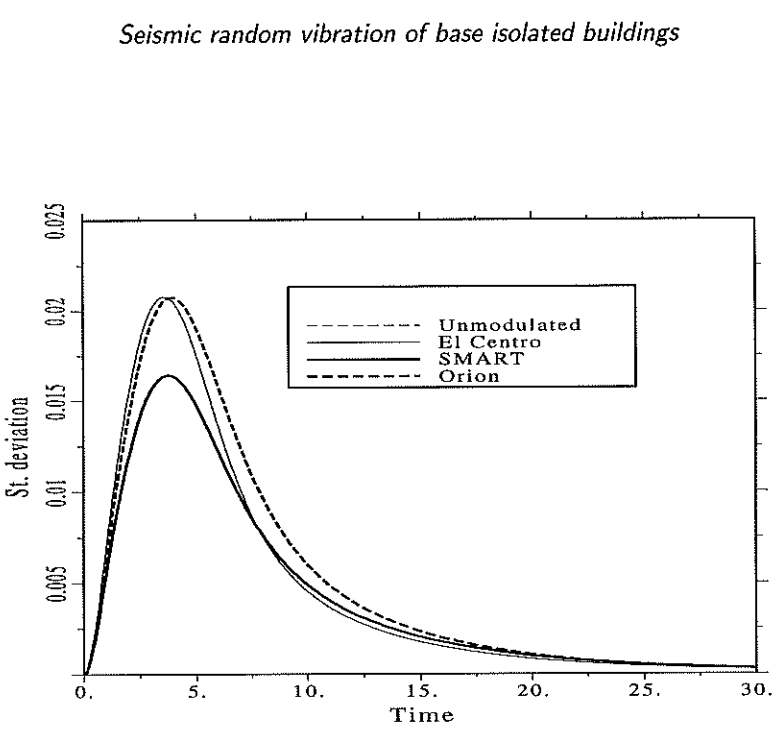

Figure 8.10 Base displacement of a building on lead-rubber bearings. Short duration earthquake

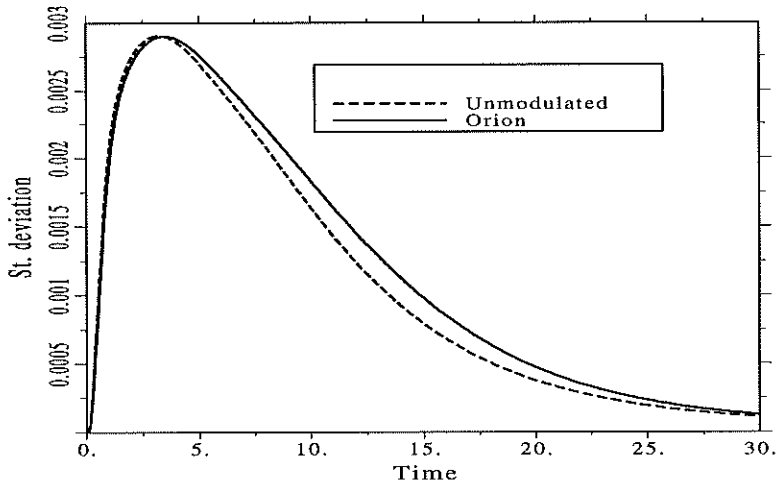

Figure 8.11 First story drift of a building on lead-rubber bearings. Short duration earthquake

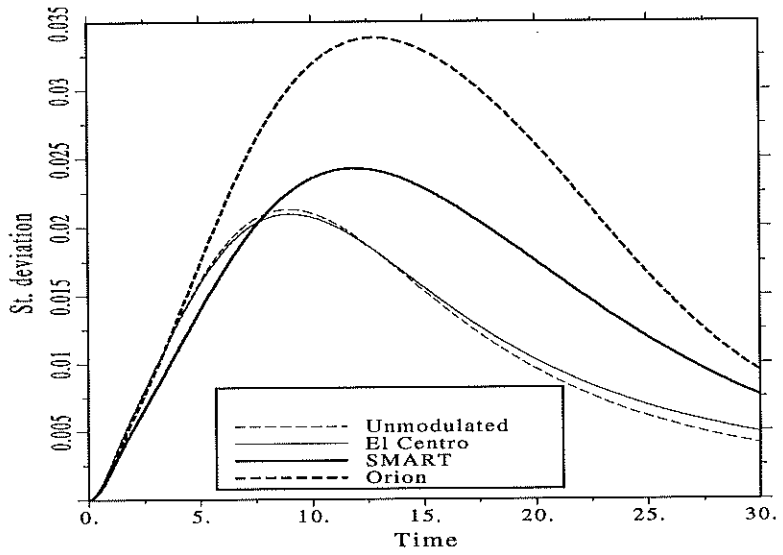

Figure 8.12 Base displacement of a building on lead-rubber bearings. Long duration earthquake

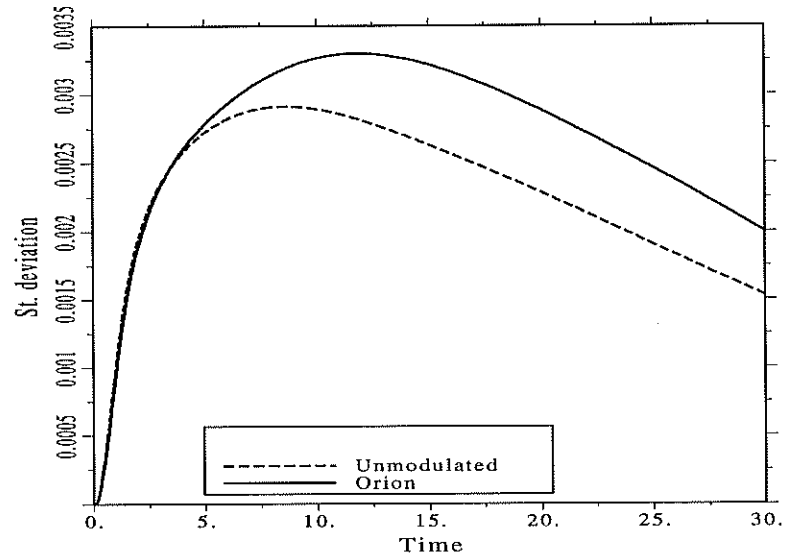

Figure 8.13 First story drift of a building on lead-rubber bearings. Long duration earthquake

seen that the evolution of frequencies can produce a large increase of the displacements of both the base isolation system and the structure if it is associated with a long effective duration. In the opposite case the effects are minimal. It must be noted also that such an effect is not captured by a stationary analysis nor by a nonstationary one in which the seismic action is modelled as a uniformly modulated process.

The importance of considering these nonstationary effects in practical design can be appreciated in figure 8.14 and 8.15, which correspond to the same building as above with 10 and 30 lead-rubber devices. It is apparent that the only way of controlling the increase of base displacement produced by a severe frequency evolution is the stiffening of the base. However, this decision would imply an important cost increase and the reduction of the effects pursued with base isolation.

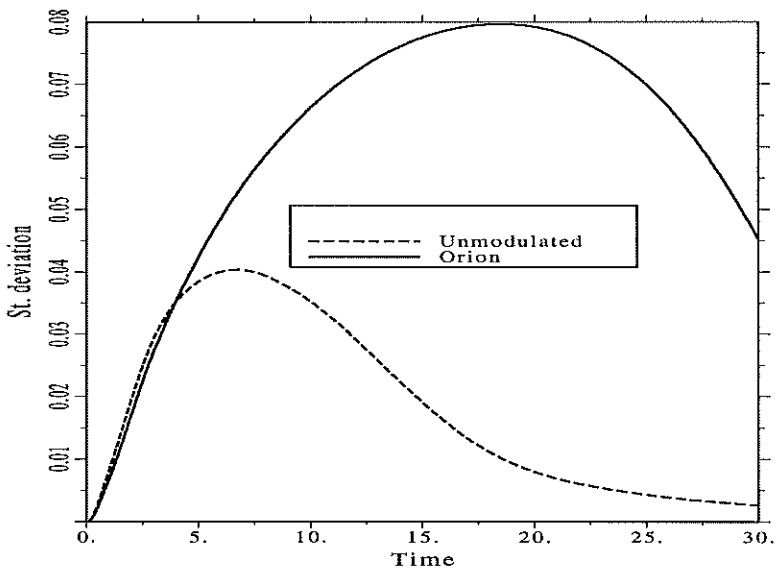

Figure 8.14 Base displacement of a building on 10 lead-rubber bearings

A similar result for a six-story building supported on a frictional pendula with $\mu = 0.1$ is depicted in figure 8.16. Only the case of long duration earthquake with the Orion frequency modulating function has been considered. It can be observed that this kind of system is similarly sensitive to the frequency evolution as the lead-rubber one. This is due to the imposition of a high period at the base system for restoring the final position.

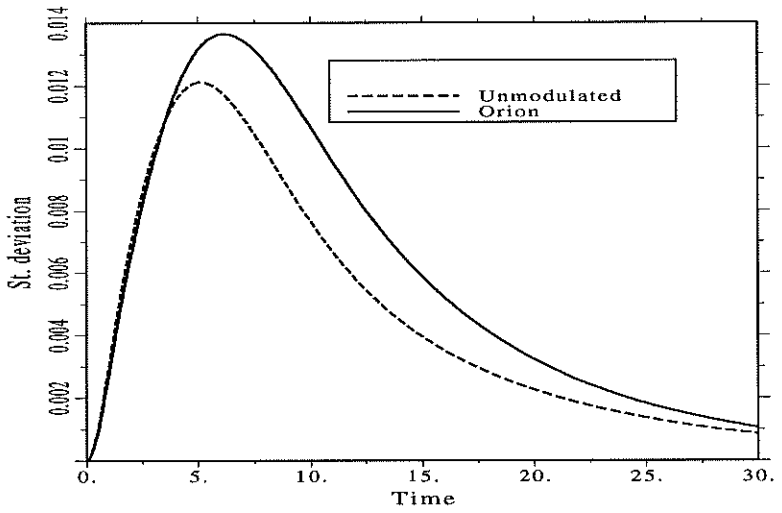

Figure 8.15 Base displacement of a building on 30 lead-rubber bearings

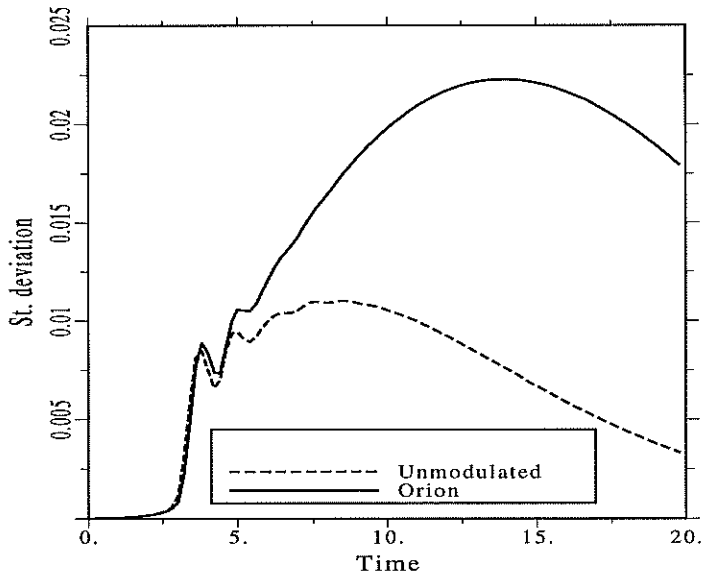

Figure 8.16 Base displacement of a 6-story building on frictional pendula. $\mu = 0.1$

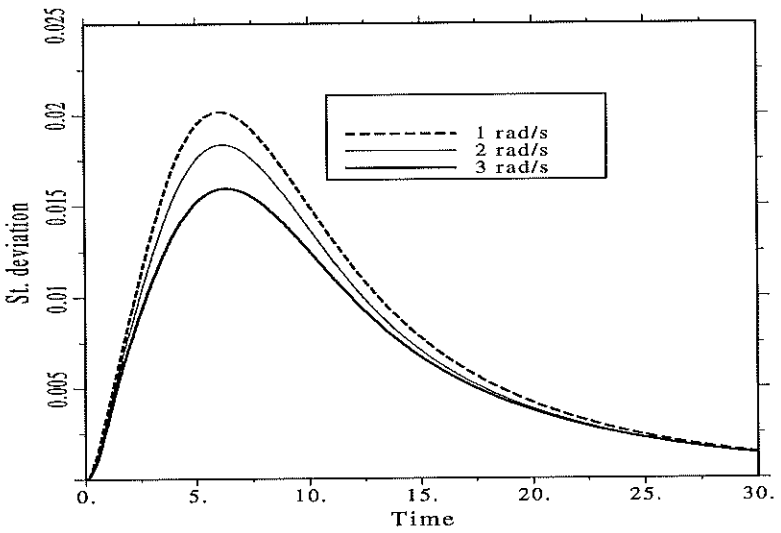

Figure 8.17 On the influence of ω_f on base displacement

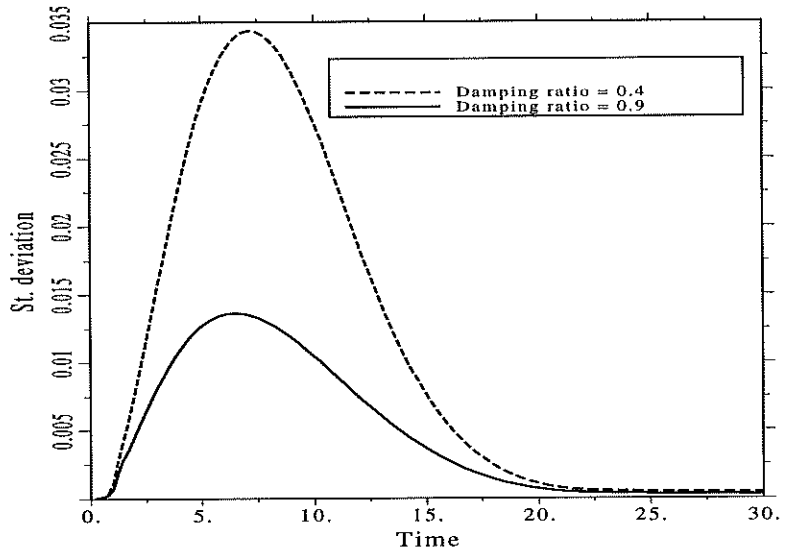

Figure 8.18 On the influence of ν_f on base displacement

8.4.2 Influence of seismic spectrum parameters.

Being a large period structural system, the response of buildings supported by lead-rubber or frictional pendulum bearings can be expected to be insensitive to the main damping and frequency parameters (ν_g, ω_g) of the Clough-Penzien spectrum as given by table 2.2. This was confirmed by some numerical analyses performed on both type of systems whose results are not shown. In contrast, a high sensitivity to the low-cut filter parameters ν_f and ω_f can be anticipated. To confirm this hypothesis, an analysis was performed on the two-story lead-rubber and frictional pendulum buildings using the SMART function and an intermediate duration envelope defined with $a = 0.15$ and $b = 0.3$. As figures 8.17 and 8.18 illustrate, the decision on these values in practical applications must be done carefully, because their influence is crucial in the assessment of the response statistics.

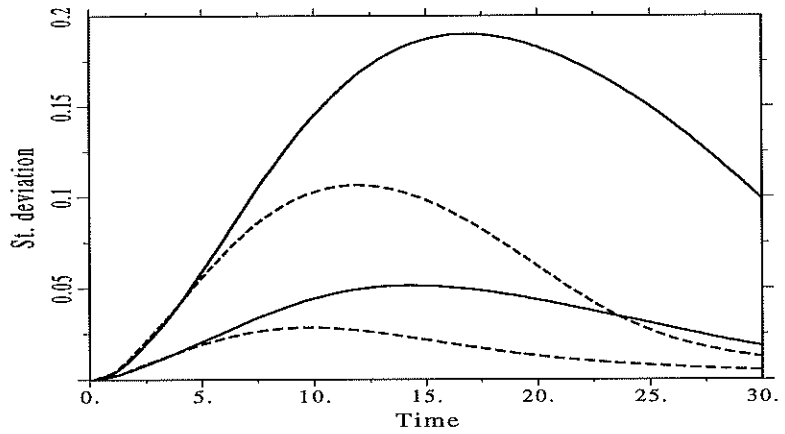

Figure 8.19 On the influence of S_w

Finally, an analysis was carried out in order to examine whether the increase of the displacement statistics produced by the consideration of frequency modulation is affected by the strength of the excitation. To this purpose a six-story building with 20 lead-rubber devices subject to Clough-Penzien spectra with driving white noises of strengths 50 and 200 cm^2/s^3 was analysed. It can be observed in figure 8.19 that the percent of increase in both cases is similar. Therefore, it can be concluded that a rigth modelling of earthquake actions for analysing this type of buildings should always consider the possibility of ocurrence of high energy, low frequency waves.

8.4.3 Influence of structural nonlinearities.

Another aspect that deserve examination is the effect of nonlinear incursions of the elements composing the upper stories. To model such nonlinear behaviour, the strength of each story j was set equal to

$$h_{uj} = C_s \sum_{i=1}^{j} m_i g \tag{8.24}$$

where C_s is the so-called seismic coefficient in earthquake-resistant design, whose typical values are in the range 0.05 to 0.2. Figures 8.20 and 8.21 display the results of the standard deviation of the displacement of the isolation system and bottom story of the two-story building supported on 20 lead-rubber bearings with $C_s = 0.1$ in all stories. It can be observed that, while the nonlinear behaviour of the structure reduces the base displacement, it increases that of the stories. If such greater structural drift does not become critical for the safety of structural and non-structural elements, this can be considered a positive effect as a whole.

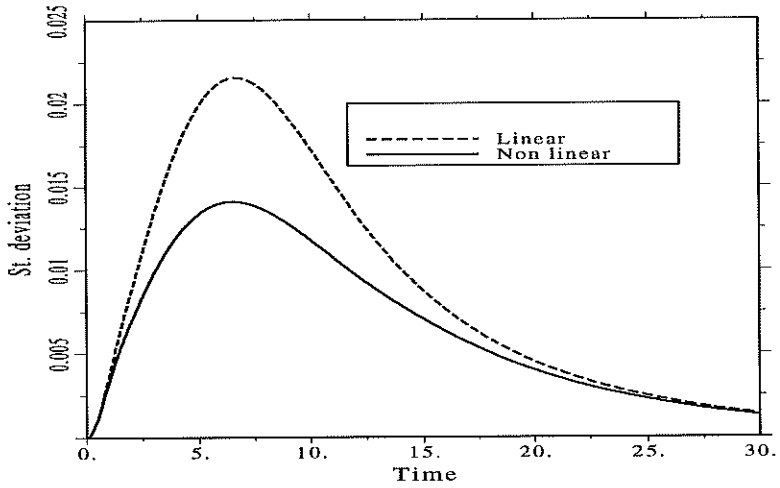

Figure 8.20 Influence of structural nonlinearity on base displacement

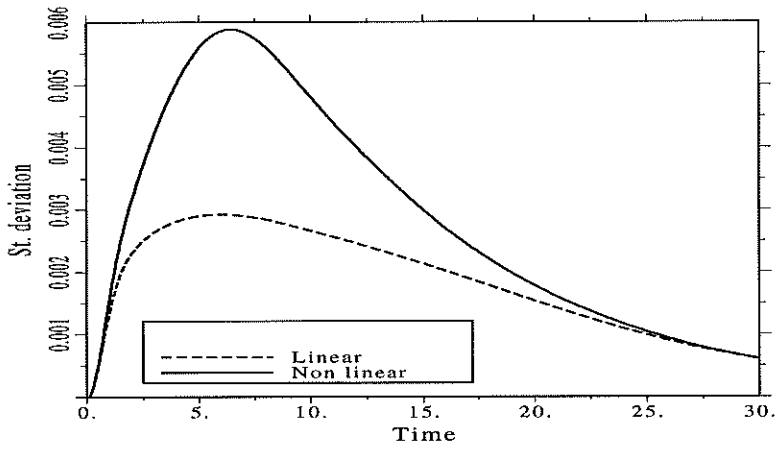

Figure 8.21 Influence of structural nonlinearity on bottom story drift

8.5 Influence of strength uncertainty

As said in the introduction, the seismic behaviour of base isolated buildings depends narrowly on the structural characteristics of the isolation devices and much less on the characteristics of the structure, due to the tendency of the latter to move as a rigid body. This means that the uncertainty about the isolation model parameters affects directly the assessment of the response in stochastic terms. Specifically, to what extent the randomness of the strength of the base isolation system affects the estimation of the maximum base displacement is the question that will be briefly examined in this section using the method of perturbation introduced in chapter 3 and developped in chapter 5 for hysteretic systems. Using the results of the analysis of a two-story building supported on lead-rubber bearings, the probability distribution for the maximum base displacement was calculated by the method of section 3.4 with $t_1 = 5\,\mathrm{s}$ and $t_2 = 30\,\mathrm{s}$.

Figure 8.22 shows the assumed Gaussian distribution of the displacement inferred with the peak value of the standard deviation and the Gumbel distribution of the maximum. The mean and standard deviation of the maximum are 28.5 and 10.9599 cm, respectively. The solution of the sensitivity differential equation (3.60) with respect to the strength of the isolation devices h_u, using the equations of section 5.4, and the posterior calculation of the perturbed deviation by equation (3.58) yields 10.9607 or 10.9631 cm if the coefficient of

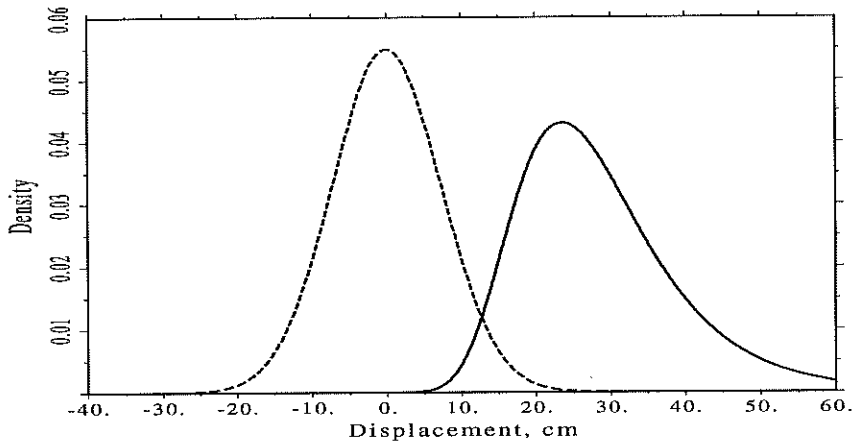

Figure 8.22 Estimated density functions of base displacement and its maximum

variation of the strength is set equal to 0.1 or 0.2, respectively. Since these increments are negligible, it can be concluded that the lead-rubber system is robust with respect to the uncertainty in its strength.

Such a sheer insensitivity of the maximum base displacement to the strength of the isolation devices is due to the fact that the latter is a parameter of little significance in a system whose behaviour is close to linear, as illustrated by figure 8.5. In last analysis, it can be attributted to the high value of the post-yield ratio α of the model. Note that a much higher value ($\alpha = 0.6$) has been proposed by other researches for this very same system (Yang *et al.* 1992a, b; Yang *et al.* 1994).

References

Amin, M. and A.H.S. Ang (1966): *A nonstationary stochastic model for strong motion earthquakes.* Structural Research Series, 306, University of Illinois, Department of Civil Engineering

Augusti, G., A. Baratta and F. Casciati (1984): *Probabilistic Methods in Structural Engineering.* Chapman and Hall, London.

Asano, K. and W. D. Iwan (1984): An alternative approach to the random response of bilinear hysteretic systems. *Earthquake Engineering and Structural Dynamics*, 12:229-236.

Atalik, T. S. and S. Utku (1976): Stochastic linearization of multi-degree of freedom non-linear systems. *Earthquake Engineering and Structural Dynamics*, 4:411-420.

Baber, T. T. and Y. K. Wen (1979): *Stochastic equivalent linearization for hysteretic, degrading, multistory structures*, Structural Research Series, 471, University of Illinois, Department of Civil Engineering

Baber, T. T. and Y. K. Wen (1981): Random vibration of hysteretic, degrading systems. *Journal of the Engineering Mechanics Division ASCE*, 107:1069-1087.

Baber, T. T. and Y. K. Wen (1982): Stochastic response of multistorey yielding frames. *Earthquake Engineering and Structural Dynamics*, 10:403-416.

Baber, T. T. (1985): Nonzero mean random vibration of hysteretic frames. *Computers and Structures*, 23:265-277.

Baber, T. T. (1986): Modal analysis for random vibration of hysteretic frames. *Earthquake Engineering and Structural Dynamics*, 14:841-859.

Baratta, A. (1993): Approximate solution of the Fokker-Planck equation for dynamical systems, in *Dynamic Motion: Chaotic and Stochastic Behaviour*, edited by F. Casciati. Springer-Verlag, Wien.

Barbat, A. H., J. Rodellar, N. Molinares and E. P. Ryan (1994): Seismic performance of buildings with a class of adaptive nonlinear hybrid systems. *Journal of Structural Control*, 1:117-141.

Barbat, A. H. and L. M. Bozzo (1997): Seismic analysis of base isolated buildings. *Archives of Computational Methods in Engineering*, 4:153-192.

Bard, Y. (1974): *Nonlinear Parameter Estimation.* Academic Press, San Diego.

Bartels, R. H. and G. W. Stewart (1972): Solution of the matrix equation $AX + BX = C$, Algorithm 432. *Communications of the ACM*, 15:820-826.

Beavers, A. N. and E. D. Denman (1975): A new solution method for the Lyapounov matrix equation. *SIAM Journal of Applied Mathematics*, 29:416-421.

Beck, J. L. and C. Papadimitrou (1993): Moving resonance in nonlinear response to fully nonstationary stochastic ground motion. *Probabilistic Engineering Mechanics* 8:157-167.

Bendat, J. S and A. G. Piersol (1971): *Random Data: Analysis and Measurement Procedures.* John Wiley and Sons, New York.

Benjamin, J. R. and C.A. Cornell (1970): *Probability, Statistics and Decisions for Civil Engineers.* McGraw-Hill, New Jersey.

Bergman, L. A. and J. C. Heinrich (1981): On the moments of time to first passage of the linear oscillator. *Earthquake Engineering and Structural Dynamics*, 9:197-204.

Bergman, L. A. and J. C. Heinrich (1982): On the reliability of the linear oscillator and systems of coupled oscillators. *International Journal for Numerical Methods in Engineering*, 18:1271-1295.

Bergman, L. A. and B. F. Spencer (1997): Application of the FE method to the solution of forward and backward Kolmogorov equations, in *IASSAR report on Computational Stochastic Mechanics*, edited by G. I. Schuëller. *Probabilistic Engineering Mechanics* 12:251-256.

Boas, M. L. (1983): *Mathematical Methods in the Physical Sciences.* John Wiley and Sons, New York.

Bogoliubov, N. N. and Y. A. Mitropolski (1964): *Asymptotic Methods in the Theory of Nonlinear Oscillators.* Gordon and Breach, London.

Boore, D. M. and W. B. Joyner (1982): The empirical prediction of ground motion. *Bulletin of the Seismological Society of America* 72:S43-S60.

Boore, D. M. (1986): Short-period P- and S- wave radiation from large earthquakes: implications for spectral scaling relations. *Bulletin of the Seismological Society of America* 76:43-64.

Boore, D. M. and G. M. Atkinson (1987): Stochastic prediction of ground motion and spectral parameters at hard-rock sites in eastern north- America. *Bulletin of the Seismological Society of America* 77:440-467.

Bouc, R. (1967): Forced vibration of mechanical systems with hysteresis (Abstract), in: *Proceedings of the Fourth Conference on Nonlinear Oscillation*, Prague, Czechoslovakia.

Box, G. E. P. and N. R. Draper (1987): *Empirical Model-building and Response Surfaces.* John Wiley and Sons, New York.

Bozzo, L. and A. H. Barbat (1995): Nonlinear response of structures with sliding base isolation. *Journal of Structural Control* 2:59-77

Bratley, P., B. L. Fox and L. E. Schrage (1987): *A Guide to Simulation.* Springer-Verlag, New York.

Bullen, K. E. and B. A. Bolt (1985): *An Introduction to the Theory of Seismology.* Cambridge University Press, Cambridge.

Bycroft, G. N. (1960): White noise representation of earthquakes. *Journal of the Engineering Mechanics Division ASCE*, 86:1-16.

Carli, F. (1992): Nonstationary models of earthquake accelerograms, in *Earthquake Engineering. Proceedings of the Tenth World Conference*, held in Madrid, 1992. 2:829-834. Balkema, Rotterdam.

Carli, F. (1995): Smooth frequency modulating function for strong ground motion. in *Proceedings of the 10th European Conference on Earthquake Engineering* held in Vienna, 1994, edited by G. Duma. 1:155-160. Balkema, Rotterdam.

Casciati, F. and L. Faravelli (1985a): Reliability assessment for non-linear random frames, in *Probabilistic Methods in the Mechanics of Solids and Structures*, edited by S. Eggwertz and N. C. Lind. Springer-Verlag, Berlin.

Casciati, F. and L. Faravelli (1985b): Methods of non-linear stochastic dynamics for the assessment of structural fragility. *Nuclear Engineering and Design*, 90:341-356.

Casciati, F., L. Faravelli and M. P. Singh (1986): Non-linear structural response and modeling uncertainty on system parameters and seismic excitation. *Proceedings of the Eigth European Conference on Earthquake Engineering*, held in Lisbon. 3:6.3, 41-48.

Casciati, F. (1987a): Non linear stochastic dynamics of large structural systems by equivalent linearization, Proceedings ICASP5, Vancouver.

Casciati, F. (1987b): Approximate methods in non linear stochastic dynamics, in *Stochastic methods in structural dynamics*, edited by G. I. Schuëller and M. Shinozuka. Martinus Nijhoff Publishers.

Casciati, F. and L. Faravelli (1988): Non linear stochastic dynamics of frames, in *Proceeding of the 3rd. International Conference on Recent Advances in Structural Dynamics* 781-789. Southampton.

Casciati, F. (1989): Stochastic dynamics of hysteretic media. *Structural Safety*, 6:259-269.

Casciati, F. and L. Faravelli (1988): Stochastic equivalent linearization for 3-D frames. *Journal of Engineering Mechanics ASCE*, 114:1760-1771.

Casciati, F. and L. Faravelli (1991): *Fragility Analysis of Complex Structural Systems*. Research Studies Press Ltd., Taunton.

Casciati, F., L. Faravelli and P. Venini (1991): Stochastic equivalent linearization of nonlinear complex structures, in: *Computational Stochastic Mechanics*, edited by P. D. Spanos and C. A. Brebbia, pp. 349-358. Computational Mechanics Publications, Southampton and Elsevier Applied Science, London.

Casciati, F., L. Faravelli and A. M. Hasofer (1993): A new philosophy for stochastic equivalent linearization. *Probabilistic Engineering Mechanics*, 8:179-185.

Casciati, F. and P. Venini (1994): Discussion to Y. J. Park (1992): Equivalent linearization for seismic responses. I: Formulation and error analysis. *Journal of Engineering Mechanics ASCE*, 120:676-679.

Casciati, F., L. Faravelli and P. Venini (1994): Frequency Analysis in Stochastic Linearization. *Journal of Engineering Mechanics ASCE*, 120:2498-2518.

Casciati, F. and P. Venini (1995): Irregular structures under stochastic excitation, in *Proceedings of the 10th European Conference on Earthquake Engineering* held in Vienna, 1994, edited by G. Duma. 2:1297-1302. Balkema, Rotterdam.

Caughey, T. K. (1963): Equivalent linearization techniques. *Journal of the Acoustical Society of America*, 35:1706-1711.

Chang, T. P. (1985) *Seismic response analysis of nonlinear structures using the stochastic equivalent linearization technique.* PhD. Thesis. Columbia University, New York.

Chen, Y. and G. Ahmadi (1994): Performance of a high damping rubber bearing base isolation system for a shear beam structure. *Earthquake Engineering and Structural Dynamics*, 23:729-744.

Clough, R. W. and J. Penzien (1993): *Dynamics of Structures*, 2nd edition. McGraw Hill, New York, U. S. A.

Colangelo, F., R. Giannini and P. E. Pinto (1995): Stochastic linearization for the assessment of behavior factors and capacity design provisions in Eurocode 8, in *Proceedings of the 10th European Conference on Earthquake Engineering* held in Vienna, 1994, edited by G. Duma. 2:947-952. Balkema, Rotterdam.

Constantinou, M. C. and I. G. Tadjbakhsh (1985): Hysteretic dampers in base isolation: Random Approach. *Journal of Structural Engineering*, 111:705-721.

Cunha, A. A. M. F. (1990): *Dinamica estructural estocástica. Aplicaçes a engenharia sísmica.* PhD. Thesis. Universidade do Porto. (in Portuguese)

Cunha, A. A. M. F. (1992): Structural safety assessment of building structures under earthquake hazard by the stochastic equivalent linearization method, in *Earthquake Engineering. Proceedings of the Tenth World Conference*, held in Madrid, 1992. Balkema, Rotterdam.

Cunha, A. A. M. F. (1994): The role of the stochastic equivalent linearization method in the analysis of the non-linear seismic response of building structures. *Earthquake Engineering and Structural Dynamics*, 23:837-857.

Di Paola, M. (1993): Stochastic differential calculus, in *Dynamic motion: chaotic and stochastic behaviour*, edited by F. Casciati. Springer-Verlag, Wien.

Di Paola, M. and G. Falsone (1994): Stochastic dynamics of MDOF structural systems under non-normal filtered inputs. *Probabilistic Engineering Mechanics*, 9:265-272.

DiPaola, M., G. Ricciardi and M. Vasta (1995): A method for the probabilistic analysis of nonlinear systems. *Probabilistic Engineering Mechanics* 10:1-10

Dmitriev, V. I. (1991): *Teoría de información aplicada.* Mir, Moscow. (in Spanish)

Donley, M. G. and P. D. Spanos (1991): Statistical quadratization for nonlinear systems in offshore engineering, in *Stochastic Structural Dynamics 2*, edited by Y. K. Lin and I. Elishakoff. Springer-Verlag, Berlin.

Einstein, A. (1956): *Investigations on the Theory of Brownian Movement.* Dover, New York.

Eliopoulos, D. E. and Y. K. Wen (1991): Evaluation of response statistics of moment resisting steel frames under seismic excitation, in: *Computational*

Stochastic Mechanics, edited by P. D. Spanos and C. A. Brebbia, pp.673-684. Computational Mechanics Publications, Southampton and Elsevir Applied Science, London.

Elishakoff, I. (1991): Method of stochastic linearization revised and improved, in: *Computational Stochastic Mechanics*, edited by P. D. Spanos and C. A. Brebbia, pp. 101-112. Computational Mechanics Publications, Southampton and Elsevier Applied Science, London.

Elishakoff, I. and Colombi, P. (1993): Succesful combination of the stochastic linearization and Monte Carlo methods, *Journal of Sound and Vibration*, 160:554-558.

Falsone, G. (1991): Stochastic linearization for the response of MDOF systems subjected to external and parametric Gaussian excitations, in: *Computational Stochastic Mechanics*, edited by P. D. Spanos and C. A. Brebbia, pp. 303-314. Computational Mechanics Publications, Southampton and Elsevier Applied Science, London.

Fan, F. and G. Ahmadi (1990): Nonstationary Kanai-Tajimi models for El Centro 1940 and Mexico City 1985 earthquakes. *Probabilistic Engineering Mechanics*, 5:171-181.

Fan, F. and G. Ahmadi (1991): Random response analysis of frictional base isolation system. *Journal of Engineering Mechanics ASCE*, 116:1881-1901.

Faravelli, L. (1988a): Stochastic modeling of the seismic excitation for structural dynamics purposes, *Probabilistic Engineering Mechanics*, 3:189-195.

Faravelli, L. (1988b): Source-to-site seismic models in structural dynamics, in *Proceeding of the 3rd. International Conference on Recent Advances in Structural Dynamics*, held in Southampton, 1988. 1021-1032.

Faravelli, L., F. Casciati and M. P. Singh (1988): Stochastic equivalent linearization algoritms and their applicability to hysteretic systems. *Meccanica*, 23:107-112.

Faravelli, L. (1993): Dynamic analysis of complex structural systems, in *Dynamic Motion: Chaotic and Stochastic Behaviour*, edited by F. Casciati. Springer- Verlag, Wien.

Foliente, G. C., M. P. Singh and M. N. Noori (1996): Equivalent linearization of generally pinching hysteretic, degrading systems. *Earthquake Engineering and Structural Dynamics*, 25:611-629.

Gantmacher, F. R. (1966) :*Théorie des matrices.* Dunod, Paris. (in French)

Gardiner, C. W. (1985): *Handbook of Stochastic Methods*, 2nd edition. Springer-Verlag, Berlin.

Ghanem, R. G. and P. D. Spanos (1991):*Stochastic Finite Elements: A spectral Approach.* Springer-Verlag, New York.

Grigoriu, M., S. E. Ruiz, E. Rosenblueth (1988): The Mexico earthquake of September 19, 1985 - Nonstationary models of seismic ground acceleration. *Earthquake Spectra*, 4:551-568.

Gzyl, H. (1995): *The Method of Maximum Entropy.* World Scientific, Singapore.

Hagen, Ø. (1993): Outcrossing of stationary Gaussian process from 2D elliptical region, *Journal of Engineering Mechanics ASCE*, 119:973-996.

Hämmerlin, G. and K. H. Hoffmann (1991): *Numerical Mathematics.* Springer-VErlag, New York.

Hampl, N. C. and G. I. Schuëller (1989): Probability density of the response of nonlinear structures under stochastic dynamic excitation. *Probabilistic Engineering Mechanics*, 4:2-9.

Hao, H. (1996): Characteristics of torsional ground motion. *Earthquake Engineering and Structural Dynamics*, 25:599-610.

Housner, G. W. (1947): Characteristics of strong motion earthquakes. *Bulletin of the Seismological Society of America*, 37:1-19.

Hurtado, J.E. and A.H. Barbat (1996a): Improved stochastic linearization method using mixed distributions. *Structural Safety*, 18:49-62

Hurtado, J.E. and A.H. Barbat (1996b) Stochastic control of base isolated structures, in *Proceedings of the First European Conference on Structural Control*, held in Barcelona, 1996, edited by A. Baratta and J. Rodellar. World Scientific, Singapore

Hurtado, J.E., A.H. Barbat and A. A. M. F. da Cunha (1996c): Nonlinear random vibration of base isolated buildings under evolutionary seismic input, in *Earthquake Engineering. Proceedings of the Eleventh World Conference*, held in Acapulco, Mexico, 1996, paper 249. Balkema, Rotterdam.

Hurtado, J.E. and A.H. Barbat (1998): Monte Carlo Techniques in Computational Stochastic Mechanics. *Archives of Computational Methods in Engineering* 5:3-30

Ibrahim, R. A. (1985) *Parametric Random Vibration.* Research Studies Press Ltd., Taunton, England.

Iwan, W. D. and I. M. Yang (1972): Application of statistical linearization techniques to nonlinear multidegree of freedom systems. *Journal of Applied Mechanics*, 39:545-550.

Iwan, W. D. (1973): A generalization of the concept of equivalent linearization. *International Journal of Nonlinear Mechanics*, 8:279-287.

Iwan, W. D. and L. G. Paparizos (1988): The stochastic response of strongly yielding systems. *Probabilistic Engineering Mechanics* 3:75-82.

Jennings, A. and J. J. McKeown (1992): *Matrix Computation.* John Wiley and Sons, Chichester.

Johnson, N. L., S. Kotz and N. Balakrishnan (1994): *Continuous Univariate Distributions*, 2nd. edition. John Wiley and Sons, New York.

Kameda, H. and Nojima, N. (1988): Simulation of risk-consistent earthquake motion. *Earthquake Engineering and Structural Dynamics*, 16:1007-1019.

Kanai, K. (1961): An empirical formula for the spectrum of strong earthquake motions. *Bulletin of the Earthquake Research Institute*, University of Tokio. 39:85-95.

Kapur, J.N. (1989): *Maximum Entropy Models in Science and Engineering.* John Wiley and Sons, New Delhi.

Kelly, J. M. (1993): *Earthquake-Resistant Design with Rubber.* Springer-Verlag, London.

Khan, A. S. and S. Huang (1995): *Continuum Theory of Plasticity.* John Wiley and Sons, New York.

Kimura, K., H. Yasumuro and M. Sakata (1994): Non-Gaussian equivalent linearization for nonstationary random vibration of hysteretic system. *Probabilistic Engineering Mechanics*, 9:15-22.

Kleiber, M. and Hien, T. D. (1992): *The Stochastic Finite Element Method* John Wiley and Sons, New York.

Kloeden, P. E. and E. Platten (1995): *Numerical Solution of Stochastic Differential Equations.* Springer-Verlag, Berlin.

Kobori, T., R. Minai and Y. Suzuki (1977): Stochastic response of hysteretic structures, *Bulletin of the Disaster Prevention Research Institute*, Kyoto University, 26:57-70.

Kovalenko, I. N., N. Yu. Kuznetsov, and V. M. Shurenkov (1996): *Models of Random Processes.* CRC Press, Boca Raton.

Krylov, N. and N. Bogoliubov (1943): *Introduction to Nonlinear Mechanics.* Princenton University Press, New York.

Lai, S. P. (1982): Statistical characterization of strong ground motions using power spectral density function. *Bulletin of the Seismological Society of America* 72:259-274.

Langtangen, H. P. (1991): A general numerical solution for Fokker-Planck equations with applications to structural reliability. *Probabilistic Engineering Mechanics*, 6:33-48.

Leadbetter, M. R., G. Lindgren and H. Rootzen (1983): *Extremes and Related Properties of Stochastic Processes.* Springer-Verlag, New York.

Leira, B. (1994): Multivariate distributions of maxima and extremes for Gaussian vector-processes, *Structural Safety*, 14:247-265.

Li, J., W. Yuan and L. Fan (1994): Optimal design of aseismic rubber bearings for continuous bridges, in *Proceedings of the First World Conference on Structural Control*, held in Los Angeles, 1994. IV:23-29.

Li, W. (1990): A non-Gaussian stochastic linearization technique based on the cumulant-neglect closure method, in *Structural Dynamics - Proceedings of the European Conference on Structural Dynamics EURODYN'90*, held in Bochum, 1990, edited by W. B. Krätzig, O. T.. Bruhns, H. L. Jessberger, K. Meskouris, H.-J. Niemann, G. Schmid, F. Stangenberg, A. N. Kounadis and G. I. Schuëller (613-618). Balkema, Rotterdam.

Li, Z. and H. Katsukura (1990): Markovian hysteretic characteristics. *Journal of Engineering Mechanics ASCE*, 116:1798-1811.

Lin, B.C., I. G. Tadjbakhsh, A.S. Papageorgiu and G. Ahmadi (1989): Response of base-isolated building to random excitations described by the Clough-Penzien spectral model. *Earthquake Engineering and Structural Dynamics*, 18:49-62.

Lin, B.C., I. G. Tadjbakhsh, A.S. Papageorgiu and G. Ahmadi (1990a): Performace of earthquake isolation systems. *Journal of Engineering Mechanics*, 116:446-461.

Lin, S., G. Ahmadi and I. G. Tadjbakhsh (1990b): Comparative study of base isolated systems. *Journal of Engineering Mechanics*, 115:1976-1992.

Lin, Y. K. (1976): *Probabilistic Theory of Structural Dynamics.* Robert E. Krieger Publishing Company, Malabar, Florida.

Lin, Y. K., F. Kozin, Y. K. Wen, F. Casciati, G. I. Schuëller, A. Der Kiureghian, O. Ditlevsen and E. H. Vanmarcke (1986): Methods of stochastic structural dynamics. *Structural Safety*, 3:167-194

Lin, Y. K. (1987a): Evolutionary Kanai-Tajimi earthquake models. *Journal of Engineering Mechanics*, 113:1119-1137

Lin, Y. K. (1987b): Application of Markov process theory to nonlinear random vibration problems, in *Stochastic Methods in Structural Dynamics*, edited by G. I. Schuëller and M. Shinozuka. Martinus Nijhoff Publishers.

Lin, Y. K. and C. Q. Cai (1995):*Probabilistic Structural Dynamincs. Advanced Theory and Applications.* McGraw Hill, New York.

Liu, P. and A. der Kiurghian (1986): Multivariate distribution models with prescribed marginals and covariances. *Probabilistic Engineering Mechanics*, 1:105-112.

Lutes, L. D. and S. Sarkani (1997): *Stochastic analysis of structural and mechanical vibrations.* Prentice - Hall, Upper Saddle River, New Jersey.

MacCann, M. W. and Shah, H. C. (1979): A statistically rational approach to ground motion studies, in *Proceedings of the Speciality Conference on Probabilistic Mechanics and Structural Reliability*, held in Tucson, Arizona, 1979, edited by A.H.S. Ang and M. Shinozuka. American Society of Civil Engineers, New York.

Malhotra, P. K. (1997): Dynamics of seismic impacts in base-isolated buildings. *Earthquake Engineering and Structural Dynamics*, 26:797-813.

Moayyad, P. and B. Mohraz (1982): A study of power spectral density of earthquake accelerograms. Civil Engineering department, Southern Methodist University, Dallas.

Mochio, T. (1991): Stochastic response of nonlinear multi-degree-of-freedom structures subjeted to combined random loads, in: *Computational Stochastic Mechanics*, edited by P. D. Spanos and C. A. Brebbia, pp. 255-266. Computational Mechanics Publications, Southampton and Elsevier Applied Science, London.

Muscolino, G. (1993): Response of linear and non-linear structural systems under Gaussian or non-Gaussian filtered input, in *Dynamic Motion: Chaotic and Stochastic Behaviour*, edited by F. Casciati. Springer - Verlag, Wien.

Naess, A. and Johnsen, J. M. (1991): The path integral solution technique applied to the random vibration of hysteretic systems, in: *Computational Stochastic Mechanics*, edited by P. D. Spanos and C. A. Brebbia, pp. 279-291. Computational Mechanics Publications, Southampton and Elsevier Applied Science, London.

Naess, A. (1995): Prediction of extreme response of nonlinear structures by extended stochastic linearization. *Probabilistic Engineering Mechanics*, 10:153-160.

Nataf, A. (1962): Determination des distributions dont les marges sont donées. *Comptes rendues de l'Academie des Sciences*, 225:42-43. (in French)

Nau, R. F., R. M. Oliver and K. S. Pister (1982): Simulating and analyzing artificial nonstationary earthquake ground motions. *Bulletin of the Seismological Society of America* 72:615-636.

Newmark, N. M. and E. Rosenblueth (1971): *Fundamentals of Earthquake Engineering.* Prentice-Hall, Englewood Cliffs.

Nielsen, S.R.K., K.J. Mørk and P. Thoft-Christensen (1990a): Stochastic Response of Hysteretic Systems. *Earthquake Engineering and Structural Dynamics*, 18:655-666.

Nielsen, S.R.K., K.J. Mørk and P. Thoft-Christensen (1990b): Response analysis of Hysteretic multi-storey frames under earthquake excitation. *Structural Safety*, 9:59-71.

Nigam, N. C. (1983): *Introduction to random vibrations.* The MIT Press, Cambridge, Massachussets.

Nigam, N. C. and S. Narayanan (1994): *Applications of random vibrations.* Springer-Verlag - Narosa Publishing House, Delhi.

Noori, M. m. Saffar, G. Ghantous, A. Guran, H. Davoodi and T. T. Baber: (1991): Equivalent linearization of a newly introduced general hysteretic model, in: *Computational Stochastic Mechanics*, edited by P. D. Spanos and C. A. Brebbia, pp. 315-326. Computational Mechanics Publications, Southampton and Elsevier Applied Science, London.

Noori, M., M. Dimentberg, Z. Hou, R. Christodoulidou and A. Alexandrou (1995): First-passage study and stationary response of a BWB hysteresis model using quasi-conservative stochastic averaging method. *Probabilistic Engineering Mechanics*, 10:161-170.

Øksendal, B. (1995): *Stochastic Differential Equations.* Springer Verlag, Berlin.

Oppenheim, A. V. and R. W. Schafer (1989): *Discrete-Time Signal Processing.* Prentice-Hall, Englewood Cliffs, New Jersey.

Papoulis, A. (1991): *Probability, random variables and stochastic processes*, 3rd edition. McGraw-Hill, Singapore.

Park, Y.J., Y.K. Wen and A.H.S. Ang (1986): Random vibration of hysteretic systems under bi-directional ground motions. *Earthquake Engineering and Structural Dynamics*, 14:543-557

Park, Y.J. (1992): Equivalent linearization for seismic responses. I: Formulation and error analysis. *Journal of Engineering Mechanics ASCE*, 118:2207-2226.

Penzien, J. and Watabe, M. (1975): Characteristics of 3-dimensional earthquake ground motions. *Earthquake Engineering and Structural Dynamics*, 3:365-373.

Pires, J. E. A., Y. K. Wen and A. H. S. Ang (1983): *Stochastic analysis of liquefaction under earthquake loading*, Structural Research Series, 504, University of Illinois, Department of Civil Engineering

Pirotta, A. and R. A. Ibrahim (1997): Experimental investigation of friction-base isolation. *Probabilistic Engineering Mechanics*, 12:125-136.

Polidori, D. C. and J. L. Beck (1996): Approximate solutions for non-linear random vibration problems. *Probabilistic Engineering Mechanics*, 11:179-185.

Pradlwarter, H. J., G. I. Schuëller and X. W. Chen (1988): Consideration of non-Gaussian response properties by use of stochastic equivalent linearization, in *Proceedings of the 3rd. International Conference on Recent Advances in Structural Dynamics*, held in Southampton, 1988. 737-752.

Pradlwarter, H. J. (1990): Stochastic nonlinear hysteretic finite element analysis, in *Structural Dynamics - Proceedings of the European Conference on Structural Dynamics EURODYN'90*, held in Bochum, 1990, edited by W. B. Krätzig, O. T.. Bruhns, H. L. Jessberger, K. Meskouris, H.-J. Niemann, G. Schmid, F. Stangenberg, A. N. Kounadis and G. I. Schuëller (637-644). Balkema, Rotterdam.

Pradlwarter, H. J. and W. Li (1991): On the computation of the stochastic response of highly nonlinear large MDOF-systems modeled by finite elements, in *Stochastic Structural Dynamics 2*, edited by Y. K. Lin and I. Elishakoff. Springer-Verlag, Berlin.

Pradlwarter, H. J. and G. I. Schuëller (1991): The method of statistical equivalent linearization, in *Structural Dynamics - Recent Advances*, edited by G. I. Schuëller. Springer-Verlag, Berlin.

Pradlwarter, H. J. and G. I. Schuëller (1992): Equivalent linearization – a suitable tool for analyzing MDOF-systems. *Probabilistic Engineering Mechanics*, 8:115-126.

Press. W. H., S. A. Teukolsky, W. T. Vetterling and B. P. Flannery (1992): *Numerical Recipes in FORTRAN*, 2nd edition. Cambridge University Press, Cambridge.

Priestley, M. B. (1981): *Spectral Analysis and Time Series.* Academic Press, London.

Quek, S, Teo, Y. and Balendra, T. (1990): Non-stationary structural response with evolutionary spectra using seismological input model. *Earthquake Engineering and Structural Dynamics*, 19:275-288.

Rahman, S. and M. Grigoriu (1994): *A Markov model for local and global damage indices in seismic analysis*, Technical Report NCEER-94-0003, National Center for Earthquake Engineering Research, State University of New York at Buffalo.

Ripley, B. D. (1987): *Stochastic Simulation.* John Wiley, New York.

Risken, H. (1989): *The Fokker-Planck Equation*, 2nd edition. Springer-Verlag, Berlin.

Roberts, J. B. and P. D. Spanos (1990): *Random Vibration and Statistical Linearization.* John Wiley and Sons, Chichester.

Roberts, J. B. (1991): Random vibration and first passage failure, in *Reliability Problems: General Principles and Applications in Mechanics of Solids and Structures*, edited by F. Casciati and J. B. Roberts. Springer-Verlag, Wien.

Roy, R. V. and P. D. Spanos (1991): Padé-type Approach to Nonlinear Random Vibration Analysis, in *Stochastic Structural Dynamics 1*, edited by Y. K. Lin and I. Elishakoff. Springer-Verlag, Berlin.

Rubinstein, R. Y. (1981): *Simulation and the Monte Carlo Method.* John Wiley and Sons, New York.

Sawada, T., K. Hirao, O. Tsujihara and H. Yamamoto (1992): Relationship between maximum amplitude ratio ($\frac{a}{v}$, $\frac{ad}{v^2}$) and spectral parameters of earthquake ground motion", *Earthquake Engineering. Proceedings of the Tenth World Conference*, 2:617-621. Balkema, Rotterdam.

Shames, I. H. and F. A. Cozzarelli (1992): *Elastic and Inelastic Stress Analysis.* Prentice-Hall, Englewood Cliffs, New Jersey.

Schetzen, M. (1989): *The Volterra and Wiener Theories of Nonlinear Systems.* Krieger Publishing Company, Malabar, Florida.

Schuëller, G. I., Bucher, C. G. and H. J. Pradlwarter (1990): Computational methods in stochastic structural dynamics, in *Structural Dynamics - Proceedings of the European Conference on Structural Dynamics EURODYN'90* held in Bochum, 1990, edited by W. B. Krätzig, O. T.. Bruhns, H. L. Jessberger, K. Meskouris, H.-J. Niemann, G. Schmid, F. Stangenberg, A. N. Kounadis and G. I. Schuëller (599-605). Balkema, Rotterdam.

Schuëller, G. I., M. D. Pandey and H. J. Pradlwarter (1994): Equivalent linearization (EQL) in engineering practice for aseismic design. *Probabilistic Engineering Mechanics*, 9:95-102.

Shiau. L. and Wu, T. (1996): A finite-element mothod for analysis of a nonlinear system under stochastic parametric and external excitation, *International Journal of Non-Linear Mechanics* 31:193-201.

Shinozuka, M. (1964): Probability of failure under random loading. *Journal of Engineering Mechanics ASCE* 90:147-171.

Shinozuka, M. and Y. Sato (1967): Simulation of nonstationary random processes. *Journal of the Engineering Mechanics Division*, 93:11-40.

Shinozuka, M. and Lenoe, R. (1976): A Probabilistic model for spatial distribution of material properties. *Engineering Fracture Mechanics*, 8:217-227.

Shinozuka, M. (1983): Basic analysis of structural safety. *Journal of Structural Engineering ASCE* 109:721-740.

Shinozuka, M. (1987): Stochastic fields and their digital simulation, in *Stochastic Methods in Structural Dynamics*, edited by G. I. Schuëller and M. Shinozuka. Martinus Nijhoff Publishers.

Simulescu, I., Mochio, T. and M. Shinozuka (1989): Equivalent linearization method in nonlinear FEM, *Journal of Engineering Mechanics Division ASCE*, 115:475-492.

Skinner, R. I., W. H. Robinson and G. H. McVerry (1993): *An Introduction to Seismic Isolation.* John Wiley and Sons, Chichester.

Sobczyk, K. and J. Trębicki (1990): Maximum entropy principle in stochastic dynamics. *Probabilistic Engineering Mechanics* 5:102-110.

Sobczyk, K. (1997): Probability distributions for stochastic systems and maximum entropy method, in *IASSAR report on Computational Stochastic Mechanics*, edited by G. I. Schuëller. *Probabilistic Engineering Mechanics* 12:266-269.

Socha, L. (1986): The sensitivity analysis of stochastic non-linear dynamical systems. *Journal of Sound and Vibration*, 110:271-288.

Socha, L. and G. Zasucha (1991): The sensitivity analysis of stochastic hysteretic dynamic systems. in: *Computational Stochastic Mechanics*, edited by P. D. Spanos and C. A. Brebbia, pp. 71-80. Computational Mechanics Publications, Southampton and Elsevier Applied Science, London.

Soize, C. (1994): *The Fokker-Planck Equation for Stochastic Systems and its Explicit Steady State Solutions.* World Scientific, Singapore.

Soong, T. T. (1973): *Random Differential Equations in Science and Engineering.* Academic Press, New York.

Soong, T. T. (1990): *Active Structural Control: Theory and Practice*, Longman Scientific & Technical, Avon.

Soong, T. T. and M. Grigoriu (1993): *Random Vibration of Mechanical and Structural Systems*, Prentice-Hall, Englewood Cliffs, New Jersey.

Spanos, P. D. and W. D. Iwan (1978): On the existence and uniqueness of solutions generated by equivalent linearization, *International Journal of Non-Linear Mechanics* 13:71-78.

Spanos, P. D., W. Y. Tein and R. Ghanem (1992): Spectral estimation of bivariate non-stationary processes, in *Earthquake Engineering. Proceedings of the Tenth World Conference*, held in Madrid, 1992. 2:839-844. Balkema, Rotterdam.

Spencer, B. F. and L. A. Bergman (1985): On the reliability of a simple hysteretic system. *Journal of Engineering Mechanics ASCE*, 111:1502-1514.

Spencer, B. F. and L. A. Bergman (1991): Numerical solution of the Fokker-Planck equation for first passage probabilities, in: *Computational Stochastic Mechanics*, edited by P. D. Spanos and C. A. Brebbia, pp. 359-370. Computational Mechanics Publications, Southampton and Elsevier Applied Science, London.

Spencer, B. F. and L. A. Bergman (1993): On the numerical solution of the Fokker-Planck equation for nonlinear stochastic systems, *Nonlinear Dynamics* 4:357-372.

Stengel, R. F. (1986): *Stochastic Optimal Control.* John Wiley and Sons, New York.

Stratonovitch, P. L. (1961): *Selected Topics of the Theory of Fluctuations in Radiotechnics.* Sovietskoe Radio, Moscow. (in Russian)

Sues, R. H., Y. K. Wen and A. H.-S. Ang (1985): Stochastic evaluation of seismic structural performance, *Journal of Structural Engineering*, 111:1204-1218.

Sues, R. H., S. T. Mau and Y. K. Wen (1988): Systems identification of degrading hysteretic restoring forces. *Journal of Engineering Mechanics*, 114:833-846.

Szidarovszky, F. and A. T. Bahill (1992): *Linear System Theory.* CRC Press, Boca Raton, Florida.

Tagliani, A. (1990): On the existence of maximum entropy distributions with four and more assigned moments. *Probabilistic Engineering Mechanics*, 5:167-170.

Tajimi, H. (1960): A statistical method of determining the maximum response of a building structure during an earthquake, in *Proceedings of the Second World Conference on Earthquake Engineering*, held in Tokio and Kyoto, 1960. Science Council. 2:781-797.

Tan, D. and Yang, Q. (1995): Structural random vibration analysis by using recursive formulas, *Probabilistic Engineering Mechanics*, 10:11-21.

Thyagarajan, R. S. and W. D. Iwan (1990): Performance characteristics of a widely used hysteretic model in structural dynamics, in *Proceedings of Fourth U.S. National Conference on Earthquake Engineering* held in Palm Springs. EERI, Oakland.

Tikhonov, B. I. (1982): *Statistical Radiotechnics* 2nd edition. Radio i sviaz, Moscow. (in Russian)

Tikhonov, B. I. (1986): *Nonlinear Transformations of Stochastic Processes.* Radio i sviaz, Moscow. (in Russian)

To, C. W. S. and D. M. Li (1991): Equivalent nonlinearization of nonlinear system to random excitations, in *Stochastic Structural Dynamics 1*, edited by Y. K. Lin and I. Elishakoff. Springer-Verlag, Berlin.

Trębicki, J. and K. Sobczyk (1996): Maximum Entropy Principle and Non-stationary Distributions of Stochastic Systems. *Probabilistic Engineering Mechanics* 11:169-178.

Vanmarcke, E. H. (1976): Structural response to earthquakes, in *Seismic Risk and Engineering Decisions*, edited by C. Lomnitz and E. Rosenblueth. Elsevier Scientific Publishing Company, Amsterdam.

Vanmarcke, E. H. and S. P. Lai (1980): Strong-motion duration and RMS amplitude of earthquake records. *Bulletin of the Seismological Society of America* 70:1293-1307.

Venziano, D., M. Grigoriu and C. A. Cornell (1977) Vector-process models for system reliability. *Journal of the Engineering Mechanics Division ASCE*, 103:441-460.

Wen, Y. K. (1975): Approximate method for non-linear random vibration. *Journal of Engineering Mechanics*, 101:389-401.

Wen, Y. K. (1976): Method for random vibration of hysteretic systems. *Journal of Engineering Mechanics*, 102:249-263.

Wen, Y. K. (1980): Equivalent linearization for hysteretic systems under random excitation. *Journal of Applied Mechanics*, 47:150-154.

Wen, Y.K. and C. H. Yeh (1989): Biaxial and torsional response of inelastic structures under random excitation. *Structural Safety*, 6:137-152

Wen, Y.K. (1990): *Structural Load Modeling and Combination for Performance and Safety Evaluation.* Elsevier, Amsterdam.

Wen, Y.K. (1991): Application of nonlinear stochastic dynamics and damage accumulation in seismic engineering, in *Reliability Problems: General Principles and Applications in Mechanics of Solids and Structures*, edited by F. Casciati and J. B. Roberts. Springer-Verlag, Wien.

Wen, Y. K. and D. Eliopoulos (1994): Method for nonstationary random vibration of inelastic structures. *Probabilistic Engineering Mechanics*, 9:115-123.

Wiener, N. (1958):*Nonlinear problems in random theory*, Technology Press of the Massachussets Institute of Technology and John Wiley and Sons, New York.

Wirsching, P. H., T. L. Paez and K. Ortiz (1995): *Random Vibrations: Theory and Practice.* John Wiley and Sons, New York.

Yang, J.N. and S.C. Liu (1981): Distribution of maximum and statistical response spectra. *Journal of the Engineering Mechanics Division*, 107:1089-1102.

Yang, C. Y., A. H. D. Cheng and R. V. Roy (1991): Chaotic and stochastic dynamics for inelastic systems with hysteresis and degradation, in *Stochastic Structural Dynamics 1*, edited by Y. K. Lin and I. Elishakoff. Springer-Verlag, Berlin.

Yang, J.N. and A. Akbarpour (1990): Effect of system uncertainty on control of seismic-excited buildings. *Journal of Engineering Mechanics*, 116:462-478.

Yang, J.N., Z. Li, A. Danielians and S.C. Liu (1992a): Aseismic hybrid control of nonlinear hysteretic structures I. *Journal of Engineering Mechanics*, 118:1423-1440.

Yang, J.N., Z. Li, A. Danielians and S.C. Liu (1992b): Aseismic hybrid control of nonlinear hysteretic structures II. *Journal of Engineering Mechanics*, 118:1441-1456

Yang, J.N., Z. Li and S.C. Liu (1991): Instantaneous optimal control with acceleration and velocity feedback, in *Stochastic Structural Dynamics 1*, edited by Y. K. Lin - I. Elishakoff, Springer-Verlag, Berlin.

Yang, J. N., Z. Li and S. Vongchavalitkul (1994): Stochastic hybrid control of hysteretic structures. *Probabilistic Engineering Mechanics*, 9:125-133.

Yeh, C.H. (1989): *Modelling of nonstationary earthquake ground motion and biaxial and torsional response of inelastic structures.* Ph. D. thesis. University of Illinois.

Yeh, C.H. and Y. K. Wen (1990): Modeling of nonstationary ground motion and analysis of inelastic structural response. *Structural Safety*, 8:281-298.

Zayezdny, A., D. Tabak and D. Wulich (1989): *Engineering Applications of Stochastic Processes.* Research Studies Press Ltd., Taunton, England.

Zhang, R., M. Shinozuka and M. Q. Feng (1994): Statistical analysis of hybrid isolation system with new stochastic linearization approach, in *Structural Safety & Reliability. Proceedings of ICOSSAR - 93*, held in Innsbruck, 1993, edited by G. I. Schüeller, M. Shinozuka and C. P. Yao. 3:1607-1614. Balkema, Rotterdam.

Zhang, T. S. and T. Fang (1991): Analysing nonstationary random response to evolutionary random excitation by complex modal method, in *Stochastic Structural Dynamics 1*, edited by Y. K. Lin and I. Elishakoff, Springer-Verlag, Berlin.

Zhang, X., I. Elishakoff and R. Zhang (1991): A stochastic linearization technique based on minimum mean square deviation of potential energy, in *Stochastic Structural Dynamics 1*, edited by Y. K. Lin and I. Elishakoff. Springer-Verlag, Berlin.

Zienkiewicz, O. C. and R. L. Taylor (1995): *El método de los elementos finitos*, Vol. 2. McGraw-Hill / CIMNE, Barcelona. (in Spanish)

CENTRO INTERNACIONAL DE METODOS NUMERICOS EN INGENIERIA

Lista de monografías publicadas en la Serie de Ingeniería Sísmica

Las monografías pueden adquirirse dirigiéndose al Departamento de Publicaciones del Centro Internacional de Métodos Numericos en Ingeniería, Edificio C1, Campus Norte UPC, c/ Gran Capitán s/n, 08034 Barcelona, telefóno: 93-401.60.37, Fax: 93-401-65-17.

IS-1 *Qualitative Reasoning for Earthquake Resistant Buildings,* Luís M. Bozzo, 149 pp., ISBN 84-87867-36-7, 1993.

IS-2 *Control predictivo en sistemas de protección sísmica de estructuras,* R. Andrade Cascante, J. Rodellar, F. López Almasa, 143 pp., ISBN 84-87867-37-5, 1993.

IS-3 *Simulación numérica del comportamiento no lineal de presas de hormigón ante acciones sísmicas,* M. Galindo, J. Oliver, M. Cervera, 255 pp., ISBN 84-87867-38-3, 1994.

IS-4 *Simulación del daño sísmico en edificios de hormigón armado,* A. Hanganu, A.H. Barbat, S. Oller, E. Oñate, 96 pp., ISBN 84-87867-40-5, 1994.

IS-5 *Edificios con aislamiento de base no lineal,* N. Molinares, A.H. Barbat, 96 pp., ISBN: 84-87867-41-3, 1994.

IS-6 *Vulnerabilidad sísmica de edificios,* C. Caicedo, A.H. Barbat, J.A. Canas, R. Aguiar 100 pp., ISBN 84-87867-43-X, 1994.

IS-7 *Análisis de terremotos históricos por sus efectos,* J. R. Arango Gonzalez, 119 pp., ISBN 84-87867-44-8, 1994.

IS-8 *Control activo no lineal de edificios con aislamiento de base,* A.H. Barbat, N. Molinares, J. Rodellar, 124 pp., ISBN 84-87867-46-4, 1994.

IS-9 *Análise estocástica da resposta sísmica nao-linear de estructuras,* A.M. F. Cunha, 199 pp., ISBN: 84-87867-47-2, 1994

IS-10 *Definición de la acción sísmica,* A.H. Barbat, L. Orosco, J.E. Hurtado, M. Galindo, 122 pp., ISBN: 84-87867-448-0, 1994

IS-11 *Sismología y peligrosidad sísmica,* J.A. Canas Torres, C. Pujades Beneit, E. Banda Tarradellas, 87 pp., ISBN: 84-87867-49-9, 1994

IS-12 *Riesgo, peligrosidad y vulnerabilidad sísmica de edificios de mampostería,* F. Yépez, A.H. Barbat, J.A. Canas, 104 pp., ISBN: 84-87867-50-2, 1995

IS-13 *Estudios de ingeniería sismológica y sísmica,* J.A. Canas, ISBN: 84-87867-57-X, 13 pp., 1995

IS-14 *Simulación de escenarios de daño para estudios de riesgo sísmico,* F. Yépez, A.H. Barbat y J.A. Canas, ISBN: 84-87867-58-8, 103 pp., 1995

IS-15 *Diseño sismorresistente de edificios de hormigón armado,* L. Bozzo, A.H. Barbat, ISBN: 84-87867-59-6, 185 pp., 1995

IS-16 *Modelo tridimensional de atenuación anelástica de las ondas sísmicas en la Península Ibérica,* J.O. Caselles, J. A. Canas, Ll. G. Pujades, R.B. Herrmann, ISBN: 84-87867-60-X, 119 pp., 1995

IS-17 *Índices de daño sísmico en edificios de hormigón armado,* R. Aguiar ISBN: 84-87867-43-X, 99 pp., 1996

IS-18 *Experimental study of a reduced scale model seismically base isolated with Rubber-Layer Roller Bearings (RLRB),* D. Foti, J.M. Kelly ISBN: 84-87867-82-0, 112 pp., 1996

IS-19 *Modelos de evaluación del comportamiento sísmico no lineal de estructuras de hormigón armado,* F. Yépez Moya ISBN: 84-87867-80-4., 96pp., 1996

IS-20 *Evaluación probabilista de la vulnerabilidad y riesgo sísmico de estructuras de hormigón armado por medio de simulación,* F. Yépez Moya, A.H. Barbat, J.A. Canas, ISBN: 84-87867-81-2, 1996

IS-21 *Modelización de la peligrosidad sísmica. Aplicación a Cataluña,* J.A. Canas, J.J. Egozcue, J. Miquel Canet y A.H. Barbat, ISBN: 84-87867-83-9, 101pp., 1996

IS-22 *Evaluación del daño sísmico global en edificios porticados de hormigón armado,* R. Aguiar, A.H. Barbat and J. Canas, ISBN: 84-87867-96-0, 173pp., 1997

IS-23 *Daño sísmico global en edificios con muros de cortante,* R. Aguiar, ISBN: 84-89925-00-3, 101 pp., 1997

Los autores interesados en publicar monografías en esta serie deben contactar con el editor para concretar las normas de preparación del texto.